BIOMECHANICAL MODELLING OF A HORSE RIDER

A THESIS SUBMITTED TO
THE GRADUATE SCHOOL OF NATURAL AND APPLIED SCIENCES
OF
MIDDLE EAST TECHNICAL UNIVERSITY

BY

SİNEM GÖZDE DEFTERLİ

IN PARTIAL FULFILLMENT OF THE REQUIREMENTS
FOR
THE DEGREE OF MASTER OF SCIENCE
IN
MECHANICAL ENGINEERING

FEBRUARY 2014

Approval of the thesis:

BIOMECHANICAL MODELLING OF A HORSE RIDER

Submitted by **SİNEM GÖZDE DEFTERLİ** in partial fulfillment of the requirements for the degree of **Master of Science in Mechanical Engineering Department, Middle East Technical University** by,

Prof. Dr. Canan Özgen
Dean, Graduate School of **Natural and Applied Sciences** _____

Prof. Dr. Süha Oral
Head of Department, **Mechanical Engineering** _____

Prof. Dr. Reşit Soylu
Supervisor, **Mechanical Engineering Dept., METU** _____

Examining Committee Members:

Prof. Dr. M. Kemal Özgören
Mechanical Engineering Dept., METU _____

Prof. Dr. Reşit Soylu
Mechanical Engineering Dept., METU _____

Prof. Dr. Tuna Balkan
Mechanical Engineering Dept., METU _____

Assist. Prof. Dr. Ergin Tönük
Mechanical Engineering Dept., METU _____

Assist. Prof. Dr. Kutluk Bilge Arıkan
Mechatronics Engineering Dept., ATILIM University _____

Date: 04.02.2014

I hereby declare that all information in this document has been obtained and presented in accordance with academic rules and ethical conduct. I also declare that, as required by these rules and conduct, I have fully cited and referenced all material and results that are not original to this work.

Name, Last name: Sinem Gözde Defterli

Signature:

ABSTRACT

BIOMECHANICAL MODELLING OF A HORSE RIDER

Defterli, Sinem Gözde
M.Sc., Department of Mechanical Engineering
Supervisor: Prof. Dr. Reşit Soylu

February 2014, 178 pages

In this study, a biomechanical horse rider model is developed. The rider is modeled, on the sagittal plane, using link segments representing the limbs of the body. The model which is a tree type structure kinematically, consists of 11 links connected by the revolute joints. Assuming that each of the joints is actuated by an equivalent muscle torque, the equations of motion of the rider model is developed. In this study, it is assumed that the actuating muscle torques applied by the rider and the equivalent forces applied by the horse on the rider are to be minimized. An appropriate performance measure is defined in order to achieve this goal. This performance measure is minimized subject to the biological constraints regarding the movement and torque limits of a human joint. A constraint, which ensures that the rider does not fall down from horseback, is also imposed. As two case studies, sitting trot and a sudden stop scenario are considered. Computer codes are developed, in MATLAB®, in order to realize these case studies.

Keywords: rider modeling, equestrian dynamics, kinematics of rider, trot, horse-rider interaction

ÖZ

AT BİNİCİSİNİN BİYOMEKANİK MODELLENMESİ

Defterli, Sinem Gözde
Yüksek Lisans, Makina Mühendisliği Bölümü
Tez Yöneticisi: Prof. Dr. Reşit Soylu

Şubat 2014, 178 sayfa

Bu çalışmada, biyomekanik bir at binicisi modeli geliştirilmiştir. Binici, yanal düzlemde, bedeninin her bir uzvunu temsil edecek şekilde çubuk parçaları ile modellenmiştir.Kinematik olarak ağacımsı yapıda olan bu model, döner mafsallarla bağlanmış 11 parçadan oluşmaktadır. Her eklemin eşdeğer bir kas torku ile tahrik edildiğini göz önünde bulundurarak, binici modelinin hareket denklemleri elde edilmiştir. Bu çalışmada, binici tarafından uygulanan kas tahrik torklarının ve atın biniciye uyguladığı eşdeğer kuvvetlerin minimize edilmesi amaçlandı. Bu hedefe ulaşmak için uygun bir performans ölçüsü tanımlanmıştır. Bu performans ölçüsü, bir insan ekleminin hareket ve tork limitleri gibi biyolojik kısıtlar göz önüne alınarak minimize edilmiştir. Binicinin düşmesini engellemek amacıyla ayrı bir kısıt daha kullanılmıştır. Örnek çalışma olarak, adi süratli biniş ve ani duruş senaryoları ele alınmıştır. Bu çalışmaları gerçekleştirmek için de MATLAB® kullanılarak kodlar geliştirilmiştir.

Anahtar Kelimeler: binici modellenmesi, at binicisi dinamiği, binici kinematiği, tırıs, at-binici etkileşimi

To my family,

ACKNOWLEDGEMENTS

I wish to express my sincere appreciation and thanks to my supervisor Prof. Dr. Reşit Soylu for his precious guidance, valuable advices, moral support and for enlightening my professional and academic vision throughout my study.

I would like to express my great thanks to Gözde Tanıl for her data support and especially to Tuğçe Aydil , Fulya Erol and Ni Li for their friendship and moral support throughout my study.

I would like to give the biggest thanks to my family who have made everything possible for me with their endless love, affection, and support throughout my whole life. The completion of this study would not have been possible without them.

TABLE OF CONTENTS

LIST OF TABLES

TABLES

LIST OF FIGURES

FIGURES

LIST OF SYMBOLS

COP	: Center of Pressure
FR	: Front-Rear
LR	: Left-Right
PCA	: Principal Component Analysis
AR	: Axial Rotation
SAD	: Shoulder Angle Displacement
LLI	: Leg Length Inequality
dof	: Degree of freedom
CM	: Center of Mass
WFF	: World Fixed Frame
MRF	: Motion Reference Frame
BRF	: Body Reference Frame
C_i	: Center of mass of the ith Link
A	: Hip-thigh joint of the rider model
B	: Knee joint of the rider model
C	: Ankle joint of the rider model
L_5	: Abdomen-pelvis joint of the rider model
M_4	: 4^{th} marker on the saddle
T12	: Trunk-abdomen joint/12^{th} trunk vertebrae of the rider model
D	: Shoulder joint of the rider model
E	: Elbow joint of the rider model
F	: Wrist joint of the rider model
T1	: Neck-trunk joint of the rider model
CS1	: Head-neck joint of the rider model
$\mathbf{u}_1^i$	: Body reference frames' first axis of the rider model
$\mathbf{u}_2^i$	: Body reference frames' second axis of the rider model
$\mathbf{u}_3$	: Body reference frames' third axis of the rider model

$u_1^{(0)}$: First axis of World Fixed Frame of the rider model

$u_2^{(0)}$: Second axis of World Fixed Frame of the rider model

$u_3^{(0)}$: Third axis of World Fixed Frame of the rider model

$\mathcal{F}_0\{O\}$: World Fixed Frame at origin point O

$\mathcal{F}_2\{A\}$: Body Reference Frame of Link-2 at origin point A

$\mathcal{F}_3\{B\}$: Body Reference Frame of Link-3 at origin point B

$\mathcal{F}_4\{C\}$: Body Reference Frame of Link-4 at origin point C

$\mathcal{F}_5\{L_5\}$: Body Reference Frame of Link-5 at origin point L5

$\mathcal{F}_6\{T_{12}\}$: Body Reference Frame of Link-6 at origin point T12

$\mathcal{F}_7\{D\}$: Body Reference Frame of Link-7 at origin point D

$\mathcal{F}_8\{E\}$: Body Reference Frame of Link-8 at origin point E

$\mathcal{F}_9\{F\}$: Body Reference Frame of Link-9 at origin point F

$\mathcal{F}_{10}\{T_1\}$: Body Reference Frame of Link-10 at origin point T1

$\mathcal{F}_{11}\{CS_1\}$: Body Reference Frame of Link-11 at origin point CS1

$\mathcal{F}_a\{A\}$: Body Reference Frame at origin point A

$\mathcal{F}_0\{O\}$: Global Fixed Reference Frame at origin point O

DCM : Direction Cosine Matrix

θ : Rotation angle from global frame $\mathcal{F}_0\{O\}$ to body reference frame $\mathcal{F}_a\{A\}$

$C^{(0,a)}$: Direction Cosine Matrix of from $\mathcal{F}_0\{O\}$ to $\mathcal{F}_a\{A\}$

$R_i(\theta)$: Rotation Matrix about $u_i^{(0)}$ axis with θ angle

$C^{(0,1)}$: Transformation Matrix from Frame-0 $\mathcal{F}_0\{O\}$ to Frame-1 $\mathcal{F}_1\{O\}$

$\bar{r}_{P/A}^{(a)}$: Position vector of point P relative to A in fixed frame $\mathcal{F}_a\{A\}$

$C^{(a,b)}$: Transformation Matrix from frame $\mathcal{F}_b\{B\}$ to frame $\mathcal{F}_a\{A\}$

$\bar{r}_{P/B}^{(b)}$: Position vector of point P relative to point B in the body reference frame $\mathcal{F}_b\{B\}$

$\overline{r}_{B/A}^{(a)}$: Position vector of point B relative to A in fixed frame $\mathcal{F}_a\{A\}$

$u_1^{(1)}$: First unit vector from 1st marker to 2nd marker

$u_{2d}^{(1)}$: Second dummy unit vector from 1st marker to 3rd marker

$u_3^{(1)}$: Third unit vector of body reference frame of Link-1

$\overline{r}_k$: Position vector of kth marker in world fixed frame

$\overline{n}$: Rotation axis unit vector

$tr(R)$: Trace of Rotation Matrix R

θ_{01} : The rotation angle of Link-1 from $\mathcal{F}_0\{O\}$ to $\mathcal{F}_1\{M_1\}$

β : Constant

$\widetilde{\omega}_{b/a}{}^{(b)}$: Angular velocity cross product matrix of $\mathcal{F}_b\{B\}$ with respect to $\mathcal{F}_a\{A\}$

I : Identity Matrix

$\overline{v}_{P/A}^{(a)}$: Velocity vector of point P relative to A in fixed frame $\mathcal{F}_a\{A\}$

$\overline{v}_{P/B}^{(b)}$: Velocity vector of point P relative to B in body reference frame $\mathcal{F}_b\{B\}$

$\overline{v}_{B/A}^{(a)}$: Velocity vector of point P relative to B in fixed frame $\mathcal{F}_a\{A\}$

$\widetilde{\omega}_{b/a}$: Angular velocity cross product matrix of $\mathcal{F}_b\{B\}$ relative to fixed frame $\mathcal{F}_a\{A\}$

$\overline{r}_{M4/O}^{(0)}$: 4th marker position vector in world fixed frame $\mathcal{F}_0\{O\}$ global coordinates

$\overline{v}_{M4/O}^{(0)}$: 4th marker velocity vector in world fixed frame $\mathcal{F}_0\{O\}$ global coordinates

$\overline{a}_{M4/O}^{(0)}$: 4th marker acceleration vector in world fixed frame $\mathcal{F}_0\{O\}$ global coordinates

$\bar{a}^{(a)}_{P/A}$: Acceleration vector of point P with respect to point A in $\mathcal{F}_a\{A\}$

$\bar{a}^{(b)}_{P/B}$: Acceleration vector of point P with respect to point B in $\mathcal{F}_b\{B\}$

$\tilde{\alpha}_{b/a}$: Angular acceleration cross poduct matrix of $\mathcal{F}_b\{B\}$ relative to fixed frame $\mathcal{F}_a\{A\}$

$\bar{\omega}_{1/0}$: Angular velocity vector of Link-1 in world fixed frame $\mathcal{F}_0\{O\}$ global coordinates

$\bar{\alpha}_{1/0}$: Angular acceleration vector of Link-1 in world fixed frame $\mathcal{F}_0\{O\}$ global coordinates

$\bar{F}^{(0)}$: The resultant of the external forces vector in the world fixed frame coordinates

m : Total mass of the body

$\bar{L}^{(0)}$: Angular momentum vector of the body in the world fixed frame coordinates

$\bar{L}^{(b)}$: Angular momentum vector of the body in the body reference coordinates

$\hat{J}$: Mass Moment Matrix of the rigid body

$\bar{F}^{(0)}_{ji}$: Reaction force vector applied by Link-j exerted on Link-i in $\mathcal{F}_0\{O\}$ global coordinates

$m_i\bar{g}^{(0)}$: Weight of Link-i, in $\mathcal{F}_0\{O\}$ global coordinates

$\bar{M}^{(0)}_j$: Reaction moment vector exerted on Link-j, in $\mathcal{F}_0\{O\}$ global coordinates

$\bar{T}^{(0)}_k$: Joint Actuator Torque at Point k represented in $\mathcal{F}_0\{O\}$ global coordinates

$\hat{J}^{(0)}_i$: Inertia Matrix of Link-i in $\mathcal{F}_0\{O\}$ global coordinates

$\widetilde{AB}^{(0)}$: Cross product matrix of position vector from point A to point B in $\mathcal{F}_0\{O\}$ global coordinates

t_0 : Initial time value of all time intervals that the generated functions are valid

t_f : Final time value of all time intervals that the generated functions are valid

n_p : Number of piecewise polynomials

d_p : Degree of polynomials at each time interval

d_c : Degree of continuity at knot points

Δt : Equal time increment in $[t_0, t_f]$ interval

n_k : Number of knot points

A : Symbolic parameter matrix of coefficients of the continuous piecewise polynomials

f : column vector composed of each piecewise polynomial functions in whole time interval

$\dot{f}$: First derivative of each piecewise polynomial functions

$\ddot{f}$: Second derivative of each piecewise polynomial functions

f_{knots} : column vector of zeroth order function equality at knot points

$\dot{f}_{knots}$: column vector of first order function equality at knot points

$\ddot{f}_{knots}$: column vector of second order function equality at knot points

θ_0 : Zeroth order initial condition at t_0 for piecewise polynomial

$\dot{\theta}_0$: First order initial condition at t_0 for piecewise polynomial

$\ddot{\theta}_0$: Second order initial condition at t_0 for piecewise polynomial

θ_f : Zeroth order final condition at t_0 for piecewise polynomial

$\dot{\theta}_f$: First order final condition at t_0 for piecewise polynomial

$\ddot{\theta}_f$: Second order final condition at t_0 for piecewise polynomial

f_{eqn} : Column vector of zeroth order equalities of the piecewise polynomials at knot points

$\dot{f}_{eqn}$: Column vector of first order equalities of the piecewise polynomials at knot points

$\ddot{f}_{eqn}$: Column vector of second order equalities of the piecewise polynomials at knot points

C : Coefficient matrix

$\overline{a}$: Parameters vector

$\overline{b}$: Initial and Boundary conditions vector

C_{mod} : Modified coefficient matrix after column elimination

$\overline{a}_{mod}$: Modified parameters vector after column elimination

fps : Frame per second

J : Performance measure functional

w_i : Weighting factors of each joint torque squares

$\overline{a}_m$: Independent parameters vector (design parameters)

$h_i\ (\overline{a}_m)$: Equality constraints

$p_j(\overline{a}_m)$: Inequality constraints

$\overline{x}_{CG,rider}$: Center of gravity position of the rider along x-direction

$\overline{x}_{4th\ marker}$: Position of 4^{th} marker along x-direction

CHAPTER 1

INTRODUCTION

1.1 Aim of the Thesis Study

One of the objectives of this thesis study is to create a dynamic horse-rider model in the sagittal plane. The human body is modeled by link segments as a tree-type structure and each link represents a segment of a human body. The equations of motion are obtained in symbolic form by performing kinematic and dynamic analyses. The second objective of this study is to create continuous piecewise parametric polynomials to define each joint angle, angular velocity and angular acceleration by selected design parameters. Hence, the reaction forces and actuation torques at each joint can be represented via these design parameters.

Lastly, the third objective is to minimize a performance measure, subject to some constraints, for two case studies. An objective function is created as the sum of the squares of each joint actuation torque together with reaction forces and moments at the saddle-horse interaction interface. A nonlinear optimization solver available in MATLAB® is used to find the optimum design parameters which minimize the performance measure and also satisfy the constraints during the case studies.

1.2 Outline of the Thesis Study

In Chapter 2, a literature survey is conducted for the horse rider modeling studies. In Chapter 3, definitions of the natural horse gaits and horse riding equipment are given and the correct rider posture is discussed. Next, rider modeling studies are introduced in Chapter 4. After modeling the rider body, the kinematic analysis (position, velocity, acceleration analysis) and inverse dynamic analysis by Newton-Euler method is performed in Chapter 5. In Chapter 6, the continuous piecewise polynomial creation process, the performance measure used in the optimization problem and the constraints are mentioned. In Chapter 7, two case studies are presented and the discussions about the results obtained are given in Chapter 8. Conclusions and future work are presented in Chapter 9.

CHAPTER 2

LITERATURE SURVEY

2.1 Horse-Rider Studies

From the early years of history, horse riding has a significant influence on the civilization of humanity. With the improvements in horse riding, decreasing the travelling time and massive struggles at war results were seen as the obvious effects **[1]**. However, due to the technological development over the decades, today horse riding is a branch of sports. In literature, generally, veterinary departments are interested in horse and rider related studies and investigate the effects of rider on the horse with different experimental methods.

2.1.1 Loading on Horseback Applied by the Rider

Horse related studies are much more common in equestrian sports since the full performance is thought to be affected much more by the horse kinematics and kinetics, rather than the influence of the rider. It is believed that the only intervention of the rider is the total load on the horseback due to his/her weight.

In **[1]**, the forces acting on the saddle and COP (center of pressure) variability along transversal and longitudinal directions of the riders are examined during three stages of the trotting gait of the horse, namely: rising trot, sitting trot and two-point seat. For data collection, a pressure mat is placed under the saddle and measurements are carried out while the horse is on a treadmill. Overall effecting forces are directly calculated from the pressure mat measurements using the known area of the pressure mat. In addition, the moments and the overall forces in three directions are measured and then COP values of the rider are obtained. Next, comparisons are made between different horse gaits. This study shows that the maximum load applied on the back of

the horse occurs during rising trot. The load in sitting trot is lower and the minimum overall force is observed for the two-point seat position of the rider. Figure 2.1 shows the graphical representation of the overall force during one motion cycle **[1]**.

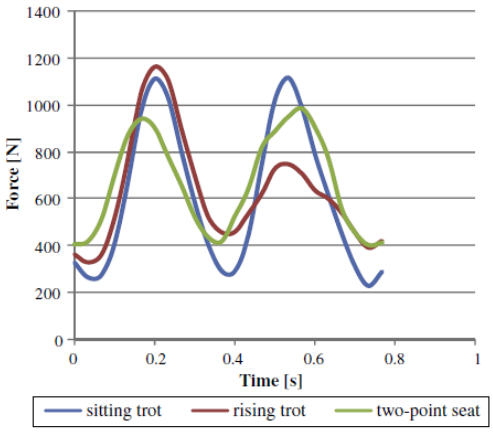

Figure 2.1 Overall forces during one motion cycle in all three stages of the trotting gait **[1]**

The forces applied by the rider on the horseback are vital especially in dressage. It is known that the difference in body orientation and the horizontal motion of the horses in dressage are influenced by the weight distribution, the position of the riders' leg and asymmetry between the leg forces of the rider. For this aim, in **[2]**, a pressure mat is used to obtain pressure measurements under the saddle and to calculate the vertical-lateral forces on the horseback during shoulder-in, traverse and straight on gaits of horses (see Figure 2.2).

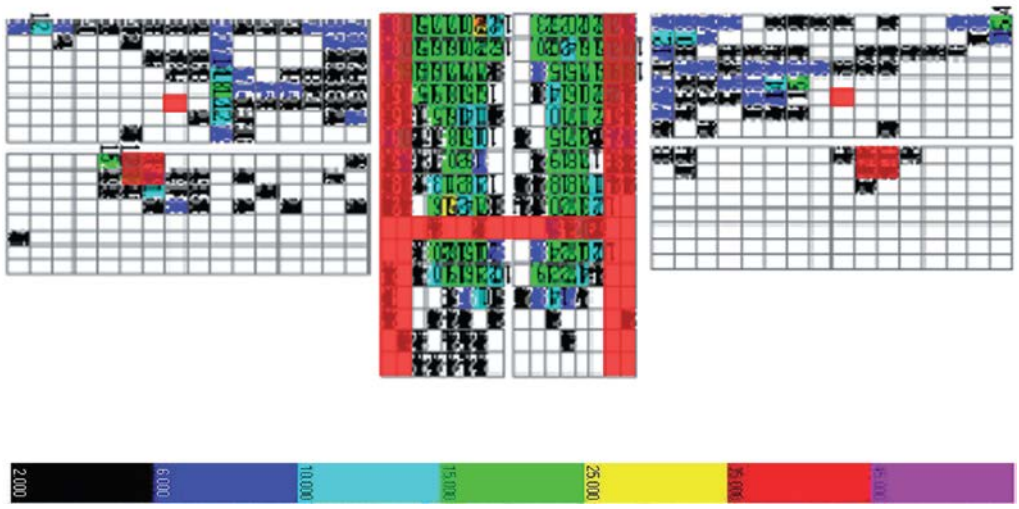

Figure 2.2 Three pressure mat measurements under left leg-saddle-right leg respectively from left to right (red areas are not considered for analysis and the rest shows the pressure values according to color scale) **[2]**

2.1.2 Horse-Rider Interaction

Although the forces exerted by the rider on the horseback are worth studying, another vital point is investigating the haptic interaction between the rider and the horse. In dressage, the horse's motion with the given music is evaluated by the jury considering the harmony between the horse and the rider. That harmony is created with the balance, the seat location on saddle and the weight distribution of the rider. In **[3]**, the relationship between some of the joint angles (hock and stifle) of dressage horses' and the riders' hip and knee angles are determined. Six reflective markers and a camera system (of two pan and tilt cameras), positioned in an indoor manage, are used for the data collection. Six reflective markers are placed at predefined positions on the horse's and the rider's right side limbs to observe the studied joint angles. The rider and the horse modeling are done in the sagittal plane.Figure-2.3 shows the positions of the reflective markers, the horse's stifle- hock angles and the rider's hip and knee angles **[3]**.

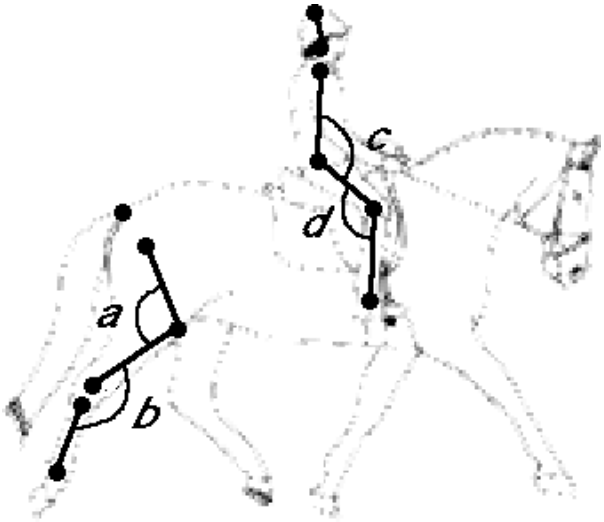

Figure 2.3 Horse and rider marker locations and the related joint angles (a=stifle, b=hock, c=hip, d=knee) **[3]**

As a result, it is observed that any angular change in the hip angle of the rider directly affects the stifle angle of the horse. So, there is a strong direct relationship between these two angles. On the other hand, this is not true for the relationship between the hip angle of the rider and the hock angle of the horse **[3]**.

Hence, it is clearly observed that horse kinematics is directly related with the angular change of the rider's limbs and the existence of the rider affects the horse motion. In **[4]**, the horse motion is compared during trot for the ridden and unridden cases. Also the saddle fitness effect is considered regarding the variability of the equine gait. Reflective markers are only attached along the spinal dorsal for the unridden case and two markers are used for the ridden case to collect the kinematic data. The data were collected from horses while they trot on a treadmill platform using a motion analysis system with six cameras. Three case studies are performed for each horse such as riding with a well-fitted saddle, riding with a non-fitted saddle and unridden cases. In Figure 2.4, the experiment set up and the locations of the reflective markers for the ridden and unridden cases are shown **[4]**.

In this study, the effect of saddle fitness on the horse gait is observed and it is found that a well–fitted saddle positively effects the interaction between the rider and the horse. A saddle that is not well fitted causes disturbances and irregularities in the motion of the horse **[4]**.

Figure 2.4 Experimental set up for ridden (A) and unridden (B) cases **[4]**

The rider has a controlling intervention of the horse motion and this is related with the experience level of the horse rider during the gait of the horse. In the article **[5]**, expert and inexperienced riders are compared while the horses are walking and trotting. The horse rider is modeled as a link-joint arrangement (see Figure 2.5) in the sagittal plane. Some of the joint angles are measured and compared for the expert and novice riders during a 24 week-exercise period. Three observations and data

collection processes are realized in the 0th, 12th and 24th weeks of the exercise period. The angles of the shoulder, elbow, hip; knee, ankle, and front-back angle have been measured from the sagittal plane. The left-right angles have been measured from the front plane and the data collection has been done with four digital camcorders, utilizing 21 round reflective markers attached on the rider's joints **[5]**.

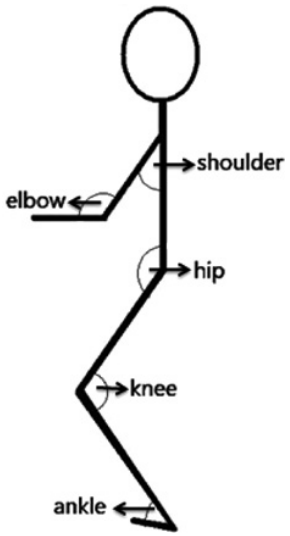

Figure 2.5 Relative angles of the rider **[5]**

During the walk gait, novice riders get closer to the posture of experienced riders as the exercise period lengthens. In the beginners group, the shoulder and the elbow angles get nearly close to the advanced rider posture at the end of the 24^{th} week exercise period. On the other hand, for a trotting horse, many angles of the beginners do not get similar to the ones of the advanced riders at the end of exercise period **[5]**.

Perturbations on the horse back are investigated in **[6]** for novice and expert riders while the horse is trotting. Oscillations about the vertical axis are further studied and statistically determined by using haptic information regarding the communication between the horse and the rider. Markers on the limbs of the horse and on the rider are used for data collection. Sphere-shaped reflective markers are used on the rider 's right side segments such as right shoulder, elbow, hand, hip, knee, heel and the tip of boot. The locations of the markers attached to the horse can be seen in Figure 2.6.

Six cameras are used for data collecting via markers placed on the right side of the rider's body **[6]**.

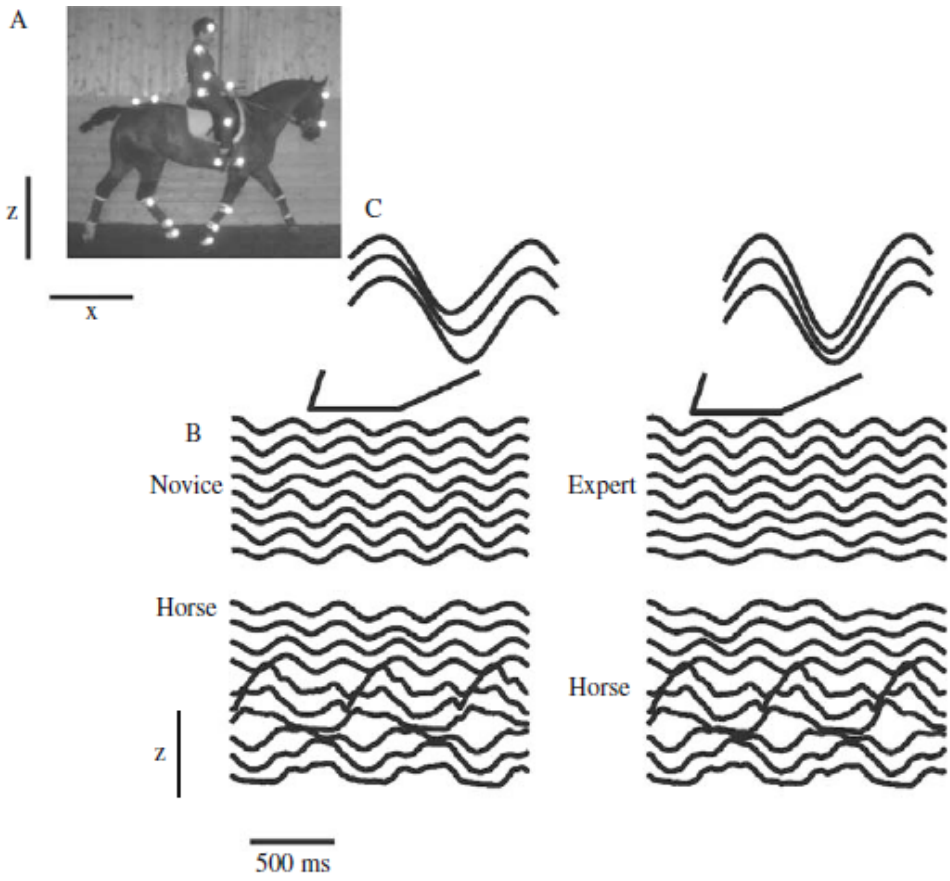

Figure 2.6 Locations of the reflective markers on the rider and the horse-Vertical perturbations of the novice and expert riders **[6]**

The haptic information is obtained from the reins, stirrups, saddle seat and the inside of the rider leg and the horse trunk. Novice riders cannot use this contact information and they hold a straight posture, this causes vertical disturbances on not only the horseback, but also on the rider seat. Advanced riders can locate their pelvis on the saddle deeply and correctly so that the rider can follow the motion of the horse. The harmony thus obtained prevents oscillations, leading to a comfortable ride **[6]**.

The fitness between the pelvis of the rider and the saddle has an influence on the harmony of the rider and the horse. So, the saddle type has an effect on the rider synchrony with the horse motion.

The aim in **[7]** is to describe a mathematical model for the horse–rider system and to present the angular differences of the limbs between side saddle and English saddle. To this purpose, PCA (Principal Component Analysis) is used for the three horse gaits namely, walk, trot and canter and these gaits are characterized by a few variables. By identifying the variables, the riding dynamics is studied via phase plots. Furthermore, two saddle types (Side saddle and English saddle) are compared. Motion has been recorded using the Expert Vision System with six video cameras (sample frequency 120 Hz). Fourteen markers (eleven markers attached to the horse and three markers attached to the rider's body) (see Figure 2.7) on the right-hand side of the horse has been used for the kinematical analysis.

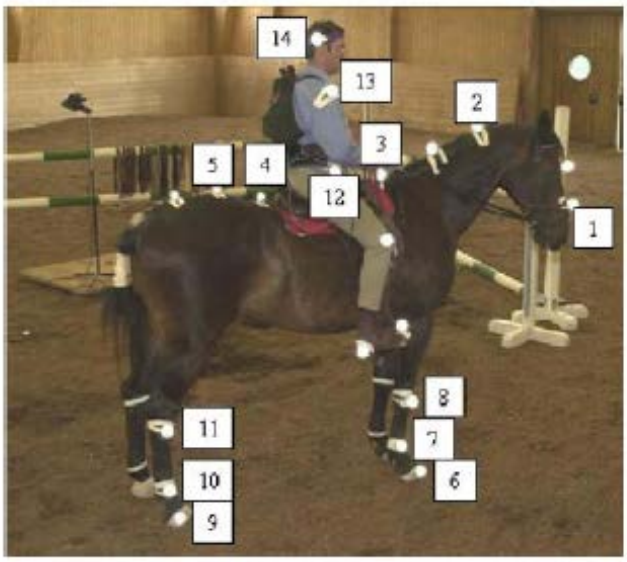

Figure 2.7 Location of the reflective markers on horse skin and rider body **[7]**

In the literature, saddle motion is generally investigated without the rider. In **[8]**, the aim is to express the movements of the saddle and the high-level dressage rider

together. The relationship between the horse and the rider movements at walk is a background a starting point to identify with the equine orthopedic injuries which are directly related to the contact on a saddle by the rider. Data collection is achieved on a high-speed treadmill platform (Mustang 2200) and spherical reflective markers are used on the horse, on the rider and the saddle. These markers are recorded by 12 infrared cameras (ProReflex). Seven high-level dressage horses with riders have walked on a treadmill and kinematic measurements have been taken**.** Angles associated with the rider arm and legs and the angles associated with the horse's trunk and neck are measured and incorporated into the rigid body model **[8]**.

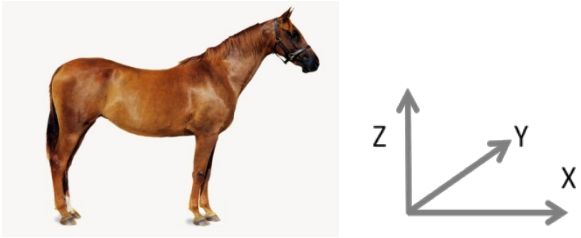

Figure 2.8 The coordinate system of the experiment

The coordinate system of the experiment system is constructed by considering the X-axis to be horizontal and along the direction of translational motion. Y-axis is on the horizontal plane and positive along the left directon and the Z-axis to be vertical and positive upwards (see Figure 2.8). For defining the rider position and angular orientation (roll, pitch and yaw angles) in the XZ, YZ and XY – planes, these markers are used for data processing of the angles such as saddle roll, rider pelvis pitch and rider upper body yaw **[8]**.

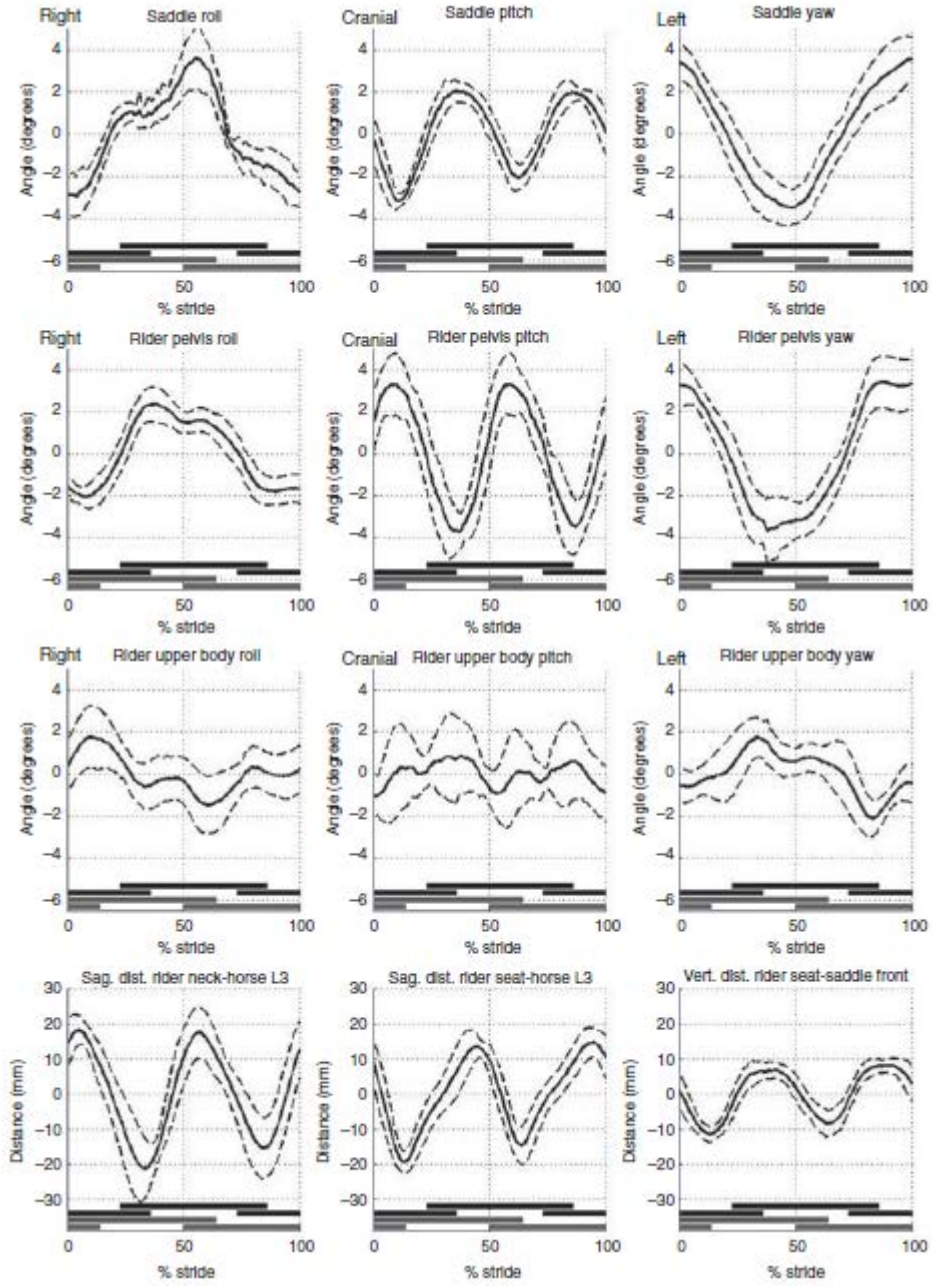

Figure 2.9 Stride cycles for the related defined angles **[8]**

From this study, it is observed that the yaw and pitch angles of the rider and the saddle are mostly related with the movement of the hind limbs of the horse. However, the roll angle is affected by the forelimbs of the horse during the stance of the walk gait **[8]**.

In order to improve the performance of the riders, the main differences in posture should be investigated for different experience levels. In **[9]**, the aim is to observe some defined angles of the rider upper and lower limbs (such as hip, knee, upper arm, trunk, thigh and lower leg (see Figure 2.10)) for levels of experience such as beginner, intermediate and advanced. In this study, walk, posting trot and sitting trot gaits are considered. The analysis is done by a high speed camera system (Motion Analysis Corporation) and reflective markers are located on the left limbs of the rider in the sagittal plane **[9]**.

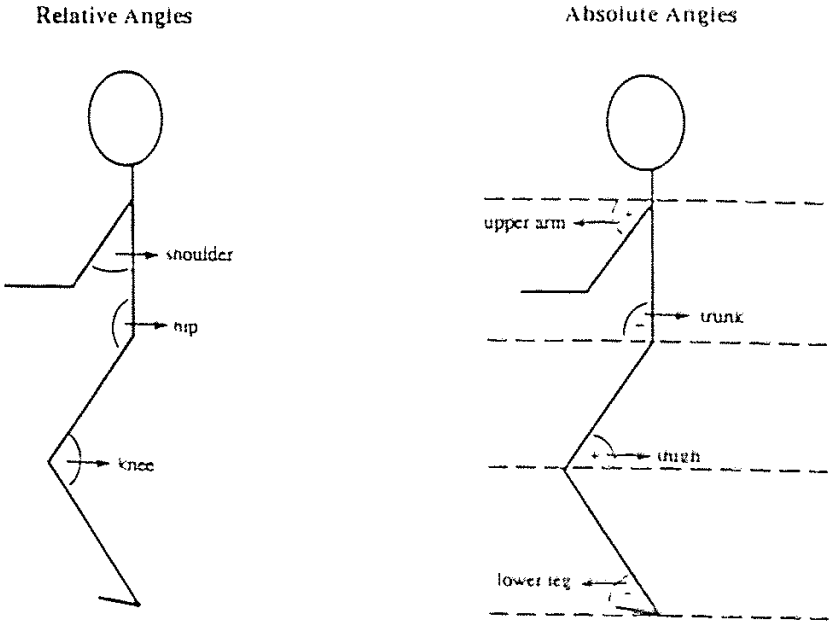

Figure 2.10 Relative and absolute angles of the rider model **[9]**

According to the level of the riders (beginner, intermediate, advanced), the absolute angles of trunk, thigh and upper arm differ; on the other hand, the relative angle of the knee is not related to the experience level of the rider **[9]**.

The rider seat position has a great influence on the kinematics of the rider and the horse. This kinematics is also related with the symmetry of the rider along the longitudinal and transverse directions on horseback. In **[10]**, the authors studied rider asymmetry by considering the axial rotation of the rider (AR), shoulder angle displacement (SAD) and leg length inequality (LLI) in order to find a relationship

between them. Two camera-video systems obtained images from the sagittal and transverse planes during the horses' walk, trot, right and left canter gaits. At the end, it has been observed that rider posture shows an asymmetry during the gaits (especially, the right shoulder range of motion varies a lot (see Figure 2.11)) **[10]**.

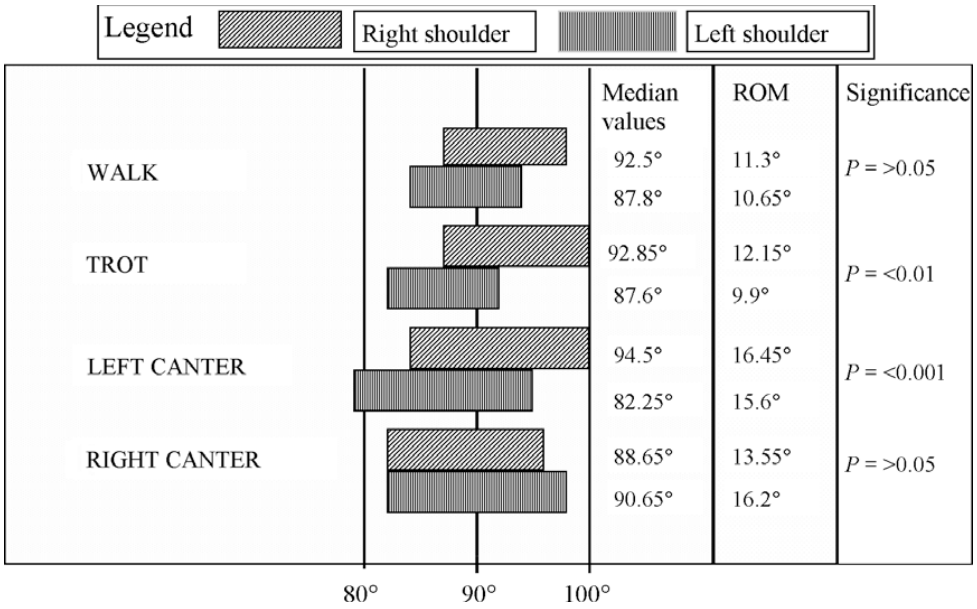

Figure 2.11 Left and right shoulder displacement in each gait **[10]**

According to various horse-rider studies in the literature, it is observed that many parameters that affect the performance of the rider also affect the performance of the horse. These open problems in that field of study are generally as saddle effect on riding (saddle design and saddle fit), rider-related factors on horse performance (rider experience and skill levels, rider bodyweight distribution and the rider's center of mass on horseback, the rider's influence on head and neck position of the horse) and horse-related factors (asymmetry of movement of horse during riding) **[11]**.

2.2 Similar Rider Modeling Studies in Other Sport Branches

The rider modeling approach in **[12]**, is quite different than the others. Wobbling masses are considered in order to take into account the rider comfort. The passive posture maintenance and the active motion generation actuators have to be

implemented at each joint of the human body model. The torque values, which are acting between the two coupling points at the segments, have been calculated.

Human modeling is achieved by considering wobbling masses to add flexibility to the limbs of the human model link segments which make a more realistic approach for the practical cases and simulation results. For horse riders, this human modeling can also be used and wobbling masses may be added in order to relax the rigidity assumption **[12]**.

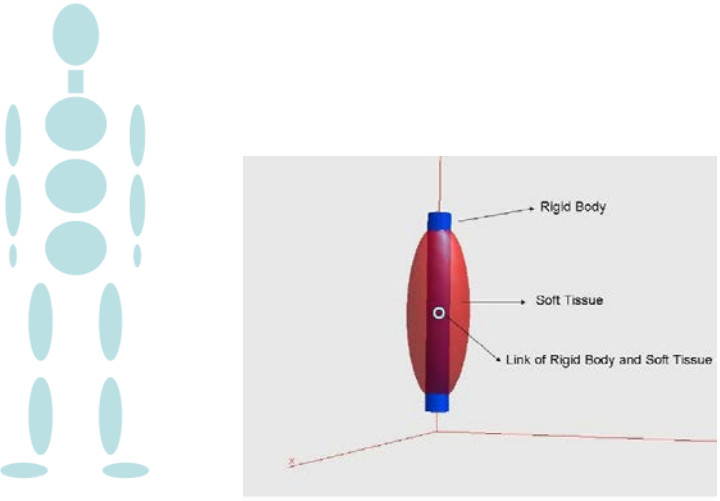

Figure 2.12 Human modeling with 17 segments and wobbling mass model **[12]**

Human body model is developed by using a seventeen segments which are foot, shank, thigh for two legs ; hand, forearm, upper arm for two arms; three portioned trunk and neck, head.**[13]**. To control the steering of handlebars, active joint torque actuation is needed for shoulders and elbows; on the other hand, the lower segments, trunk, neck and head are controlled passively. **[13]**.

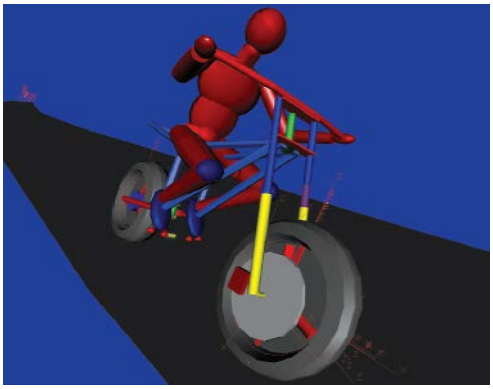

Figure 2.13 Steering through a crossover road track **[13]**

CHAPTER 3

RIDING CONCEPTS

3.1 Natural Horse Gaits

3.1.1 Walk

Walk is one of the natural gaits which have a four-beat sequence. The sequences of the beats are shown in Figure 3.1 and Figure 3.2.It is a lateral gait and each beat can be heard easily. Walk is the slowest natural gait and the average speed is 5-7 km/h. During walking, Beat-1: right hind leg, Beat-2: right front leg, Beat-3: Left hind leg, Beat-4: left front leg (see Figure 3.2). At the walk, the horse always has one foot raised and the other three feet on the ground **[14]**.

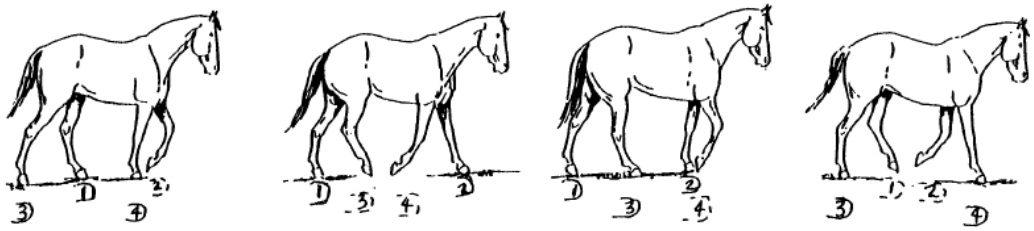

Figure 3.1 Horse's four beats of the walk gait **[15]**

Figure 3.2 Four-beat sequences of the hooves

During the walking gait of the horse, the weight distribution of the horse is carried by one foot to another one during sequences of the hooves. Due to that reason, the rider feels a side-to-side motion in lateral direction on horseback. Since the horse transmits its center of mass from one point to another while changing the sequence of its beat, this causes joggling for the rider.

3.1.2 Trot

The trot is a two-beat diagonal gait. The right hind and left front legs move together, and the left hind and right front legs move together. The red diagonal legs represent right front leg and left hind leg and right front and left hind leg that move together during gait (see Figure 3.3). Since the horse uses its diagonal legs for each beat, that causes a more stable motion and also more comfort for the rider. In trotting, there are two types of riding techniques, one is sitting trot and the other is posting trot.

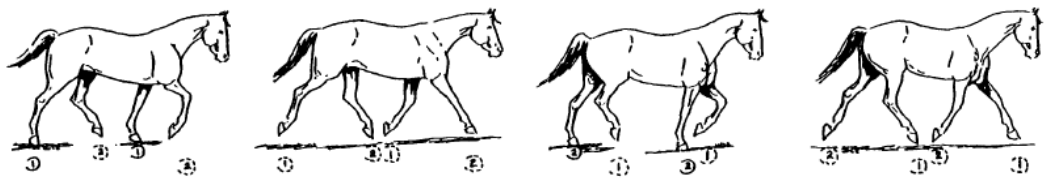

Figure 3.3 Horse's two diagonal beats of the trot gait **[15]**

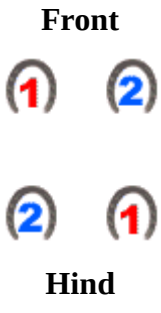

Figure 3.4 Two-beat sequences of the hooves

Although, sitting trot is hard for the rider, this position provides optimum control. The sitting trot makes the rider to follow the movement of the horse by his/her abdomen and pelvis, so that work performance is achieved by most of lumbar spine and pelvis of the rider. The upper extremities such as the shoulder, upper arm, elbow, forearm and hands keep their position during riding. On the other hand; for the posting trot, the rider makes an up-down movement on the horseback while first diagonal beat rising phase occurs and during the second one, rider sits on saddle. If posting is applied correctly, riding comfort can be achieved for both the rider and the horse. Trotting is faster than the walk gait and the average speed of it is generally 8-10 km/h.

3.1.3 Canter

This natural gait is a three-beat gait and the sequences of the hooves are shown in Figure 3.5 and Figure 3.6. The average speed of cantering is 16-27 km/h. Figure 3.6a shows the left-lead canter where the first beat starts with the left hind leg and the right-lead canter sequence is indicated in Figure 3.6b. For the right-lead, canter starts with grounding the first beat with the left hind leg and the second beat continue with the right hind and left front beat together (see Figure 3.5). The last beat is the grounding phase of the right front leg. For the left-lead, canter begins with first beat of the right hind leg and second one follows as left hind and right front leg simultaneously and finished by the third beat as grounding of left front leg (see Figure 3.6).

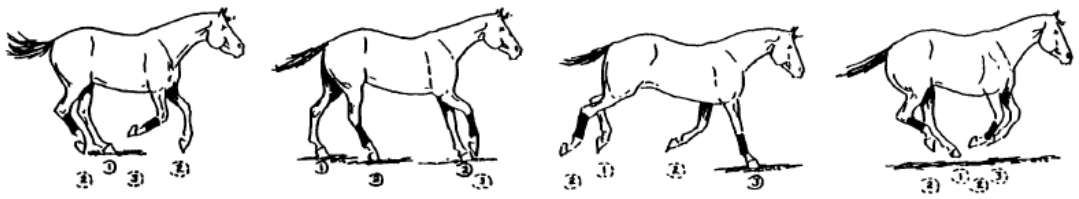

Figure 3.5 Horse's three-beat gait sequence during cantering-Right Lead **[15]**

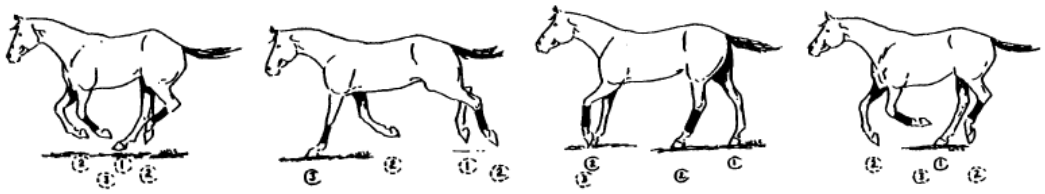

Figure 3.6 Horse's three-beat gait sequence during cantering-Left Lead **[15]**

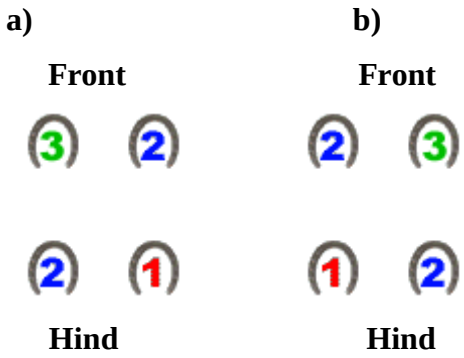

Figure 3.7 Three-beat sequence of hooves a) Left-Lead Canter b) Right-Lead Canter

In cantering, the rider should follow the rhythm of the horse by an up and down motion as well as a back-forth swing. Although the lower extremity of the rider, such as the thigh, calf and foot remain nearly still, the upper extremity; hip, abdomen, trunk, shoulder and arms of the rider are in synchrony with the horse's three beat.

3.2 Equipment of the Horse and the Rider

Riding equipment consists of many subparts and some of them are shown in Figure 3.8. Riding equipment may be divided into two main groups, namely the saddle and the bridle. The saddle group includes the stirrup leather/iron, girth, flap, skirt, seat, pommel, cantle and pad. The bridle group consists of the headpiece, head band/noseband, straps, snaffle/curb bit, snaffle/curb rein.

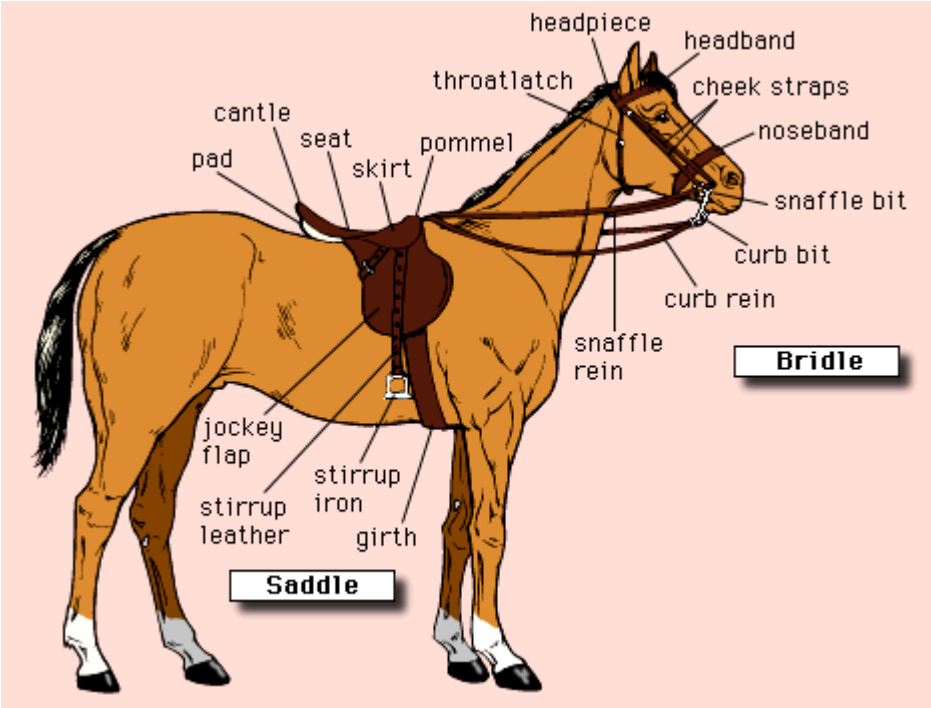

Figure 3.8 Riding equipment of the horse **[16]**

3.2.1 Saddle

Saddle is the most important part of the riding equipment since most of the haptic information is transmitted via the saddle. According to the riding style and the purpose of the riding, the saddles vary in type. The most vital point is the proper selection of the saddle according to the rider and the fitness of it to the horse body.

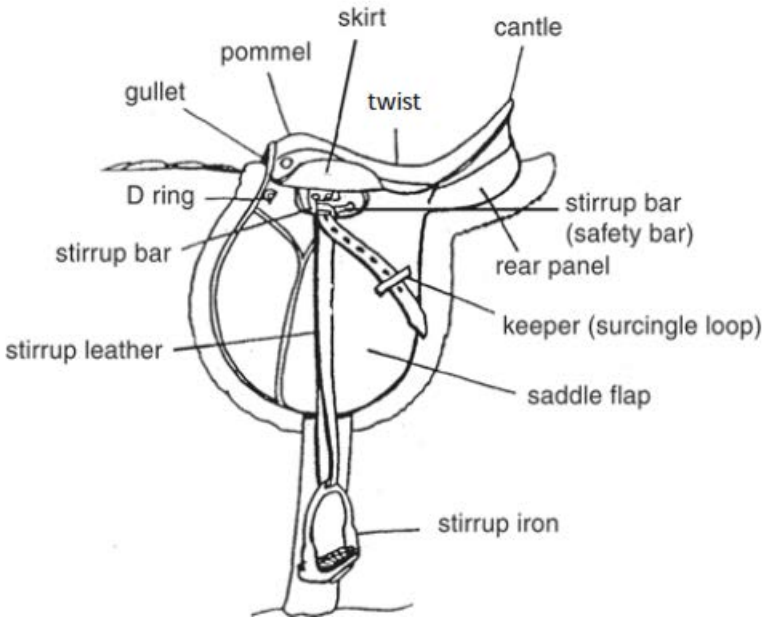

Figure 3.9 Detailed description of an English saddle **[15]**

As English saddle is shown in Figure 3.9, cantle is the back of the saddle and the level of it is a bit higher for preventing the rider to move back and lose the position of the seat during riding. Twist is the deep curvature which allows the rider to locate his/her hip at the correct position. The pommel is the front part of the seat. The rider should feel that his/her hip (pelvis) is as if it is “in” the saddle, not “on” the saddle. That is the critical point for the correct location of the rider on horseback.

i) Stirrup Leather/Iron:

Stirrups are attached to the saddle with stirrup leathers and are used for holding the rider foot to adapt and control the movement of the horse. In Figure 3.10, some stirrup types are shown. The stirrup leather is adjustable according to the rider leg length.

Figure 3.10 Stirrup types **[15]**

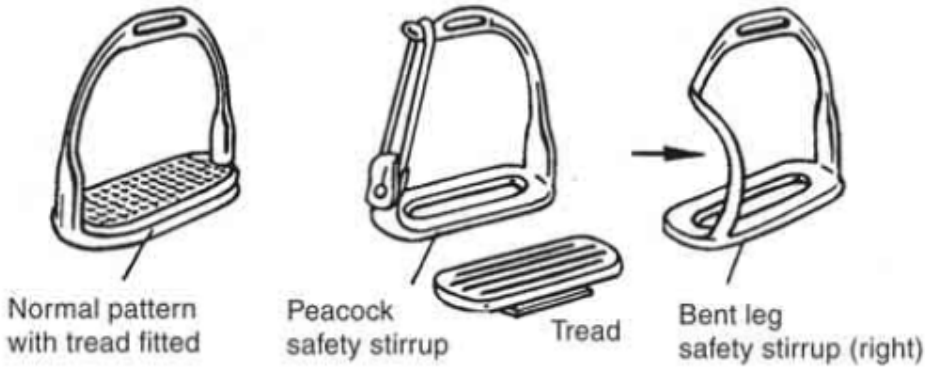

Figure 3.11 Stirrup irons **[15]**

It should be noted that the location of the foot on the stirrup is vital and the friction between the threaded pattern and the rider's boots is considerable for preventing falling off from the horseback (see Figure 3.11).

3.2.2 Bridle

Bridle is the equipment related to the head of the horse and consists of the headband, noseband, cheek piece, snaffle bit and reins (see Figure 3.12). These elements provide control of the horse head by the rider in order to manipulate the horse movement according to the rider's will.

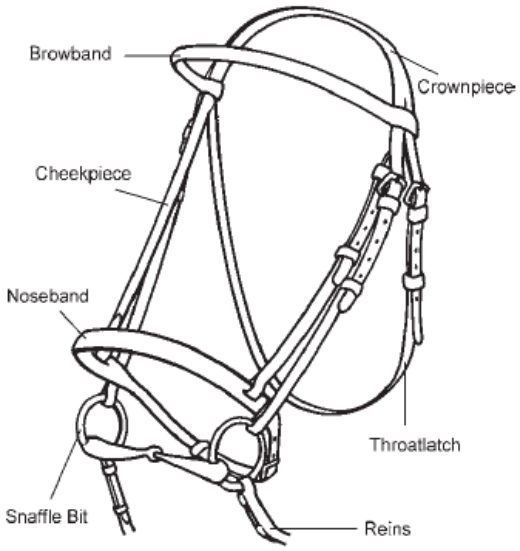

Figure 3.12 Detailed description of an English bridle **[15]**

There are many types of sniffle bits and reins are attached to that element which passes through the horse mouth.

i) Rein:

Control of the horse movement is achieved by the help of reins. It provides contact information from the mouth of the horse to the rider's hand. Depending upon the riding style, there are many types of reins.

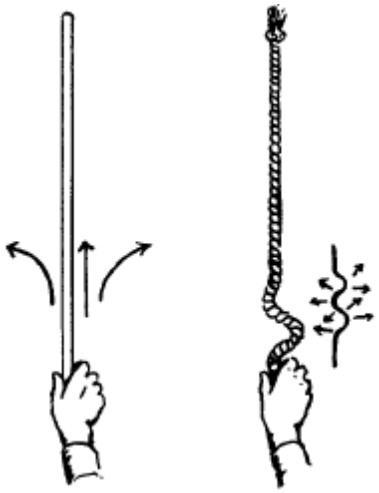

Figure 3.13 The handling of a stick and a rein rope **[15]**

As shown in Figure 3.13, it should be always remembered that the rein behaves as a rope not a stick, i.e., it should be only in tension in order to control the horse movement.

3.3 Rider Posture on Horseback

During riding, the control of the horse movement depends on the information sent by the rider to the horse. The rider's weight distribution, balance, center of mass, rein tension, stirrup tension, inside leg pressure are significant parameters that affect a good posture.

As shown in Figure 3.14, the rider's correct alignment is described by two main direction lines. The first line passes through the ear, shoulder, hip and heel. The second line passes through the elbow, forearm, wrist, hand, rein and the horse's mouth.

Figure 3.14 Rider's correct posture and alignment lines **[17]**

For correct posturing, there are some concerns for the alignment and location of certain limbs, such as pelvis/hip, thigh, abdomen/trunk and elbow/wrist/hand.

3.3.1 Pelvis

During riding, the rider posture on horseback is the key point for balance, safety and good performance. Pelvis orientation is an important consideration for making the rider's center of mass closer to the horse mass center. As shown in Figure 3.15, in photo-3 the rider pelvis orientation is backward more like sitting on a chair that is not safe. This relax position makes the rider lose control easily. In photo-4, pelvis orientation is forward which is a common mistake is during riding. This orientation causes extra loading on the lumbar spine in the waist region of the rider body. On the other hand, in Figure 3.16, it can be seen that the correct pelvis orientation is the vertical (neutral) position. The neutral position keeps the rider straight and in control during riding.

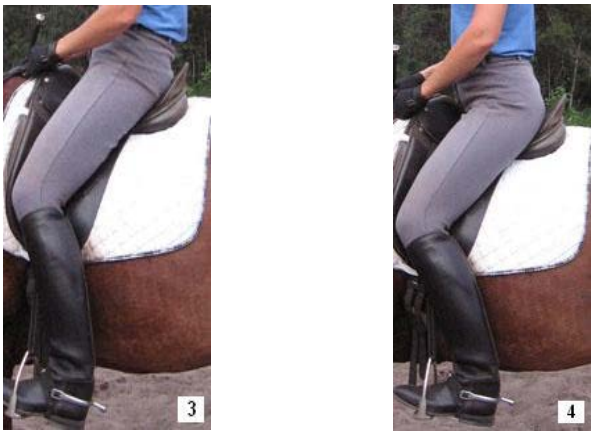

Figure 3.15 Pelvis backward rotation (3) and forward rotation (4) **[18]**

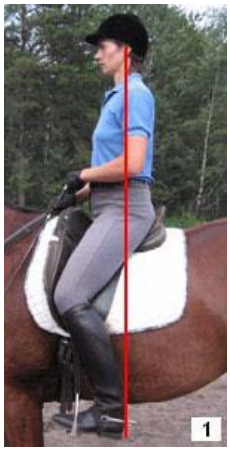

Figure 3.16 Correct posture for pelvis of the rider (neutral position) **[18]**

3.3.2 Thigh

In relation with the pelvis orientation, thigh position at each side of the horse body is a way of controlling the horse's abdomen and energy along the movement direction. If the rider grasps the horse abdomen with his/her thighs, it is an effective way of gaining awareness of the horse motion and forwarding the appropriate signals in order to direct the movement according to rider's will. If the pelvis rotation is backward, the knee is along the outward direction and the thighs don't cover the horse abdomen enough (see Figure 3.17). This orientation of the rider body creates a risk.

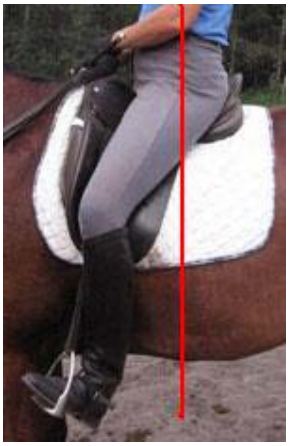

Figure 3.17 Rider's wrong thigh position **[18]**

In Figure 3.18, the pelvis orientation is in the neutral position, as a consequence the knee is inward and the thigh wraps the horse abdomen region well. The correct posture shown (satisfying the red line alignment) in the figure creates a vital interaction between the rider body and the horse body.

Figure 3.18 Rider's correct thigh position **[18]**

3.3.3 Trunk and Abdomen

The upper extremity's posture on horseback is mostly significant for preventing rider injuries. In Figure 3.19, in photo-2 and photo-3, the rider pelvis is rotated backward and forward respectively. Furthermore, the abdomen is compressed and the shoulders

turn inward. In these two situations, the rider's spine is forced to carry an extra loading, especially in lumbar region. Although these two alignments seem like a relaxed position, it is even more tiring (not only for the rider, but also for the horse).

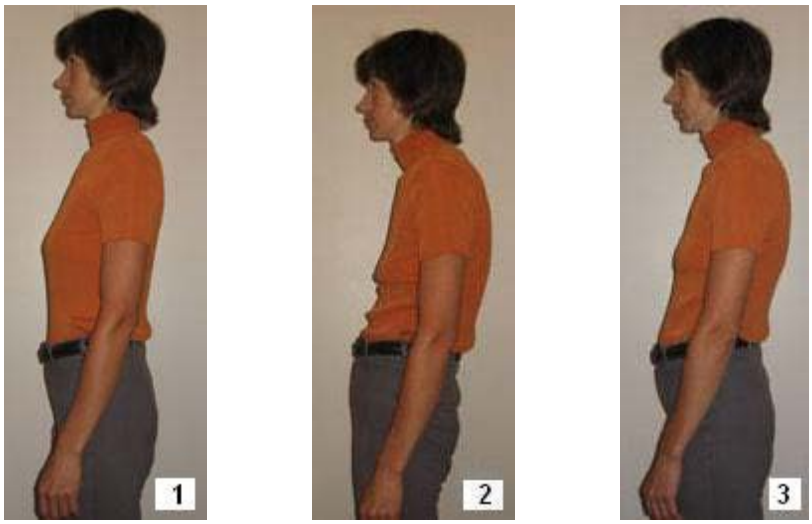

Figure 3.19 Posture of the abdomen/trunk of the rider **[18]**

In Figure 3.19 photo-1, on the other hand, the correct posture for the trunk and abdomen of the rider body can be seen. In this correct posture, the pelvis orientation is neutral, and the shoulders are straight and relaxed. If the rider sits in the saddle with this trunk posture, balance can be kept easily and extra energy consumption of the rider and the horse can be prevented.

Figure 3.20 Correct posture of the rider's abdomen/trunk **[18]**

3.3.4 Elbow, Wrist and Hand

After having a correct posture for the pelvis, abdomen/trunk and thigh, the last adjustment should be realized regarding the elbow-wrist-hand configuration (see Figure 3.21).

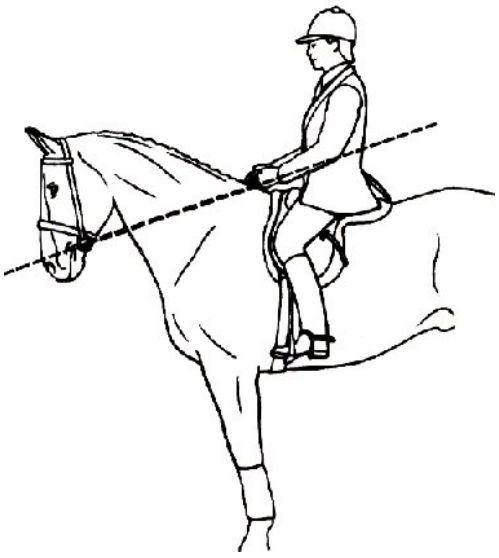

Figure 3.21 Correct alignment directions for elbow/lower arm/wrist/hand/rein **[19]**

The position of the rider hand should be below the waist region of the rider body and at the top of the withers of the horse. Hands should be in front of the saddle and this region causes a safe area for good control of the reins coming from the mouth of the horse. If the rider moves his/her hand forward or backward, this makes his/her center of mass to move forward or backward and cause a loss of balance. In addition to that, grasping the rein is important for feeling the horse mouth easily and directing during riding and one of the methods, 3-in-1 Method, is shown in Figure 3.22.

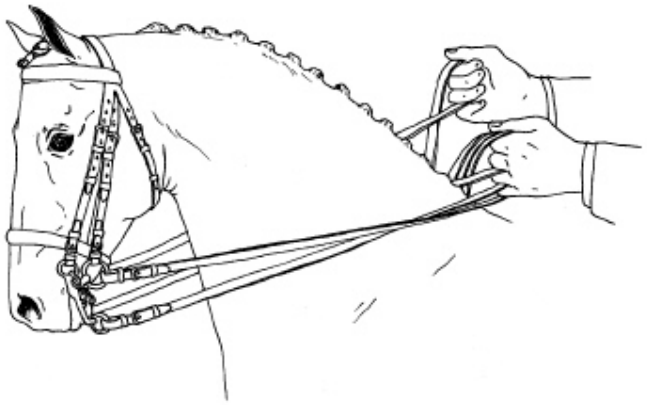

Figure 3.22 Double bridle reins - 3 in 1 method **[20]**

CHAPTER 4

RIDER MODELING STUDY

4.1 Segmentation of Human Body

Segmentation of the human body is significant for the biomechanics of human motion. Better formulations can be done via reliable physical models with the help of human body segmentation. In literature, the human body is defined by three anatomical planes and six directions. As shown in Figure 4.1, the transverse plane divides the human body into the upper and lower extremities. The frontal plane separates the body into front and back and lastly the mid-sagittal plane (sagittal plane) goes through the body by separating the left and the right limbs. The Cartesian coordinate system used is shown in Figure 4.1. Along the x-axis, anterior and posterior directions refer to the front and back directions, respectively. Along the y-axis, the left and right sides are defined as the lateral directions and lastly the upper extremities are along the superior direction on the z-axis, whereas the lower extremities are along the interior one. These planes and directions are commonly used for the biomechanical modeling studies of the human body. In this study the body is assumed to be bilaterally symmetrical **[21]**. In the rider modeling study, medium-size male aviator anthropometric data is used in the kinematic and inverse dynamic analyses **[21]**.

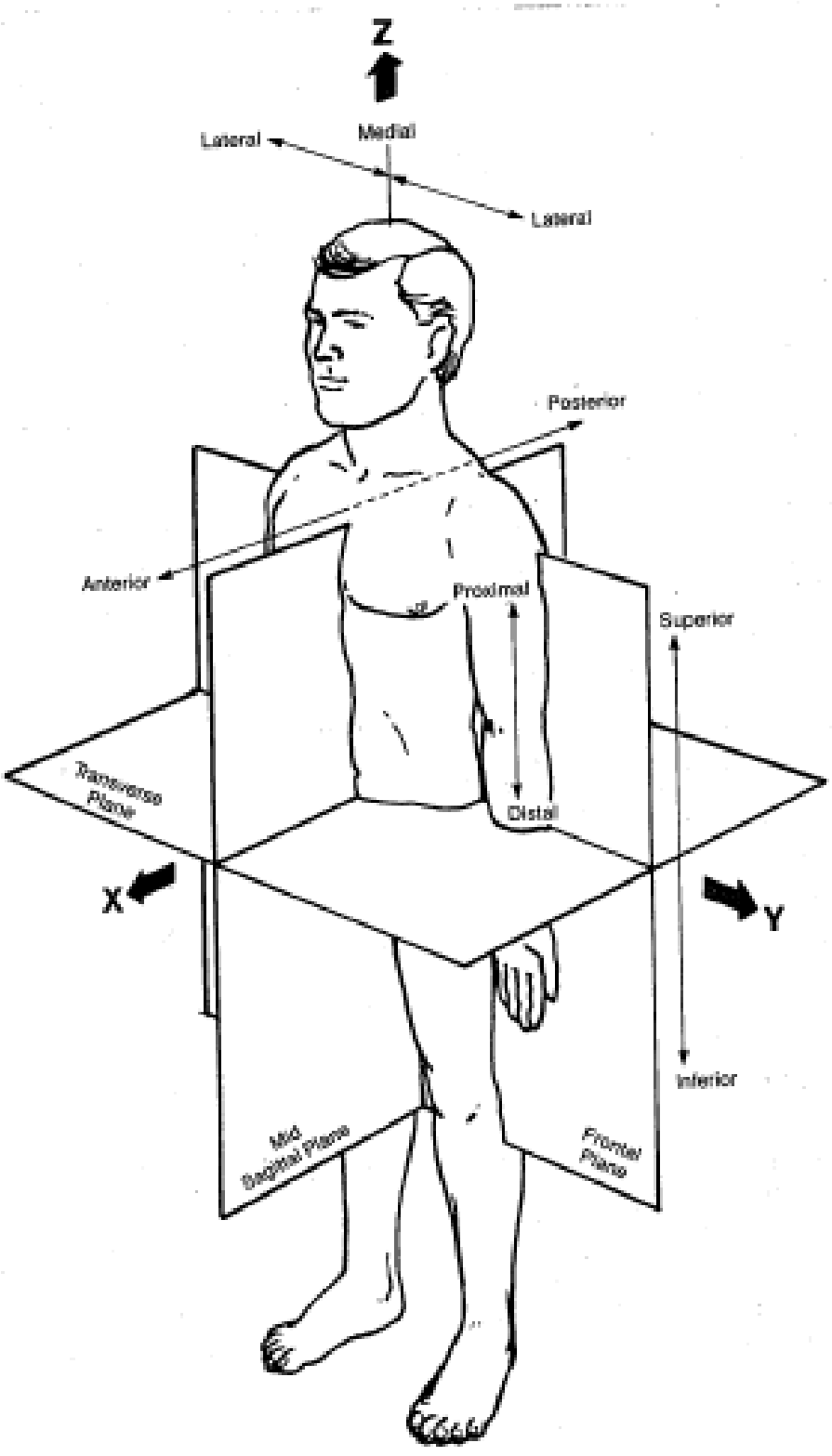

Figure 4.1 Anatomical planes and directions of human body **[21]**

Human body segmentation is defined by 10 anatomical planes (see Figure 4.2) which are listed in Table 4.1. The definitions of the limbs are given below.

i. above Plane-1: Head
ii. between Plane-1 and Plane-2 : Neck
iii. between Plane-2 and Plane-3 : Thorax
iv. between Plane-3 and Plane-4 : Abdomen
v. between Plane-4 and Plane-5 : Hip/Pelvis
vi. between Plane-5 and Plane-6 : Thigh
vii. between Plane-6 and Plane-7 : Shank
viii. limb below Plane-7: Foot
ix. between Plane-8 and Plane-9 : Upper arm
x. between Plane-9 and Plane-10 : Fore arm
xi. limb below Plane-10: Hand

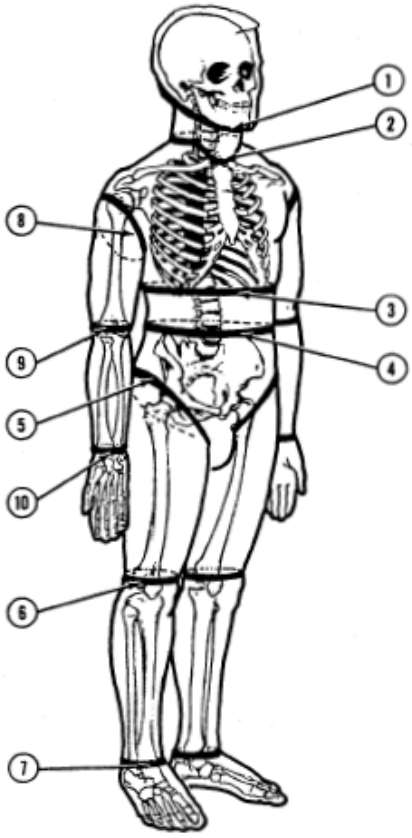

Figure 4.2 Planes of body segmentation **[21]**

Table 4.1 Segmentation Planes **[21]**

Head Plane	**1**
Neck Plane	**2**
Thorax Plane	**3**
Abdominal Plane	**4**
Hip Plane	**5**
Knee Plane	**6**
Wrist Plane	**7**
Shoulder Plane	**8**
Elbow Plane	**9**
Wrist Plane	**10**

4.2 Anthropometric Data

The mass, center of mass locations, dimensions of the limbs and inertia values, obtained from **[21]**, are given in the Appendix. The center of mass locations of each limb is on the symmetry axis. In addition, the center of mass of each body segments is assumed to be the same both in the standing and sitting positions of the human body. Hence, the anthropometric data can be implemented directly while the rider is in the sitting position.

4.2.1 Geometry

The dimensions of each limb such as length, perimeter, diameter and also joint locations are listed in the Appendix. The distances between the center of mass and joint locations of each limb are calculated based on the medium-size male aviator data in order to be implemented in the kinematic and inverse dynamic analyses.

4.2.2 Center of Mass

When it is looked at the sagittal plane of the human body in the standing position, the center of masses of each limb are on the same vertical line and they are all on the symmetric according to z-axis.

4.2.3 Mass

Mass distributions of each limb are calculated via regression analyses **[21]** and all values of the medium-size male aviator are listed in Appendix.

4.2.4 Inertia

Inertia values according to the principal reference frames are given **[21]** however these matrices are subjected to rotation due to the different orientation of body-fixed frames of each link of the kinematical model.

4.3 Kinematic Model

Horse rider studies are usually realized by the help of reflective markers located on the joints of the rider and the horse. The motions of the rider and the horse are recorded by video cameras during different gaits. Image processing is utilized to obtain the kinematic data in order to compare the performances of different riders and horses.

In this study, a kinematic rider model is proposed in order to determine the joint reaction forces and joint torques associated with the rider.

The horse rider is modeled in the sagittal plane as link segments (rigid bodies) which represent the limbs of the human body. The links are connected to each other by revolute joints (see Figure 4.3). The multi-segmented human body is a tree-type structure that is modeled as planar in this study. The rider model is divided into two sub-regions, namely, the upper extremity and the lower extremity.

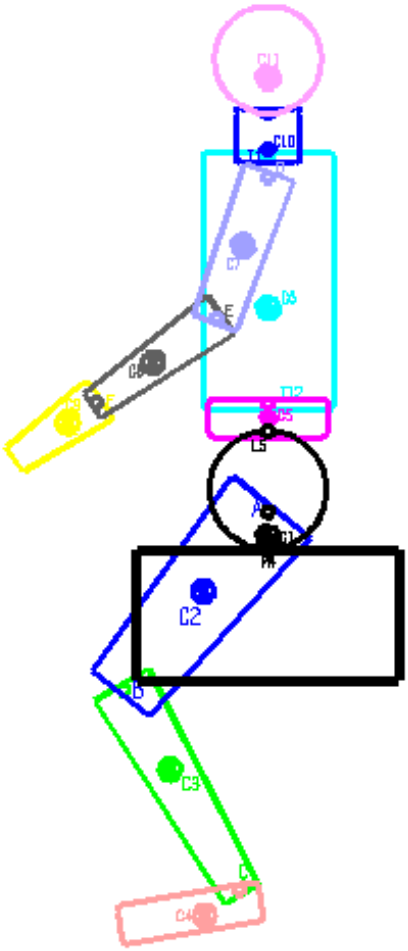

Figure 4.3 Rider model represented by 11 body links

4.3.1 Lower Extremity and Saddle

Lower extremity of the rider model consists of the hip-saddle, thigh, shank and foot. Here, it should be noted that during the three gaits, i.e., walk, trot and canter, it is assumed that the rider's hip never loses contact with the saddle. It should be recalled that, in the rising trot, the rider's hip and saddle contact instantaneously only. In contrast to the rising trot, during the sitting trot, the rider's hip and the saddle is always in contact. Since only sitting trot is investigated in this study, it is assumed that the hip and the saddle is a single body, namely Link-1.The thigh, or the upper leg, is labelled as Link-2. All of the revolute joints have their rotational freedoms about the body fixed frames' $\mathbf{u}_3^i$ axes. Link-3 represents the shank, or lower leg, of

the body and the foot is labelled as Link-4. All links are assumed to be symmetrical with respect to their own longitudinal, since this is a realistic and popular assumption. As seen in Figure 4.4, the origin of the body-fixed reference frames of each link is located at the joint center and $\mathbf{u}_1^{\,i}$ axis is always along the symmetry axis. Furthermore, $\mathbf{u}_2^{\,i}$ is perpendicular to $\mathbf{u}_1^{\,i}$ and $\mathbf{u}_3^{\,i}$ comes out of the plane.

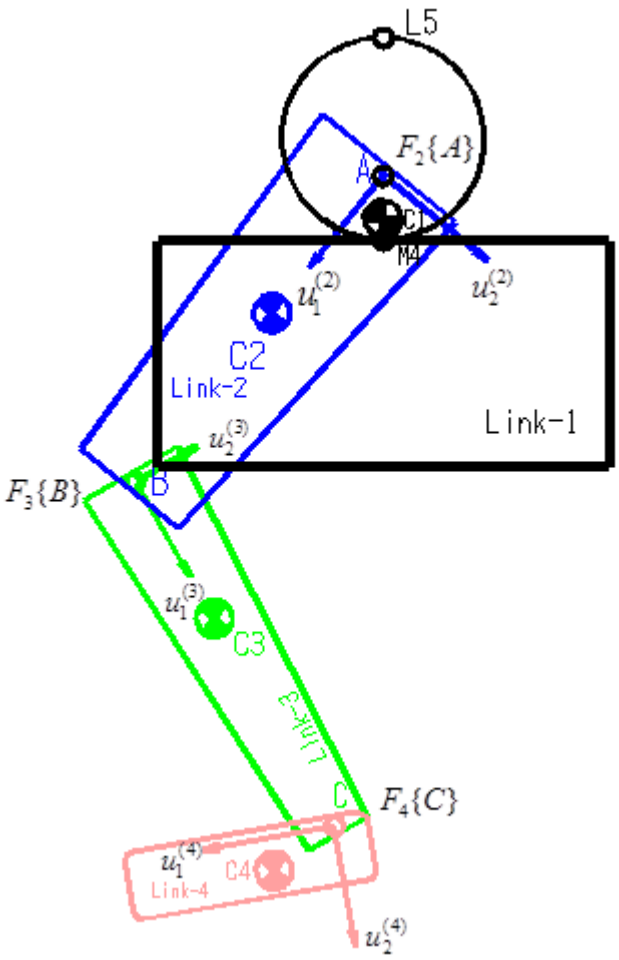

Figure 4.4 Lower extremity of rider model

The center of mass of links 1, 2, 3 and 4 are indicated by C_1, C_2, C_3 and C_4 . The revolute joints are indicated by A (hip joint/pivot), B (knee), C (ankle) and L_5 (abdomen-pelvis pivot). For Link-1, which is a composite body consisting of the hip and the saddle, the center of mass is calculated by assuming that the saddle geometry as a rectangle. As seen in Figure 4.5, M_4 represents the fourth marker, the kinematic

data of which is obtained in a previous study **[22]**. The marker M_4, hip pivot A, center of mass C_1, and the abdomen-pelvis pivot L_5 are on the same vertical symmetry axis **[21]**.

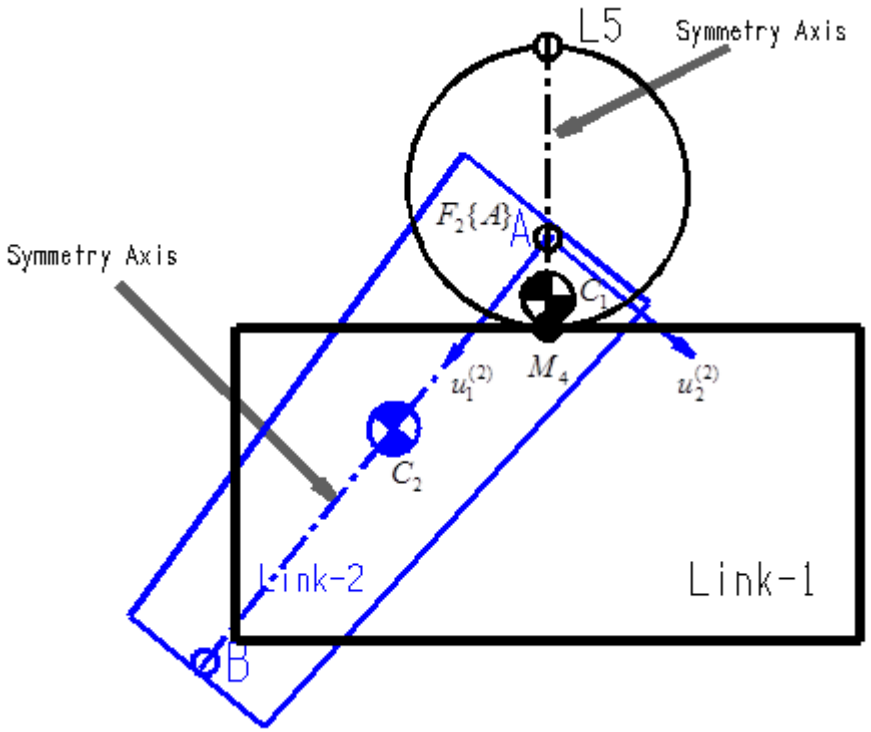

Figure 4.5 CM locations on symmetry axis of each links such as Link-1 and Link-2

4.3.2 Upper Extremity

The upper extremity of the rider body consists of the abdomen, trunk, upper arm, lower arm, hand, neck and head. Starting from the bottom, Link-5 is the abdomen segment; Link-6 is the trunk segment. Furthermore, Link-7, Link-8 and Link-9 represent the upper arm, the lower arm and the hand respectively. Link-10 and Link-11 refer to the neck and the head. These limbs (links) are connected to each other by single-dof revolute joints which are at the points L5 (abdomen-pelvis pivot/5th lumbar vertebrae), T12 (trunk-abdomen pivot/12th trunk vertebrae), D (shoulder pivot), E (elbow), F (wrist), T1 (neck-trunk pivot) and CS1 (head-neck pivot). The origins of the body-fixed reference frames are located at these points and the $\mathbf{u}_1^{\,i}$ axis

is always along the symmetry axis direction. Additionally, $\mathbf{u}_2^i$ axis is perpendicular to the $\mathbf{u}_1^i$ axis and $\mathbf{u}_3^i$ comes out of the plane. The center of masses of the limbs are labelled as C_5, C_6, C_7, C_8, C_9, C_{10} and C_{11} are also along the symmetry axis of each link also providing that L5, C_6 and T1 are all on the same symmetry line. All of these details are drawn in Figure 4.6

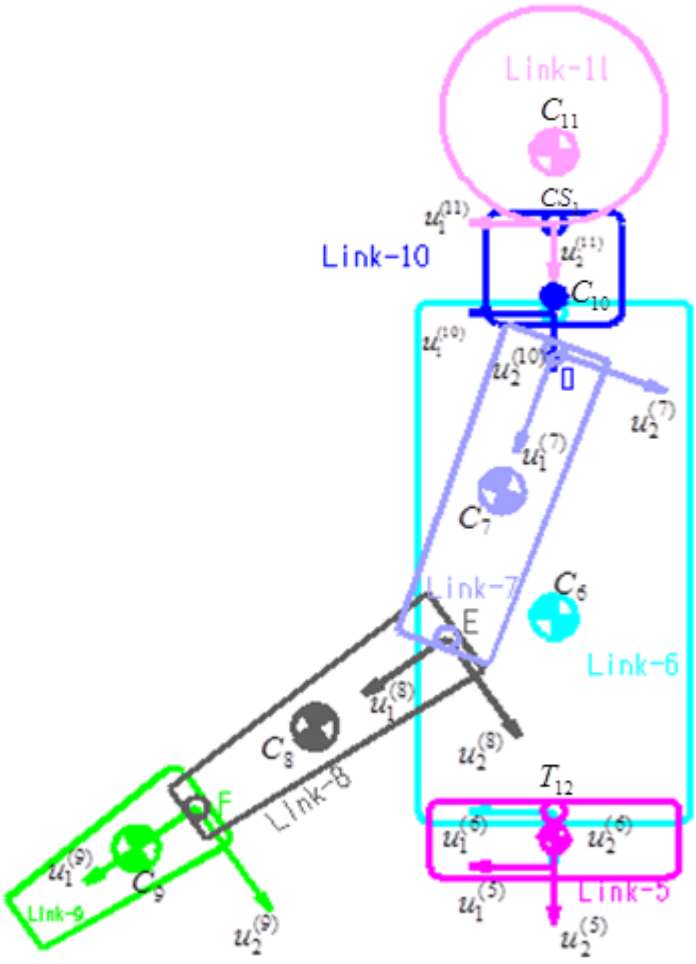

Figure 4.6 Upper Extremity of Rider Model

CHAPTER 5

EQUATIONS OF MOTION BY INVERSE MODELLING

5.1 Rigid Body Motion Kinematics

5.1.1 Reference Frames Definitions

In the rider model, two types of reference frames are used for all kinematic and dynamic calculations. The first one is the world-fixed frame (WFF) that is the same as the motion reference frame (MRF) in **[22]**. This frame has been used to express the kinematics of the saddle motion. The positive x-axis is parallel to the motion of the horse, the positive y-axis is along the gravity direction and the positive z- axis is out of the sagittal plane. In this study, the axes of the MRF (fixed frame) are labelled as $u_1^{(0)}$ (x-axis), $u_2^{(0)}$ (y-axis) and $u_3^{(0)}$ (z-axis). The origin of the world fixed frame is O and the frame is named as $\mathcal{F}_0\{\mathrm{O}\}$. The second type of reference frame that is used in this study is the body-reference frame (BRF) the origin of which is located at the connection points of the links. The number of the frame is the same as the labelling of the link number (see Figure 5.1). The BRF definitions are given in Table 5.1. All of the kinematic vectors (position, velocity, acceleration) of the rider model's links are represented with respect to origin point "O" of WFF as in global coordinates.

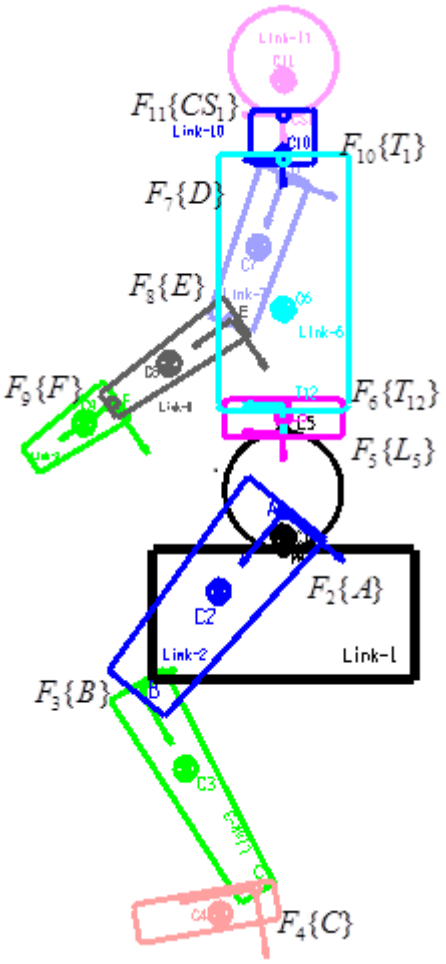

Figure 5.1 Rider model with BRF and WFF.

Table 5.1 Links and BRF representations

Link-1	**Link-2**	**Link-3**	**Link-4**	**Link-5**
$F_1\{M\}$	$F_2\{A\}$	$F_3\{B\}$	$F_4\{C\}$	$F_5\{L_5\}$
Link-6	**Link-7**	**Link-8**	**Link-9**	**Link-10**
$F_6\{T_{12}\}$	$F_7\{D\}$	$F_8\{E\}$	$F_9\{F\}$	$F_{10}\{T_1\}$
Link-11				
$F_{11}\{CS_1\}$				

5.1.2 Direction Cosine Matrix and Elementary Rotations

In this study, the links of the horse rider model have both translational and rotational motion. Since the model is represented in the sagittal plane, only rotations about the u_3 axis are considered. Consider, now, a body reference frame $\mathcal{F}_a\{\mathrm{A}\}$ that represents a rigid body A and a global coordinate system $\mathcal{F}_0\{\mathrm{O}\}$ which is fixed to the ground at origin O. Let the origins of these two frames be coincident. Assuming that the rigid body A rotates θ degrees about the $u_3^{(0)}$- axis, the direction cosine matrix (DCM) $C^{(0,a)}$ is written as:

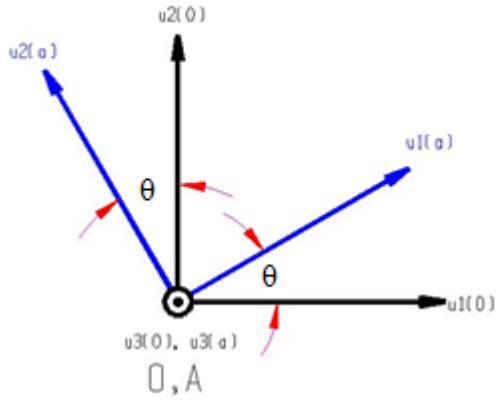

Figure 5.2 Frame rotation $u_3^{(0)}$

$$R_3(\theta) = C^{(0,a)} = \begin{bmatrix} \cos(\theta) & -\sin(\theta) & 0 \\ \sin(\theta) & \cos(\theta) & 0 \\ 0 & 0 & 1 \end{bmatrix} \quad \textbf{(5.1)}$$

where

$C^{(0,a)}$: Direction Cosine Matrix from $\mathcal{F}_0\{\mathrm{O}\}$ to $\mathcal{F}_a\{\mathrm{A}\}$,

$R_3(\theta)$: Rotation Matrix corresponding to a rotation of θ about the $u_3^{(0)}$ axis.

The remaining elementary rotations about the $u_1^{(0)}$ and $u_2^{(0)}$ axes are represented in a similar manner as given below:

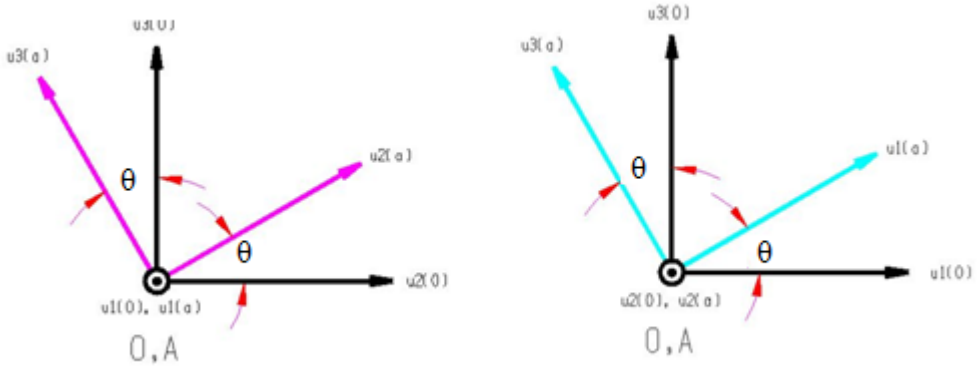

Figure 5.3 Frame rotations about $u_1^{(0)}$ and $u_2^{(0)}$

with the corresponding rotation matrices as

$$R_1(\theta)=\begin{bmatrix}1 & 0 & 0\\ 0 & \cos(\theta) & -\sin(\theta)\\ 0 & \sin(\theta) & \cos(\theta)\end{bmatrix}, \qquad \textbf{(5.2)}$$

$R_1(\theta)$: Rotation Matrix corresponding to a rotation of θ about the $u_1^{(0)}$ axis,

and

$$R_2(\theta)=\begin{bmatrix}\cos(\theta) & 0 & \sin(\theta)\\ 0 & 1 & 0\\ -\sin(\theta) & 0 & \cos(\theta)\end{bmatrix}, \qquad \textbf{(5.3)}$$

$R_2(\theta)$: Rotation Matrix corresponding to a rotation of θ about the $u_2^{(0)}$ axis.

5.1.3 Successive Rotations

If a body reference frame is rotated more than once, the resulting rotation matrix and the direction cosine matrix is formulated as given below.

Transformation sequence is:

$$\mathcal{T}_0\{\mathrm{O}\} \longrightarrow \mathcal{T}_1\{\mathrm{O}\} \longrightarrow \mathcal{T}_2\{\mathrm{O}\}$$

The transformation matrix from Frame-0 $\mathcal{T}_0\{\mathrm{O}\}$ to Frame-2 $\mathcal{T}_2\{\mathrm{O}\}$:

$$C^{(0,2)} = C^{(0,1)}C^{(1,2)} \qquad \textbf{(5.4)}$$

$C^{(0,1)}$: Transformation Matrix from Frame-0 $[\mathcal{T}_0\{\mathrm{O}\}]$ to Frame-1 $[\mathcal{T}_1\{\mathrm{O}\}]$,

$C^{(1,2)}$: Transformation Matrix from Frame-1 $[\mathcal{T}_1\{\mathrm{O}\}]$ to Frame-2 $[\mathcal{T}_2\{\mathrm{O}\}]$,

$C^{(0,2)}$: Transformation matrix from Frame-0 $[\mathcal{T}_0\{\mathrm{O}\}]$ to Frame-2 $[\mathcal{T}_2\{\mathrm{O}\}]$.

5.1.4 Position of a Body as Observed in Different Frames

Consider a body reference frame $\mathcal{F}_b\{\mathrm{B}\}$ attached to body B and a fixed frame $\mathcal{F}_a\{\mathrm{A}\}$ as seen in Figure 5.4. The position vector of a random point P on body B is represented, in the fixed frame $\mathcal{F}_a\{\mathrm{A}\}$, as:

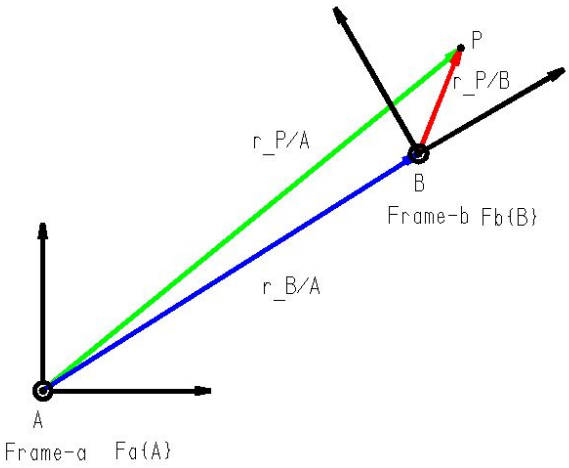

Figure 5.4 Different frames position vector

$$\overline{r}_{P/A}^{(a)} = C^{(a,b)}\,\overline{r}_{P/B}^{(b)} + \overline{r}_{B/A}^{(a)}\,. \qquad \textbf{(5.5)}$$

Here,

$\overline{r}_{P/A}^{(a)}$: Position vector of point P relative to A expressed in the fixed frame $\mathcal{F}_a\{\mathrm{A}\}$,

$C^{(a,b)}$: Transformation Matrix from frame $\mathcal{F}_b\{\mathrm{B}\}$ to frame $\mathcal{F}_a\{\mathrm{A}\}$,

$\overline{r}_{P/B}^{(b)}$: Position vector of point P relative to point B expressed in the body reference frame $\mathcal{F}_b\{\mathrm{B}\}$,

$\overline{r}_{B/A}^{(a)}$: Position vector of point B relative to A expressed in the fixed frame $\mathcal{F}_a\{\mathrm{A}\}$.

This formulation is used to determine the position vectors of the center of mass points of each link expressed in the world-fixed frame coordinates.

5.2 Kinematic Analysis

5.2.1 Position Analysis

5.2.1.1 Lower Extremity

i) Link-1 (Saddle-Hip)

As mentioned before, Link-1 consists of the horse saddle and the hip of the rider body. In a previous study **[22]**, the kinematic data of the saddle has been obtained via four reflective markers placed on the saddle (see Figure 5.5).

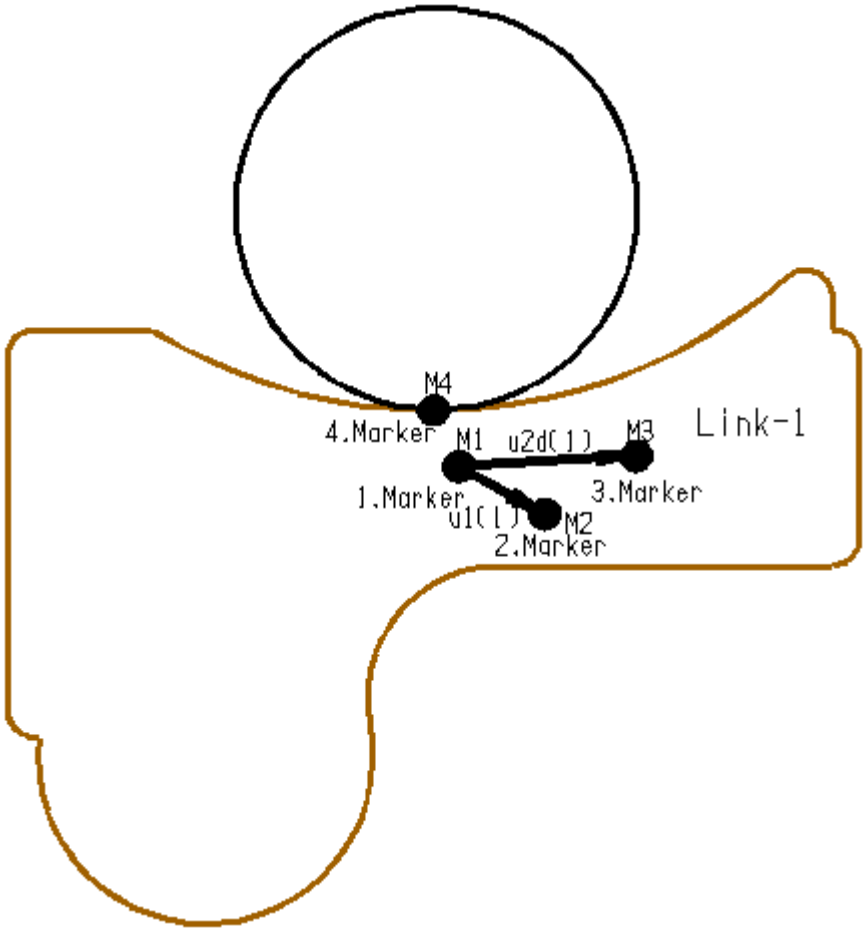

Figure 5.5 Reflective markers on saddle and BRF of Link-1

The position vectors of the four markers have been obtained via a vision system. Hence, the origin of the body reference frame of Link-1, $\mathcal{F}_1\{M_1\}$, is placed on the 1st marker. The $u_1^{(1)}$, $u_2^{(1)}$ and $u_3^{(1)}$ axes, on the other hand, are obtained as described

below. The $u_1^{(1)}$ unit vector is from the 1st marker to the 2nd marker and the dummy $u_{2d}^{(1)}$ vector is from the 1st marker to the 3rd marker. The cross product of these two vectors gives the $u_3^{(1)}$ unit vector which is then used to determine the exact $u_2^{(1)}$ axis by taking the cross product with $u_1^{(1)}$. **[22]** The related equations are follows:

$$\overline{u}_1^{(1)} = \frac{\overline{r_2} - \overline{r_1}}{|\overline{r_2} - \overline{r_1}|}, \quad \textbf{(5.6)}$$

$$\overline{u}_{2d}^{(1)} = \frac{\overline{r_3} - \overline{r_1}}{|\overline{r_3} - \overline{r_1}|}, \quad \textbf{(5.7)}$$

where $\overline{r}_3, \overline{r}_1$ and $\overline{r}_2$ are the position vectors of 3rd marker, 1st marker and 2nd marker in WFF global coordinates, respectively.

$$\overline{u}_3^{(1)} = \frac{\overline{u}_1^1 x \overline{u}_{2d}^1}{\left|\overline{u}_1^1 x \overline{u}_{2d}^1\right|}, \quad \textbf{(5.8)}$$

$$\overline{u}_2^{(1)} = \frac{\overline{u}_3^1 x \overline{u}_1^1}{\left|\overline{u}_3^1 x \overline{u}_1^1\right|} \ . \quad \textbf{(5.9)}$$

The transformation matrix from Frame-0 to Frame-1, on the other hand, is given by

$$C^{(0,1)} = [u_1^1 \quad u_2^1 \quad u_3^1], \quad \textbf{(5.10)}$$

where $C^{(0,1)}$ denotes for the transformation matrix of Link-1 with $\mathcal{T}_1\{M_1\}$ frame whose origin is located at point M_1 (1st marker location).

After finding the rotation matrix of Link-1, the rotation angle θ_{01} can be found by the formula **[23]**:

$$R = I\cos\theta + \tilde{n}\sin\theta + \overline{n}\,\overline{n}^t(1 - \cos\theta), \quad \textbf{(5.11)}$$

where θ denotes for the rotation angle and n is rotation axis unit vector.

Equation (5.11) written in matrix form is

$$\begin{bmatrix} r_{11} & r_{12} & r_{13} \\ r_{21} & r_{22} & r_{23} \\ r_{31} & r_{32} & r_{33} \end{bmatrix} =$$

$$\begin{bmatrix} 1 & 0 & 0 \\ 0 & 1 & 0 \\ 0 & 0 & 1 \end{bmatrix} \cos\theta + \begin{bmatrix} 0 & -n_3 & n_2 \\ n_3 & 0 & -n_1 \\ -n_2 & n_1 & 0 \end{bmatrix} \sin\theta + \begin{bmatrix} n_1^2 & n_1 n_2 & n_1 n_3 \\ n_1 n_2 & n_2^2 & n_2 n_3 \\ n_1 n_3 & n_2 n_3 & n_3^2 \end{bmatrix} (1 - \cos\theta) . \quad \textbf{(5.12)}$$

Equating the diagonal elements in (5.12), one obtains:

$$r_{11} = \cos\theta + n_1^2(1 - \cos\theta), \quad \textbf{(5.13)}$$

$$r_{22} = \cos\theta + n_2^2(1 - \cos\theta), \quad \textbf{(5.14)}$$

$$r_{33} = \cos\theta + n_3^2(1 - \cos\theta). \quad \textbf{(5.15)}$$

Adding (5.13) – (5.15) side by side, one obtains

$$r_{11} + r_{22} + r_{33} = 3\cos\theta + (n_1^2 + n_2^2 + n_3^2)\ (1 - \cos\theta) \quad \textbf{(5.16)}$$

which, using

$$(n_1^2 + n_2^2 + n_3^2) = 1 \quad \textbf{(5.17)}$$

yields

$$\cos\theta = \frac{(r_{11} + r_{22} + r_{33}) - 1}{2} = \frac{tr(R) - 1}{2} \quad \textbf{(5.18)}$$

where $tr(R)$ is the trace of rotation matrix.

Hence,

$$\cos\theta = \frac{tr(R) - 1}{2} = \beta\ (constant) \quad \textbf{(5.19)}$$

leading to $\sin\theta = \sigma\sqrt{1 - \beta^2}$ with $\sigma = \mp 1$.

Therefore, the rotation angle θ is obtained as:

$$\theta = atan2[\sigma\sqrt{1 - \beta^2}, \beta\ ]. \quad \textbf{(5.20)}$$

Hence, the rotation angle of Link-1, θ_{01}, can be found, after determining the $C^{(0,1)}$ matrix, via the equation

$$\theta_{01} = atan2[\sigma\sqrt{1 - \beta^2}, \beta\ ] \quad \textbf{(5.21)}$$

where

$$\cos\theta_{01} = \frac{tr(C^{(0,1)}) - 1}{2} = \beta\ (constant), \quad \textbf{(5.22)}$$

$$\sin\theta_{01} = \sigma\sqrt{1-\beta^2} \qquad \sigma = \mp 1\ . \tag{5.23}$$

n_1, n_2, n_3 on the other hand, may be obtained by considering the off-diagonal elements of R as described below:

$$r_{12} = -n_3 \sin\theta + n_1 n_2 (1 - \cos\theta), \tag{5.24}$$

$$r_{21} = n_3 \sin\theta + n_1 n_2 (1 - \cos\theta). \tag{5.25}$$

By subtracting Equation (5.24) from Equation (5.25), one obtains

$$r_{21} - r_{12} = 2n_3 \sin\theta. \tag{5.26}$$

Hence,

$$n_3 = \frac{r_{21}-r_{12}}{2\sin\theta} = \frac{r_{21}-r_{12}}{2\sigma\sqrt{1-\beta^2}}\ . \tag{5.27}$$

Similarly it can be shown that

$$n_2 = \frac{r_{13}-r_{31}}{2\sin\theta} = \frac{r_{13}-r_{31}}{2\sigma\sqrt{1-\beta^2}}\,, \tag{5.28}$$

$$n_1 = \frac{r_{32}-r_{23}}{2\sin\theta} = \frac{r_{32}-r_{23}}{2\sigma\sqrt{1-\beta^2}}\,. \tag{5.29}$$

If $\sin\theta \neq 0$, hence one obtains

$$\overline{n} = [n_1; n_2; n_3]\ . \tag{5.30}$$

ii) Link-2 (Thigh)

Link-2 and Link-1 are connected by using the revolute joint at point A. The origin of the body reference frame of Link-2, $\mathcal{T}_2\{\mathrm{A}\}$, is located at point A and the u_1^2 axis direction is towards the center of mass C_2. Link-2 is symmetric along its longitudinal axis and C_2 is on that symmetry axis. As seen from Figure 5.6, the position of C_2 with respect to $\mathcal{T}_0\{\mathrm{O}\}$, in global coordinates, is given by the following equation

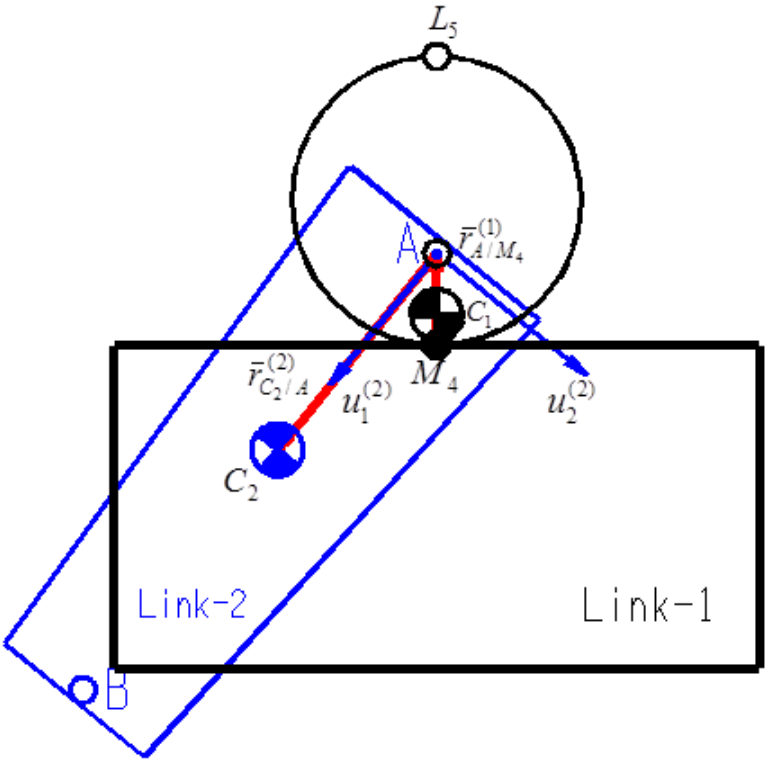

Figure 5.6 Position vector of CM of Link-2 (Thigh)

$$\overline{\{r_{C2/O}\}}^{(0)} = C^{(0,2)}\overline{\{r_{C2/A}\}}^{(2)} + C^{(0,1)}\overline{\{r_{A/M4}\}}^{(1)} + \overline{\{r_{M4/O}\}}^{(0)}\ , \qquad \textbf{(5.31)}$$

where

$\overline{\{r_{C2/O}\}}^{(0)}$: Position vector from Point O to Point C_2 expressed in WFF, $\mathcal{T}_0\{\mathrm{O}\}$,

$\overline{\{r_{C2/A}\}}^{(2)}$: Position vector from Point A to Point C_2 expressed in $\mathcal{T}_2\{\mathrm{A}\}$,

$\overline{\{r_{A/M4}\}}^{(1)}$: Position vector from Point M_4 to Point A expressed in $\mathcal{T}_1\{M_1\}$,

$\overline{\{r_{M4/O}\}}^{(0)}$: Position vector of Point M_4 expressed in $\mathcal{T}_0\{\mathrm{O}\}$ (which is taken from

the previous study **[22]** and see Appendix A.7 **)**,

$C^{(0,2)}$: Transformation Matrix from $\mathcal{F}_2\{\mathrm{A}\}$ to $\mathcal{F}_0\{\mathrm{O}\}$,

$C^{(0,1)}$: Transformation Matrix from $\mathcal{F}_1\{M_1\}$ to $\mathcal{F}_0\{\mathrm{O}\}$,

θ_{02} : Rotation angle about $\overline{u}_3{}^{(2)}$ from $\mathcal{F}_2\{\mathrm{A}\}$ to $\mathcal{F}_0\{\mathrm{O}\}$, and

$$C^{(0,2)} = \begin{bmatrix} \cos\theta_{02} & -\sin\theta_{02} & 0 \\ \sin\theta_{02} & \cos\theta_{02} & 0 \\ 0 & 0 & 1 \end{bmatrix}, \tag{5.32}$$

$$C^{(0,1)} = \begin{bmatrix} \cos\theta_{01} & -\sin\theta_{01} & 0 \\ \sin\theta_{01} & \cos\theta_{01} & 0 \\ 0 & 0 & 1 \end{bmatrix}. \tag{5.33}$$

iii) Link-3 (Shank)

Link-3 and Link-2 are connected by using the revolute joint at point B. The origin of the body reference frame of Link-3, $\mathcal{F}_3\{\mathrm{B}\}$, is located at point B and the u_1^3 axis direction is towards the center of mass location. Link-3 is symmetric along its longitudinal axis and C_3 is on that symmetry axis. As seen from Figure 5.7, the position of C_3 with respect to $\mathcal{F}_0\{\mathrm{O}\}$, in global coordinates is given by the following equation

$$\overline{\{r_{C3/O}\}}^{(0)} = C^{(0,3)}\overline{\{r_{C3/B}\}}^{(3)} + C^{(0,2)}\overline{\{r_{B/C2}\}}^{(2)} + \overline{\{r_{C2/O}\}}^{(0)}, \tag{5.34}$$

where

$\overline{\{r_{C3/O}\}}^{(0)}$: Position vector from Point C_3 expressed in WFF, $\mathcal{F}_0\{\mathrm{O}\}$,

$\overline{\{r_{C3/B}\}}^{(3)}$: Position vector from Point B to Point C_3 expressed in $\mathcal{F}_3\{\mathrm{B}\}$,

$\overline{\{r_{B/C2}\}}^{(2)}$: Position vector from Point C_2 to Point B expressed in $\mathcal{F}_2\{\mathrm{A}\}$,

$\overline{\{r_{C2/O}\}}^{(0)}$: Position vector of Point C_2 expressed in $\mathcal{F}_0\{\mathrm{O}\}$,

$C^{(0,3)}$: Transformation Matrix from $\mathcal{F}_3\{\mathrm{B}\}$ to $\mathcal{F}_0\{\mathrm{O}\}$,

θ_{03} : Rotation angle about $\overline{u}_3{}^{(3)}$ from $\mathcal{F}_3\{\mathrm{B}\}$ to $\mathcal{F}_0\{\mathrm{O}\}$, and

$$C^{(0,3)} = \begin{bmatrix} \cos\theta_{03} & -\sin\theta_{03} & 0 \\ \sin\theta_{03} & \cos\theta_{03} & 0 \\ 0 & 0 & 1 \end{bmatrix}. \quad \textbf{(5.35)}$$

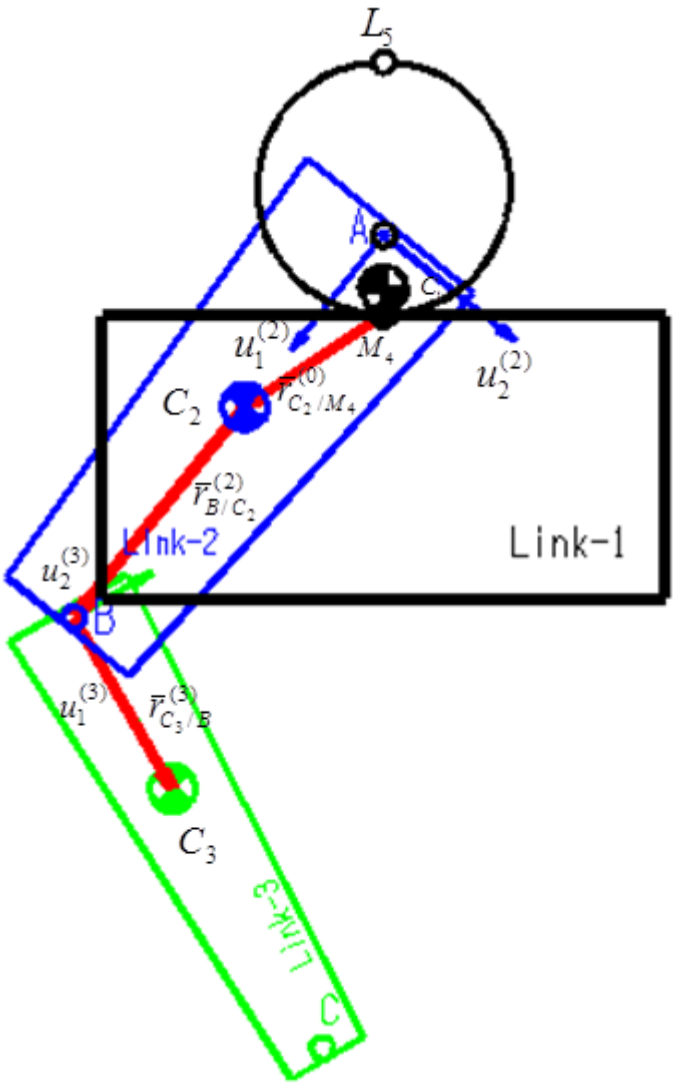

Figure 5.7 Position vector of CM of Link-3 (Shank)

iv) Link-4 (Foot)

Link-4 and Link-3 are connected by using the revolute joint at point C. The origin of the body reference frame of Link-4, $\mathcal{T}_4\{\mathrm{C}\}$, is located at point C and the u_1^4 axis direction is towards to center of mass, C_4. Link-4 is symmetric along its longitudinal axis and C_4 is on that symmetry axis. As seen from Figure 5.8, the position of C_4 with respect to $\mathcal{T}_0\{\mathrm{O}\}$, in global coordinates, is given by the following equation

$$\overline{\{r_{C4/O}\}}^{(0)} = C^{(0,4)}\overline{\{r_{C4/C}\}}^{(4)} + C^{(0,3)}\overline{\{r_{C/C3}\}}^{(3)} + \overline{\{r_{C3/O}\}}^{(0)}, \quad \textbf{(5.36)}$$

where

$\overline{\{r_{C4/O}\}}^{(0)}$: Position vector from Point C_4 expressed in WFF, $\mathcal{T}_0\{O\}$,

$\overline{\{r_{C4/C}\}}^{(4)}$: Position vector from Point C to Point C_4 expressed in $\mathcal{T}_4\{C\}$,

$\overline{\{r_{C/C3}\}}^{(3)}$: Position vector from Point C_3 to Point C expressed in $\mathcal{T}_3\{B\}$,

$\overline{\{r_{C3/O}\}}^{(0)}$: Position vector of Point C_3 expressed in $\mathcal{T}_0\{O\}$,

$C^{(0,4)}$: Transformation Matrix from $\mathcal{T}_4\{C\}$ to $\mathcal{T}_0\{O\}$,

θ_{04} : Rotation angle about $\overline{u}_3^{(4)}$ from $\mathcal{T}_4\{C\}$ to $\mathcal{T}_0\{O\}$, and

$$C^{(0,4)} = \begin{bmatrix} \cos\theta_{04} & -\sin\theta_{04} & 0 \\ \sin\theta_{04} & \cos\theta_{04} & 0 \\ 0 & 0 & 1 \end{bmatrix}. \quad \textbf{(5.37)}$$

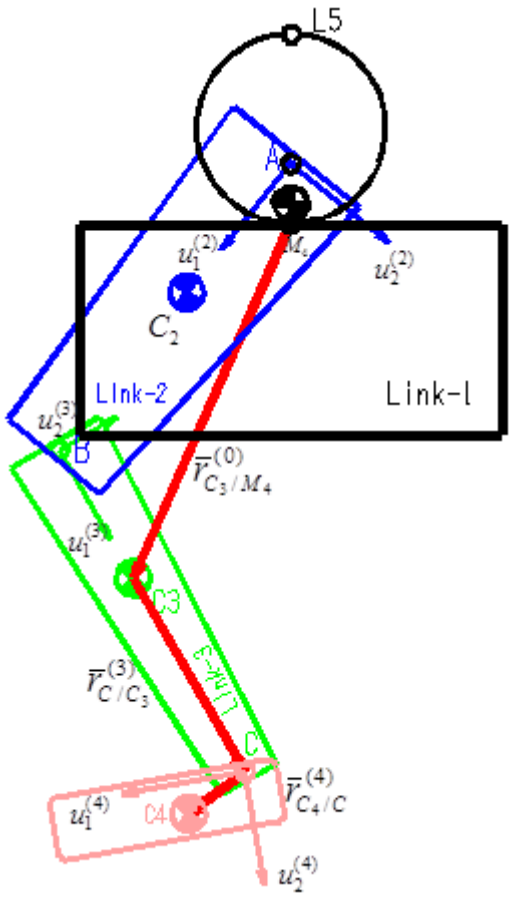

Figure 5.8 Position vector of CM of Link-4 (Foot)

5.2.1.2 Upper Extremity

i) Link-5 (Abdomen)

Link-5 and Link-1 are connected by using the revolute joint at point L_5. The origin of the body reference frame of Link-5, $\mathcal{T}_5\{L_5\}$, is located at point L_5 and the u_1^5 axis direction is towards the center of mass, C_5. Link-5 is symmetric along its longitudinal axis and C_5 is on that symmetry axis. As seen from Figure 5.9, the position of C_5 with respect to $\mathcal{T}_0\{\mathrm{O}\}$, in global coordinates, is given by the following equation

$$\overline{\{r_{C5/O}\}}^{(0)} = C^{(0,5)}\overline{\{r_{C5/L5}\}}^{(5)} + C^{(0,1)}\overline{\{r_{L5/M4}\}}^{(1)} + \overline{\{r_{M4/O}\}}^{(0)}\ , \qquad \textbf{(5.38)}$$

where

$\overline{\{r_{C5/O}\}}^{(0)}$: Position vector from Point C_5 expressed in WFF, $\mathcal{T}_0\{\mathrm{O}\}$,

$\overline{\{r_{C5/L5}\}}^{(5)}$: Position vector from Point L_5 to Point C_5 expressed in $\mathcal{T}_5\{L_5\}$,

$\overline{\{r_{L5/M4}\}}^{(1)}$: Position vector from Point M_4 to Point L_5 expressed in $\mathcal{T}_1\{M_1\}$,

$\overline{\{r_{M4/O}\}}^{(0)}$: Position vector of Point M_4 expressed in $\mathcal{T}_0\{\mathrm{O}\}$ (which is taken from previous study **[22]**, see Appendix A.7) ,

$C^{(0,5)}$: Transformation Matrix from $\mathcal{T}_5\{L_5\}$ to $\mathcal{T}_0\{\mathrm{O}\}$,

θ_{05} : Rotation angle about $\overline{u}_3^{(5)}$ from $\mathcal{T}_5\{L_5\}$ to $\mathcal{T}_0\{\mathrm{O}\}$, and

$$C^{(0,5)} = \begin{bmatrix} \cos\theta_{05} & -\sin\theta_{05} & 0 \\ \sin\theta_{05} & \cos\theta_{05} & 0 \\ 0 & 0 & 1 \end{bmatrix}. \qquad \textbf{(5.39)}$$

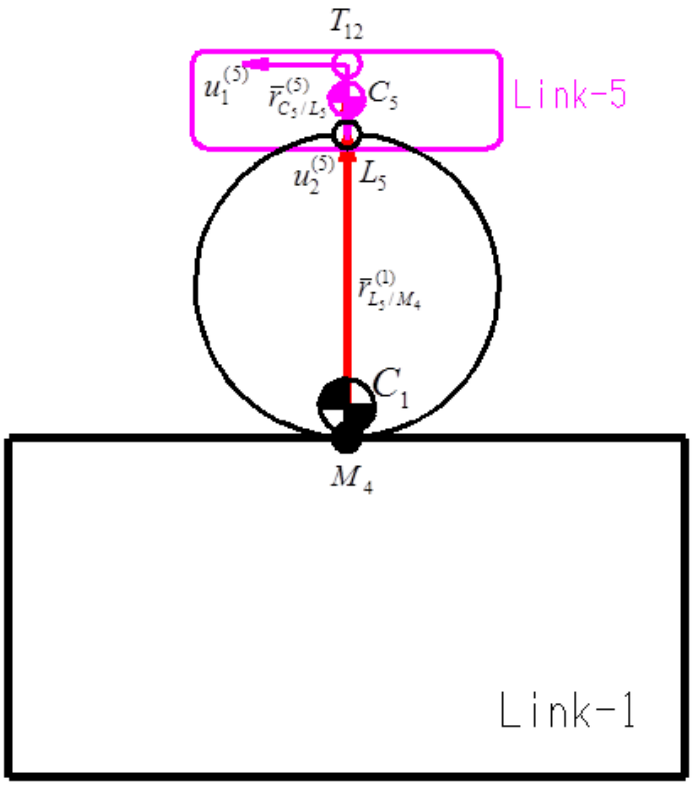

Figure 5.9 Position vector of CM of Link-5 (Abdomen)

ii) Link-6 (Trunk)

Link-6 and Link-5 are connected by using the revolute joint at point T_{12}. The origin of the body reference frame of Link-6, $\mathcal{T}_6\{T_{12}\}$, is located at point T_{12} and the u_1^6 axis direction is towards the center of mass, C_6. Link-6 is symmetric along its longitudinal axis and C_6 is on that symmetry axis. As seen from Figure 5.10, the position of C_6 with respect to $\mathcal{T}_0\{\mathrm{O}\}$, in global coordinates, is given by the following equation

$$\overline{\{r_{C6/O}\}}^{(0)} = C^{(0,6)}\overline{\{r_{C6/T12}\}}^{(6)} + C^{(0,5)}\overline{\{r_{T12/C5}\}}^{(5)} + \overline{\{r_{C5/O}\}}^{(0)}, \qquad \textbf{(5.40)}$$

where

$\overline{\{r_{C6/O}\}}^{(0)}$: Position vector from Point C_6 expressed in WFF, $\mathrm{T}_0\{\mathrm{O}\}$,

$\overline{\{r_{C6/T12}\}}^{(6)}$: Position vector from Point T_{12} to Point C_6 expressed in $\mathrm{T}_6\{T_{12}\}$,

$\overline{\{r_{T12/C5}\}}^{(5)}$: Position vector from Point C_5 to Point T_{12} expressed in $\mathrm{T}_5\{L_5\}$,

$C^{(0,6)}$: Transformation Matrix from $\mathrm{T}_6\{T_{12}\}$ to $\mathrm{T}_0\{\mathrm{O}\}$,

θ_{06} : Rotation angle about $\overline{u}_3^{(6)}$ from $\mathrm{T}_6\{T_{12}\}$ to $\mathcal{T}_0\{\mathrm{O}\}$, and

$$C^{(0,6)} = \begin{bmatrix} \cos\theta_{06} & -\sin\theta_{06} & 0 \\ \sin\theta_{06} & \cos\theta_{06} & 0 \\ 0 & 0 & 1 \end{bmatrix} \quad \textbf{(5.41)}$$

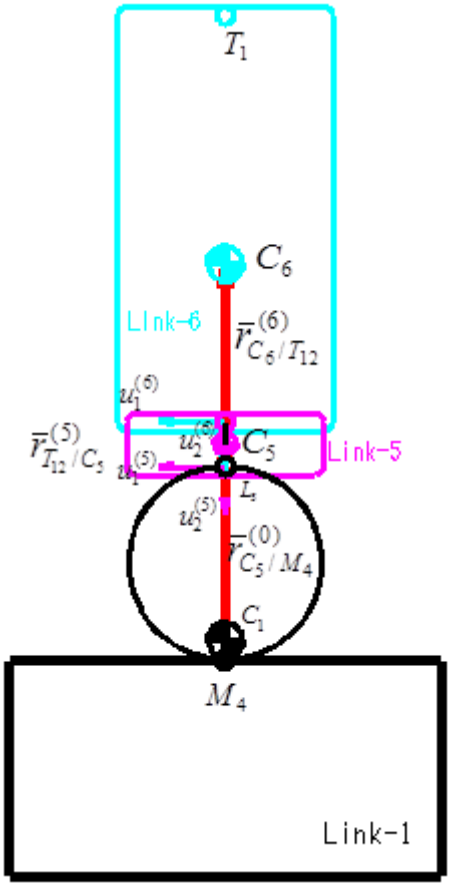

Figure 5.10 Position vector of CM of Link-6 (Trunk)

iii) Link-7 (Upper Arm)

Link-7 and Link-6 are connected by using the revolute joint at point D. The origin of the body reference frame of Link-6, $\mathrm{T}_7\{D\}$, is located at point D and the u_1^7 axis direction is towards the center of mass, C_7. Link-7 is symmetric along its longitudinal axis and C_7 is on that symmetry axis. As seen from Figure 5.11, the position of C_7

with respect to $\mathrm{T}_0\{\mathrm{O}\}$, in global coordinates, is given by the following equation

$$\overline{\{r_{C7/O}\}}^{(0)} = C^{(0,7)}\overline{\{r_{C7/D}\}}^{(7)} + C^{(0,6)}\overline{\{r_{D/C6}\}}^{(6)} + \overline{\{r_{C6/O}\}}^{(0)}, \qquad \textbf{(5.42)}$$

where

$\overline{\{r_{C7/O}\}}^{(0)}$: Position vector from Point C_7 expressed in WFF, $\mathrm{T}_0\{\mathrm{O}\}$,

$\overline{\{r_{C7/D}\}}^{(7)}$: Position vector from Point D to Point C_7 expressed in $\mathrm{T}_7\{D\}$,

$\overline{\{r_{D/C6}\}}^{(6)}$: Position vector from Point C_6 to Point D expressed in $\mathrm{T}_6\{T_{12}\}$,

$\overline{\{r_{C6/O}\}}^{(0)}$: Position vector of Point C_6 expressed in $\mathrm{T}_0\{\mathrm{O}\}$,

$C^{(0,7)}$: Transformation Matrix from $\mathrm{T}_7\{D\}$ to $\mathrm{T}_0\{\mathrm{O}\}$,

θ_{07} : Rotation angle about $\overline{u}_3{}^{(7)}$ from $\mathrm{T}_7\{D\}$ to $\mathrm{T}_0\{\mathrm{O}\}$, and

$$C^{(0,7)} = \begin{bmatrix} \cos\theta_{07} & -\sin\theta_{07} & 0 \\ \sin\theta_{07} & \cos\theta_{07} & 0 \\ 0 & 0 & 1 \end{bmatrix}. \qquad \textbf{(5.43)}$$

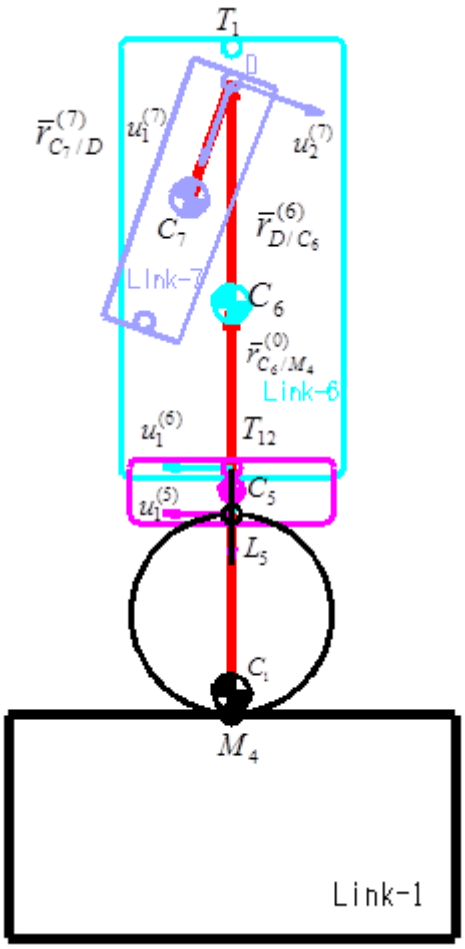

Figure 5.11 Position vector of CM of Link-7 (Upper Arm)

iv) Link-8 (Lower Arm)

Link-8 and Link-7 are connected by using the revolute joint at point E. The origin of the body reference frame of Link-8, $\mathrm{T}_8\{E\}$, is located at point E and the u_1^8 axis direction is towards to the center of mass, C_8. Link-8 is symmetric along its longitudinal axis and C_8 is on that symmetry axis. As seen from Figure 5.12, the position of C_8 with respect to $\mathrm{T}_0\{\mathrm{O}\}$, in global coordinates, is given by the following equation

$$\overline{\{r_{C8/O}\}}^{(0)} = C^{(0,8)}\overline{\{r_{C8/E}\}}^{(8)} + C^{(0,7)}\overline{\{r_{E/C7}\}}^{(7)} + \overline{\{r_{C7/O}\}}^{(0)}\,, \qquad \textbf{(5.44)}$$

where

$\overline{\{r_{C8/O}\}}^{(0)}$: Position vector from Point C_8 expressed in WFF, $\mathfrak{T}_0\{O\}$,

$\overline{\{r_{C8/E}\}}^{(8)}$: Position vector from Point E to Point C_8 expressed in $\mathfrak{T}_8\{E\}$,

$\overline{\{r_{E/C7}\}}^{(7)}$: Position vector from Point C_7 to Point E expressed in $\mathfrak{T}_7\{D\}$,

$\overline{\{r_{C7/O}\}}^{(0)}$: Position vector of Point C_7 expressed in $\mathfrak{T}_0\{O\}$,

$C^{(0,8)}$: Transformation Matrix from $\mathfrak{T}_8\{E\}$ to $\mathfrak{T}_0\{O\}$,

θ_{08} : Rotation angle about $\overline{u}_3^{(8)}$ from $\mathfrak{T}_8\{E\}$ to $\mathfrak{T}_0\{O\}$, and

$$C^{(0,8)} = \begin{bmatrix} \cos\theta_{08} & -\sin\theta_{08} & 0 \\ \sin\theta_{08} & \cos\theta_{08} & 0 \\ 0 & 0 & 1 \end{bmatrix}. \qquad \textbf{(5.45)}$$

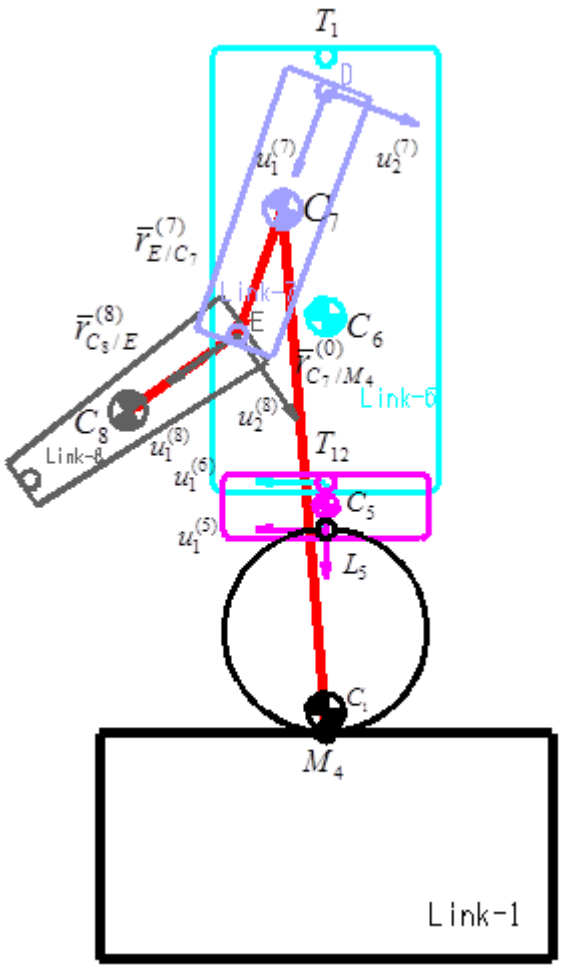

Figure 5.12 Position vector of CM of Link-8 (Lower Arm)

v) Link-9 (Hand)

Link-9 and Link-8 are connected by using the revolute joint at point F. The origin of the body reference frame of Link-9, $\mathrm{T}_9\{F\}$, is located at point F and the u_1^9 axis direction is towards the center of mass, C_9. Link-9 is symmetric along its longitudinal axis and C_9 is on that symmetry axis. As seen from Figure 5.13, the position of C_9 with respect to $\mathrm{T}_0\{\mathrm{O}\}$, in global coordinates, is given by the following equation

$$\overline{\{r_{C9/O}\}}^{(0)} = C^{(0,9)}\overline{\{r_{C9/F}\}}^{(9)} + C^{(0,8)}\overline{\{r_{F/C8}\}}^{(8)} + \overline{\{r_{C8/O}\}}^{(0)}, \qquad \textbf{(5.46)}$$

where

$\overline{\{r_{C9/O}\}}^{(0)}$: Position vector from Point C_9 expressed in WFF, $\mathrm{T}_0\{\mathrm{O}\}$,

$\overline{\{r_{C9/F}\}}^{(9)}$: Position vector from Point F to Point C_9 expressed in $\mathrm{T}_9\{F\}$,

$\overline{\{r_{F/C8}\}}^{(8)}$: Position vector from Point C_8 to Point F expressed in $\mathrm{T}_8\{E\}$,

$\overline{\{r_{C8/O}\}}^{(0)}$: Position vector of Point C_8 expressed in $\mathrm{T}_0\{\mathrm{O}\}$,

$C^{(0,9)}$: Transformation Matrix from $\mathrm{T}_9\{F\}$ to $\mathrm{T}_0\{\mathrm{O}\}$,

θ_{09} : Rotation angle about $\overline{u}_3^{(9)}$ from $\mathrm{T}_9\{F\}$ to $\mathcal{T}_0\{\mathrm{O}\}$, and

$$C^{(0,9)} = \begin{bmatrix} \cos\theta_{09} & -\sin\theta_{09} & 0 \\ \sin\theta_{09} & \cos\theta_{09} & 0 \\ 0 & 0 & 1 \end{bmatrix}. \qquad \textbf{(5.47)}$$

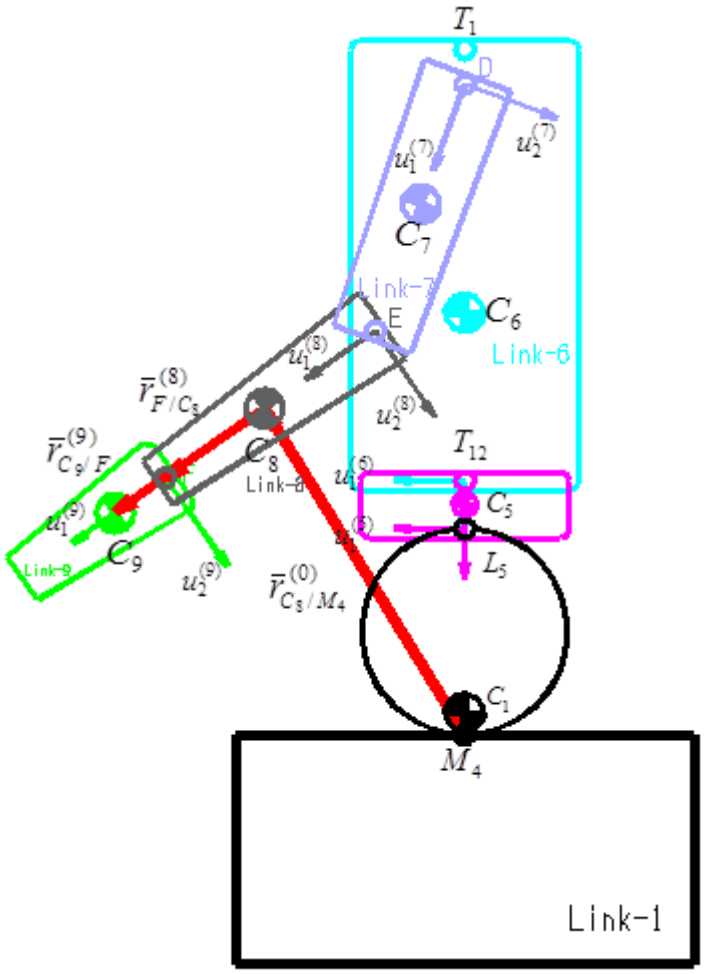

Figure 5.13 Position vector of CM of Link-9 (Hand)

vi) Link-10 (Neck)

Link-10 and Link-6 are connected by using the revolute joint at point T_1. The origin of the body reference frame of Link-10, $\mathfrak{T}_{10}\{T_1\}$, is located at point T_1 and the u_1^{10} axis direction is towards the center of mass, C_{10}. Link-10 is symmetric along its longitudinal axis and C_{10} is on that symmetry axis. As seen from Figure 5.14, the position of C_{10} with respect to $\mathfrak{T}_0\{O\}$, in global coordinates, is given by the following equation

$$\overline{\{r_{C10/O}\}}^{(0)} = C^{(0,10)}\overline{\{r_{C10/T1}\}}^{(10)} + C^{(0,6)}\overline{\{r_{T1/C6}\}}^{(6)} + \overline{\{r_{C6/O}\}}^{(0)}, \qquad \textbf{(5.48)}$$

where

$\overline{\{r_{C10/O}\}}^{(0)}$: Position vector from Point C_{10} expressed in WFF, $\mathrm{T}_0\{\mathrm{O}\}$,

$\overline{\{r_{C10/T1}\}}^{(10)}$: Position vector from Point T_1 to Point C_{10} expressed in $\mathrm{T}_{10}\{T_1\}$,

$\overline{\{r_{T1/C6}\}}^{(6)}$: Position vector from Point C_6 to Point T_1 expressed in $\mathrm{T}_6\{T_{12}\}$,

$\overline{\{r_{C6/O}\}}^{(0)}$: Position vector of Point C_6 expressed in $\mathrm{T}_0\{\mathrm{O}\}$,

$C^{(0,10)}$: Transformation Matrix from $\mathrm{T}_{10}\{T_1\}$ to $\mathrm{T}_0\{\mathrm{O}\}$,

θ_{010} : Rotation angle about $\overline{u}_3{}^{(10)}$ from $\mathrm{T}_{10}\{T_1\}$ to $\mathrm{T}_0\{\mathrm{O}\}$,

$$C^{(0,10)} = \begin{bmatrix} \cos\theta_{010} & -\sin\theta_{010} & 0 \\ \sin\theta_{010} & \cos\theta_{010} & 0 \\ 0 & 0 & 1 \end{bmatrix}. \qquad \textbf{(5.49)}$$

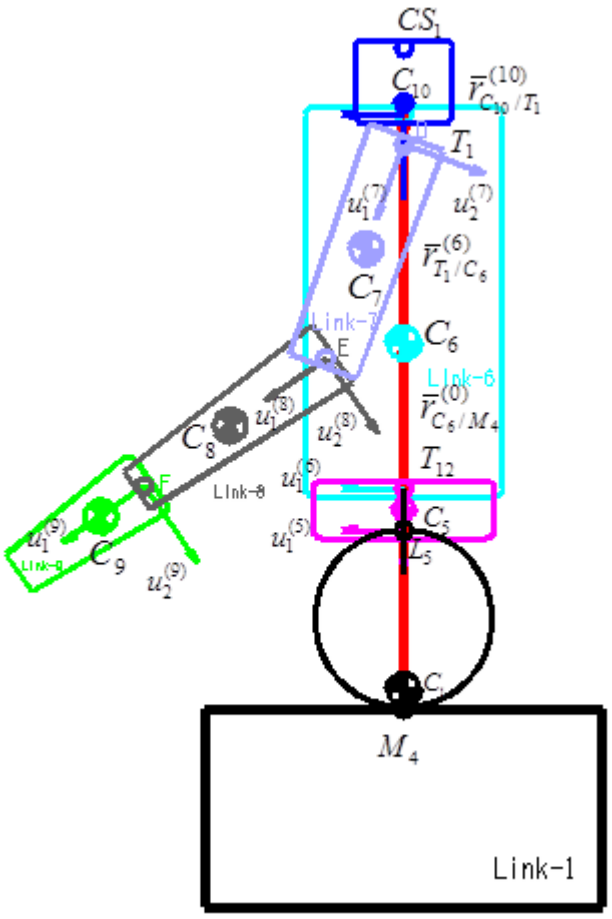

Figure 5.14 Position vector of CM of Link-10 (Neck)

vii) Link-11 (Head)

Link-11 and Link-10 are connected by using the revolute joint at point CS_1. The origin of the body reference frame of Link-11, $\mathrm{T}_{11}\{CS_1\}$, is located at point CS_1 and the u_1^{11} axis direction is towards the center of mass, C_{11}. Link-11 is symmetric along its longitudinal axis and C_{11} is on that symmetry axis. As seen from Figure 5.15, the position of C_{11} with respect to $\mathrm{T}_0\{\mathrm{O}\}$, in global coordinates, is given by the following equation

$$\overline{\{r_{C11/O}\}}^{(0)} = C^{(0,11)}\overline{\{r_{C11/CS1}\}}^{(11)} + C^{(0,10)}\overline{\{r_{CS1/C10}\}}^{(10)} + \overline{\{r_{C10/O}\}}^{(0)}\,, \qquad \textbf{(5.50)}$$

where

$\overline{\{r_{C11/O}\}}^{(0)}$: Position vector from Point C_{11} expressed in WFF, $\mathrm{T}_0\{\mathrm{O}\}$,

$\overline{\{r_{C11/CS1}\}}^{(11)}$: Position vector from Point CS_1 to Point C_{11}expressed in $\mathrm{T}_{11}\{CS_1\}$,

$\overline{\{r_{CS1/C10}\}}^{(10)}$: Position vector from Point C_{10} to Point CS_1 expressed in $\mathrm{T}_{10}\{T_1\}$,

$\overline{\{r_{C10/O}\}}^{(0)}$: Position vector of Point C_{10} expressed in $\mathrm{T}_0\{\mathrm{O}\}$,

$C^{(0,11)}$: Transformation Matrix from $\mathrm{T}_{11}\{CS_1\}$ to $\mathrm{T}_0\{\mathrm{O}\}$,

θ_{011} : Rotation angle about $\overline{u}_3^{(11)}$from $\mathrm{T}_{11}\{CS_1\}$ to $\mathcal{T}_0\{\mathrm{O}\}$, and

$$C^{(0,11)} = \begin{bmatrix} \cos\theta_{011} & -\sin\theta_{011} & 0 \\ \sin\theta_{011} & \cos\theta_{011} & 0 \\ 0 & 0 & 1 \end{bmatrix}. \qquad \textbf{(5.51)}$$

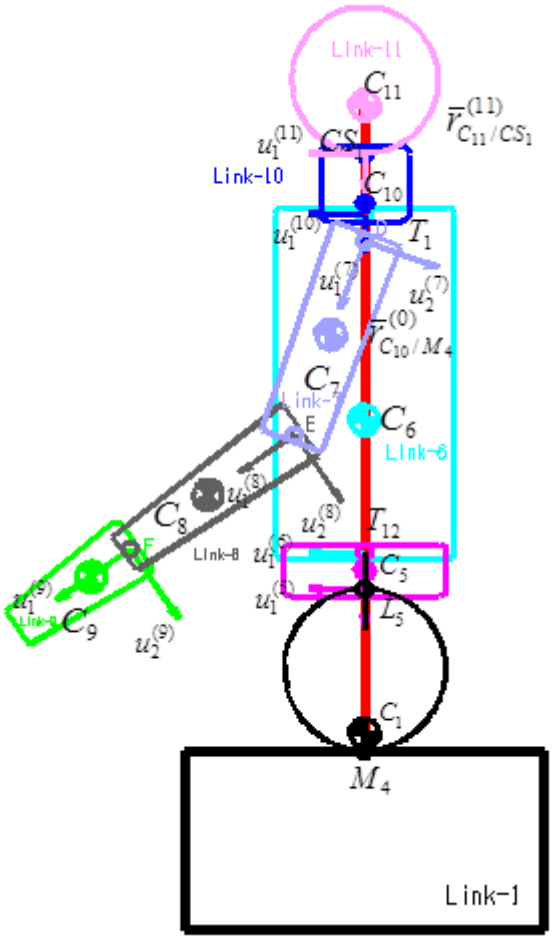

Figure 5.15 Position vector of CM of Link-11 (Head)

5.2.2 Velocity Analysis

Next, velocity analysis is achieved by obtaining the velocity vectors of the center of masses for each link in the global coordinates. From this point, differentiation of position vectors is performed in order to find the related velocity vectors of the links. Consider Transport (Coriolis) Theorem **[23]** which states that the relation between the velocities in two different frames as:

$$\overline{r}^{(a)} = C^{(a,b)}\,\overline{r}^{(b)} \quad \textbf{(5.52)}$$

$$\dot{\overline{r}}^{(a)} = C^{(a,b)}\,\dot{\overline{r}}^{(b)} + \dot{C}^{(a,b)}\,\overline{r}^{(b)} \quad \textbf{(5.53)}$$

$$\dot{\overline{r}}^{(a)} = C^{(a,b)}[\dot{\overline{r}}^{(b)} + C^{(b,a)}\,\dot{C}^{(a,b)}\,\overline{r}^{(b)}]. \quad \textbf{(5.54)}$$

Therefore, the relationship between direction cosine matrix and angular velocity can be expressed as follows:

$C^{(b,a)}\,\dot{C}^{(a,b)} = \widetilde{\omega}_{b/a}{}^{(b)}$ and $\dot{C}^{(a,b)}C^{(b,a)} = \widetilde{\omega}_{b/a}{}^{(a)}$ (by Coriolis Theorem) **(5.55)**

where $\widetilde{\omega}_{b/a}{}^{(b)}$ denotes for the angular velocity cross product matrix of $\mathrm{T}_b\{\mathrm{B}\}$ with respect to $\mathrm{T}_a\{\mathrm{A}\}$ and has the form

$$\widetilde{\omega}_{b/a} = \begin{bmatrix} 0 & -\omega_3 & \omega_2 \\ \omega_3 & 0 & -\omega_1 \\ \omega_2 & \omega_1 & 0 \end{bmatrix} \quad \text{with} \quad \overline{\omega}_{b/a} = \begin{bmatrix} \omega_1 \\ \omega_2 \\ \omega_3 \end{bmatrix}. \quad \textbf{(5.56)}$$

Finally, Equation (5.54) can be rewritten as in the following

$$\dot{\overline{r}}^{(a)} = C^{(a,b)}[\dot{\overline{r}}^{(b)} + \widetilde{\omega}_{b/a}{}^{(b)}\,\overline{r}^{(b)}]. \quad \textbf{(5.57)}$$

Consider a body reference frame $\mathrm{T}_b\{\mathrm{B}\}$ which is attached to body B and a fixed frame $\mathrm{T}_a\{\mathrm{A}\}$ as seen in Figure 5.4. The velocity vector of a random point P at body B, represented in the fixed frame $\mathrm{T}_a\{\mathrm{A}\}$ can be obtained by taking time derivative of Equation (5.5), yielding

$$\overline{v}_{P/A}^{(a)} = C^{(a,b)}\left(\overline{v}_{P/B}^{(b)}\right) + C^{(a,b)}\left(\widetilde{\omega}_{b/a}\,\overline{r}_{P/B}^{(b)}\right) + (\overline{v}_{B/A}^{(a)}), \qquad \textbf{(5.58)}$$

where

$\overline{v}_{P/A}^{(a)}$: Velocity vector of point P relative to A expressed in the fixed frame $\mathrm{T}_a\{\mathrm{A}\}$,

$\overline{v}_{P/B}^{(b)}$: Velocity vector of point P relative to B expressed in the body reference frame $\mathrm{T}_b\{\mathrm{B}\}$,

$\overline{v}_{B/A}^{(a)}$: Velocity vector of point B relative to A expressed in the fixed frame $\mathrm{T}_a\{\mathrm{A}\}$,

$\overline{r}_{P/B}^{(b)}$: Position vector of point P relative to B expressed in the body reference frame $\mathrm{T}_b\{\mathrm{B}\}$,

$\widetilde{\omega}_{b/a}$: Angular velocity cross product matrix of $\mathrm{T}_b\{\mathrm{B}\}$ relative to fixed frame $\mathrm{T}_a\{\mathrm{A}\}$, given by

$$\widetilde{\omega}_{b/a} = \begin{bmatrix} 0 & -\omega_3 & \omega_2 \\ \omega_3 & 0 & -\omega_1 \\ \omega_2 & \omega_1 & 0 \end{bmatrix} \text{ with } \overline{\omega}_{b/a} = \begin{bmatrix} \omega_1 \\ \omega_2 \\ \omega_3 \end{bmatrix}. \qquad \textbf{(5.59)}$$

Equation (5.58) is used to find the velocity vectors of the center of mass points of each link expressed in the world-fixed frame coordinates.

5.2.2.1 Lower Extremity

i) Link-1 (Hip and Saddle)

In **[22]**, the kinematic data of the saddle is obtained via three reflective markers placed on the saddle (see Figure 5.5). The origin of the body reference frame of Link-1, $\mathrm{T}_1\{M_1\}$ is placed on 1st marker. The known kinematic data related to 4th marker are the position $\overline{r}_{M4/O}^{(0)}$, the velocity $\overline{v}_{M4/O}^{(0)}$, at the acceleration $\overline{a}_{M4/O}^{(0)}$ of the marker. Furthermore, the angular velocity $\overline{\omega}_{1/0}$ and the angular acceleration $\overline{\alpha}_{1/0}$ of body-1 is also known in the WFF global coordinates, $\mathrm{T}_0\{\mathrm{O}\}$. By using these data, the velocities of the center of masses of the links and the angular velocities of the links in the rider model may be obtained as described in the following sections.

ii) Link-2 (Thigh)

The velocity vector of C_2 expressed in the WFF, $\mathrm{T}_0\{\mathrm{O}\}$, is obtained in global coordinates as

$$\overline{v}^{(0)}_{C2/O} = D_0\,\{\overline{r}^{(0)}_{C2/O}\}^{(0)}, \qquad \textbf{(5.60)}$$

where D_0 denotes the time derivative of the related vector with respect to $\mathrm{T}_0\{\mathrm{O}\}$.

Hence,

$$\overline{v}^{(0)}_{C2/O} = C^{(0,2)}\,\dot{\overline{r}}^{(2)}_{C2/A} + \dot{C}^{(0,2)}\,\overline{r}^{(2)}_{C2/A} + \{C^{(0,1)}\,\dot{\overline{r}}^{(1)}_{A/M4} + \dot{C}^{(0,1)}\,\overline{r}^{(1)}_{A/M4}\} + \dot{\overline{r}}^{(0)}_{M4/O}. \qquad \textbf{(5.61)}$$

Now, defining

$$\widetilde{\omega}_{1/0}{}^{(1)} = C^{(1,0)}\,\dot{C}^{(0,1)}, \qquad \textbf{(5.62)}$$

$$\widetilde{\omega}_{2/0}{}^{(2)} = C^{(2,0)}\,\dot{C}^{(0,2)}, \qquad \textbf{(5.63)}$$

Equation (5.61) becomes

$$\begin{aligned}\overline{v}^{(0)}_{C2/O} &= C^{(0,2)}\left[\dot{\overline{r}}^{(2)}_{C2/A} + \widetilde{\omega}_{2/0}{}^{(2)}\,\overline{r}^{(2)}_{C2/A}\right] + C^{(0,1)}\left[\dot{\overline{r}}^{(1)}_{A/M4} + \widetilde{\omega}_{1/0}{}^{(1)}\,\overline{r}^{(1)}_{A/M4}\right] + \dot{\overline{r}}^{(0)}_{M4/O} \\ &= C^{(0,2)}\left[\overline{v}^{(2)}_{C2/A} + \widetilde{\omega}_{2/0}{}^{(2)}\,\overline{r}^{(2)}_{C2/A}\right] + C^{(0,1)}\left[\overline{v}^{(1)}_{A/M4} + \widetilde{\omega}_{1/0}{}^{(1)}\,\overline{r}^{(1)}_{A/M4}\right] + \overline{v}^{(0)}_{M4/O}.\end{aligned} \qquad \textbf{(5.64)}$$

Since points C_2 and A are on Link-2 and points A and M are on Link-1, one has

$$\overline{v}^{(2)}_{C2/A} = 0 \quad \text{and} \quad \overline{v}^{(1)}_{A/M4} = 0. \qquad \textbf{(5.65)}$$

Hence, Equation (5.66) yields

$$\overline{v}^{(0)}_{C2/O} = C^{(0,2)}\left[\widetilde{\omega}_{2/0}{}^{(2)}\,\overline{r}^{(2)}_{C2/A}\right] + C^{(0,1)}\left[\widetilde{\omega}_{1/0}{}^{(1)}\,\overline{r}^{(1)}_{A/M4}\right] + \overline{v}^{(0)}_{M4/O}, \qquad \textbf{(5.66)}$$

where

$\overline{v}^{(0)}_{C2/O}$: Velocity vector of C_2 expressed in the $\mathrm{T}_0\{\mathrm{O}\}$ global coordinates,

$\overline{v}^{(0)}_{M4/O}$: Velocity vector of the 4th marker M_4 expressed in the $\mathrm{T}_0\{\mathrm{O}\}$ global coordinates,

$\widetilde{\omega}_{1/0}{}^{(1)}$: Angular velocity cross product matrix of $\mathrm{T}_1\{M_1\}$ relative to fixed frame $\mathrm{T}_0\{\mathrm{O}\}$ expressed in $\mathrm{T}_1\{M_1\}$ local coordinates,

$\widetilde{\omega}_{2/0}{}^{(2)}$: Angular velocity cross product matrix of $\mathrm{T}_2\{\mathrm{A}\}$ relative to fixed frame $\mathrm{T}_0\{\mathrm{O}\}$ expressed in $\mathrm{T}_2\{\mathrm{A}\}$ local coordinates.

iii) Link-3 (Shank)

The velocity vector of C_3 expressed in the WFF, $\mathrm{T}_0\{\mathrm{O}\}$, is obtained in global coordinates as

$$\overline{v}^{(0)}_{C3/O} = D_0\,\{\overline{r}^{(0)}_{C3/O}\}^{(0)}. \qquad \textbf{(5.67)}$$

Hence,

$$\overline{v}^{(0)}_{C3/O} = C^{(0,3)}\left[\overline{v}^{(3)}_{C3/B} + \widetilde{\omega}_{3/0}{}^{(3)}\,\overline{r}^{(3)}_{C3/B}\right] + C^{(0,2)}\left[\overline{v}^{(2)}_{B/C2} + \widetilde{\omega}_{2/0}{}^{(2)}\,\overline{r}^{(2)}_{B/C2}\right] + \overline{v}^{(0)}_{C2/O}. \qquad \textbf{(5.68)}$$

Since points C_3 and B are on Link-3 and points B and C_2 are on Link-2, one has

$$\overline{v}^{(3)}_{C3/B} = 0 \quad \text{and} \quad \overline{v}^{(2)}_{B/C2} = 0. \qquad \textbf{(5.69)}$$

Hence, Equation (5.68) yields

$$\overline{v}^{(0)}_{C3/O} = C^{(0,3)}\left[\widetilde{\omega}_{3/0}{}^{(3)}\,\overline{r}^{(3)}_{C3/B}\right] + C^{(0,2)}\left[\widetilde{\omega}_{2/0}{}^{(2)}\,\overline{r}^{(2)}_{B/C2}\right] + \overline{v}^{(0)}_{C2/O}, \qquad \textbf{(5.70)}$$

where

$\overline{v}^{(0)}_{C3/O}$: Velocity vector of C_3 expressed in the $\mathrm{T}_0\{\mathrm{O}\}$ global coordinates,

$\overline{v}^{(0)}_{C2/O}$: Velocity vector of C_2 expressed in the $\mathrm{T}_0\{\mathrm{O}\}$ global coordinates,

$\widetilde{\omega}_{2/0}{}^{(2)}$: Angular velocity cross product matrix of $\mathrm{T}_2\{\mathrm{A}\}$ relative to fixed frame $\mathrm{T}_0\{\mathrm{O}\}$ expressed in $\mathrm{T}_2\{\mathrm{A}\}$ local coordinates,

$\widetilde{\omega}_{3/0}{}^{(3)}$: Angular velocity cross product matrix of $\mathrm{T}_3\{\mathrm{B}\}$ relative to fixed frame $\mathrm{T}_0\{\mathrm{O}\}$ expressed in $\mathrm{T}_3\{\mathrm{B}\}$ local coordinates.

iv) Link-4 (Foot)

The velocity vector of C_4 expressed in the WFF, $\mathrm{T}_0\{\mathrm{O}\}$, is obtained in global coordinates as

$$\overline{v}^{(0)}_{C4/O} = D_0\,\{\overline{r}^{(0)}_{C4/O}\}^{(0)}. \qquad \textbf{(5.71)}$$

Hence,

$$\overline{v}^{(0)}_{C4/O} = C^{(0,4)}\left[\overline{v}^{(4)}_{C4/C} + \widetilde{\omega}_{4/0}{}^{(4)}\,\overline{r}^{(4)}_{C4/C}\right] + C^{(0,3)}\left[\overline{v}^{(3)}_{C/C3} + \widetilde{\omega}_{3/0}{}^{(3)}\,\overline{r}^{(3)}_{C/C3}\right] + \overline{v}^{(0)}_{C3/O}. \qquad \textbf{(5.72)}$$

Since points C_4 and C are on Link-4 and points C and C_3 are on Link-3 one has

$$\overline{v}^{(4)}_{C4/C} = 0 \text{ and } \overline{v}^{(3)}_{C/C3} = 0 . \quad \textbf{(5.73)}$$

Hence, Equation (5.72) yields

$$\overline{v}^{(0)}_{C4/O} = C^{(0,4)} \left[\widetilde{\omega}_{4/0}{}^{(4)} \overline{r}^{(4)}_{C4/C} \right] + C^{(0,3)} \left[\widetilde{\omega}_{3/0}{}^{(3)} \overline{r}^{(3)}_{C/C3} \right] + \overline{v}^{(0)}_{C3/O}, \quad \textbf{(5.74)}$$

where

$\overline{v}^{(0)}_{C4/O}$: Velocity vector of C_4 expressed in the $\mathfrak{T}_0\{O\}$ global coordinates,

$\overline{v}^{(0)}_{C3/O}$: Velocity vector of C_3 expressed in the $\mathfrak{T}_0\{O\}$ global coordinates,

$\widetilde{\omega}_{3/0}{}^{(3)}$: Angular velocity cross product matrix of $\mathfrak{T}_3\{B\}$ relative to fixed frame $\mathfrak{T}_0\{O\}$ expressed in $\mathfrak{T}_3\{B\}$ local coordinates,

$\widetilde{\omega}_{4/0}{}^{(4)}$: Angular velocity cross product matrix of $\mathfrak{T}_4\{C\}$ relative to fixed frame $\mathfrak{T}_0\{O\}$ expressed in $\mathfrak{T}_4\{C\}$ local coordinates.

5.2.2.2 Upper Extremity

i) Link-5 (Abdomen)

The velocity vector of C_5 expressed in the WFF, $\mathfrak{T}_0\{O\}$, is obtained in global coordinates as

$$\overline{v}^{(0)}_{C5/O} = D_0 \{\overline{r}^{(0)}_{C5/O}\}^{(0)}, \quad \textbf{(5.75)}$$

$$\overline{v}^{(0)}_{C5/O} = C^{(0,5)} \left[\overline{v}^{(5)}_{C5/L5} + \widetilde{\omega}_{5/0}{}^{(5)} \overline{r}^{(5)}_{C5/L5} \right] + C^{(0,1)} \left[\overline{v}^{(1)}_{L5/M4} + \widetilde{\omega}_{1/0}{}^{(1)} \overline{r}^{(1)}_{L5/M4} \right] + \overline{v}^{(0)}_{M4/O} . \quad \textbf{(5.76)}$$

Since the points C_5 and L_5 are on Link-5 and points L_5 and M_4 are on Link-1, one has

$$\overline{v}^{(5)}_{C5/L5} = 0 \quad \text{and} \quad \overline{v}^{(1)}_{L5/M4} = 0. \quad \textbf{(5.77)}$$

Hence, Equation (5.76) yields

$$\overline{v}^{(0)}_{C5/O} = C^{(0,5)} \left[\widetilde{\omega}_{5/0}{}^{(5)} \overline{r}^{(5)}_{C5/L5} \right] + C^{(0,1)} \left[\widetilde{\omega}_{1/0}{}^{(1)} \overline{r}^{(1)}_{L5/M4} \right] + \overline{v}^{(0)}_{M4/O}, \quad \textbf{(5.78)}$$

Where

$\overline{v}^{(0)}_{C5/O}$: Velocity vector of C_5 expressed in the $\mathrm{T}_0\{\mathrm{O}\}$ global coordinates,

$\overline{v}^{(0)}_{M4/O}$: Velocity vector of 4th marker M_4 expressed in the $\mathrm{T}_0\{\mathrm{O}\}$ global coordinates,

$\widetilde{\omega}_{5/0}{}^{(5)}$: Angular velocity cross product matrix of $\mathrm{T}_5\{L_5\}$ relative to fixed frame $\mathrm{T}_0\{\mathrm{O}\}$ expressed in $\mathrm{T}_5\{L_5\}$ local coordinates,

$\widetilde{\omega}_{1/0}{}^{(1)}$: Angular velocity cross product matrix of $\mathrm{T}_1\{M_1\}$ relative to fixed frame $\mathrm{T}_0\{\mathrm{O}\}$ expressed in $\mathrm{T}_1\{M_1\}$ local coordinates.

ii) Link-6 (Trunk)

The velocity vector of C_6 expressed in the WFF, $\mathrm{T}_0\{\mathrm{O}\}$, is obtained in global coordinates as

$$\overline{v}^{(0)}_{C6/O} = D_0\,\{\overline{r}^{(0)}_{C6/O}\}^{(0)}, \qquad \textbf{(5.79)}$$

$$\overline{v}^{(0)}_{C6/O} = C^{(0,6)}\left[\overline{v}^{(6)}_{C6/T12} + \widetilde{\omega}_{6/0}{}^{(6)}\,\overline{r}^{(6)}_{C6/T12}\right] + C^{(0,5)}\left[\overline{v}^{(5)}_{T12/C5} + \widetilde{\omega}_{5/0}{}^{(5)}\,\overline{r}^{(5)}_{T12/C5}\right] + \overline{v}^{(0)}_{C5/O}\,. \qquad \textbf{(5.80)}$$

Since the points C_6 and T_{12} are on Link-6 and points T_{12} and C_5 are on Link-5, one has

$$\overline{v}^{(6)}_{C6/T12} = 0 \text{ and } \overline{v}^{(5)}_{T12/C5} = 0\,. \qquad \textbf{(5.81)}$$

Hence, Equation (5.80) yields

$$\overline{v}^{(0)}_{C6/O} = C^{(0,6)}\left[\widetilde{\omega}_{6/0}{}^{(6)}\,\overline{r}^{(6)}_{C6/T12}\right] + C^{(0,5)}\left[\widetilde{\omega}_{5/0}{}^{(5)}\,\overline{r}^{(5)}_{T12/C5}\right] + \overline{v}^{(0)}_{C5/O}, \qquad \textbf{(5.82)}$$

where

$\overline{v}^{(0)}_{C6/O}$: Velocity vector of C_6 expressed in the $\mathrm{T}_0\{\mathrm{O}\}$ global coordinates,

$\overline{v}^{(0)}_{C5/O}$: Velocity vector of C_5 expressed in the $\mathrm{T}_0\{\mathrm{O}\}$ global coordinates,

$\widetilde{\omega}_{6/0}{}^{(6)}$: Angular velocity cross product matrix of $\mathrm{T}_6\{T_{12}\}$ relative to fixed frame $\mathrm{T}_0\{\mathrm{O}\}$ expressed in $\mathrm{T}_6\{T_{12}\}$ local coordinates,

$\widetilde{\omega}_{5/0}{}^{(5)}$: Angular velocity cross product matrix of $\mathrm{T}_5\{L_5\}$ relative to fixed frame

$\mathrm{T}_0\{\mathrm{O}\}$ expressed in $\mathrm{T}_5\{\ L_5\}$ local coordinates.

iii) Link-7 (Upper Arm)

The velocity vector of C_7 expressed in the WFF, $\mathrm{T}_0\{\mathrm{O}\}$, is obtained in global coordinates as

$$\overline{v}^{(0)}_{C7/O} = D_0\ \{\overline{r}^{(0)}_{C7/O}\}^{(0)}\ , \tag{5.83}$$

$$\overline{v}^{(0)}_{C7/O} = C^{(0,7)}\left[\ \overline{v}^{(7)}_{C7/D} + \widetilde{\omega}_{7/0}{}^{(7)}\ \overline{r}^{(7)}_{C7/D}\right] + C^{(0,6)}\left[\ \overline{v}^{(6)}_{D/C6} + \widetilde{\omega}_{6/0}{}^{(6)}\ \overline{r}^{(6)}_{D/C6}\right] + \overline{v}^{(0)}_{C6/O}. \tag{5.84}$$

Since points C_7 and D are on Link-7 and points D and C_6 are on Link-6, one has

$$\overline{v}^{(7)}_{C7/D} = 0 \text{ and } \overline{v}^{(6)}_{D/C6} = 0. \tag{5.85}$$

Hence, Equation (5.84) yields

$$\overline{v}^{(0)}_{C7/O} = C^{(0,7)}\left[\ \widetilde{\omega}_{7/0}{}^{(7)}\ \overline{r}^{(7)}_{C7/D}\right] + C^{(0,6)}\left[\ \widetilde{\omega}_{6/0}{}^{(6)}\ \overline{r}^{(6)}_{D/C6}\ \right] + \overline{v}^{(0)}_{C6/O}, \tag{5.86}$$

where

$\overline{v}^{(0)}_{C7/O}$: Velocity vector of C_7 expressed in the $\mathrm{T}_0\{\mathrm{O}\}$ global coordinates,

$\overline{v}^{(0)}_{C6/O}$: Velocity vector of C_6 expressed in the $\mathrm{T}_0\{\mathrm{O}\}$ global coordinates,

$\widetilde{\omega}_{7/0}{}^{(7)}$: Angular velocity cross product matrix of $\mathrm{T}_7\{D\}$ relative to fixed frame $\mathrm{T}_0\{\mathrm{O}\}$ expressed in $\mathrm{T}_7\{D\}$ local coordinates,

$\widetilde{\omega}_{6/0}{}^{(6)}$: Angular velocity cross product matrix of $\mathrm{T}_6\{\ T_{12}\}$ relative to fixed frame $\mathrm{T}_0\{\mathrm{O}\}$ expressed in $\mathrm{T}_6\{\ T_{12}\}$ local coordinates.

iv) Link-8 (Lower Arm)

The velocity vector of C_8 expressed in the WFF, $\mathrm{T}_0\{\mathrm{O}\}$, is obtained in global coordinates as

$$\overline{v}^{(0)}_{C8/O} = D_0\ \{\overline{r}^{(0)}_{C8/O}\}^{(0)}, \tag{5.87}$$

$$\overline{v}^{(0)}_{C8/O} = C^{(0,8)}\left[\ \overline{v}^{(8)}_{C8/E} + \widetilde{\omega}_{8/0}{}^{(8)}\ \overline{r}^{(8)}_{C8/E}\right] + C^{(0,7)}\left[\ \overline{v}^{(7)}_{E/C7} + \widetilde{\omega}_{7/0}{}^{(7)}\ \overline{r}^{(7)}_{E/C7}\right] + \overline{v}^{(0)}_{C7/O}. \tag{5.88}$$

Since points C_8 and E are on Link-8 and points E and C_7 are on Link-7, one has

$$\overline{v}^{(8)}_{C8/_E} = 0 \text{ and } \overline{v}^{(7)}_{E/_{C7}} = 0. \quad \textbf{(5.89)}$$

Hence, Equation (5.88) yields

$$\overline{v}^{(0)}_{C8/_O} = C^{(0,8)}\left[\ \widetilde{\omega}_{8/0}{}^{(8)}\,\overline{r}^{(8)}_{C8/_E}\right] + C^{(0,7)}\left[\ \widetilde{\omega}_{7/0}{}^{(7)}\,\overline{r}^{(7)}_{E/_{C7}}\ \right] + \overline{v}^{(0)}_{C7/_O}, \quad \textbf{(5.90)}$$

where

$\overline{v}^{(0)}_{C8/_O}$: Velocity vector of C_8 expressed in the $\mathrm{T}_0\{\mathrm{O}\}$ global coordinates,

$\overline{v}^{(0)}_{C7/_O}$: Velocity vector of C_7 expressed in the $\mathrm{T}_0\{\mathrm{O}\}$ global coordinates,

$\widetilde{\omega}_{8/0}{}^{(8)}$: Angular velocity cross product matrix of $\mathrm{T}_8\{E\}$ relative to fixed frame $\mathrm{T}_0\{\mathrm{O}\}$ expressed in $\mathrm{T}_8\{E\}$ local coordinates,

$\widetilde{\omega}_{7/0}{}^{(7)}$: Angular velocity cross product matrix of $\mathrm{T}_7\{D\}$ relative to fixed frame $\mathrm{T}_0\{\mathrm{O}\}$ expressed in $\mathrm{T}_7\{D\}$ local coordinates.

v) Link-9 (Hand)

The velocity vector of C_9 expressed in the WFF, $\mathrm{T}_0\{\mathrm{O}\}$, is obtained in global coordinates.

$$\overline{v}^{(0)}_{C9/_O} = D_0\,\{\overline{r}^{(0)}_{C9/_O}\}^{(0)}, \quad \textbf{(5.91)}$$

$$\overline{v}^{(0)}_{C9/_O} = C^{(0,9)}\left[\ \overline{v}^{(9)}_{C9/_F} + \widetilde{\omega}_{9/0}{}^{(9)}\,\overline{r}^{(9)}_{C9/_F}\right] + C^{(0,8)}\left[\ \overline{v}^{(8)}_{F/_{C8}} + \widetilde{\omega}_{8/0}{}^{(8)}\,\overline{r}^{(8)}_{F/_{C8}}\right] + \overline{v}^{(0)}_{C8/_O}. \quad \textbf{(5.92)}$$

Since points C_9 and F are on Link-9 and points F and C_8 are on Link-3, one has

$$\overline{v}^{(9)}_{C9/_F} = 0 \quad \text{and} \quad \overline{v}^{(8)}_{F/_{C8}} = 0\ . \quad \textbf{(5.93)}$$

Hence, Equation (5.92) yields

$$\overline{v}^{(0)}_{C9/_O} = C^{(0,9)}\left[\ \widetilde{\omega}_{9/0}{}^{(9)}\,\overline{r}^{(9)}_{C9/_F}\right] + C^{(0,8)}\left[\ \widetilde{\omega}_{8/0}{}^{(8)}\,\overline{r}^{(8)}_{F/_{C8}}\ \right] + \overline{v}^{(0)}_{C8/_O}, \quad \textbf{(5.94)}$$

where

$\overline{v}^{(0)}_{C9/_O}$: Velocity vector of C_9 expressed in the $\mathrm{T}_0\{\mathrm{O}\}$ global coordinates,

$\overline{v}^{(0)}_{C8/_O}$: Velocity vector of C_8 expressed in the $\mathrm{T}_0\{\mathrm{O}\}$ global coordinates,

$\widetilde{\omega}_{9/0}{}^{(9)}$: Angular velocity cross product matrix of $\mathrm{T}_9\{F\}$ relative to fixed frame $\mathrm{T}_0\{\mathrm{O}\}$ expressed in $\mathrm{T}_9\{F\}$ local coordinates,

$\widetilde{\omega}_{8/0}{}^{(8)}$: Angular velocity cross product matrix of $\mathrm{T}_8\{E\}$ relative to fixed frame $\mathrm{T}_0\{\mathrm{O}\}$ expressed in $\mathrm{T}_8\{E\}$ local coordinates.

vi) Link-10 (Neck)

The velocity vector of C_{10} expressed in the WFF, $\mathrm{T}_0\{\mathrm{O}\}$, is obtained in global coordinates

$$\overline{v}^{(0)}_{C10/_O} = D_0\,\{\overline{r}^{(0)}_{C10/_O}\}^{(0)}, \qquad \textbf{(5.95)}$$

$$\overline{v}^{(0)}_{C10/_O} = C^{(0,10)}\left[\overline{v}^{(10)}_{C10/_{T1}} + \widetilde{\omega}_{10/0}{}^{(10)}\,\overline{r}^{(10)}_{C10/_{T1}}\right] + C^{(0,6)}\left[\overline{v}^{(6)}_{T1/_{C6}} + \widetilde{\omega}_{6/0}{}^{(6)}\,\overline{r}^{(6)}_{T1/_{C6}}\right] + \overline{v}^{(0)}_{C6/_O}. \qquad \textbf{(5.96)}$$

Since points C_{10} and T_1 are on Link-10 and points T_1 and C_6 are on Link-6, one has

$$\overline{v}^{(10)}_{C10/_{T1}} = 0 \quad \text{and} \quad \overline{v}^{(6)}_{T1/_{C6}} = 0\,. \qquad \textbf{(5.97)}$$

Hence, Equation (5.96) yields

$$\overline{v}^{(0)}_{C10/_O} = C^{(0,10)}\left[\widetilde{\omega}_{10/0}{}^{(10)}\,\overline{r}^{(10)}_{C10/_{T1}}\right] + C^{(0,6)}\left[\widetilde{\omega}_{6/0}{}^{(6)}\,\overline{r}^{(6)}_{T1/_{C6}}\right] + \overline{v}^{(0)}_{C6/_O}\,, \qquad \textbf{(5.98)}$$

where

$\overline{v}^{(0)}_{C10/_O}$: Velocity vector of C_{10} expressed in the $\mathrm{T}_0\{\mathrm{O}\}$ global coordinates,

$\overline{v}^{(0)}_{C6/_O}$: Velocity vector of C_6 expressed in the $\mathrm{T}_0\{\mathrm{O}\}$ global coordinates,

$\widetilde{\omega}_{10/0}{}^{(10)}$: Angular velocity cross product matrix of $\mathrm{T}_{10}\{T_1\}$ relative to fixed frame $\mathrm{T}_0\{\mathrm{O}\}$ expressed in $\mathrm{T}_{10}\{T_1\}$ local coordinates,

$\widetilde{\omega}_{6/0}{}^{(6)}$: Angular velocity cross product matrix of $\mathrm{T}_6\{T_{12}\}$ relative to fixed frame $\mathrm{T}_0\{\mathrm{O}\}$ expressed in $\mathrm{T}_6\{T_{12}\}$ local coordinates.

vii) Link-11 (Head)

The velocity vector of C_{11} expressed in the WFF, $\mathrm{T}_0\{\mathrm{O}\}$, is obtained in global coordinates as

$$\overline{v}^{(0)}_{C11/O} = D_0 \{\overline{r}^{(0)}_{C11/O}\}^{(0)}, \quad \textbf{(5.99)}$$

yielding

$$\overline{v}^{(0)}_{C11/O} = C^{(0,11)}\left[\overline{v}^{(11)}_{C11/CS1} + \widetilde{\omega}_{11/0}{}^{(11)}\overline{r}^{(11)}_{C11/CS1}\right] + C^{(0,10)}\left[\overline{v}^{(10)}_{CS1/C10} + \widetilde{\omega}_{10/0}{}^{(10)}\overline{r}^{(10)}_{CS1/C10}\right] + \overline{v}^{(0)}_{C10/O}. \quad \textbf{(5.100)}$$

Since points C_{11} and CS_1 are on Link-11 and points CS_1 and C_{10} are on Link-10, one has

$$\overline{v}^{(11)}_{C11/CS1} = 0 \quad \text{and} \quad \overline{v}^{(10)}_{CS1/C10} = 0\,. \quad \textbf{(5.101)}$$

Hence, Equation (5.100) yields

$$\overline{v}^{(0)}_{C11/O} = C^{(0,11)}\left[\widetilde{\omega}_{11/0}{}^{(11)}\,\overline{r}^{(11)}_{C11/CS1}\right] + C^{(0,10)}\left[\widetilde{\omega}_{10/0}{}^{(10)}\,\overline{r}^{(10)}_{CS1/C10}\right] + \overline{v}^{(0)}_{C10/O}, \quad \textbf{(5.102)}$$

where

$\overline{v}^{(0)}_{C11/O}$: Velocity vector of C_{11} expressed in the $\mathrm{T}_0\{\mathrm{O}\}$ global coordinates,

$\overline{v}^{(0)}_{C10/O}$: Velocity vector of C_{10} expressed in the $\mathrm{T}_0\{\mathrm{O}\}$ global coordinates,

$\widetilde{\omega}_{11/0}{}^{(11)}$: Angular velocity cross product matrix of $\mathrm{T}_{11}\{CS_1\}$ relative to fixed frame $\mathrm{T}_0\{\mathrm{O}\}$ expressed in $\mathrm{T}_{11}\{CS_1\}$ local coordinates,

$\widetilde{\omega}_{10/0}{}^{(10)}$: Angular velocity cross product matrix of $\mathrm{T}_{10}\{T_1\}$ relative to fixed frame $\mathrm{T}_0\{\mathrm{O}\}$ expressed in $\mathrm{T}_{10}\{T_1\}$ local coordinates.

5.2.3 Acceleration Analysis

Next, acceleration analysis is performed in order to obtain the acceleration vectors of the center of masses for each link. Acceleration vectors are then used in the inverse dynamic analysis in order to find the joint moments and reaction forces. Acceleration of a point as observed in different frames (see Figure 5.4) is as followed:

$$a_{P/A}^{(a)} = a_{P/B}^{(b)} + 2\tilde{\omega}_{b/a} v_{P/B}^{(b)} + \tilde{\alpha}_{b/a}\, r_{P/B}^{(b)} + \tilde{\omega}_{b/a}\tilde{\omega}_{b/a} r_{P/B}^{(b)} + a_{B/A}^{(a)}, \qquad \textbf{(5.103)}$$

where

$a_{P/A}^{(a)}$: Acceleration vector of point P with respect to point A in $\mathrm{T}_a\{\mathrm{A}\}$,

$a_{P/B}^{(b)}$: Acceleration vector of point P with respect to point B in $\mathrm{T}_b\{\mathrm{B}\}$,

$\tilde{\omega}_{b/a}$: Angular velocity cross product matrix of $\mathrm{T}_b\{\mathrm{B}\}$ relative to fixed frame $\mathrm{T}_a\{\mathrm{A}\}$,

$\overline{v}_{P/B}^{(b)}$: Velocity vector of point P relative to B in body reference frame $\mathrm{T}_b\{\mathrm{B}\}$,

$\tilde{\alpha}_{b/a}$: Angular acceleration cross product matrix of $\mathrm{T}_b\{\mathrm{B}\}$ relative to fixed frame $\mathrm{T}_a\{\mathrm{A}\}$,

$\overline{r}_{P/B}^{(b)}$: Position vector of point P relative to B in body reference frame $\mathrm{T}_b\{\mathrm{B}\}$,

$\overline{a}_{B/A}^{(a)}$: Acceleration vector of point P relative to B in fixed frame $\mathrm{T}_a\{\mathrm{A}\}$.

5.2.3.1 Lower Extremity

i) Link-1 (Hip and Saddle)

In **[22]**, the kinematic data of the saddle is obtained via three reflective markers placed on saddle (see Figure 5.5).

The origin of the body reference frame of Link-1, $\mathrm{T}_1\{M_1\}$ is placed on the 1st marker. The known kinematic data related to 4th marker are the position $\overline{r}_{M4/O}^{(0)}$, the velocity $\overline{v}_{M4/O}^{(0)}$, and the acceleration $\overline{a}_{M4/O}^{(0)}$ of the marker. Furthermore, the angular

velocity $\overline{\omega}_{1/0}$ and the angular acceleration $\overline{\alpha}_{1/0}$ of body-1 are also known in the WFF global coordinates, $\mathrm{T}_0\{\mathrm{O}\}$. By using these data, the acceleration of the center of masses of the links and the angular accelerations of the links in the rider model may be obtained as described in the following sections.

ii) Link-2 (Thigh)

The acceleration vector of C_2 expressed in the WFF, $\mathrm{T}_0\{\mathrm{O}\}$, is obtained in global coordinates as

$$\overline{a}^{(0)}_{C2/_O} = D_0\,\{\overline{v}^{(0)}_{C2/_O}\}^{(0)}\,, \qquad \textbf{(5.104)}$$

yielding

$$\overline{a}^{(0)}_{C2/_O} = C^{(0,2)}\left[2\widetilde{\omega}_{2/0}{}^{(2)}\,\overline{v}^{(2)}_{C2/_A} + \widetilde{\omega}_{2/0}{}^{(2)}\left(\widetilde{\omega}_{2/0}{}^{(2)}\,\overline{r}^{(2)}_{C2/_A}\right) + \overline{a}^{(2)}_{C2/_A} + \tilde{\alpha}^{(2)}_{2/0}\;\overline{r}^{(2)}_{C2/_A}\right] + C^{(0,1)}\left[2\,\widetilde{\omega}_{1/0}{}^{(1)}\overline{v}^{(1)}_{A/_{M4}} + \widetilde{\omega}_{1/0}{}^{(1)}\left(\widetilde{\omega}_{1/0}{}^{(1)}\,\overline{r}^{(1)}_{A/_{M4}}\right) + \overline{a}^{(1)}_{A/_{M4}} + \tilde{\alpha}^{(1)}_{1/0}\;\overline{r}^{(1)}_{A/_{M4}}\right] + \overline{a}^{(0)}_{M4/_O}\,. \qquad \textbf{(5.105)}$$

Since points C_2 and A are on Link-2 and points A and M are on Link-1, one has

$$\overline{v}^{(2)}_{C2/_A} = 0\,,\;\; \overline{v}^{(1)}_{A/_{M4}} = 0 \;\text{ and }\; \overline{a}^{(2)}_{C2/_A} = 0\,,\; \overline{a}^{(1)}_{A/_{M4}} = 0. \qquad \textbf{(5.106)}$$

Hence, Equation (5.105) yields

$$\overline{a}^{(0)}_{C2/_O} = C^{(0,2)}\left[\,\widetilde{\omega}_{2/0}{}^{(2)}\left(\widetilde{\omega}_{2/0}{}^{(2)}\,\overline{r}^{(2)}_{C2/_A}\right) + \tilde{\alpha}^{(2)}_{2/0}\,\overline{r}^{(2)}_{C2/_A}\,\right] + C^{(0,1)}\left[\widetilde{\omega}_{1/0}{}^{(1)}\left(\widetilde{\omega}_{1/0}{}^{(1)}\,\overline{r}^{(1)}_{A/_{M4}}\right) + \tilde{\alpha}^{(1)}_{1/0}\;\overline{r}^{(1)}_{A/_{M4}}\,\right] + \overline{a}^{(0)}_{M4/_O}\,, \qquad \textbf{(5.107)}$$

where

$\overline{a}^{(0)}_{M4/_O}$: Acceleration of the 4th Marker on the saddle, Point M_4, expressed in the $\mathrm{T}_0\{\mathrm{O}\}$ global coordinates,

$\overline{a}^{(0)}_{C2/_O}$: Acceleration of C_2 expressed in the $\mathrm{T}_0\{\mathrm{O}\}$ global coordinates,

$\tilde{\alpha}_{2/0}$: Angular acceleration cross product matrix of $\mathrm{T}_2\{\mathrm{A}\}$ relative to fixed frame $\mathrm{T}_0\{\mathrm{O}\}$.

iii) Link-3 (Shank)

The acceleration vector of C_3 expressed in the WFF, $\mathrm{T}_0\{\mathrm{O}\}$, is obtained in global coordinates as

$$\overline{a}^{(0)}_{C3/O} = D_0\,\{\overline{v}^{(0)}_{C3/O}\}^{(0)}\,, \qquad \textbf{(5.108)}$$

yielding

$$\overline{a}^{(0)}_{C3/O} = C^{(0,3)}\left[2\tilde{\omega}_{3/0}{}^{(3)}\,\overline{v}^{(3)}_{C3/B} + \tilde{\omega}_{3/0}{}^{(3)}\left(\tilde{\omega}_{3/0}{}^{(3)}\,\overline{r}^{(3)}_{C3/B}\right) + \overline{a}^{(3)}_{C3/B} + \tilde{\alpha}^{(3)}_{3/0}\,\overline{r}^{(3)}_{C3/B}\right] +$$
$$C^{(0,2)}\left[2\,\tilde{\omega}_{2/0}{}^{(2)}\,\overline{v}^{(2)}_{B/C2} + \tilde{\omega}_{2/0}{}^{(2)}\left(\tilde{\omega}_{2/0}{}^{(2)}\overline{r}^{(2)}_{B/C2}\right) + \overline{a}^{(2)}_{B/C2} + \tilde{\alpha}^{(2)}_{2/0}\,\overline{r}^{(2)}_{B/C2}\right] + \overline{a}^{(0)}_{C2/O}\,. \qquad \textbf{(5.109)}$$

Since points C_3 and B are on Link-3 and points B and C_2 are on Link-2, one has

$$\overline{v}^{(3)}_{C3/B} = 0 \;\;,\;\; \overline{v}^{(2)}_{B/C2} = 0 \;\; \text{and} \;\; \overline{a}^{(3)}_{C3/B} = 0 \;\;,\;\; \overline{a}^{(2)}_{B/C2} = 0. \qquad \textbf{(5.110)}$$

Hence, Equation (5.109) yields

$$\overline{a}^{(0)}_{C3/O} =$$
$$C^{(0,3)}\left[\,\tilde{\omega}_{3/0}{}^{(3)}\,\left(\tilde{\omega}_{3/0}{}^{(3)}\,\overline{r}^{(3)}_{C3/B}\right) + \tilde{\alpha}^{(3)}_{3/0}\,\overline{r}^{(3)}_{C3/B}\,\right] +$$
$$C^{(0,2)}\left[\,\tilde{\omega}_{2/0}{}^{(2)}\,\left(\tilde{\omega}_{2/0}{}^{(2)}\,\overline{r}^{(2)}_{B/C2}\right) + \tilde{\alpha}^{(2)}_{2/0}\,\overline{r}^{(2)}_{B/C2}\,\right] + \overline{a}^{(0)}_{C2/O}\,, \qquad \textbf{(5.111)}$$

where

$\overline{a}^{(0)}_{C3/O}$: Acceleration of C_3 expressed in the $\mathrm{T}_0\{\mathrm{O}\}$ global coordinates,

$\overline{a}^{(0)}_{C2/O}$: Acceleration of C_2 expressed in the $\mathrm{T}_0\{\mathrm{O}\}$ global coordinates,

$\tilde{\alpha}_{3/0}$: Angular acceleration cross product matrix of $\mathrm{T}_3\{\mathrm{B}\}$ relative to fixed frame $\mathrm{T}_0\{\mathrm{O}\}$,

$\tilde{\alpha}_{2/0}$: Angular acceleration cross product matrix of $\mathrm{T}_2\{\mathrm{A}\}$ relative to fixed frame $\mathrm{T}_0\{\mathrm{O}\}$.

iv) Link-4 (Foot)

The acceleration vector of C_4 expressed in the WFF, $\mathrm{F}_0\{\mathrm{O}\}$, is obtained in global coordinates as

$$\overline{a}^{(0)}_{C4/O} = D_0\,\{\overline{v}^{(0)}_{C4/O}\}^{(0)}\,, \qquad \textbf{(5.112)}$$

yielding

$$\overline{a}^{(0)}_{C4/O} = C^{(0,4)}\left[2\widetilde{\omega}_{4/0}{}^{(4)}\,\overline{v}^{(4)}_{C4/C} + \widetilde{\omega}_{4/0}{}^{(4)}\left(\widetilde{\omega}_{4/0}{}^{(4)}\,\overline{r}^{(4)}_{C4/C}\right) + \overline{a}^{(4)}_{C4/C} + \tilde{\alpha}^{(4)}_{4/0}\,\overline{r}^{(4)}_{C4/C}\right] +$$

$$C^{(0,3)}\left[\,2\,\widetilde{\omega}_{3/0}{}^{(3)}\,\overline{v}^{(3)}_{C/C3} + \widetilde{\omega}_{3/0}{}^{(3)}\left(\widetilde{\omega}_{3/0}{}^{(3)}\,\overline{r}^{(3)}_{C/C3}\right) + \overline{a}^{(3)}_{C/C3} + \widetilde{\alpha}^{(3)}_{3/0}\,\overline{r}^{(3)}_{C/C3}\right] +$$

$$\overline{a}^{(0)}_{C3/O}\,. \qquad \textbf{(5.113)}$$

Since points C_4 and C are on Link-4 and points C and C_3 are on Link-3, one has

$$\overline{v}^{(4)}_{C4/C} = 0 \;\;, \overline{v}^{(3)}_{C/C3} = 0 \;\; \text{and} \;\; \overline{a}^{(4)}_{C4/C} = 0 \;\;, \;\; \overline{a}^{(3)}_{C/C3} = 0. \qquad \textbf{(5.114)}$$

Hence, Equation (5.113) yields

$$\overline{a}^{(0)}_{C4/O} =$$

$$C^{(0,4)}\left[\,\widetilde{\omega}_{4/0}{}^{(4)}\left(\widetilde{\omega}_{4/0}{}^{(4)}\,\overline{r}^{(4)}_{C4/C}\right) + \widetilde{\alpha}^{(4)}_{4/0}\,\overline{r}^{(4)}_{C4/C}\right] +$$

$$C^{(0,3)}\left[\,\widetilde{\omega}_{3/0}{}^{(3)}\left(\widetilde{\omega}_{3/0}{}^{(3)}\,\overline{r}^{(3)}_{C/C3}\right) + \widetilde{\alpha}^{(3)}_{3/0}\,\overline{r}^{(3)}_{C/C3}\right] + \overline{a}^{(0)}_{C3/O}\,, \qquad \textbf{(5.115)}$$

where

$\overline{a}^{(0)}_{C4/O}$: Acceleration of C_4 expressed in the $\mathrm{F}_0\{\mathrm{O}\}$ global coordinates,

$\overline{a}^{(0)}_{C3/O}$: Acceleration of C_3 expressed in the $\mathrm{F}_0\{\mathrm{O}\}$ global coordinates,

$\tilde{\alpha}_{4/0}$: Angular acceleration cross product matrix of $\mathrm{F}_4\{\mathrm{C}\}$ relative to fixed frame $\mathrm{F}_0\{\mathrm{O}\}$,

$\tilde{\alpha}_{3/0}$: Angular acceleration cross product matrix of $\mathrm{F}_3\{\mathrm{B}\}$ relative to fixed frame $\mathrm{F}_0\{\mathrm{O}\}$.

5.2.3.2 Upper Extremity

i) Link-5 (Abdomen)

The acceleration vector of C_5 expressed in the WFF, $\mathrm{T}_0\{\mathrm{O}\}$, is obtained in global coordinates as

$$\overline{a}^{(0)}_{C5/O} = D_0\,\{\overline{v}^{(0)}_{C5/O}\}^{(0)}, \tag{5.116}$$

yielding

$$\overline{a}^{(0)}_{C5/O} = C^{(0,5)}\left[2\widetilde{\omega}_{5/0}{}^{(5)}\,\overline{v}^{(5)}_{C5/L5} + \widetilde{\omega}_{5/0}{}^{(5)}\left(\widetilde{\omega}_{5/0}{}^{(5)}\overline{r}^{(5)}_{C5/L5}\right) + \overline{a}^{(5)}_{C5/L5} + \tilde{\alpha}^{(5)}_{5/0}\,\overline{r}^{(5)}_{C5/L5}\right] + C^{(0,1)}\left[2\widetilde{\omega}_{1/0}{}^{(1)}\overline{v}^{(1)}_{L5/M4} + \widetilde{\omega}_{1/0}{}^{(1)}\left(\widetilde{\omega}_{1/0}{}^{(1)}\,\overline{r}^{(1)}_{L5/M4}\right) + \overline{a}^{(1)}_{L5/M4} + \tilde{\alpha}^{(1)}_{1/0}\,\overline{r}^{(1)}_{L5/M4}\right] + \overline{a}^{(0)}_{M4/O}. \tag{5.117}$$

Since points C_5 and L_5 are on Link-5 and points L_5 and M_4 are on Link-1, one has

$$\overline{v}^{(5)}_{C5/L5} = 0 \;\;,\;\; \overline{v}^{(1)}_{L5/M4} = 0 \;\; \text{and} \;\; \overline{a}^{(5)}_{C5/L5} = 0 \;\;,\;\; \overline{a}^{(1)}_{L5/M4} = 0. \tag{5.118}$$

Hence, Equation (5.117) yields

$$\overline{a}^{(0)}_{C5/O} = C^{(0,5)}\left[\,\widetilde{\omega}_{5/0}{}^{(5)}\left(\widetilde{\omega}_{5/0}{}^{(5)}\,\overline{r}^{(5)}_{C5/L5}\right) + \widetilde{\alpha}^{(5)}_{5/0}\,\overline{r}^{(5)}_{C5/L5}\,\right] + C^{(0,1)}\left[\,\widetilde{\omega}_{1/0}{}^{(1)}\left(\widetilde{\omega}_{1/0}{}^{(1)}\,\overline{r}^{(1)}_{L5/M4}\right) + \widetilde{\alpha}^{(1)}_{1/0}\,\overline{r}^{(1)}_{L5/M4}\,\right] + \overline{a}^{(0)}_{M4/O}\,, \tag{5.119}$$

where

$\overline{a}^{(0)}_{M4/O}$: Acceleration of the 4th Marker on the saddle, Point M_4, expressed in the $\mathrm{T}_0\{\mathrm{O}\}$ global coordinates,

$\overline{a}^{(0)}_{C5/O}$: Acceleration of C_5 expressed in the $\mathrm{T}_0\{\mathrm{O}\}$ global coordinates,

$\tilde{\alpha}_{1/0}$: Angular acceleration cross product matrix of $\mathrm{T}_1\{M_1\}$ relative to fixed frame $\mathrm{T}_0\{\mathrm{O}\}$,

$\tilde{\alpha}_{5/0}$: Angular acceleration cross product matrix of $\mathrm{T}_5\{\mathrm{L5}\}$ relative to fixed frame $\mathrm{T}_0\{\mathrm{O}\}$.

ii) Link-6 (Trunk)

The acceleration vector of C_6 expressed in the WFF, $\mathrm{F}_0\{\mathrm{O}\}$, is obtained in global coordinates as

$$\overline{a}^{(0)}_{C6/O} = D_0\,\{\overline{v}^{(0)}_{C6/O}\}^{(0)}, \qquad \textbf{(5.120)}$$

yielding

$$\overline{a}^{(0)}_{C6/O} =$$

$$C^{(0,6)}\left[2\widetilde{\omega}_{6/0}{}^{(6)}\,\overline{v}^{(6)}_{C6/T12} + \widetilde{\omega}_{6/0}{}^{(6)}\left(\widetilde{\omega}_{6/0}{}^{(6)}\,\overline{r}^{(6)}_{C6/T12}\right) + \overline{a}^{(6)}_{C6/T12} + \widetilde{\alpha}^{(6)}_{6/0}\,\overline{r}^{(6)}_{C6/T12}\right] +$$

$$C^{(0,5)}\left[2\,\widetilde{\omega}_{5/0}{}^{(5)}\,\overline{v}^{(5)}_{T12/C5} + \widetilde{\omega}_{5/0}{}^{(5)}\left(\widetilde{\omega}_{5/0}{}^{(5)}\,\overline{r}^{(5)}_{T12/C5}\right) + \overline{a}^{(5)}_{T12/C5} + \widetilde{\alpha}^{(5)}_{5/0}\,\overline{r}^{(5)}_{T12/C5}\right] + \overline{a}^{(0)}_{C5/O}.$$

(5.121)

Since points C_6 and T_{12} are on Link-6 and points T_{12} and C_5 are on Link-5, one has

$$\overline{v}^{(6)}_{C6/T12} = 0 \quad , \quad \overline{v}^{(5)}_{T12/C5} = 0 \quad \text{and} \quad \overline{a}^{(6)}_{C6/T12} = 0\,, \quad \overline{a}^{(5)}_{T12/C5} = 0. \qquad \textbf{(5.122)}$$

Hence, Equation (5.121) yields

$$\overline{a}^{(0)}_{C6/O} =$$

$$C^{(0,6)}\left[\widetilde{\omega}_{6/0}{}^{(6)}\left(\widetilde{\omega}_{6/0}{}^{(6)}\overline{r}^{(6)}_{C6/T12}\right) + \tilde{\alpha}^{(6)}_{6/0}\,\overline{r}^{(6)}_{C6/T12}\right] +$$

$$C^{(0,5)}\left[\widetilde{\omega}_{5/0}{}^{(5)}\left(\widetilde{\omega}_{5/0}{}^{(5)}\,\overline{r}^{(5)}_{T12/C5}\right) + \widetilde{\alpha}^{(5)}_{5/0}\,\overline{r}^{(5)}_{T12/C5}\right] + \overline{a}^{(0)}_{C5/O}$$

(5.123)

where

$\overline{a}^{(0)}_{C6/O}$: Acceleration of C_6 expressed in the $\mathrm{F}_0\{\mathrm{O}\}$ global coordinates,

$\overline{a}^{(0)}_{C5/O}$: Acceleration of C_5 expressed in the $\mathrm{F}_0\{\mathrm{O}\}$ global coordinates,

$\tilde{\alpha}_{5/0}$: Angular acceleration cross product matrix of $\mathrm{F}_5\{L_5\}$ relative to fixed frame $\mathrm{F}_0\{\mathrm{O}\}$,

$\tilde{\alpha}_{6/0}$: Angular acceleration cross product matrix of $\mathrm{F}_6\{T_{12}\}$ relative to fixed frame $\mathrm{F}_0\{\mathrm{O}\}$.

iii) Link-7 (Upper Arm)

The acceleration vector of C_7 expressed in the WFF, $\mathrm{T}_0\{\mathrm{O}\}$, is obtained in global coordinates as

$$\overline{a}^{(0)}_{C7/O} = D_0\,\{\overline{v}^{(0)}_{C7/O}\}^{(0)}, \tag{5.124}$$

yielding

$$\overline{a}^{(0)}_{C7/O} = C^{(0,7)}\left[2\tilde{\omega}_{7/0}{}^{(7)}\overline{v}^{(7)}_{C7/D} + \tilde{\omega}_{7/0}{}^{(7)}\left(\tilde{\omega}_{7/0}{}^{(7)}\overline{r}^{(7)}_{C7/D}\right) + \overline{a}^{(7)}_{C7/D} + \tilde{\alpha}^{(7)}_{7/0}\ \overline{r}^{(7)}_{C7/D}\right] +$$
$$C^{(0,6)}\left[2\ \tilde{\omega}_{6/0}{}^{(6)}\ \overline{v}^{(6)}_{D/C6} + \tilde{\omega}_{6/0}{}^{(6)}\left(\tilde{\omega}_{6/0}{}^{(6)}\ \overline{r}^{(6)}_{D/C6}\right) + \overline{a}^{(6)}_{D/C6} + \tilde{\alpha}^{(6)}_{6/0}\ \overline{r}^{(6)}_{D/C6}\right] + \overline{a}^{(0)}_{C6/O}. \tag{5.125}$$

Since points C_7 and D are on Link-7 and points D and C_6 are on Link-6, one has

$$\overline{v}^{(7)}_{C7/D} = 0\ \ ,\ \ \overline{v}^{(6)}_{D/C6} = 0\ \ \text{and}\ \ \overline{a}^{(7)}_{C7/D} = 0,\ \overline{a}^{(6)}_{D/C6} = 0. \tag{5.126}$$

Hence, Equation (5.125) yields

$$\overline{a}^{(0)}_{C7/O} = C^{(0,7)}\left[\tilde{\omega}^{(7)}_{7/0}\left(\tilde{\omega}^{(7)}_{7/0}\overline{r}^{(7)}_{C7/D}\right) + \tilde{\alpha}^{(7)}_{7/0}\ \overline{r}^{(7)}_{C7/D}\right]$$
$$+ C^{(0,6)}\left[\tilde{\omega}^{(6)}_{6/0}\left(\tilde{\omega}^{(6)}_{6/0}\overline{r}^{(6)}_{D/C6}\right) + \tilde{\alpha}^{(6)}_{6/0}\ \overline{r}^{(6)}_{D/C6}\right] + \overline{a}^{(0)}_{C6/O} \tag{5.127}$$

where

$\overline{a}^{(0)}_{C7/O}$: Acceleration of C_7 expressed in the $\mathrm{T}_0\{\mathrm{O}\}$ global coordinates,

$\overline{a}^{(0)}_{C6/O}$: Acceleration of C_6 expressed in the $\mathrm{T}_0\{\mathrm{O}\}$ global coordinates,

$\tilde{\alpha}_{7/0}$: Angular acceleration cross product matrix of $\mathrm{T}_7\{D\}$ relative to fixed frame $\mathrm{T}_0\{\mathrm{O}\}$,

$\tilde{\alpha}_{6/0}$: Angular acceleration cross product matrix of $\mathrm{T}_6\{T_{12}\}$ relative to fixed frame $\mathrm{T}_0\{\mathrm{O}\}$,

iv) Link-8 (Lower Arm)

The acceleration vector of C_8 expressed in the WFF, $\mathrm{T}_0\{\mathrm{O}\}$, is obtained in global coordinates as

$$\overline{a}^{(0)}_{C8/O} = D_0 \{\overline{v}^{(0)}_{C8/O}\}^{(0)}, \quad \textbf{(5.128)}$$

yielding

$$\overline{a}^{(0)}_{C8/O} =$$

$$C^{(0,8)}\left[2\widetilde{\omega}_{8/0}{}^{(8)}\, \overline{v}^{(8)}_{C8/E} + \widetilde{\omega}_{8/0}{}^{(8)} \left(\widetilde{\omega}_{8/0}{}^{(8)}\, \overline{r}^{(8)}_{C8/E}\right) + \overline{a}^{(8)}_{C8/E} + \widetilde{\alpha}^{(8)}_{8/0}\, \overline{r}^{(8)}_{C8/E} \right] +$$

$$C^{(0,7)}\left[2\, \widetilde{\omega}_{7/0}{}^{(7)}\, \overline{v}^{(7)}_{E/C7} + \widetilde{\omega}_{7/0}{}^{(7)} \left(\widetilde{\omega}_{7/0}{}^{(7)}\, \overline{r}^{(7)}_{E/C7}\right) + \overline{a}^{(7)}_{E/C7} + \widetilde{\alpha}^{(7)}_{7/0}\, \overline{r}^{(7)}_{E/C7} \right] +$$

$$\overline{a}^{(0)}_{C7/O}. \quad \textbf{(5.129)}$$

Since points C_8 and E are on Link-8 and points E and C_7 are on Link-7, one has

$$\overline{v}^{(8)}_{C8/E} = 0 \;\; , \;\; \overline{v}^{(7)}_{E/C7} = 0 \;\; \text{and} \;\; \overline{a}^{(8)}_{C8/E} = 0 \;\; , \;\; \overline{a}^{(7)}_{E/C7} = 0. \quad \textbf{(5.130)}$$

Hence, Equation (5.129) yields

$$\overline{a}^{(0)}_{C8/O} =$$

$$C^{(0,8)}\left[\widetilde{\omega}_{8/0}{}^{(8)} \left(\widetilde{\omega}_{8/0}{}^{(8)}\, \overline{r}^{(8)}_{C8/E}\right) + \widetilde{\alpha}^{(8)}_{8/0}\, \overline{r}^{(8)}_{C8/E} \right] +$$

$$C^{(0,7)}\left[\widetilde{\omega}_{7/0}{}^{(7)} \left(\widetilde{\omega}_{7/0}{}^{(7)}\, \overline{r}^{(7)}_{E/C7}\right) + \widetilde{\alpha}^{(7)}_{7/0}\, \overline{r}^{(7)}_{E/C7} \right] + \overline{a}^{(0)}_{C7/O}, \quad \textbf{(5.131)}$$

where

$\overline{a}^{(0)}_{C8/O}$: Acceleration of C_8 expressed in the $\mathfrak{T}_0\{O\}$ global coordinates,

$\overline{a}^{(0)}_{C7/O}$: Acceleration of C_7 expressed in the $\mathfrak{T}_0\{O\}$ global coordinates,

$\tilde{\alpha}_{8/0}$: Angular acceleration cross product matrix of $\mathfrak{T}_8\{E\}$ relative to fixed frame $\mathfrak{T}_0\{O\}$,

$\tilde{\alpha}_{7/0}$: Angular acceleration cross product matrix of $\mathfrak{T}_7\{D\}$ relative to fixed frame $\mathfrak{T}_0\{O\}$.

v) Link-9 (Hand)

The acceleration vector of C_9 expressed in the WFF, $\mathfrak{T}_0\{O\}$, is obtained in global coordinates as

$$\overline{a}^{(0)}_{C9/O} = D_0 \left\{\overline{v}^{(0)}_{C9/O}\right\}^{(0)}, \quad \textbf{(5.132)}$$

yielding

$$\overline{a}^{(0)}_{C9/O} =$$

$$C^{(0,9)}\left[\, 2\tilde{\omega}_{9/0}{}^{(9)}\,\overline{v}^{(9)}_{C9/F} + \tilde{\omega}_{9/0}{}^{(9)}\left(\tilde{\omega}_{9/0}{}^{(9)}\,\overline{r}^{(9)}_{C9/F}\right) + \overline{a}^{(9)}_{C9/F} + \tilde{\alpha}^{(9)}_{9/0}\,\overline{r}^{(9)}_{C9/F}\,\right] +$$

$$C^{(0,8)}\left[\, 2\,\tilde{\omega}_{8/0}{}^{(8)}\,\overline{v}^{(8)}_{F/C8} + \tilde{\omega}_{8/0}{}^{(8)}\left(\tilde{\omega}_{8/0}{}^{(8)}\,\overline{r}^{(8)}_{F/C8}\right) + \overline{a}^{(8)}_{F/C8} + \tilde{\alpha}^{(8)}_{8/0}\,\overline{r}^{(8)}_{F/C8}\,\right] +$$

$$\overline{a}^{(0)}_{C8/O}. \qquad \textbf{(5.133)}$$

Since points C_9 and F are on Link-9 and points F and C_8 are on Link-8, one has

$$\overline{v}^{(9)}_{C9/F} = 0 \;\;,\;\; \overline{v}^{(8)}_{F/C8} = 0 \;\; \text{and} \;\; \overline{a}^{(9)}_{C9/F} = 0 \;\;,\;\; \overline{a}^{(8)}_{F/C8} = 0. \qquad \textbf{(5.134)}$$

Hence, Equation (5.133) yields

$$\overline{a}^{(0)}_{C9/O} =$$

$$C^{(0,9)}\left[\, \tilde{\omega}_{9/0}{}^{(9)}\left(\tilde{\omega}_{9/0}{}^{(9)}\,\overline{r}^{(9)}_{C9/F}\right) + \tilde{\alpha}^{(9)}_{9/0}\,\overline{r}^{(9)}_{C9/F}\,\right] +$$

$$C^{(0,8)}\left[\, \tilde{\omega}_{8/0}{}^{(8)}\left(\tilde{\omega}_{8/0}{}^{(8)}\,\overline{r}^{(8)}_{F/C8}\right) + \tilde{\alpha}^{(8)}_{8/0}\,\overline{r}^{(8)}_{F/C8}\,\right] + \overline{a}^{(0)}_{C8/O}\,, \qquad \textbf{(5.135)}$$

where

$\overline{a}^{(0)}_{C9/O}$: Acceleration of C_9 expressed in the $\mathfrak{T}_0\{O\}$ global coordinates,

$\overline{a}^{(0)}_{C8/O}$: Acceleration of C_8 expressed in the $\mathfrak{T}_0\{O\}$ global coordinates,

$\tilde{\alpha}_{9/0}$: Angular acceleration cross product matrix of $\mathfrak{T}_9\{F\}$ relative to fixed frame $\mathfrak{T}_0\{O\}$,

$\tilde{\alpha}_{8/0}$: Angular acceleration cross product matrix of $\mathfrak{T}_8\{E\}$ relative to fixed frame $\mathfrak{T}_0\{O\}$.

vi) Link-10 (Neck)

The acceleration vector of C_{10} expressed in the WFF, $\mathfrak{T}_0\{O\}$, is obtained in global coordinates as

$$\overline{a}^{(0)}_{C10/O} = D_0\,\{\overline{v}^{(0)}_{C10/O}\}^{(0)}\,, \qquad \textbf{(5.136)}$$

yielding

$$\overline{a}^{(0)}_{C10/O} = C^{(0,10)}\left[2\widetilde{\omega}^{(10)}_{10/0}\overline{v}^{(10)}_{C10/T1} + \widetilde{\omega}_{10/0}{}^{(10)}\left(\widetilde{\omega}^{(10)}_{10/0}\overline{r}^{(10)}_{C10/T1}\right) + \overline{a}^{(10)}_{C10/T1} + \tilde{\alpha}^{(10)}_{10/0}\ \overline{r}^{(10)}_{C10/T1}\right] +$$

$$C^{(0,6)}\left[2\widetilde{\omega}^{(6)}_{6/0}\overline{v}^{(6)}_{T1/C6} + \widetilde{\omega}^{(6)}_{6/0}\left(\widetilde{\omega}^{(6)}_{6/0}\overline{r}^{(6)}_{T1/C6}\right) + \overline{a}^{(6)}_{T1/C6} + \tilde{\alpha}^{(6)}_{6/0}\ \overline{r}^{(6)}_{T1/C6}\right] + \overline{a}^{(0)}_{C6/O}. \quad \textbf{(5.137)}$$

Since points C_{10} and T_1 are on Link-10 and points T_1 and C_6 are on Link-6, one has

$$\overline{v}^{(10)}_{C10/T1} = 0 \ , \ \overline{v}^{(6)}_{T1/C6} = 0 \ \text{ and } \ \overline{a}^{(10)}_{C10/T1} = 0 \ , \ \overline{a}^{(6)}_{T1/C6} = 0. \quad \textbf{(5.138)}$$

Hence, Equation (5.137) yields

$$\overline{a}^{(0)}_{C10/O} = C^{(0,10)}\left[\ \widetilde{\omega}_{10/0}{}^{(10)}\ \left(\widetilde{\omega}_{10/0}{}^{(10)}\,\overline{r}^{(10)}_{C10/T1}\right) + \ \widetilde{\alpha}^{(10)}_{10/0}\ \overline{r}^{(10)}_{C10/T1}\ \right] +$$

$$C^{(0,6)}\left[\ \widetilde{\omega}_{6/0}{}^{(6)}\ \left(\widetilde{\omega}_{6/0}{}^{(6)}\ \overline{r}^{(6)}_{T1/C6}\right) + \ \widetilde{\alpha}^{(6)}_{6/0}\ \overline{r}^{(6)}_{T1/C6}\right] + \overline{a}^{(0)}_{C6/O}, \quad \textbf{(5.139)}$$

where

$\overline{a}^{(0)}_{C10/O}$: Acceleration of C_{10} expressed in the $\mathfrak{T}_0\{O\}$ global coordinates,

$\overline{a}^{(0)}_{C6/O}$: Acceleration of C_6 expressed in the $\mathfrak{T}_0\{O\}$ global coordinates,

$\tilde{\alpha}_{6/0}$: Angular acceleration cross product matrix of $\mathfrak{T}_6\{T_{12}\}$ relative to fixed frame $\mathfrak{T}_0\{O\}$,

$\tilde{\alpha}_{10/0}$: Angular acceleration cross product matrix of $\mathfrak{T}_{10}\{T_1\}$ relative to fixed frame $\mathfrak{T}_0\{O\}$.

vii) Link-11 (Head)

The acceleration vector of C_{11} expressed in the WFF, $\mathfrak{T}_0\{O\}$, is obtained in global coordinates

$$\overline{a}^{(0)}_{C11/O} = D_0\,\{\overline{v}^{(0)}_{C11/O}\}^{(0)}, \quad \textbf{(5.140)}$$

Yielding

$$\overline{a}^{(0)}_{C11/O} =$$

$$C^{(0,11)}\left[2\widetilde{\omega}^{(11)}_{11/0}\overline{v}^{(11)}_{C11/CS1} + \widetilde{\omega}_{11/0}{}^{(11)}\left(\widetilde{\omega}^{(11)}_{11/0}\,\overline{r}^{(11)}_{C11/CS1}\right) + \overline{a}^{(11)}_{C11/CS1} + \tilde{\alpha}^{(11)}_{11/0}\,\overline{r}^{(11)}_{C11/CS1}\right] +$$

$$C^{(0,10)}\left[2\,\widetilde{\omega}^{(10)}_{10/0}\overline{v}^{(10)}_{CS1/C10} + \widetilde{\omega}_{10/0}{}^{(10)}\left(\widetilde{\omega}^{(10)}_{10/0}\overline{r}^{(10)}_{CS1/C10}\right) + \overline{a}^{(10)}_{CS1/C10} + \tilde{\alpha}^{(10)}_{10/0}\,\overline{r}^{(10)}_{CS1/C10}\right] +$$

$$\overline{a}^{(0)}_{C10/O}\ .$$

(5.141)

Since points C_{11} and CS_1 are on Link-11 and points CS_1 and C_{10} are on Link-10, one has

$$\overline{v}^{(11)}_{C11/CS1} = 0 \quad , \quad \overline{v}^{(10)}_{CS1/C10} = 0 \quad \text{and} \quad \overline{a}^{(11)}_{C11/CS1} = 0 \quad , \quad \overline{a}^{(10)}_{CS1/C10} = 0. \qquad \textbf{(5.142)}$$

Hence, Equation (5.141) yields

$$\overline{a}^{(0)}_{C11/O} = C^{(0,11)} \left[\widetilde{\omega}_{11/0}{}^{(11)} \left(\widetilde{\omega}_{11/0}{}^{(11)} \, \overline{r}^{(11)}_{C11/CS1} \right) + \widetilde{\alpha}^{(11)}_{11/0} \, \overline{r}^{(11)}_{C11/CS1} \right] +$$

$$C^{(0,10)} \left[\widetilde{\omega}_{10/0}{}^{(10)} \left(\widetilde{\omega}_{10/0}{}^{(10)} \, \overline{r}^{(10)}_{CS1/C10} \right) + \widetilde{\alpha}^{(10)}_{10/0} \, \overline{r}^{(10)}_{CS1/C10} \right] + \overline{a}^{(0)}_{C10/O}, \qquad \textbf{(5.143)}$$

where

$\overline{a}^{(0)}_{C10/O}$: Acceleration of C_{10} expressed in the $\mathrm{T}_0\{\mathrm{O}\}$ global coordinates,

$\overline{a}^{(0)}_{C11/O}$: Acceleration of C_{11} expressed in the $\mathrm{T}_0\{\mathrm{O}\}$ global coordinates,

$\tilde{\alpha}_{11/0}$: Angular acceleration cross product matrix of $\mathrm{T}_{11}\{CS_1\}$ relative to fixed frame $\mathrm{T}_0\{\mathrm{O}\}$,

$\tilde{\alpha}_{10/0}$: Angular acceleration cross product matrix of $\mathrm{T}_{10}\{T_1\}$ relative to fixed frame $\mathrm{T}_0\{\mathrm{O}\}$.

5.3 Inverse Dynamical Analysis by Newton-Euler Method

5.3.1 Equations of Dynamic Analysis

For translational dynamics of a rigid body, Newton law is used to express the equation of motion. According to Newton's law, equation of motion is expressed in the WFF coordinates as **[24]**:

$$\bar{F}^{(0)} = m_{body}\bar{a}^{(0)}, \qquad \textbf{(5.144)}$$

where

$\bar{F}^{(0)}$: The resultant of the external forces vector expressed in the WFF coordinates,

$\bar{a}^{(0)}$: Acceleration vector of body expressed in the WFF coordinates,

m: Total mass of the body.

On the other hand, the rotational motion of a rigid body is expressed by the Euler Equation. It is expressed in the WFF coordinates and BRF coordinates such as:

$$\bar{M}^{(0)} = D_0\{\bar{L}^{(0)}\}, \qquad \textbf{(5.145)}$$

$$\bar{M}^{(b)} = D_0\{\bar{L}^{(b)}\} = \dot{\bar{L}}^{(b)} + \tilde{w}_{b/0}^{(b)}\,\bar{L}^{(b)}$$

$$= \hat{J}^{(b)}\dot{\bar{w}}_{b/0}^{(b)} + \tilde{w}_{b/0}^{(b)}\,\hat{J}^{(b)}\bar{w}_{b/0}^{(b)}, \qquad \textbf{(5.146)}$$

where

$\bar{L}^{(0)}$: Angular momentum vector of the body expressed in the WFF, T_0, coordinates,

$\bar{L}^{(b)}$: Angular momentum vector of the body expressed in the BRF, T_b, coordinates,

$\bar{M}^{(0)}$: Moment vector of the body expressed in the WFF, T_0, coordinates,

$\bar{M}^{(b)}$: Moment vector of the body expressed in the BRF, T_b, coordinates,

$\hat{J}$: Mass Moment Matrix of the rigid body,

$\tilde{w}_{b/0}^{(b)}$: Angular velocity of body with respect to WFF T_0 expressed in the BRF coordinates.

5.3.1.1 Lower Extremity

i) Link-1 (Saddle-Hip)

In Figure 5.16, free body diagram (FBD) of Link-1 is shown and reaction forces and moments, joint actuation torques and weight of the link are indicated.

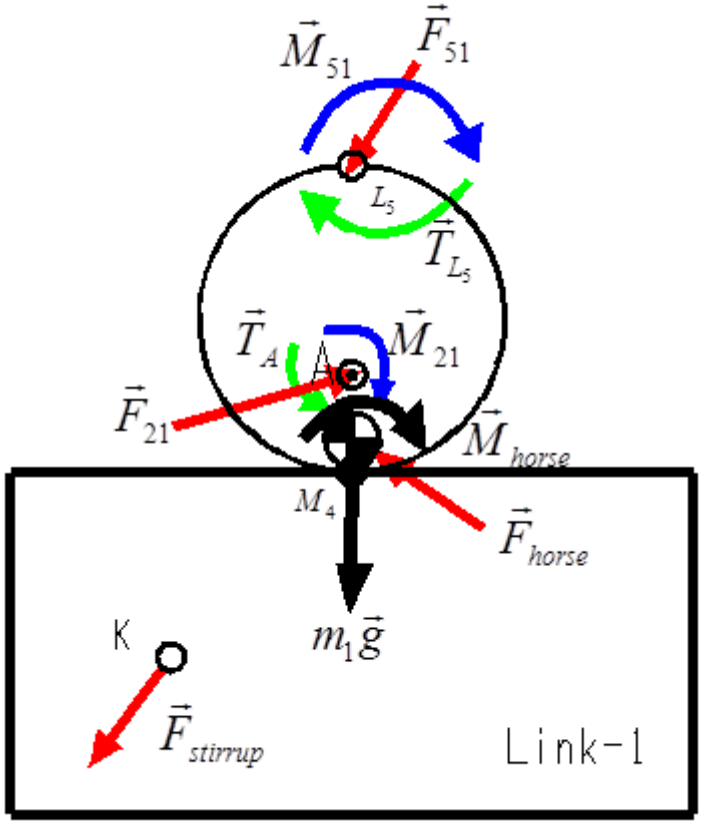

Figure 5.16 FBD of Link-1

In Matrix Form: (in world-fixed frame, $\mathcal{F}_0$)

Force Equation:

$$\bar{F}_{21}^{(0)} + \bar{F}_{stirrup}^{(0)} + \bar{F}_{horse}^{(0)} + m_1\bar{g}^{(0)} + \bar{F}_{51}^{(0)} = m_1\,\bar{a}_{C1/O}^{(0)}, \qquad \textbf{(5.147)}$$

where

$\bar{F}_{21}^{(0)}$: Reaction force vector applied by Link-2 exerted on Link-1 at point A, in $\mathcal{T}_0\{O\}$ global coordinates,

$\bar{F}_{51}^{(0)}$: Reaction force vector applied by Link-5 exerted on Link-1, in $\mathcal{T}_0\{O\}$ global coordinates,

$\bar{F}^{(0)}_{stirrup}$: Stirrup leather tension force vector applied to Link-1, in $\mathcal{F}_0\{O\}$ global coordinates,

$\bar{F}^{(0)}_{horse}$: Horse's reaction force vector (actuation force) exerted on Link-1, in $\mathcal{F}_0\{O\}$ global coordinates,

$m_1\bar{g}^{(0)}$: Weight of Link-1, in $\mathcal{F}_0\{O\}$ global coordinates.

Moment Equation: (in world-fixed frame, $\mathcal{F}_0$)

$$\sum \vec{M}_{M4} = \hat{J}_1^{(1)}\,\bar{\alpha}_{1/0}^{(1)} + \tilde{\omega}_{1/0}{}^{(1)}\,\hat{J}_1^{(1)}\bar{\omega}_{1/0}^{(1)},$$

$$\bar{M}_{horse}^{(1)} + \bar{T}_A^{(1)} + \bar{T}_{L5}^{(1)} + \widetilde{M_4}K^{(1)}\bar{F}_{stirrup}^{(1)} + \widetilde{M_4}A^{(1)}\bar{F}_{21}^{(1)} + \widetilde{M_4}L_5^{(1)}\bar{F}_{51}^{(1)} = \hat{J}_1^{(1)}\,\bar{\alpha}_{1/0}^{(1)} + \tilde{\omega}_{1/0}{}^{(1)}\,\hat{J}_1^{(1)}\bar{\omega}_{1/0}^{(1)}, \quad \textbf{(5.148)}$$

where $\bar{M}_{21}^{(1)} = 0$ *and* $\bar{M}_{51}^{(1)} = 0$. At revolute joint connection points *A* and L_5 there is no reaction moment, because there is no rotational restriction at the revolute joints.

Here,

$\bar{M}_{horse}^{(1)}$: Horse's reaction moment vector (actuation force) exerted on Link-1, in $\mathcal{F}_1\{M_1\}$ coordinates,

$\bar{T}_A^{(1)}$: Joint Actuator Torque at Point A - the connection of Link-2 and Link-1, represented in $\mathcal{F}_1\{M_1\}$ coordinates,

$\bar{T}_{L5}^{(1)}$: Joint Actuator Torque at Point L_5 - the connection of Link-5 and Link-1, represented in $\mathcal{F}_1\{M_1\}$ coordinates,

$\hat{J}_1^{(1)}$: Inertia Matrix of Link-1 in $\mathcal{F}_1\{M_1\}$ coordinates,

$\widetilde{M_4}K^{(1)}$, $\widetilde{M_4}A^{(1)}$, $\widetilde{M_4}L_5^{(1)}$: Cross product matrices of position vectors from point M_4 to points K, A and L_5 respectively, in $\mathcal{F}_1\{M_1\}$ coordinates.

ii) Link-2 (Thigh)

In Figure 5.17, free body diagram (FBD) of Link-2 is shown and reaction forces and moments, joint actuation torques and weight of the link are indicated.

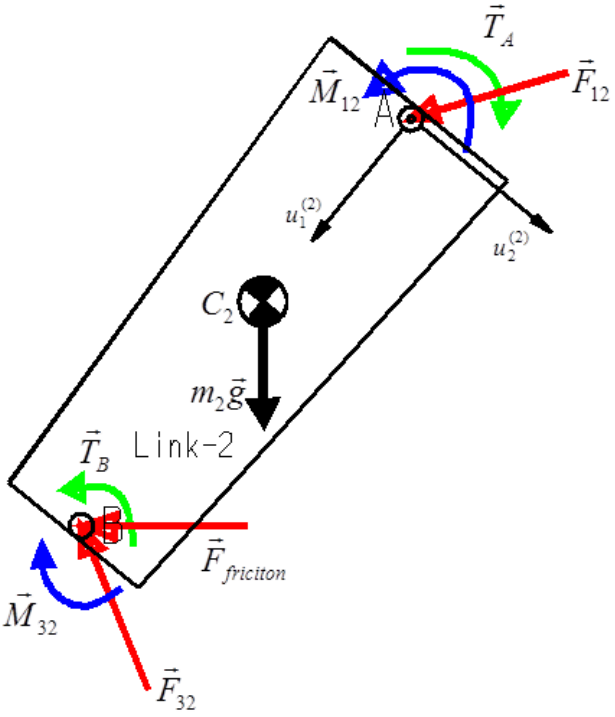

Figure 5.17 FBD of Link-2

<u>In Matrix Form</u>: (in world-fixed frame, $\mathcal{F}_0$)

Force Equation:

$$\bar{\mathrm{F}}_{\mathrm{fric}}^{(0)} + \bar{\mathrm{F}}_{12}^{(0)} + \bar{\mathrm{F}}_{32}^{(0)} + \mathrm{m}_2\bar{\mathrm{g}}^{(0)} = \mathrm{m}_2\,\bar{a}_{C2/O}^{(0)}\,, \qquad \textbf{(5.149)}$$

where $\bar{\mathrm{F}}_{12}^{(0)} = -F_{21}^{(0)}$, and

$\bar{\mathrm{F}}_{12}^{(0)}$: Reaction force vector applied by Link-1 exerted on Link-2 at point A, in $\mathrm{T}_0\{\mathrm{O}\}$ global coordinates,

$\bar{\mathrm{F}}_{32}^{(0)}$: Reaction force vector applied by Link-3 exerted on Link-2 at point B, in $\mathrm{T}_0\{\mathrm{O}\}$ global coordinates,

$\bar{\mathrm{F}}_{\mathrm{fric}}^{(0)}$: Friction force between the rider leg and the saddle lateral pad at point B in $\mathrm{T}_0\{\mathrm{O}\}$ global coordinates,

$\mathrm{m}_2\bar{\mathrm{g}}^{(0)}$: Weight of Link-2, in $\mathrm{T}_0\{\mathrm{O}\}$ global coordinates.

Friction force $\bar{\mathrm{F}}_{\mathrm{fric}}^{(0)}$, is calculated as the product of friction coefficient and the force exerted by the inside of the knee to horse body. Mean force value, which is 8.8 N, is taken as a reference value and added to the force calculations of the Link-2 **[13]**. The

direction of the friction force is along the translational motion direction $\bar{u}_1^{(0)}$.

Moment Equation: (in body-fixed frame, $\mathcal{F}_2$)

$$\bar{\mathrm{M}}_{12}^{(2)} + \bar{\mathrm{M}}_{32}^{(2)} + \bar{\mathrm{T}}_A^{(2)} + \bar{\mathrm{T}}_B^{(2)} + \widetilde{\mathrm{C}_2\mathrm{A}}^{(2)}\bar{\mathrm{F}}_{12}^{(2)} + \widetilde{\mathrm{C}_2\mathrm{B}}^{(2)}\bar{\mathrm{F}}_{32}^{(2)} + \widetilde{\mathrm{C}_2\mathrm{B}}^{(2)}\bar{\mathrm{F}}_{\mathrm{fric}}^{(2)} = \hat{\mathrm{J}}_2^{(2)}\,\bar{\alpha}_{2/0}^{(2)} + \widetilde{\omega}_{2/0}{}^{(2)}\,\hat{\mathrm{J}}_2^{(2)}\bar{\omega}_{2/0}^{(2)}, \quad \textbf{(5.150)}$$

where $\bar{\mathrm{T}}_A^{(2)} = -\widehat{\mathrm{C}}^{(2,0)}\bar{\mathrm{T}}_A^{(0)}$, $\bar{\mathrm{F}}_{32}^{(2)} = \widehat{\mathrm{C}}^{(2,0)}\bar{\mathrm{F}}_{32}^{(0)}$, $\bar{\mathrm{F}}_{12}^{(2)} = -\widehat{\mathrm{C}}^{(2,0)}\bar{\mathrm{F}}_{21}^{(0)}$, $\bar{\mathrm{M}}_{12}^{(2)} = 0$ and $\bar{\mathrm{M}}_{32}^{(2)} = 0$. At revolute joint connection points *A* and *B*, there is no reaction moment, because there is no rotational restriction at the revolute joints.

Here,

$\bar{\mathrm{T}}_A^{(2)}$: Joint Actuator Torque at Point A - the connection of Link-2 and Link-1, represented in $\mathcal{F}_2\{\mathrm{A}\}$ in local coordinates,

$\bar{\mathrm{T}}_B^{(2)}$: Joint Actuator Torque at Point B - the connection of Link-2 and Link-3, represented in $\mathcal{F}_3\{\mathrm{B}\}$ in local coordinates,

$\hat{\mathrm{J}}_2^{(2)}$: Inertia Matrix of Link-2 in $\mathcal{F}_2\{\mathrm{A}\}$ local coordinates,

$\widetilde{\mathrm{C}_2\mathrm{A}}^{(2)}$, $\widetilde{\mathrm{C}_2\mathrm{B}}^{(2)}$: Cross product matrices of position vectors from point C_2 to points A and B respectively, in $\mathcal{F}_2\{\mathrm{A}\}$ in local coordinates.

iii) Link-3 (Shank)

In Figure 5.18, free body diagram (FBD) of Link-3 is shown and reaction forces and moments, joint actuation torques and weight of the link are indicated.

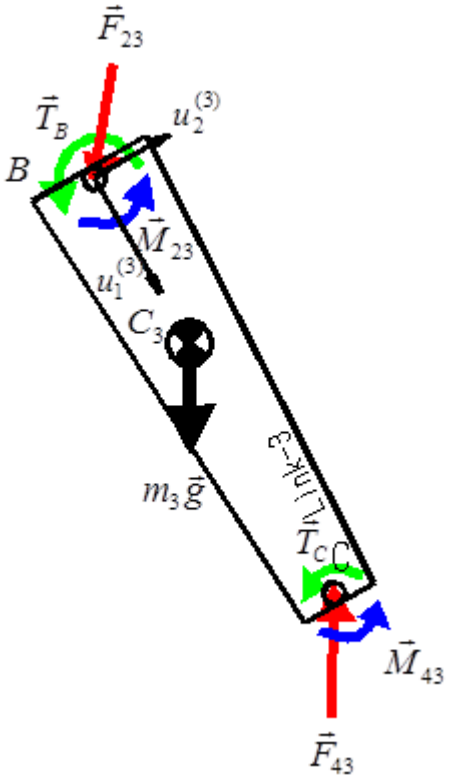

Figure 5.18 FBD of Link-3

In Matrix Form: (in world-fixed frame, $\mathcal{F}_0$)

Force Equation:

$$\bar{F}_{23}^{(0)} + \bar{F}_{43}^{(0)} + m_3\bar{g}^{(0)} = m_3\,\bar{a}_{C3/O}^{(0)}, \qquad \textbf{(5.151)}$$

where $\left[\ \bar{F}_{23}^{(0)} = -\bar{F}_{32}^{(0)}\ \right]$, and

$\bar{F}_{23}^{(0)}$: Reaction force vector applied by Link-2 exerted on Link-3 at point B, in $\mathcal{F}_0\{O\}$ global coordinates,

$\bar{F}_{43}^{(0)}$: Reaction force vector applied by Link-4 exerted on Link-3 at point C, in $\mathcal{F}_0\{O\}$ global coordinates,

$m_3\bar{g}^{(0)}$: Weight of Link-3, in $\mathcal{F}_0\{O\}$ global coordinates.

Moment Equation: (in body-fixed frame, $\mathcal{F}_3$)

$$\bar{M}_{23}^{(3)} + \bar{M}_{43}^{(3)} + \bar{T}_B^{(3)} + \bar{T}_C^{(3)} + \widetilde{C_3}B^{(3)}\,\bar{\mathrm{F}}_{23}^{(3)} + \widetilde{C_3}C\,\bar{\mathrm{F}}_{43}^{(3)} = \hat{\mathrm{J}}_3^{(3)}\,\bar{\alpha}_{3/0}^{(3)} + \tilde{\omega}_{3/0}{}^{(3)}\,\hat{\mathrm{J}}_3^{(3)}\,\bar{\omega}_{3/0}^{(3)}\,, \quad \textbf{(5.152)}$$

where $\bar{\mathrm{T}}_B^{(3)} = -\hat{\mathrm{C}}^{(3,2)}\,\bar{\mathrm{T}}_B^{(2)}$, $\bar{\mathrm{F}}_{23}^{(3)} = -\hat{\mathrm{C}}^{(3,0)}\bar{\mathrm{F}}_{32}^{(0)}$, $\bar{\mathrm{F}}_{43}^{(3)} = \hat{\mathrm{C}}^{(3,0)}\bar{\mathrm{F}}_{43}^{(0)}$, and $\bar{\mathrm{M}}_{23}^{(3)} = 0$, $\bar{\mathrm{M}}_{43}^{(3)} = 0$. At revolute joint connection points B and C, there is no reaction moment, because there is no rotational restriction at revolute joints.

Here,

$\bar{T}_B^{(3)}$: Joint Actuator Torque at Point B - the connection of Link-3 and Link-2, represented in $\mathrm{T}_3\{\mathrm{B}\}$ in local coordinates,

$\bar{T}_C^{(3)}$: Joint Actuator Torque at Point C - the connection of Link-3 and Link-4, represented in $\mathrm{T}_3\{\mathrm{B}\}$ in local coordinates,

$\hat{\mathrm{J}}_3^{(3)}$: Inertia Matrix of Link-3 in $\mathrm{T}_3\{\mathrm{B}\}$ local coordinates,

$\widetilde{C_3}B^{(3)}$, $\widetilde{C_3}C$: Cross product matrices of position vectors from point C_3 to points B and C respectively, in $\mathrm{T}_3\{\mathrm{B}\}$ in local coordinates,

$\hat{\mathrm{C}}^{(3,2)}$: Transformation Matrix from $\mathrm{T}_2\{A\}$ to $\mathrm{T}_3\{B\}$, which has the form

$$\hat{\mathrm{C}}^{(3,2)} = \begin{bmatrix} \cos\theta_{32} & -\sin\theta_{32} & 0 \\ \sin\theta_{32} & \cos\theta_{32} & 0 \\ 0 & 0 & 1 \end{bmatrix}$$

where θ_{32} : Relative angle from $\mathrm{T}_2\{A\}$ to $\mathrm{T}_3\{B\}$ about $\bar{u}_3^{(2)}$ axis.

iv) Link-4 (Foot)

In Figure 5.19, free body diagram (FBD) of Link-4 is shown and reaction forces and moments, joint actuation torques and weight of the link are indicated.

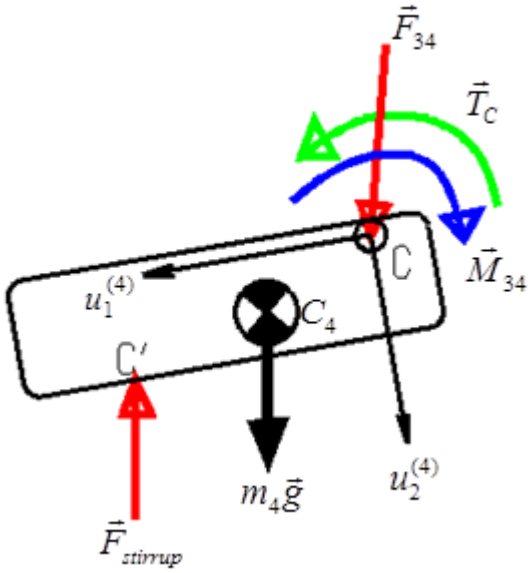

Figure 5.19 FBD of Link-4

In Matrix Form:

Force Equation: (in world-fixed frame, $\mathcal{F}_0$)

$$\bar{F}^{(0)}_{stirrup} + \bar{F}^{(0)}_{34} + m_4\bar{g}^{(0)} = m_4\,\bar{a}^{(0)}_{C4/O}, \quad \text{where} \quad \left[\,\bar{F}^{(0)}_{34} = -\bar{F}^{(0)}_{43}\,\right], \qquad \textbf{(5.153)}$$

where

$\bar{F}^{(0)}_{34}$: Reaction force vector applied by Link-3 exerted on Link-4 at point C, in $\mathcal{T}_0\{O\}$ global coordinates,

$\bar{F}^{(0)}_{stirrup}$: Stirrup leather tension force vector applied to Link-4, in $\mathcal{T}_0\{O\}$ global coordinates,

$m_4\bar{g}^{(0)}$: Weight of Link-4, in $\mathcal{T}_0\{O\}$ global coordinates.

Moment Equation: (in body-fixed frame, $\mathcal{F}_4$)

$$\bar{M}^{(4)}_{34} + T^{(4)}_C + \widetilde{C_4C}^{(4)}\bar{F}^{(4)}_{34} + \widetilde{C_4C'}^{(4)}\,\bar{F}^{(4)}_{stirrup} = \hat{J}_4{}^{(4)}\,\bar{\alpha}^{(4)}_{4/0} + \tilde{\omega}_{4/0}{}^{(4)}\hat{J}_4{}^{(4)}\,\bar{\omega}^{(4)}_{4/0}\,,$$

(5.154)

where $\overline{\mathrm{T}}_C^{(4)} = -\widehat{\mathrm{C}}^{(4,3)}\overline{\mathrm{T}}_B^{(3)}$, $\overline{\mathrm{F}}_{34}^{(4)} = \widehat{\mathrm{C}}^{(4,0)}\overline{\mathrm{F}}_{34}^{(0)}$, $\overline{\mathrm{F}}_{\text{stirrup}}^{(4)} = \widehat{\mathrm{C}}^{(4,0)}\overline{\mathrm{F}}_{\text{stirrup}}^{(0)}$ and $\overline{\mathrm{M}}_{34}^{(4)} = 0$. At revolute joint connection point *C,* there is no reaction moment, because there is no rotational restriction at revolute joints. Here,

$\overline{\mathrm{T}}_C^{(4)}$: Joint Actuator Torque at Point C - the connection of Link-4 and Link-3, represented in $\mathrm{T}_4\{\mathrm{C}\}$ in local coordinates,

$\hat{\mathrm{J}}_4^{(4)}$: Inertia Matrix of Link-4 in $\mathrm{T}_4\{\mathrm{C}\}$ local coordinates,

$\widetilde{\mathrm{C}_4\mathrm{C}}^{(4)}$, $\widetilde{\mathrm{C}_4\mathrm{C}'}^{(4)}$: Cross product matrices of position vectors from point C_4 to points C and C' respectively, in $\mathrm{T}_4\{\mathrm{C}\}$ in local coordinates,

$\widehat{\mathrm{C}}^{(4,3)}$: Transformation Matrix from $\mathrm{T}_3\{B\}$ to $\mathrm{T}_4\{C\}$, which has the form

$$\widehat{\mathrm{C}}^{(4,3)} = \begin{bmatrix} \cos\theta_{43} & -\sin\theta_{43} & 0 \\ \sin\theta_{43} & \cos\theta_{43} & 0 \\ 0 & 0 & 1 \end{bmatrix},$$

where θ_{43} : Relative angle from $\mathrm{T}_3\{B\}$ to $\mathrm{T}_4\{C\}$ about $\bar{u}_3^{(3)}$ axis.

Here, $\overline{F}_{\text{stirrup}}^{(0)}$ denotes the stirrup force. The average value of this force, which is 260 N **[25]**, is used in this study as implemented in the force equations of Link-4 and Link-1.The direction of the stirrup force is taken as a normal force to the bottom surface of the foot.

5.3.1.2 Upper Extremity

i) Link-5 (Abdomen)

In Figure 5.20, free body diagram (FBD) of Link-5 is shown and reaction forces and moments, joint actuation torques and weight of the link are indicated.

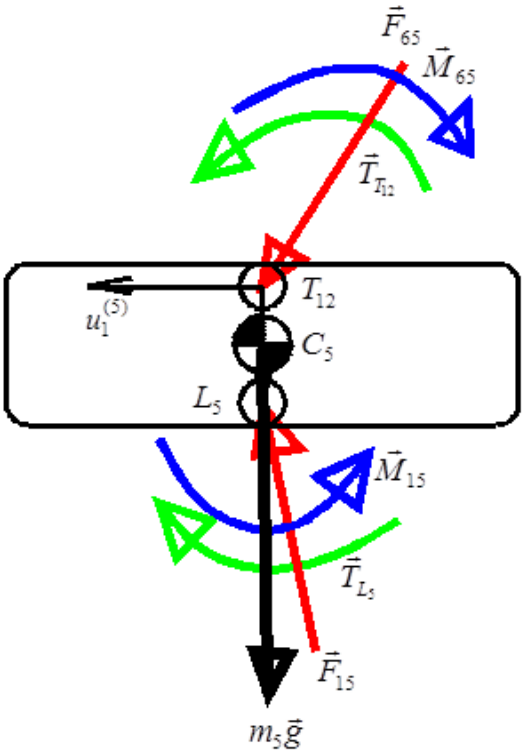

Figure 5.20 FBD of Link-5

In Matrix Form:

Force Equation: (in world-fixed frame, $\mathcal{F}_0$)

$$\bar{\mathrm{F}}_{15}^{(0)} + \bar{\mathrm{F}}_{65}^{(0)} + \mathrm{m}_5\bar{\mathrm{g}}^{(0)} = \mathrm{m}_5\,\overline{a}_{C5/O}^{(0)}\,, \qquad \textbf{(5.155)}$$

where $\bar{\mathrm{F}}_{15}^{(0)} = -\bar{\mathrm{F}}_{51}^{(0)}$ and

$\bar{\mathrm{F}}_{15}^{(0)}$: Reaction force vector applied by Link-1 exerted on Link-5 at point L_5, in $\mathrm{F}_0\{\mathrm{O}\}$ global coordinates,

$\bar{\mathrm{F}}_{65}^{(0)}$: Reaction force vector applied by Link-6 exerted on Link-5 at point T_{12}, in $\mathrm{F}_0\{\mathrm{O}\}$ global coordinates,

$\mathrm{m}_5\bar{\mathrm{g}}^{(0)}$: Weight of Link-5, in $\mathrm{F}_0\{\mathrm{O}\}$ global coordinates.

Moment Equation : (in body-fixed frame, $\mathcal{F}_5$)

$$\bar{\mathrm{M}}_{15}^{(5)} + \bar{\mathrm{M}}_{65}^{(5)} + \bar{\mathrm{T}}_{L5}^{(5)} + \mathrm{T}_{T12}^{(5)} + \widetilde{C_5}L_5{}^{(5)}\,\bar{\mathrm{F}}_{15}^{(5)} + C_5\widetilde{T_{12}}^{(5)}\bar{\mathrm{F}}_{65}^{(5)} = \hat{\mathrm{J}}_5^{(5)}\,\overline{\alpha}_{5/0}^{(5)} +$$

$$\widetilde{\omega}_{5/0}{}^{(5)}\hat{\mathrm{J}}_5^{(5)}\bar{\omega}_{5/0}^{(5)}\,, \qquad \textbf{(5.156)}$$

where $\bar{\mathrm{T}}_{L5}^{(5)} = \hat{\mathrm{C}}^{(5,1)}\bar{\mathrm{T}}_{L5}^{(1)}$, $\bar{\mathrm{F}}_{15}^{(5)} = \hat{\mathrm{C}}^{(5,0)}\bar{\mathrm{F}}_{15}^{(0)}$, $\bar{\mathrm{F}}_{65}^{(5)} = \hat{\mathrm{C}}^{(5,0)}\bar{\mathrm{F}}_{65}^{(0)}$, and $\bar{\mathrm{M}}_{15}^{(5)} = 0$, $\bar{\mathrm{M}}_{65}^{(5)} = 0$. At revolute joint connection points L_5 and T_{12}, there are no reaction moments, because there is no rotational restriction at revolute joints.

Here,

$\bar{\mathrm{T}}_{L5}^{(5)}$: Joint Actuator Torque at Point L_5 - the connection of Link-5 and Link-1, represented in $\mathrm{F}_5\{L_5\}$ in local coordinates,

$\mathrm{T}_{T12}^{(5)}$: Joint Actuator Torque at Point T_{12} - the connection of Link-5 and Link-1, represented in $\mathrm{F}_5\{L_5\}$ in local coordinates,

$\hat{\mathrm{J}}_5^{(5)}$: Inertia Matrix of Link-5 in $\mathrm{F}_5\{L_5\}$ local coordinates,

$\widetilde{C_5L_5}^{(5)}$, $\widetilde{C_5T_{12}}^{(5)}$: Cross product matrices of position vectors from point C_5 to points L_5 and T_{12} respectively, in $\mathrm{F}_5\{L_5\}$ in local coordinates,

$\hat{\mathrm{C}}^{(5,1)}$: Transformation Matrix from $\mathrm{F}_1\{M_1\}$ to $\mathrm{F}_5\{L_5\}$, which has the form

$$\hat{\mathrm{C}}^{(5,1)} = \begin{bmatrix} \cos\theta_{51} & -\sin\theta_{51} & 0 \\ \sin\theta_{51} & \cos\theta_{51} & 0 \\ 0 & 0 & 1 \end{bmatrix},$$

where θ_{51} : Relative angle from $\mathrm{F}_1\{M_1\}$ to $\mathrm{F}_5\{L_5\}$ about $\bar{u}_3^{(1)}$ axis

ii) Link-6 (Trunk)

In Figure 5.21, free body diagram (FBD) of Link-6 is shown and reaction forces and moments, joint actuation torques and weight of the link are indicated.

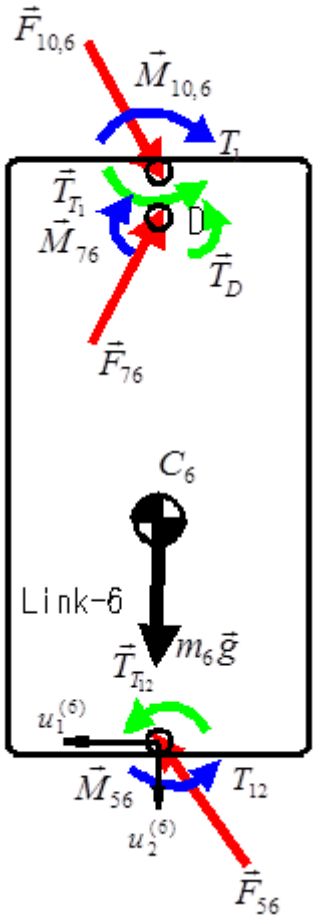

Figure 5.21 FBD of Link-6

In Matrix Form:

Force Equation: (in world-fixed frame, $\mathcal{F}_0$)

$$\bar{F}_{56}^{(0)} + \bar{F}_{10,6}^{(0)} + \bar{F}_{76}^{(0)} + m_6\bar{g}^{(0)} = m_6\,\bar{a}_{C6/O}^{(0)}, \qquad \textbf{(5.157)}$$

where $\bar{F}_{56}^{(0)} = -\bar{F}_{65}^{(0)}$ and

$\bar{F}_{56}^{(0)}$: Reaction force vector applied by Link-5 exerted on Link-6 at point T_{12}, in $\mathfrak{T}_0\{O\}$ global coordinates,

$\bar{F}_{10,6}^{(0)}$: Reaction force vector applied by Link-10 exerted on Link-6 at point T_1, in $\mathfrak{T}_0\{O\}$ global coordinates,

$\bar{F}_{76}^{(0)}$: Reaction force vector applied by Link-7 exerted on Link-6 at point D, in $\mathfrak{T}_0\{O\}$ global coordinates,

$m_6\bar{g}^{(0)}$: Weight of Link-6, in $\mathcal{F}_0\{O\}$ global coordinates.

Moment Equation: (in body-fixed frame, $\mathcal{F}_6$)

$$\bar{M}_{56}^{(6)} + \bar{M}_{76}^{(6)} + \bar{M}_{10,6}^{(6)} + \bar{T}_{T12}^{(6)} + T_{T1}^{(6)} + T_D^{(6)} + \widetilde{C}_6 T_{12}^{(6)}\, \bar{F}_{56}^{(6)} + \widetilde{C}_6 T_1^{(6)} \bar{F}_{10,6}^{(6)} +$$

$$\widetilde{C}_6 D \bar{F}_{76}^{(6)} = \hat{J}_6^{(6)}\, \bar{\alpha}_{6/0}^{(6)} + \tilde{\omega}_{6/0}{}^{(6)} \hat{J}_6^{(6)} \bar{\omega}_{6/0}^{(6)}\,, \qquad \textbf{(5.158)}$$

where $\bar{T}_{T12}^{(6)} = \hat{C}^{(6,5)}\, \bar{T}_{T12}^{(5)}$, $\bar{F}_{56}^{(6)} = \hat{C}^{(6,0)} \bar{F}_{56}^{(0)}$, and $\bar{F}_{10,6}^{(6)} = \hat{C}^{(6,0)} \bar{F}_{10,6}^{(0)}$, $\bar{F}_{76}^{(6)} = \hat{C}^{(6,0)} \bar{F}_{76}^{(0)}$. Also, $\bar{M}_{56}^{(6)} = 0$, $\bar{M}_{76}^{(6)} = 0$ and $\bar{M}_{10,6}^{(6)} = 0$.

At revolute joint connection points T_{12}, D and T_1, there are no reaction moments, because there is no rotational restriction at revolute joints.

Here,

$\bar{T}_{T12}^{(6)}$: Joint Actuator Torque at Point T_{12} - the connection of Link-6 and Link-5, represented in $\mathcal{F}_6\{T_{12}\}$ in local coordinates,

$T_{T1}^{(6)}$: Joint Actuator Torque at Point T_1 - the connection of Link-6 and Link-10, represented in $\mathcal{F}_6\{T_{12}\}$ in local coordinates,

$T_D^{(6)}$: Joint Actuator Torque at Point D - the connection of Link-6 and Link-7, represented in $\mathcal{F}_6\{T_{12}\}$ in local coordinates,

$\hat{J}_6^{(6)}$: Inertia Matrix of Link-6 in $\mathcal{F}_6\{T_{12}\}$ local coordinates,

$\widetilde{C}_6 T_{12}^{(6)}$, $\widetilde{C}_6 T_1^{(6)}$, $\widetilde{C}_6 D$: Cross product matrices of position vectors from point C_6 to points T_{12}, T_1 and D respectively, in $\mathcal{F}_6\{T_{12}\}$ in local coordinates,

$C^{(6,5)}$: Transformation Matrix from $\mathcal{F}_5\{L_5\}$ to $\mathcal{F}_6\{T_{12}\}$, which has the form

$$C^{(6,5)} = \begin{bmatrix} \cos\theta_{65} & -\sin\theta_{65} & 0 \\ \sin\theta_{65} & \cos\theta_{65} & 0 \\ 0 & 0 & 1 \end{bmatrix},$$

where θ_{65} : Relative angle from $\mathcal{F}_5\{L_5\}$ to $\mathcal{F}_6\{T_{12}\}$ about $\bar{u}_3^{(5)}$ axis.

iii) Link-7 (Upper Arm)

In Figure 5.22, free body diagram (FBD) of Link-7 is shown and reaction forces and moments, joint actuation torques and weight of the link are indicated.

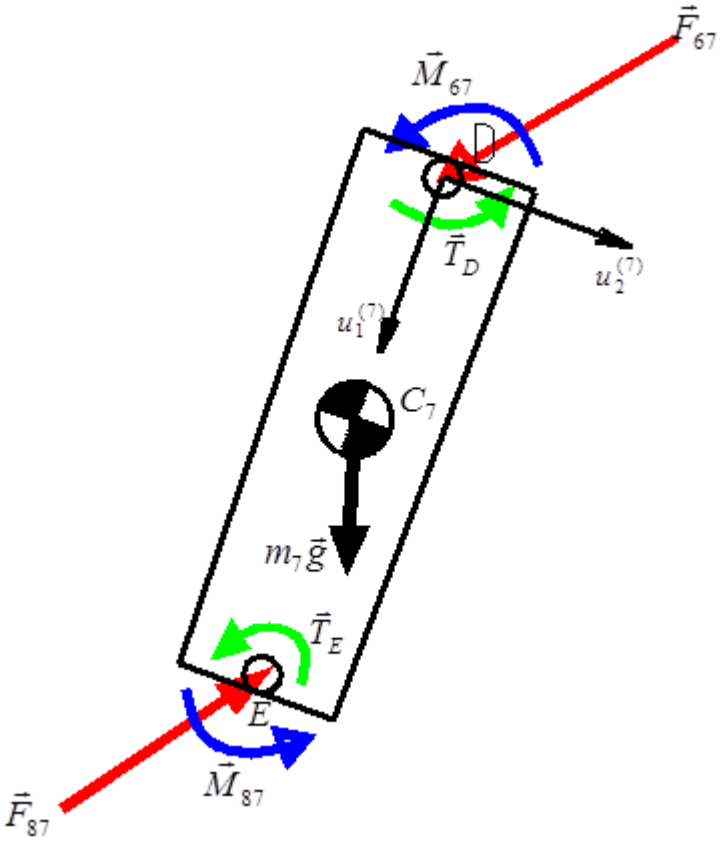

Figure 5.22 FBD of Link-7

<u>In Matrix Form</u>:

Force Equation: (in world-fixed frame, $\mathcal{F}_0$)

$$\bar{F}_{67}^{(0)} + \bar{F}_{87}^{(0)} + m_7\bar{g}^{(0)} = m_7\,\bar{a}_{C7/O}^{(0)}\,, \qquad \textbf{(5.159)}$$

where $\bar{F}_{67}^{(0)} = -\bar{F}_{76}^{(0)}$ and

$\bar{F}_{67}^{(0)}$: Reaction force vector applied by Link-6 exerted on Link-7 at point D, in $\mathfrak{T}_0\{O\}$ global coordinates,

$\bar{F}_{87}^{(0)}$: Reaction force vector applied by Link-8 exerted on Link-7 at point E, in $\mathfrak{T}_0\{O\}$ global coordinates,

$m_7\bar{g}^{(0)}$: Weight of Link-7, in $\mathfrak{T}_0\{O\}$ global coordinates.

Moment Equation: (in body-fixed frame, $\mathcal{F}_7$)

$$\bar{M}_{67}^{(7)} + \bar{M}_{87}^{(7)} + \bar{T}_D^{(7)} + T_E^{(7)} + \widetilde{C_7D}^{(7)}\bar{F}_{67}^{(7)} + \widetilde{C_7E}^{(7)}\bar{F}_{87}^{(7)} = \hat{J}_7^{(7)}\bar{\alpha}_{7/0}^{(7)} + \tilde{\omega}_{7/0}{}^{(7)}\hat{J}_7^{(7)}\bar{\omega}_{7/0}^{(7)} \quad \textbf{(5.160)}$$

where $\bar{T}_D^{(7)} = \hat{C}^{(7,6)}\bar{T}_D^{(6)}$, $\bar{F}_{67}^{(7)} = \hat{C}^{(7,0)}\bar{F}_{67}^{(0)}$, $\bar{F}_{87}^{(7)} = \hat{C}^{(7,0)}\bar{F}_{87}^{(0)}$, and $\bar{M}_{67}^{(7)} = 0$, $\bar{M}_{87}^{(7)} = 0$. At revolute joint connection points D and E, there are no reaction moments, because there is no rotational restriction at revolute joints.

Here,

$\bar{T}_D^{(7)}$: Joint Actuator Torque at Point D - the connection of Link-7 and Link-6, represented in $\mathcal{F}_7\{D\}$ in local coordinates,

$T_E^{(7)}$: Joint Actuator Torque at Point E - the connection of Link-7 and Link-8, represented in $\mathcal{F}_7\{D\}$ in local coordinates,

$\hat{J}_7^{(7)}$: Inertia Matrix of Link-7 in $\mathcal{F}_7\{D\}$ local coordinates,

$\widetilde{C_7D}^{(7)}$ and $\widetilde{C_7E}^{(7)}$: Cross product matrices of position vectors from point C_7 to points D and E respectively, in $\mathcal{F}_7\{D\}$ in local coordinates,

$C^{(7,6)}$: Transformation Matrix from $\mathcal{F}_6\{T_{12}\}$ to $\mathcal{F}_7\{D\}$, which has the form

$$C^{(7,6)} = \begin{bmatrix} \cos\theta_{76} & -\sin\theta_{76} & 0 \\ \sin\theta_{76} & \cos\theta_{76} & 0 \\ 0 & 0 & 1 \end{bmatrix},$$

where θ_{76} : Relative angle from $\mathcal{F}_6\{T_{12}\}$ to $\mathcal{F}_7\{D\}$ about $\bar{u}_3^{(6)}$ axis.

iv) Link-8 (Lower Arm)

In Figure 5.23, free body diagram (FBD) of Link-8 is shown and reaction forces and moments, joint actuation torques and weight of the link are indicated.

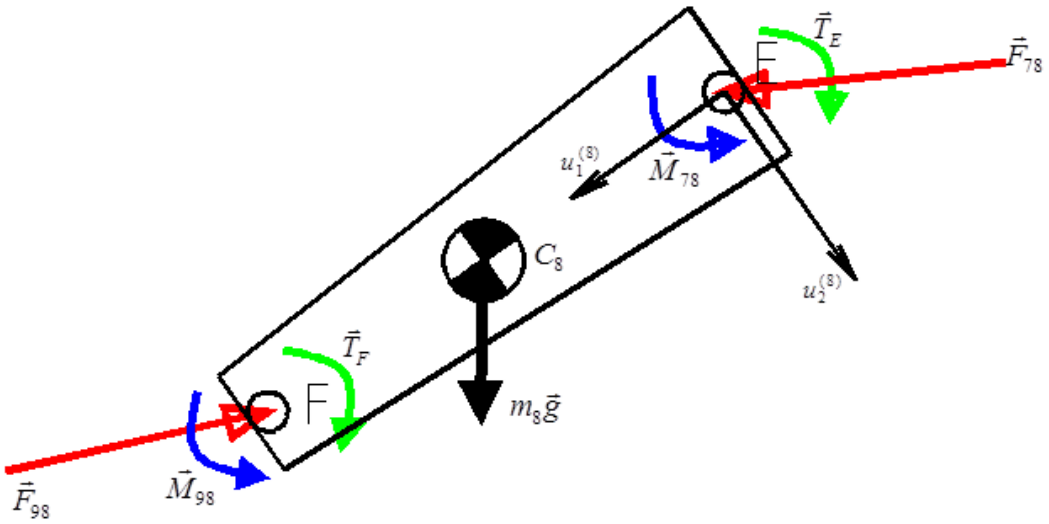

Figure 5.23 FBD of Link-8

In Matrix Form:

Force Equation: (in world-fixed frame, $\mathcal{F}_0$)

$$\bar{F}_{78}^{(0)} + \bar{F}_{98}^{(0)} + m_8\bar{g}^{(0)} = m_8\,\bar{a}_{C8/O}^{(0)}, \qquad \textbf{(5.161)}$$

where $\bar{F}_{78}^{(0)} = -\bar{F}_{87}^{(0)}$ and

$\bar{F}_{78}^{(0)}$: Reaction force vector applied by Link-7 exerted on Link-8 at point E, in $\mathfrak{T}_0\{O\}$ global coordinates,

$\bar{F}_{98}^{(0)}$: Reaction force vector applied by Link-9 exerted on Link-8 at point F, in $\mathfrak{T}_0\{O\}$ global coordinates,

$m_8\bar{g}^{(0)}$: Weight of Link-8, in $\mathfrak{T}_0\{O\}$ global coordinates.

Moment Equation: (in body-fixed frame, $\mathcal{F}_8$)

$$\bar{M}_{78}^{(8)} + \bar{M}_{98}^{(8)} + \bar{T}_E^{(8)} + T_F^{(8)} + \widetilde{C_8E}^{(8)}\,\bar{F}_{78}^{(8)} + \widetilde{C_8F}^{(8)}\bar{F}_{98}^{(8)} = \hat{J}_8^{(8)}\,\bar{\alpha}_{8/0}^{(8)} + \tilde{\omega}_{8/0}{}^{(8)}\hat{J}_8^{(8)}\bar{\omega}_{8/0}^{(8)},$$

(5.162)

where $\bar{T}_E^{(8)} = \hat{C}^{(8,7)}\,\bar{T}_E^{(7)}$, $\bar{F}_{78}^{(8)} = \hat{C}^{(8,0)}\bar{F}_{78}^{(0)}$, $\bar{F}_{98}^{(8)} = \hat{C}^{(8,0)}\bar{F}_{98}^{(0)}$, $\bar{M}_{78}^{(8)} = 0$ and $\bar{M}_{98}^{(8)} = 0$. At revolute joint connection points E and F, there are no reaction moments, because there is no rotational restriction at revolute joints.

Here,

$\bar{T}_E^{(8)}$: Joint Actuator Torque at Point E - the connection of Link-8 and Link-7, represented in $\mathfrak{T}_8\{E\}$ in local coordinates,

$T_F^{(8)}$: Joint Actuator Torque at Point F - the connection of Link-8 and Link-9, represented in $\mathfrak{T}_8\{E\}$ in local coordinates,

$\hat{J}_8^{(8)}$: Inertia Matrix of Link-8 in $\mathfrak{T}_8\{E\}$ local coordinates,

$\widetilde{C_8E}^{(8)}$, $\widetilde{C_8F^{(8)}}$: Cross product matrices of position vectors from point C_8 to points E and F respectively, in $\mathfrak{T}_8\{E\}$ in local coordinates,

$C^{(8,7)}$: Transformation Matrix from $\mathfrak{T}_7\{D\}$ to $\mathfrak{T}_8\{E\}$, which has the form

$$C^{(8,7)} = \begin{bmatrix} \cos\theta_{87} & -\sin\theta_{87} & 0 \\ \sin\theta_{87} & \cos\theta_{87} & 0 \\ 0 & 0 & 1 \end{bmatrix},$$

where θ_{87} : Relative angle from $\mathfrak{T}_7\{D\}$ to $\mathfrak{T}_8\{E\}$ about $\bar{u}_3^{(7)}$ axis.

v) Link-9 (Hand)

In Figure 5.24, free body diagram (FBD) of Link-9 is shown and reaction forces and moments, joint actuation torques and weight of the link are indicated.

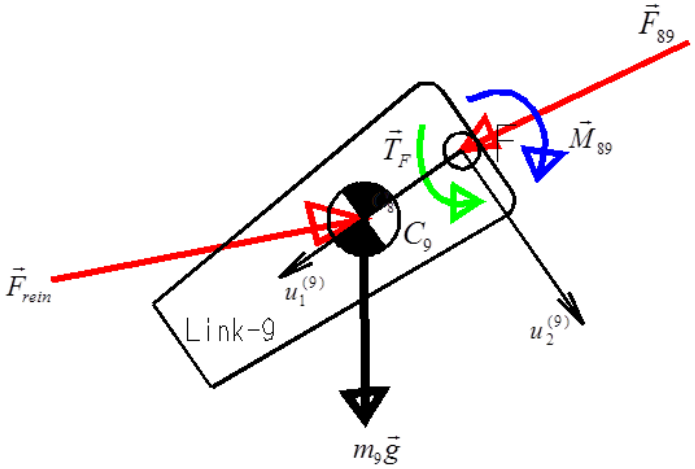

Figure 5.24 FBD of Link-9

In Matrix Form:

Force Equation: (in world-fixed frame, $\mathcal{F}_0$)

$$\bar{F}_{89}^{(0)} + \bar{F}_{rein}^{(0)} + m_9\bar{g}^{(0)} = m_9\,\bar{a}_{C9/O}^{(0)}\,, \qquad \textbf{(5.163)}$$

where $\bar{F}_{89}^{(0)} = -\bar{F}_{98}^{(0)}$ and

$\bar{F}_{89}^{(0)}$: Reaction force vector applied by Link-8 exerted on Link-9 at point F, in $\mathcal{F}_0\{O\}$ global coordinates,

$\bar{F}_{rein}^{(0)}$: Rein tension force exerted on Link-9, in $\mathcal{F}_0\{O\}$ global coordinates,

$m_9\bar{g}^{(0)}$: Weight of Link-9, in $\mathcal{F}_0\{O\}$ global coordinates.

Rein tension force is obtained from the literature survey and the average value which is 3.53 N, is inserted into the force equation **[26]**.The direction of the rein force is taken as along the direction of the hand longitudinal axis ($\bar{u}_1^{(9)}$ axis).

Moment Equation : (in body-fixed frame, $\mathcal{F}_9$)

$$\bar{M}_{89}^{(9)} + \bar{T}_F^{(9)} + \widetilde{C_9F}^{(9)}\,\bar{F}_{89}^{(9)} = \hat{J}_9^{(9)}\,\bar{\alpha}_{9/0}^{(9)} + \tilde{\omega}_{9/0}{}^{(9)}\hat{J}_9^{(9)}\bar{\omega}_{9/0}^{(9)}\,, \qquad \textbf{(5.164)}$$

where $\bar{F}_{89}^{(9)} = \hat{C}^{(9,0)}\,\bar{F}_{89}^{(0)}$, $\bar{T}_F^{(9)} = \hat{C}^{(9,8)}\,\bar{T}_F^{(8)}$, and $\bar{M}_{89}^{(9)} = 0$.

At revolute joint connection point F, there is no reaction moment, because there is no rotational restriction at revolute joints.

Here,

$\bar{T}_F^{(9)}$: Joint Actuator Torque at Point F - the connection of Link-9 and Link-8, represented in $\mathcal{F}_9\{F\}$ in local coordinates,

$\hat{J}_9^{(9)}$: Inertia Matrix of Link-9 in $\mathcal{F}_9\{F\}$ local coordinates,

$\widetilde{C_9F}^{(9)}$: Cross product matrices of position vector from point C_9 to point F , in $\mathcal{F}_9\{F\}$ in local coordinates,

$C^{(9,8)}$: Transformation Matrix from $\mathcal{F}_8\{E\}$ to $\mathcal{F}_9\{F\}$, which has the form

$$C^{(9,8)} = \begin{bmatrix} \cos\theta_{98} & -\sin\theta_{98} & 0 \\ \sin\theta_{98} & \cos\theta_{98} & 0 \\ 0 & 0 & 1 \end{bmatrix},$$

where θ_{98} : Relative angle from $\mathcal{F}_8\{E\}$ to $\mathcal{F}_9\{F\}$ about $\bar{u}_3^{(8)}$ axis.

vi) Link-10 (Neck)

In Figure 5.25, free body diagram (FBD) of Link-10 is shown and reaction forces and moments, joint actuation torques and weight of the link are indicated.

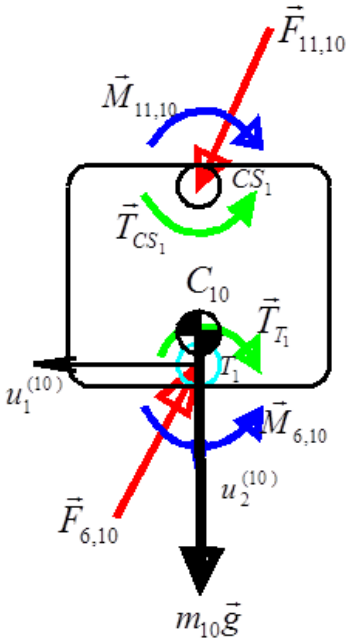

Figure 5.25 FBD of Link-10

<u>In Matrix Form</u>:

Force Equation: (in world-fixed frame, $\mathcal{F}_0$)

$$\bar{\mathrm{F}}_{6,10}^{(0)} + \bar{\mathrm{F}}_{11,10}^{(0)} + \mathrm{m}_{10}\bar{\mathrm{g}}^{(0)} = \mathrm{m}_{10}\,\bar{a}_{C10/O}^{(0)}, \qquad \textbf{(5.165)}$$

where $\bar{\mathrm{F}}_{6,\,10}^{(0)} = -\bar{\mathrm{F}}_{10,\,6}^{(0)}$ and

$\bar{\mathrm{F}}_{6,10}^{(0)}$: Reaction force vector applied by Link-6 exerted on Link-10 at point T_1, in $\mathrm{T}_0\{\mathrm{O}\}$ global coordinates,

$\bar{\mathrm{F}}_{11,10}^{(0)}$: Reaction force vector applied by Link-11 exerted on Link-10 at point CS_1, in $\mathrm{T}_0\{\mathrm{O}\}$ global coordinates,

$\mathrm{m}_{10}\bar{\mathrm{g}}^{(0)}$: Weight of Link-10, in $\mathrm{T}_0\{\mathrm{O}\}$ global coordinates.

Moment Equation: (in body-fixed frame, $\mathcal{F}_{10}$)

$$\bar{M}_{6,10}^{(10)} + \bar{M}_{11,10}^{(10)} + \bar{T}_{T1}^{(10)} + T_{CS_1}^{(10)} + \widetilde{C_{10}T_1}^{(10)} \bar{F}_{6,10}^{(10)} + \widetilde{C_{10}CS_1}^{(10)} \bar{F}_{11,10}^{(10)} =$$

$$\hat{J}_{10}^{(10)} \bar{\alpha}_{10/0}^{(10)} + \tilde{\omega}_{10/0}{}^{(10)} \hat{J}_{10}^{(10)} \bar{\omega}_{10/0}^{(10)}, \qquad \textbf{(5.166)}$$

where $\bar{F}_{6,10}^{(10)} = \hat{C}^{(10,0)} \bar{F}_{6,10}^{(0)}$, $\bar{F}_{11,10}^{(10)} = \hat{C}^{(10,0)} \bar{F}_{11,10}^{(0)}$, $\bar{T}_{T1}^{(10)} = \hat{C}^{(10,6)} \bar{T}_{T1}^{(6)}$. Also, $\bar{M}_{6,10}^{(10)} = 0$ and $\bar{M}_{11,10}^{(10)} = 0$. At revolute joint connection points T_1 and CS_1, there are no reaction moments, because there are not any rotational restriction at revolute joints. Here,

$\bar{T}_{T1}^{(10)}$: Joint Actuator Torque at Point T_1 - the connection of Link-10 and Link-6, represented in $\mathcal{F}_{10}\{T_1\}$ in local coordinates,

$T_{CS_1}^{(10)}$: Joint Actuator Torque at Point CS_1 - the connection of Link-10 and Link-11, represented in $\mathcal{F}_{10}\{T_1\}$ in local coordinates,

$\hat{J}_{10}^{(10)}$: Inertia Matrix of Link-10 in $\mathcal{F}_{10}\{T_1\}$ local coordinates,

$\widetilde{C_{10}T_1}^{(10)}$, $\widetilde{C_{10}CS_1}^{(10)}$: Cross product matrices of position vectors from point C_{10} to points T_1 and CS_1, in $\mathcal{F}_{10}\{T_1\}$ in local coordinates,

$C^{(10,6)}$: Transformation Matrix from $\mathcal{F}_6\{T_{12}\}$ to $\mathcal{F}_{10}\{T_1\}$, which has the form

$$C^{(10,6)} = \begin{bmatrix} \cos\theta_{10,6} & -\sin\theta_{10,6} & 0 \\ \sin\theta_{10,6} & \cos\theta_{10,6} & 0 \\ 0 & 0 & 1 \end{bmatrix},$$

where $\theta_{10,6}$: Relative angle from $\mathcal{F}_6\{T_{12}\}$ to $\mathcal{F}_{10}\{T_1\}$ about $\bar{u}_3^{(6)}$ axis.

vii) Link-11 (Head)

In Figure 5.26, free body diagram (FBD) of Link-11 is shown and reaction forces and moments, joint actuation torques and weight of the link are indicated.

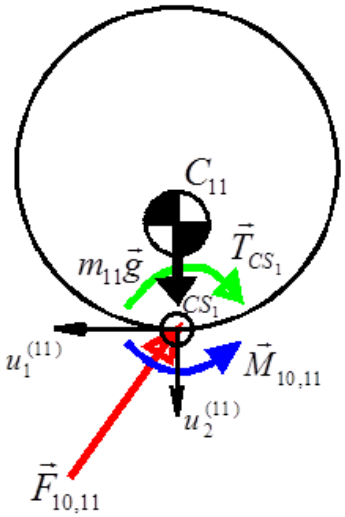

Figure 5.26 FBD of Link-11

In Matrix Form:

Force Equation: (in world-fixed frame, $\mathcal{F}_0$)

$$\bar{\mathrm{F}}_{10,11}^{(0)} + \mathrm{m}_{11}\bar{\mathrm{g}}^{(0)} = \mathrm{m}_{11}\,\bar{a}_{C11/O}^{(0)}, \qquad \textbf{(5.167)}$$

where $\bar{\mathrm{F}}_{10,11}^{(0)} = -\bar{\mathrm{F}}_{11,10}^{(0)}$ and

$\bar{\mathrm{F}}_{10,11}^{(0)}$: Reaction force vector applied by Link-10 exerted on Link-11 at point CS_1, in $\mathrm{T}_0\{\mathrm{O}\}$ global coordinates,

$\mathrm{m}_{11}\bar{\mathrm{g}}^{(0)}$: Weight of Link-11, in $\mathrm{T}_0\{\mathrm{O}\}$ global coordinates.

Moment Equation: (in body-fixed frame, $\mathcal{F}_{11}$)

$$\bar{\mathrm{M}}_{10,11}^{(11)} + \mathrm{T}_{CS_1}^{(11)} + \widetilde{C_{11}}\mathrm{CS}_1^{(11)}\bar{\mathrm{F}}_{10,11}^{(11)} = \hat{\mathrm{J}}_{11}^{(11)}\,\bar{\alpha}_{11/0}^{(11)} + \tilde{\omega}_{11/0}{}^{(11)}\hat{\mathrm{J}}_{11}^{(11)}\bar{\omega}_{11/0}^{(11)}, \qquad \textbf{(5.168)}$$

where $\bar{\mathrm{F}}_{10,11}^{(11)} = \hat{\mathrm{C}}^{(11,0)}\,\bar{\mathrm{F}}_{10,11}^{(0)}$ and $\bar{\mathrm{M}}_{10,11}^{(11)} = 0$.

At revolute joint connection point CS_1, there is no reaction moment, because there is not any rotational restriction at revolute joints. Here,

$\mathrm{T}_{CS_1}^{(11)}$: Joint Actuator Torque at Point CS_1 - the connection of Link-11 and Link-10, represented in $\mathrm{T}_{11}\{CS_1\}$ in local coordinates,

$\hat{\mathrm{J}}_{11}^{(11)}$: Inertia Matrix of Link-11 in $\mathrm{T}_{11}\{CS_1\}$ local coordinates,

$\widetilde{C_{11}}\mathrm{CS}_1^{(11)}$: Cross product matrices of position vectors from point C_{11} to point CS_1, in $\mathrm{T}_{11}\{CS_1\}$ in local coordinates.

CHAPTER 6

OPTIMIZATION PROBLEM

6.1 Piecewise Continuous Polynomial Parameterization

The joint angles, angular velocities and angular accelerations of the links are needed to get the reaction forces and the actuation torques at the joints. The joint angles are represented by parametric piecewise continuous polynomials in symbolic form. So, by taking time derivatives of these polynomials, the angular velocities and the angular accelerations are obtained. In order to create the piecewise parametric polynomials, a program is developed using MATLAB®.

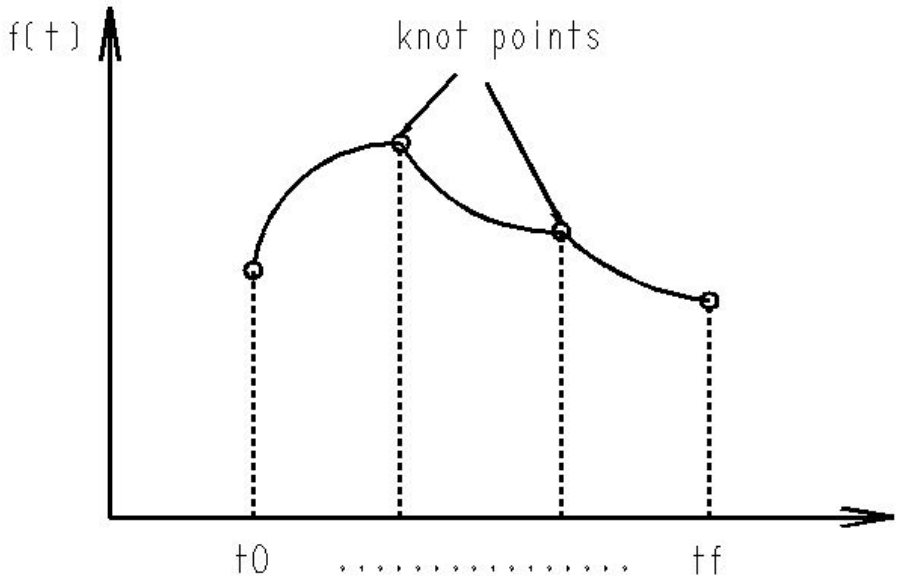

Figure 6.1 Piecewise polynomial representation

The inputs to the program are as follows:

t_0: Initial time that the generated function f(t) is valid,

t_f: Final time that the generated function f(t) is valid,

n_p: Number of piecewise polynomials,

d_p: Degree of polynomials at each time interval,

d_c: Degree of continuity at the knot points (degree of continuity can not be larger than degree of the polynomials implying that $d_c < d_p$.

After getting these inputs, Δt and n_k are calculated via the equations

$$\Delta t = \frac{t_f - t_0}{n_p}, \quad \textbf{(6.1)}$$

$$n_k = n_p - 1, \quad \textbf{(6.2)}$$

where n_k is the number of knot points.

The function $f(t)$ will be approximated by n_p polynomials. The i^{th} polynomial, which is valid in the interval

$$t_i - 1 \leq t \leq t_i \quad \textbf{(6.3)}$$

will be of the form

$$f_i(t) = a_{i0} + a_{i1}t + a_{i2}t^2 + \cdots + a_{ij}t^j, \quad \textbf{(6.4)}$$

where i = 1, 2,…, n_p and j = 0, 1, 2,…, d_p. The n_p polynomials must satisfy the continuity equations of the knot points given by

$$\frac{d^j}{dt^j} f_i(t_i) = \frac{d^j}{dt^j} f_{i+1}(t_i), \quad \textbf{(6.5)}$$

where i = 1, 2,…, $n_p - 1$ and j = 0, 1, 2,…, d_c.

In addition to satisfying the continuity equations at the knot points, the n_p polynomials may also satisfy the initial and final conditions at t_0 and t_f given by:

$$f_1(t_0) = \theta_0 \quad \textbf{(6.6)}$$

$$\dot{f}_1(t_0) = \dot{\theta}_0 \quad \textbf{(6.7)}$$

and

$$f_{np}(t_f) = \theta_f \quad \textbf{(6.8)}$$

$$\dot{f}_{np}(t_f) = \dot{\theta}_f \ . \quad \textbf{(6.9)}$$

If $f(t)$ is a periodic function [with the period being $(t_0 - t_f)$] that has to satisfy a second order differential equation, in that case, the piecewise polynomial, should also satisfy the periodicity conditions given by

$$f_1(t_0) = f_{np}(t_f) \quad \textbf{(6.10)}$$

$$\dot{f}_1(t_0) = \dot{f}_{np}(t_f) \ . \quad \textbf{(6.11)}$$

Equations (6.4) – (6.11) are n_e linear equations in the coefficients of the n_p polynomials, namely, $a_{10}, a_{11}, \ldots, a_{1dp}$; $a_{20}, a_{21}, \ldots, a_{2dp}$; ...; $a_{np0}, a_{np1}, \ldots, a_{npdp}$. Hence, by using equations (6.4) – (6.11), one may eliminate n_e of the $n_p \ x \ (d_p + 1)$ unknowns to get n_i independent unknowns which are the components of the design parameters vector $\overline{a}_m$.

6.2 Computation of Performance Measure

In this study, two scenarios are investigated in order to minimize the joint torques, reaction forces and reaction moments at the horse-saddle interface. Firstly, minimization is performed during sitting trot. The second minimization is related to a sudden stop scenario.

6.2.1 Objective Function

Consider, now, the following notation

$\theta_{01}(t)\,,\theta_{02}(t)\,,\ldots\,,\theta_{011}(t)$: Joint angle functions associated with the rider model,

$\tilde{\theta}_{01}(\overline{a}_m,t)\,,\tilde{\theta}_{02}(\overline{a}_m,t)\,,\ldots\,,\tilde{\theta}_{011}(\overline{a}_m,t)$: Approximations of the joint angle functions $\theta_{01}(t)\,,\theta_{02}(t)\,,\ldots\,,\theta_{011}(t)$ using continuous piecewise polynomials, where $\overline{a}_m$ denotes the vector of independent design parameters,

$\overline{\tilde{\theta}}_{0i}(\overline{a}_m)$: Vector with (n_p+1) elements obtained by evaluating $\overline{\tilde{\theta}}_{0i}(\overline{a}_m,t)$ at the (n_p+1) knot points $t_0, t_1, \ldots t_f$, i.e.

$$\overline{\tilde{\theta}}_{0i}(\overline{a}_m)=\begin{bmatrix}\tilde{\theta}_{01}(\overline{a}_m,t_0)\\ \tilde{\theta}_{02}(\overline{a}_m,t_1)\\ \vdots\\ \tilde{\theta}_{0i}(\overline{a}_m,t_f)\end{bmatrix},$$

$T_{CS1}(t)\,,T_{T1}(t)\,,T_F(t),T_E(t),T_D(t),T_{T12}(t),T_{L5}(t),T_C(t),T_B(t),T_A(t)$: Joint actuator torques associated with the rider model. Note that these actuator torques are related to the joint angle functions $\theta_{01}(t)\,,\theta_{02}(t)\,,\ldots\,,\theta_{011}(t)$ via Newton-Euler equations,

$\tilde{T}_{CS1}(\overline{a}_m,t)\,,\tilde{T}_{T1}(\overline{a}_m,t)\,,\ldots\,,\tilde{T}_A(\overline{a}_m,t)$: Approximations of the joint actuator torques obtained by using the approximate joint angle functions $\tilde{\theta}_{01}(\overline{a}_m,t)\,,\tilde{\theta}_{02}(\overline{a}_m,t)$, ... $\tilde{\theta}_{011}(\overline{a}_m,t)$ instead of joint angle functions $\theta_{01}(t)\,,\theta_{02}(t)\,,\ldots\,,\theta_{011}(t)$,

$\overline{\tilde{T}}_{CS1}(\overline{a}_m)$: Vector with $(n_p + 1)$ element, obtained by evaluating $\tilde{T}_{CS1}(\overline{a}_m, t)$ at the $(n_p + 1)$ knot points $t_0, t_1, \ldots\ t_f$, i.e.

$$\overline{\tilde{T}}_{CS1}(\overline{a}_m) = \begin{bmatrix} \tilde{T}_{CS1}(\overline{a}_m, t_0) \\ \tilde{T}_{CS1}(\overline{a}_m, t_1) \\ \vdots \\ \tilde{T}_{CS1}(\overline{a}_m, t_f) \end{bmatrix}.$$

Note that $\overline{\tilde{T}}_{T1}(\overline{a}_m)$, ... , $\overline{\tilde{T}}_{A}(\overline{a}_m)$ are defined in a similar manner to $\overline{\tilde{T}}_{CS1}(\overline{a}_m)$.

$\overline{F}_{horse}(t)$, $\overline{M}_{horse}(t)$: Force and moment applied by the horse on the saddle. Note that $\overline{F}_{horse}(t)$, $\overline{M}_{horse}(t)$ are related to the joint angle functions $\theta_{01}(t)$, ... , $\theta_{011}(t)$ via Newton-Euler equations.

$\overline{\tilde{F}}_{horse}(\overline{a}_m, t)$, $\overline{\tilde{M}}_{horse}(\overline{a}_m, t)$: Approximations of $\overline{F}_{horse}(t)$, $\overline{M}_{horse}(t)$ obtained by using the approximate joint angles $\tilde{\theta}_{01}(\overline{a}_m, t)$, $\tilde{\theta}_{02}(\overline{a}_m, t)$, ... , $\tilde{\theta}_{011}(\overline{a}_m, t)$.

The performance measure to be minimized in this study is given by

$$J = \int_{t_0}^{t_f} [\, w_1({T_{CS1}}^2(t)) + w_2\left({T_{T1}}^2(t)\right) + w_3\left({T_F}^2(t)\right) + w_4\left({T_E}^2(t)\right) + w_5\left({T_D}^2(t)\right) + w_6\left({T_{T12}}^2(t)\right) + w_7\left({T_{L5}}^2(t)\right) + w_8\left({T_C}^2(t)\right) + w_9\left({T_B}^2(t)\right) + w_{10}\left({T_A}^2(t)\right) + w_{11}(\| M_{horse}(t)\|^2) + w_{12}(\| F_{horse}(t)\|^2)\,]\, dt\ .$$

(6.12)

If the joint angles are approximated by continuous piecewise polynomials $\tilde{\theta}_{01}(\overline{a}_m, t)$, ... , $\tilde{\theta}_{011}(\overline{a}_m, t)$, then the performance measure given by (6.12) will become;

$$\tilde{J}\,(\overline{a}_m) = \int_{t_0}^{t_f} [\, w_1(\tilde{T}_{CS1}{}^2(\overline{a}_m, t)) + w_2\left(\tilde{T}_{T1}{}^2(\overline{a}_m, t)\right) + w_3\left(\tilde{T}_F{}^2(\overline{a}_m, t)\right) +$$
$$w_4\left(\tilde{T}_E{}^2(\overline{a}_m, t)\right) + w_5\left(\tilde{T}_D{}^2(\overline{a}_m, t)\right) + w_6\left(\tilde{T}_{T12}{}^2(\overline{a}_m, t)\right) + w_7\left(\tilde{T}_{L5}{}^2(\overline{a}_m, t)\right) +$$
$$w_8\left(\tilde{T}_C{}^2(\overline{a}_m, t)\right) + w_9\left(\tilde{T}_B{}^2(\overline{a}_m, t)\right) + w_{10}\left(\tilde{T}_A{}^2(\overline{a}_m, t)\right) +$$
$$w_{11}\left(\left\| \tilde{M}_{horse}(\overline{a}_m, t)\right\|^2\right) + w_{12}(\left\| \tilde{F}_{horse}(\overline{a}_m, t)\right\|^2)\,]\, dt\,.$$

(6.13)

Hence, minimization of J is transformed into a nonlinear optimization problem which may be described as follows:

Determine the optimal design parameters, $\overline{a}_m{}^*$, such that $\tilde{J}\,(\overline{a}_m)$ is minimized subjected to the equality and inequality constraints given by

$h_i\,(\overline{a}_m) = 0$, i = 1, 2,…, r, **(6.14)**

$p_j(\overline{a}_m) \leq 0$, j = 1, 2,…, n, **(6.15)**

where

$h_i\,(\overline{a}_m)$: equality constraints,

$p_j(\overline{a}_m)$: inequality constraints.

6.2.2 Constraints

6.2.2.1 Linear Constraints

i) Linear Equality Constraints

There are no linear equality constraints for the horse rider problem.

ii) Linear Inequality Constraints

Due to the biological limits of these human joints, there is an allowable motion range for each joint. The angular limits are listed in Table A.III.1 **[27]**. Hence, the constraints which ensure that the joint angles are within these allowable ranges at all times are given by the following inequality constraints.

Each joint angle, $\theta_{ij}(\overline{a}_m)$, is a linear function of $\overline{a}_m$, independent parameters vector (design variables).

$$\overline{p}_j^{\,lin}(\overline{a}_m) = \begin{bmatrix} \overline{\tilde{\theta}}_{12}(\overline{a}_m) - \overline{\theta}_{12,max} \\ \overline{\theta}_{12,min} - \overline{\tilde{\theta}}_{12}(\overline{a}_m) \\ \overline{\tilde{\theta}}_{23}(\overline{a}_m) - \overline{\theta}_{23,max} \\ \overline{\theta}_{23,min} - \overline{\tilde{\theta}}_{23}(\overline{a}_m) \\ \overline{\tilde{\theta}}_{34}(\overline{a}_m) - \overline{\theta}_{34,max} \\ \vdots \\ \overline{\tilde{\theta}}_{1011}(\overline{a}_m) - \overline{\theta}_{1011,max} \\ \overline{\theta}_{1011,min} - \overline{\tilde{\theta}}_{1011}(\overline{a}_m) \end{bmatrix} \leq \overline{0}\,, \qquad \textbf{(6.16)}$$

where

$\overline{\theta}_{ij,max}, \overline{\theta}_{ij,min}$ [for i = 1,2,3, ... 10 and j = 2,3,4 ... 11] are constant vectors (with appropriate dimensions) which yield the maximum allowable and minimum allowable values of the joint angle $\overline{\theta}_{0i}$ and $\overline{0}$ is a zero vector with appropriate dimensions.

6.2.2.2 Nonlinear Constraints

i) Nonlinear Equality Constraints

In both scenarios during the riding, the relative distance of the rider's center of mass position (with respect to the 4th marker position on the saddle) should not change along the x-direction. This constraint prevents the rider to fall down. This relative distance is calculated at t = t_0, and it is desired to be kept constant throughout the riding. This constraint may be expressed as follows

$$[\,\overline{x}_{CG,rider}(\,\overline{a}_m) - \overline{x}_{4th\ marker}\,] - \left[\,\overline{x}_{CG,rider}(\overline{a}_m)_{at\ t=\,t_0} - \overline{x}_{4th\ marker}(t_0)\right] = 0\,. \quad \textbf{(6.17)}$$

Another restriction is the adjustment of the stirrup leather length before riding which affects the position of the foot (Link-4). In other words, the relative distance, along the y-axis, between the center of mass location of the foot (Point C_4) and the 4th marker position (Point M_4) on the saddle seat must remain constant and must be equal to the value at t = t_0. This constraint may be expressed as follows

$$\left[\,\overline{r}^{\,(0)}{}_{M4/O} - \overline{r}^{\,(0)}{}_{C4/O}\,(\overline{a}_m)\,\right] - [\,\overline{r}^{\,(0)}{}_{M4/O}(t_0) - \overline{r}^{\,(0)}{}_{C4/O}(\overline{a}_m)_{at\ \ t=\,t_0}\,] = 0. \ \textbf{(6.18)}$$

Therefore, all of the nonlinear equality constraints are implemented in vector form as given below

$$\overline{h}_i^{\,nonlin}(\overline{a}_m) \;=$$
$$\begin{bmatrix} \left(\overline{x}_{CG,rider}(\,\overline{a}_m) - \overline{x}_{4th\ marker}\,\right) - \left(\,\overline{x}_{CG,rider}(\overline{a}_m)_{at\ t=\,t_0} - \overline{x}_{4th\ marker}(t_0)\right) \\ \left(\,\overline{r}^{\,(0)}{}_{M4/O} - \overline{r}^{\,(0)}{}_{C4/O}\,(\overline{a}_m)\,\right) - \left(\overline{r}^{\,(0)}{}_{M4/O}(t_0) - \overline{r}^{\,(0)}{}_{C4/O}(\overline{a}_m)_{at\ \ t=\,t_0}\,\right) \end{bmatrix} = 0, \quad \textbf{(6.19)}$$

where

$\overline{h}_i^{\,nonlin}(\overline{a}_m)$: Nonlinear Equality Constraint vector (in terms of $\overline{a}_m$) .

ii) Nonlinear Inequality Constraints

There is a range of allowable torque values for each joint due to the biological endurance limits of human joints. The torque limits are listed in Table A.II.1 [28]. Each joint torque in the rider model, $T(\overline{a}_m)$, is a nonlinear function of $\overline{a}_m$, independent parameters vector (design variables). So that these minimum and maximum torque limits restrict the possible values of $\overline{a}_m$ for the minimization problem.

$$\overline{p}_j^{\,nonlin}(\overline{a}_m) = \begin{bmatrix} \overline{\tilde{T}}_A(\overline{a}_m) - \overline{T}_{A,max} \\ \overline{T}_{A,min} - \overline{\tilde{T}}_A(\overline{a}_m) \\ \overline{\tilde{T}}_B(\overline{a}_m) - \overline{T}_{B,max} \\ \overline{T}_{B,min} - \overline{\tilde{T}}_B(\overline{a}_m) \\ \overline{\tilde{T}}_C(\overline{a}_m) - \overline{T}_{C,max} \\ \vdots \\ \overline{\tilde{T}}_{CS1}(\overline{a}_m) - \overline{T}_{CS1,max} \\ \overline{T}_{CS1,min} - \overline{\tilde{T}}_{CS1}(\overline{a}_m) \end{bmatrix} \leq \overline{0}\,, \qquad \textbf{(6.20)}$$

where $\overline{T}_{A,min}, \overline{T}_{A,max}$ ... $\overline{T}_{CS1,min}, \overline{T}_{CS1,max}$ are constant vectors (with appropriate dimensions) which yield the maximum allowable and minimum allowable values of the joint torque associated with $\overline{\theta}_{ij}$ and $\overline{0}$ is a zero vector with appropriate dimensions. Here,

$\overline{p}_j^{\,nonlin}(\overline{a}_m)$: Nonlinear Inequality Constraint vector in terms of $\overline{a}_m$ and torque limits.

6.3 Minimization of Performance Measure

The optimization of the objective function $\tilde{J}(\overline{a}_m)$ subject to constraints is performed using MATLAB®. Note that, this a nonlinear multivariable optimization problem with linear and nonlinear constraints and "fmincon" function in the Optimization Toolbox of MATLAB® is an appropriate solver for that kind of minimization problems. **[29]**.

The integration necessary to get the objective function $\tilde{J}(\overline{a}_m)$ (see equation 6.12) is performed by symbol-numerically, using 6-point Gauss Quadrature Method.

The performance measure functional is:

$$\tilde{J}(\overline{a}_m) = \int_{t_0}^{t_f} [\, w_1(\tilde{T}_{CS1}{}^2(\overline{a}_m, t)) + w_2\left(\tilde{T}_{T1}{}^2(\overline{a}_m, t)\right) + w_3\left(\tilde{T}_F{}^2(\overline{a}_m, t)\right) +$$
$$w_4\left(\tilde{T}_E{}^2(\overline{a}_m, t)\right) + w_5\left(\tilde{T}_D{}^2(\overline{a}_m, t)\right) + w_6\left(\tilde{T}_{T12}{}^2(\overline{a}_m, t)\right) + w_7\left(\tilde{T}_{L5}{}^2(\overline{a}_m, t)\right) +$$
$$w_8\left(\tilde{T}_C{}^2(\overline{a}_m, t)\right) + w_9\left(\tilde{T}_B{}^2(\overline{a}_m, t)\right) + w_{10}\left(\tilde{T}_A{}^2(\overline{a}_m, t)\right) +$$
$$w_{11}\left(\left\| \tilde{M}_{horse}(\overline{a}_m, t)\right\|^2\right) + w_{12}(\left\| \tilde{F}_{horse}(\overline{a}_m, t)\right\|^2) \,]\, dt\,. \qquad \textbf{(6.21)}$$

To this purpose, a code is written and the objective function to be minimized is obtained just in terms of design variables $\overline{a}_m$. The linear inequality constraint equations (angle limits) are written in matrix form and the nonlinear equality (CG of the rider and stirrup leather length) and the inequality constraint functions (torque limits) are constructed and written in separate function files to be called in the main optimization code in which *fmincon* is used.

6.4 Gaussian Quadrature Method

The definite integral of a function may not always have an exact result or may not be straight forward to obtain. Numerical quadrature is a well-known technique, which is based on interpolation polynomials, to approximate such definite integrals and it

simply has the following form **[30]**

$$\int_a^b f(x)\,dx \;\approx\; \sum_{i=0}^{n} a_i\, f(x_i).$$

(6.22)

Here, the closed interval $[a\,,b]$ is divided into $(n-1)$ subintervals by using n-distinct nodes $\{x_0, x_1, \dots, x_n\}$ where $x_0 = a$ and $x_n = b$. This formula is exact for polynomials of degree at most n. The class of quadrature methods where

$$a_i = \int_a^b L_i(x)\,dx = \int_a^b \prod_{\substack{j=0 \\ j\neq i}}^{n} \frac{(x - x_j)}{(x_i - x_j)}\,dx,$$

(6.23)

($L_i(x)$ are the Lagrange polynomials of degree n) with the error term $E(f)$

$$E(f) = \frac{1}{(n+1)!}\int_a^b \prod_{i=0}^{n}(x - x_i)\, f^{(n+1)}\big(\xi(x)\big)dx \quad \text{where } \xi(x) \in [a,b]\ \forall x\,,$$

(6.24)

are called Newton-Cotes formulas **[30]**. Note that, Trapezoidal rule, Simpson's rule and Midpoint rule are some of the well-known Newton-Cotes formulas. These formulas use the discrete function values at equally-spaced nodes which may decrease the order of accuracy. On the other hand, the nodes x_i $(i = 1,2,\dots,n)$ (which still lie in $[a\,,b]$) and the coefficients c_i $(i = 1,2,\dots,n)$ are chosen in an optimal way in Gaussian quadrature method such that the error is minimized. Therefore, there are $2n$ parameters to be selected, like in a polynomial of degree $2n-1$. One can conclude that, Gauss quadrature formula

$$\int_a^b f(x)\,dx \;\approx\; \sum_{i=1}^{n} c_i\, f(x_i)$$

(6.25)

gives exact results for the class of polynomials of degree at most $2n-1$ **[30]**. Such an accuracy can be achieved by selecting the nodes x_i's as the roots of the n^{th}-degree Legendre polynomial $P_n(x)$ such that $x_i \in$ (-1, 1). Then **[30]**,

$$\int_{-1}^{1} P(x)\,dx \;\approx\; \sum_{i=1}^{n} c_i\,P(x_i) \quad \text{where}$$

$$c_i = \int_{-1}^{1} \prod_{\substack{j=1 \\ j\neq i}}^{n} \frac{(x-x_j)}{(x_i-x_j)}\,dx \qquad (i = 1,2,\dots,n),$$

(6.26)

where c_i's and x_i 's for 6 point method are given in Table 6.1 (see in below).

Note that, it is always possible to apply Gaussian quadrature over an arbitrary interval $[a\,,b]$ by using the transformation $t = \frac{2x-a-b}{b-a}$ yielding

$$\int_a^b f(x)\,dx = \int_{-1}^{1} f\left(\frac{(b-a)t+(b+a)}{2}\right)\frac{(b-a)}{2}\,dt.$$

(6.27)

Table 6.1 6-point Gauss-Quadrature Method weighting factors and function arguments

Points	**Weighting Factors**	**Function Arguments**
6	c_1 = 0.171324492	x_1 = -0.932469514
	c_2 = 0.360761573	x_2 = -0.661209386
	c_3 = 0.467913935	x_3 = -0.2386191860
	c_4 = 0.467913935	x_4 = 0.2386191860
	c_5 = 0.360761573	x_5 = 0.661209386
	c_6 = 0.171324492	x_6 = 0.932469514

CHAPTER 7

CASE STUDIES

7.1 Minimization in Performance Measure during Sitting Trot

Firstly, minimization of a performance measure depending on the rider's joint torques and rider-horse interaction forces and moments is aimed during the sitting trot gait. The linear equality, nonlinear equality and nonlinear inequality constraints all mentioned in Section 6.2 are considered in the optimization process.

Nonlinear inequality constraints $p_j{}^{nonlin}$ provide optimized parameters,$\overline{a}_m$, satisfy that the joint torques should be in the range between minimum and the maximum torque limit values. Linear inequality constraints $p_j{}^{lin}$ provide that the optimized parameters, $\overline{a}_m$, as inserted in the equation of the angles, they should be in the range of maximum and minimum values of joint angle limits. On the other hand, $h_i{}^{nonlin}$ nonlinear equality constraints, concern that the relative distance between the rider's center of gravity and the 4th marker position along x-direction should be kept constant during riding. The stirrup length is adjusted before riding and it is kept constant during the ride. The piecewise continuous polynomials for the joint angles are created to be 3rd degree polynomials with second degree of continuity at the knot points. The initial and final values of 0th, 1st and 2nd derivatives of the joint angles are equal at t_0 and t_f in order to provide periodicity of the joint angles. The initial and final conditions for the rider posture at time t_0 and t_f are set as the correct posture for riding, i.e., the joint angles are defined at t_0 and t_f to be $f_1(t_0)$ and $f_n(t_f)$. (See Appendix Table A.21)

The optimization process for the sitting trot yields the optimal design variables and performance measure given below.

$\overline{a}_m{}^*$ = [1.0439 1.9209 -1.4523 0 -0.6905 0.8694 0 1.0519 -0.5236 -0.7643]

$J^*(\overline{a}_m) = 1.096579\text{e+}11\ (Nm)^2$

The results of the optimization are given by following plots. . In the plots, the minimum and maximum limits of the joint angles and torques are represented by square-dotted (cyan color) and the mean values of the joint angles are shown as diamond-dotted (magenta color) lines.

i) Link-1 Simulation Results

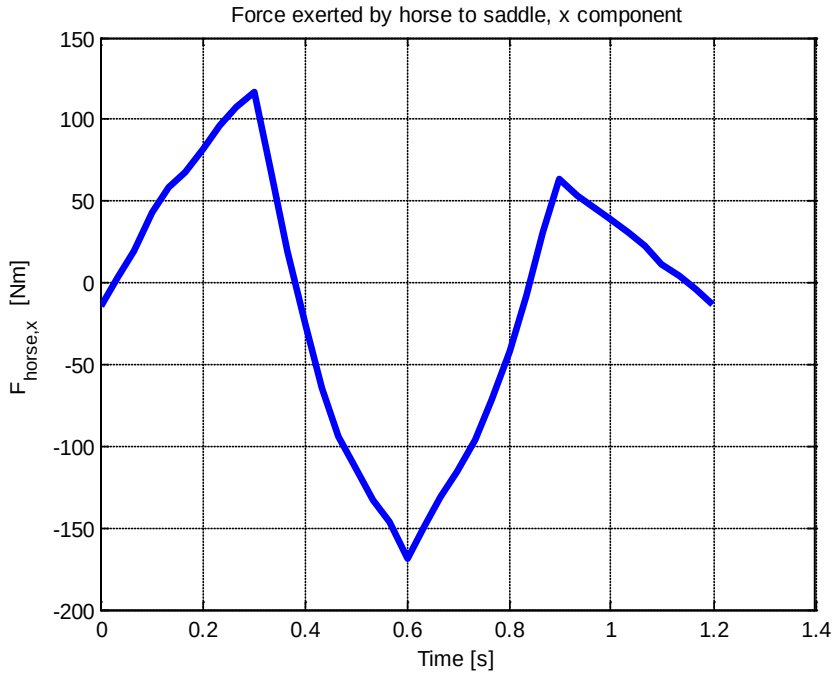

Figure 7.1 Force exerted by horse to saddle, x component during sitting trot

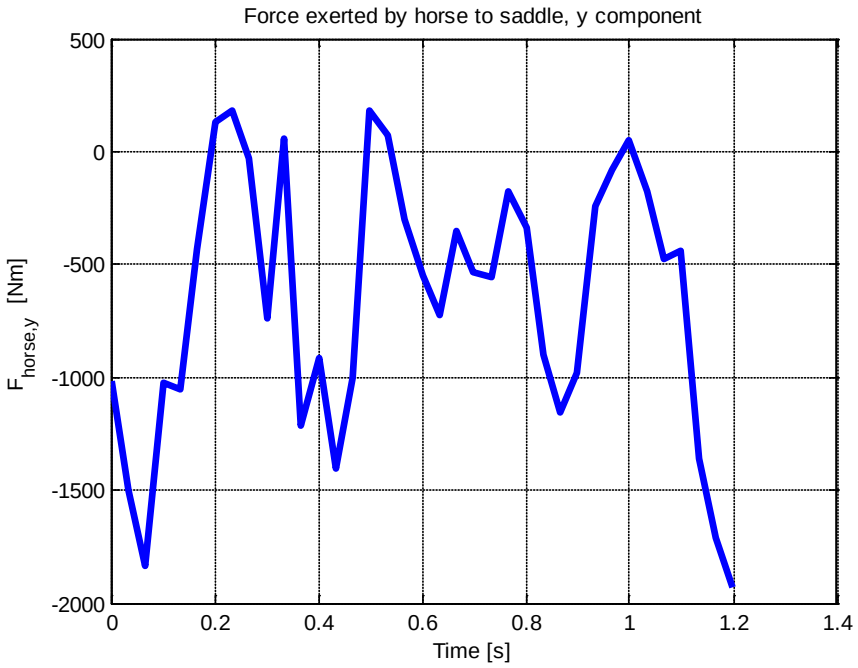

Figure 7.2 Force exerted by horse to saddle, y component during sitting trot

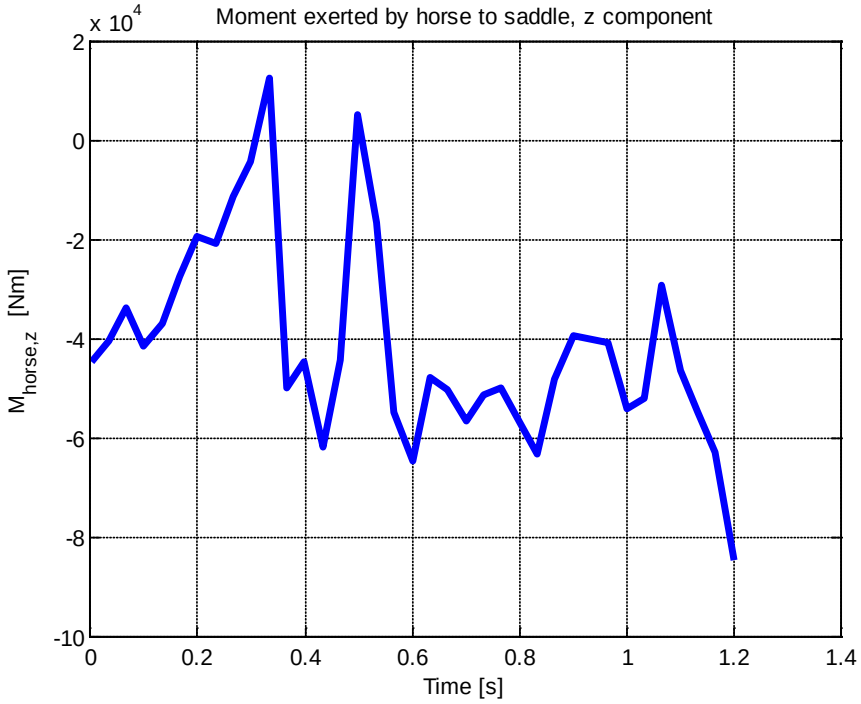

Figure 7.3 Moment exerted by horse to saddle, z component during sitting trot

ii) Link-2 Simulation Results

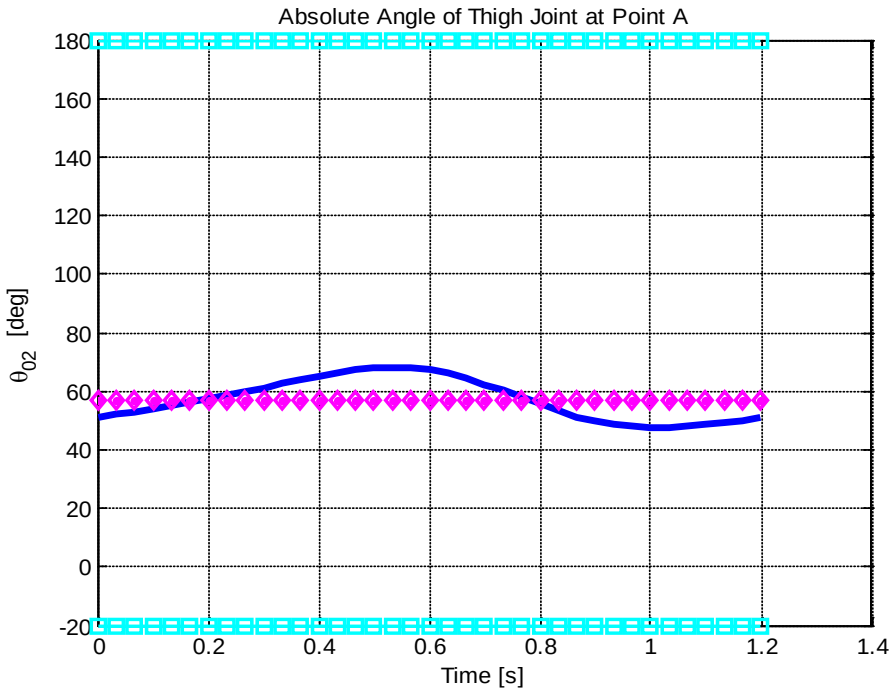

Figure 7.4 Absolute Angle of Thigh Joint at Point A during sitting trot

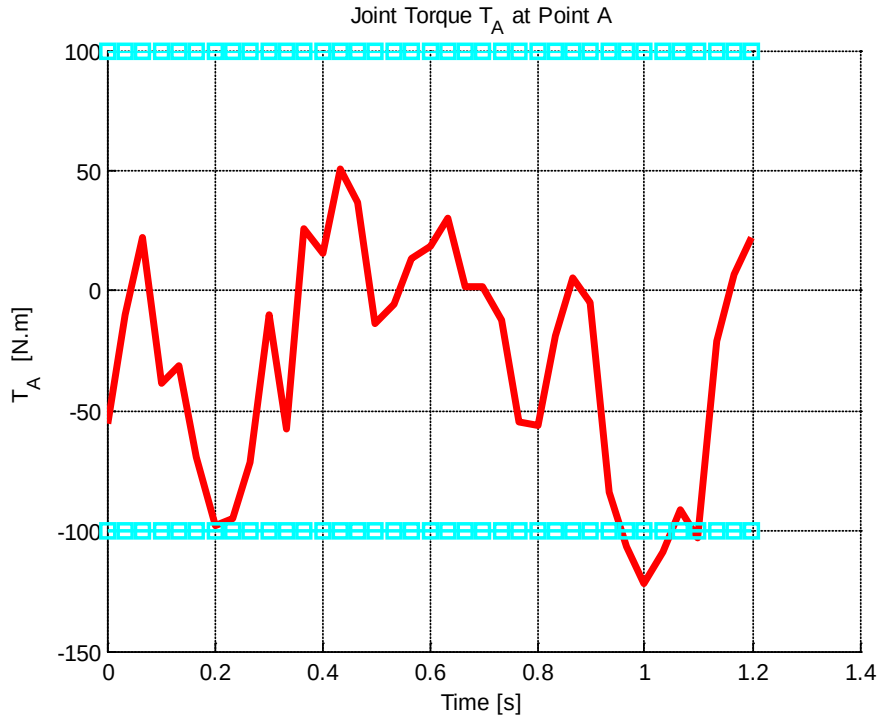

Figure 7.5 Joint Torque T_A at Point A during sitting trot

iii) Link-3 Simulation Results

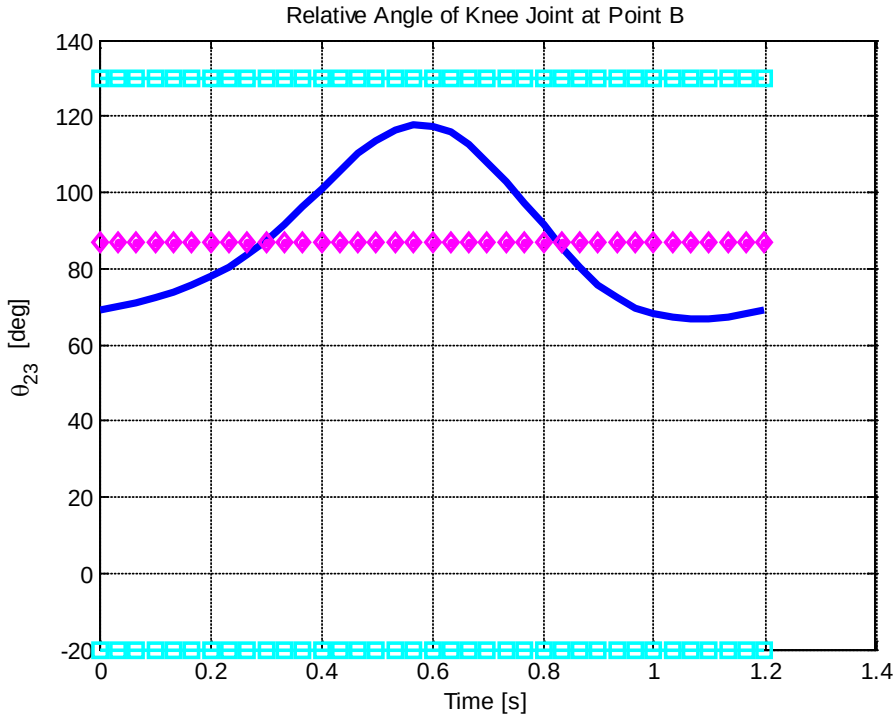

Figure 7.6 Relative Angle of Knee at Point B during sitting trot

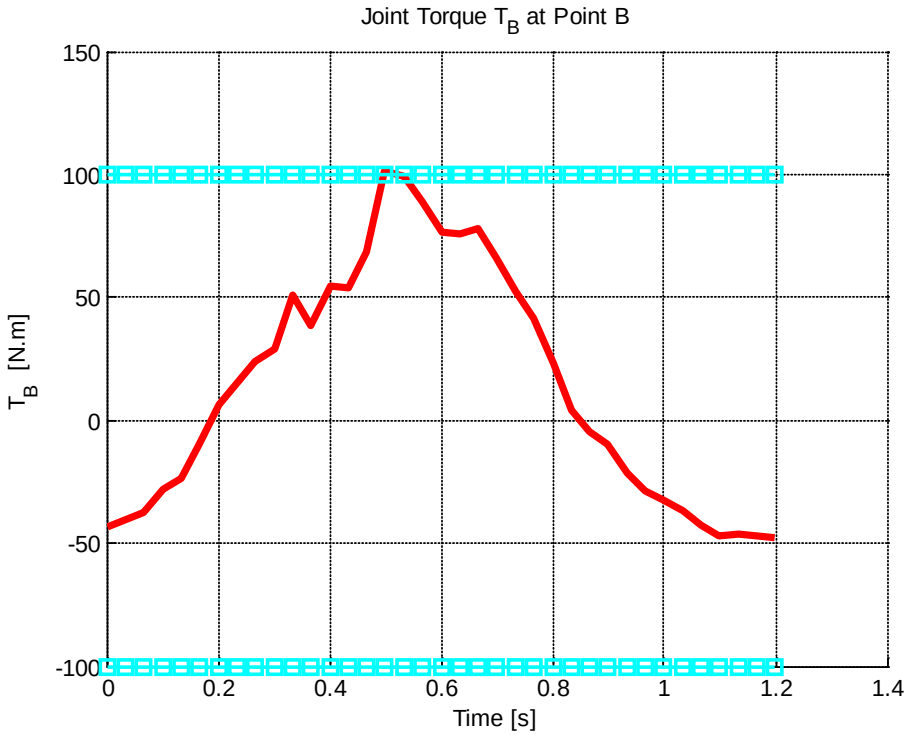

Figure 7.7 Joint Torque T_B at Point B during sitting trot

iv) Link-4 Simulation Results

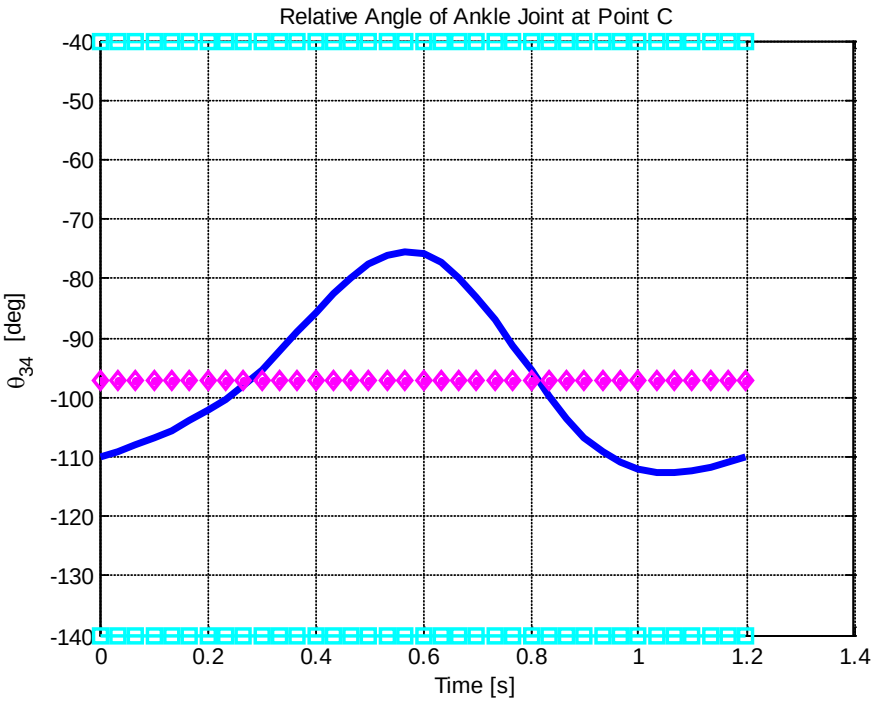

Figure 7.8 Relative Angle of Ankle Joint at Point C during sitting trot

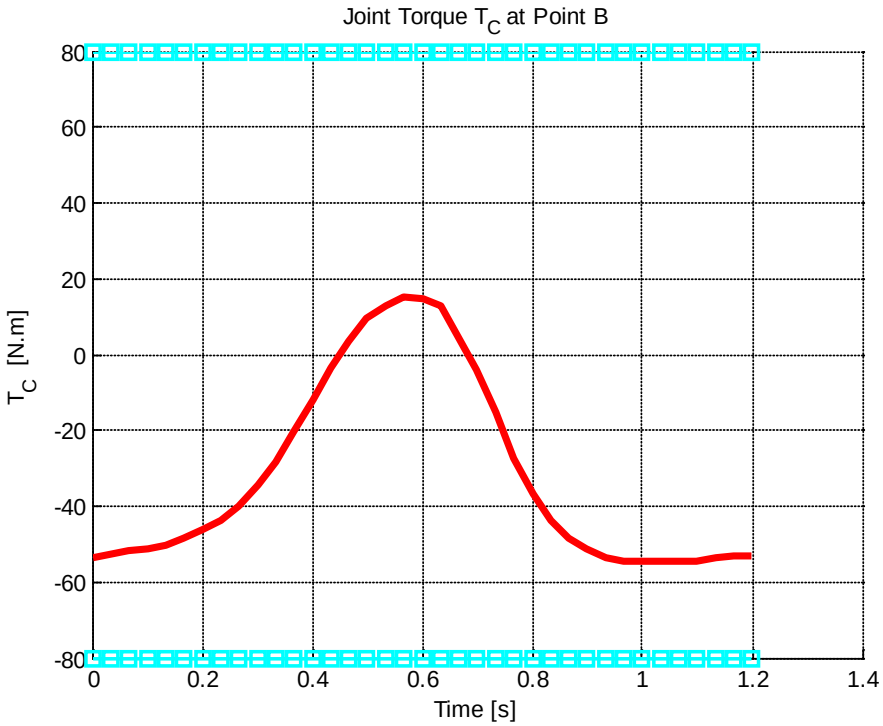

Figure 7.9 Joint Torque T_C at Point C during sitting trot

v) Link-5 Simulation Results

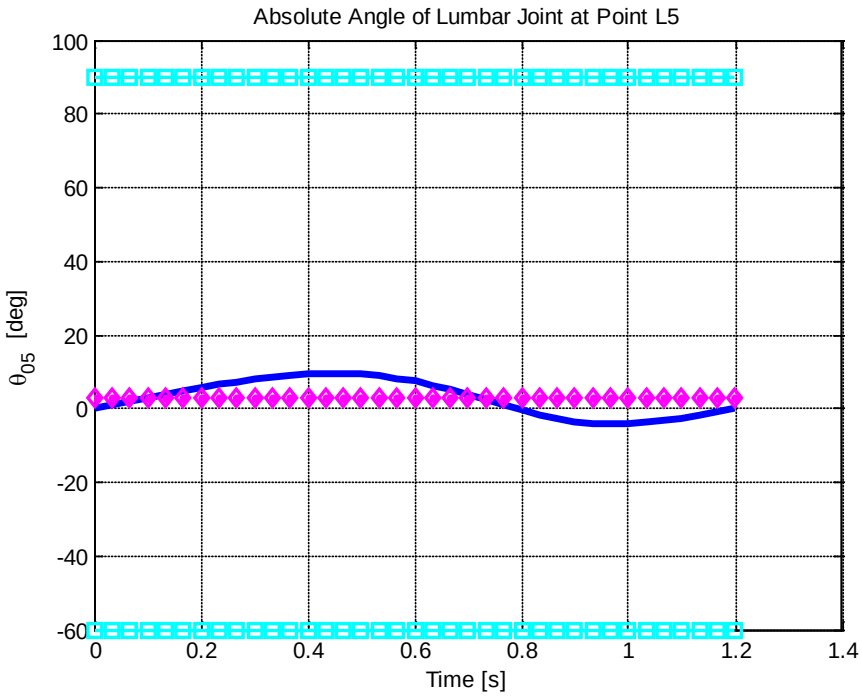

Figure 7.10 Absolute Angle of Lumbar Joint at Point L_5 during sitting trot

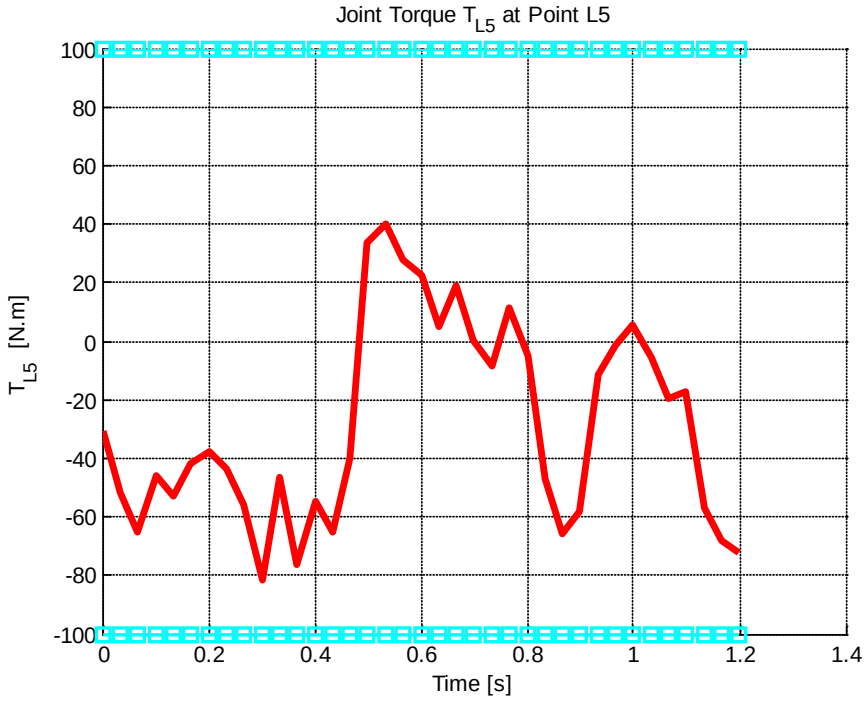

Figure 7.11 Joint Torque T_{L5} at Point L_5 during sitting trot

vi) Link-6 Simulation Results

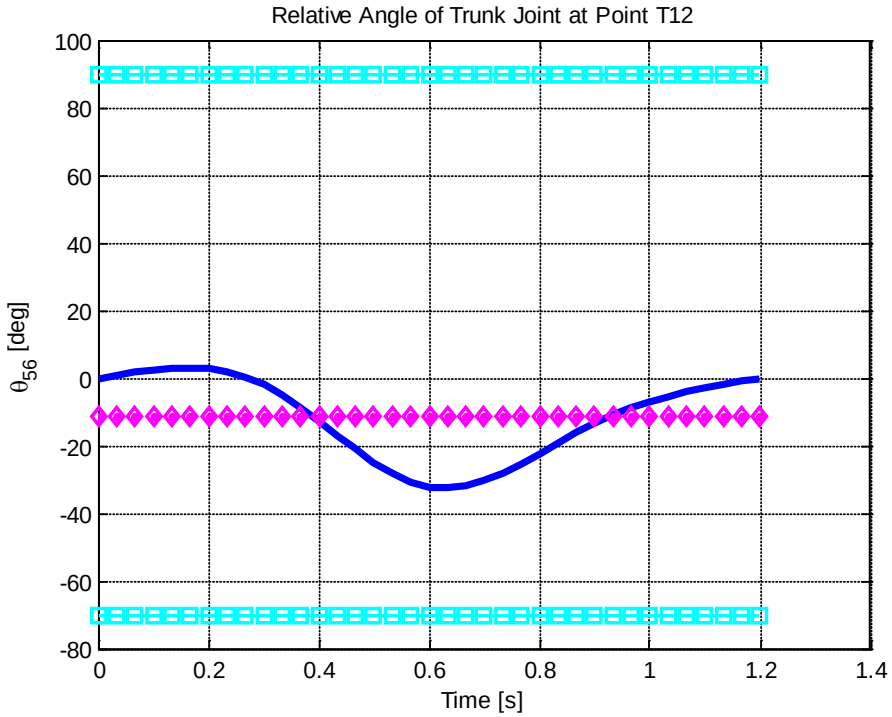

Figure 7.12 Relative Angle of Trunk at Point T_{12} during sitting trot

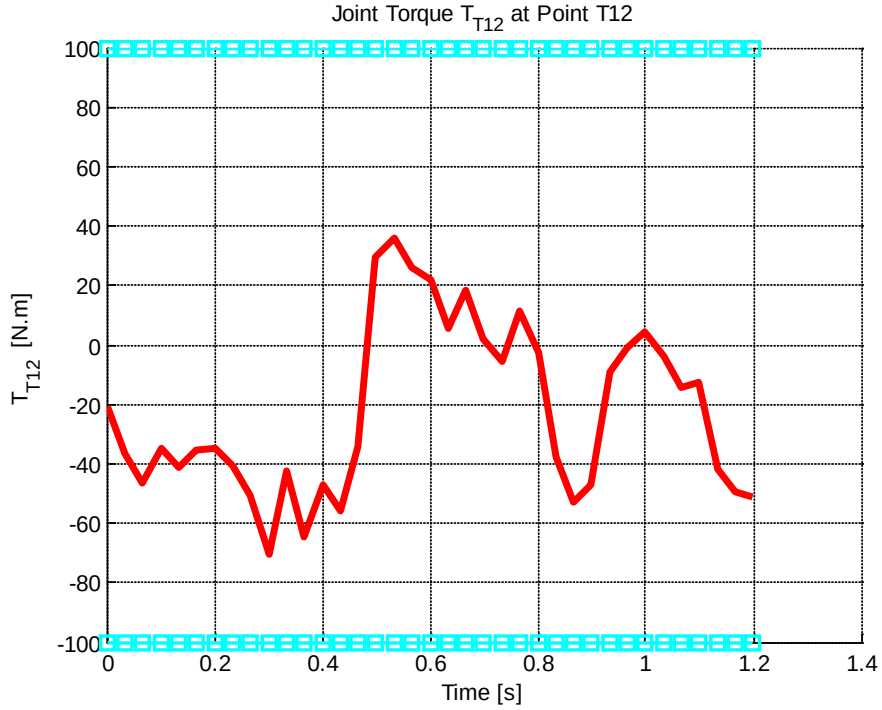

Figure 7.13 Joint Torque T_{T12} at Point T_{12} during sitting trot

vii) Link-7 Simulations Result

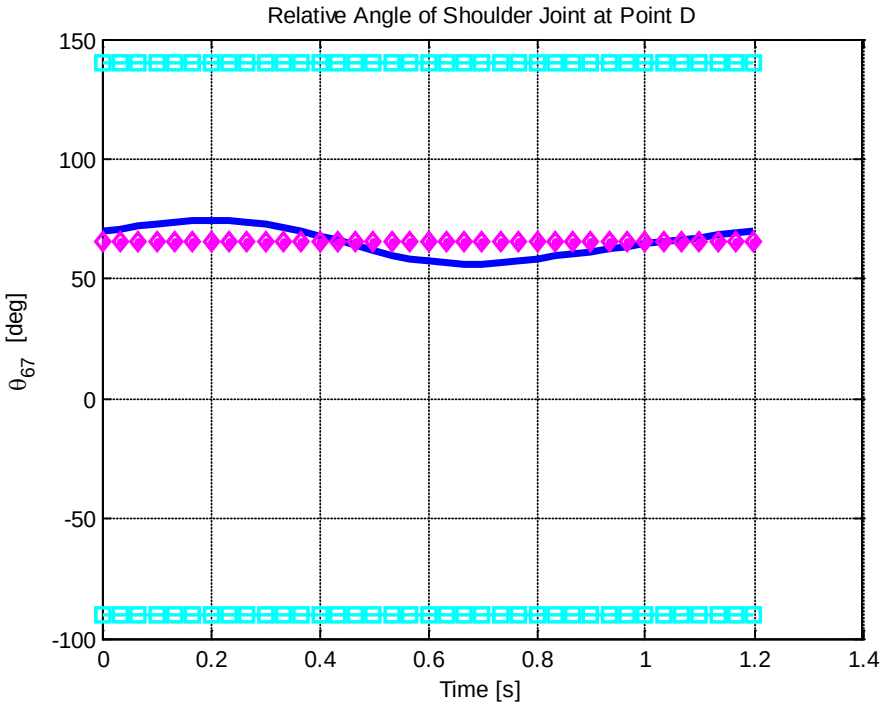

Figure 7.14 Relative Angle of Shoulder Joint at Point D during sitting trot

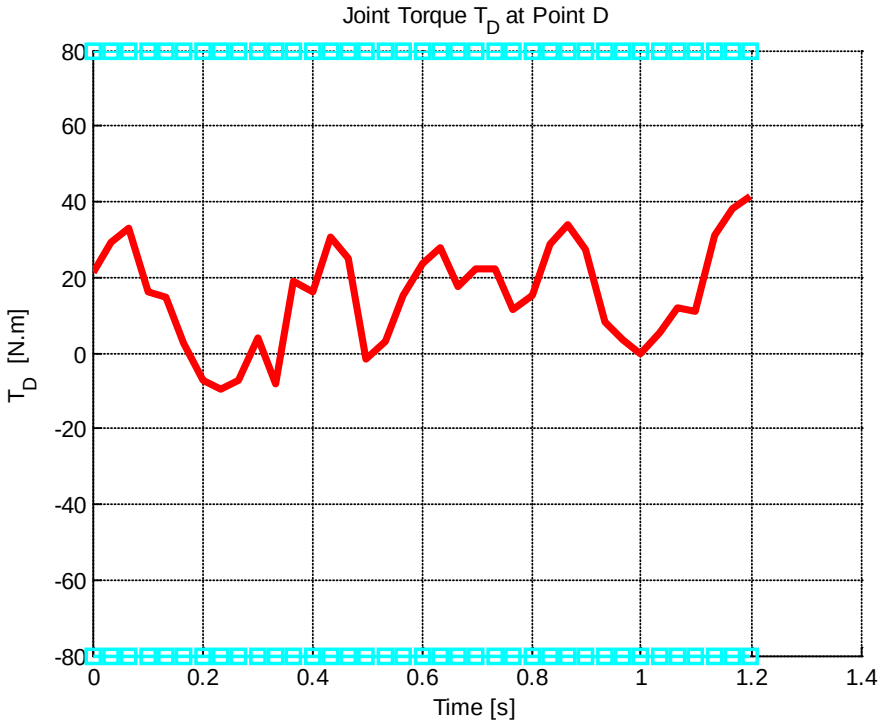

Figure 7.15 Joint Torque T_D at Point D during sitting trot

viii) Link-8 Simulation Results

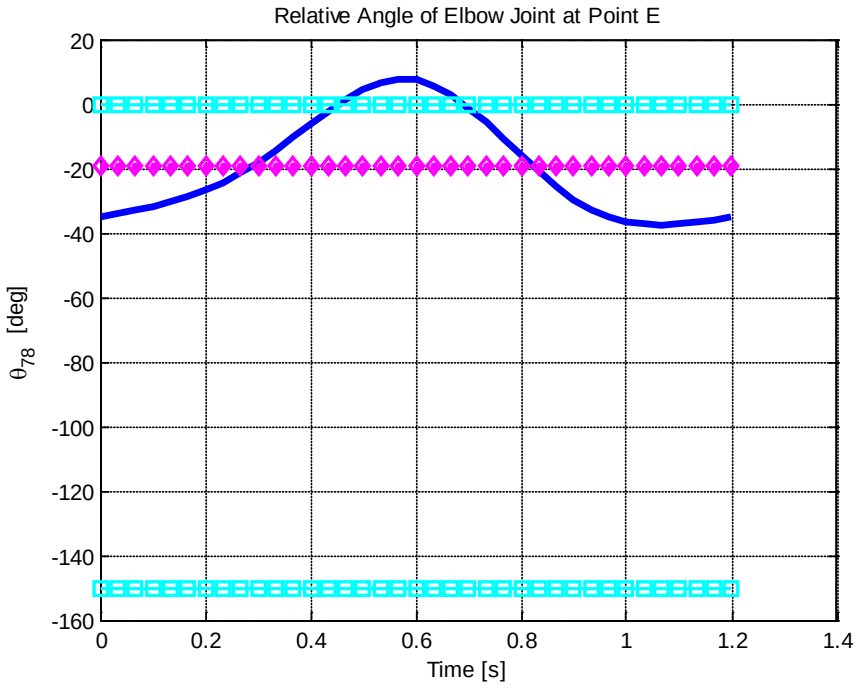

Figure 7.16 Relative Angle of Elbow Joint at Point E during sitting trot

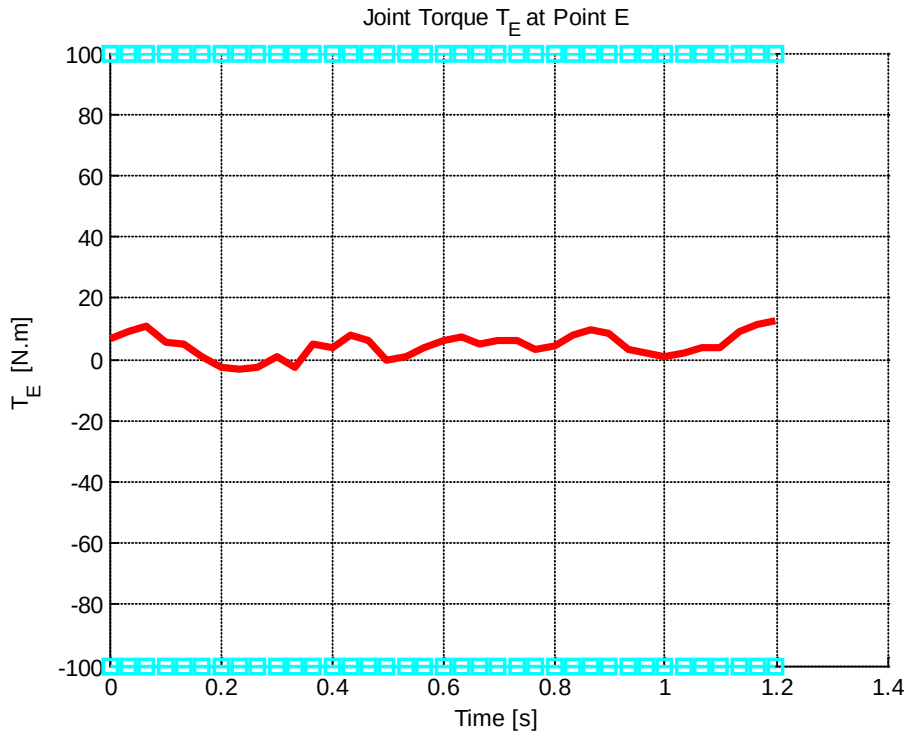

Figure 7.17 Joint Torque T_E at Point E during sitting trot

ix) Link-9 Simulation Results

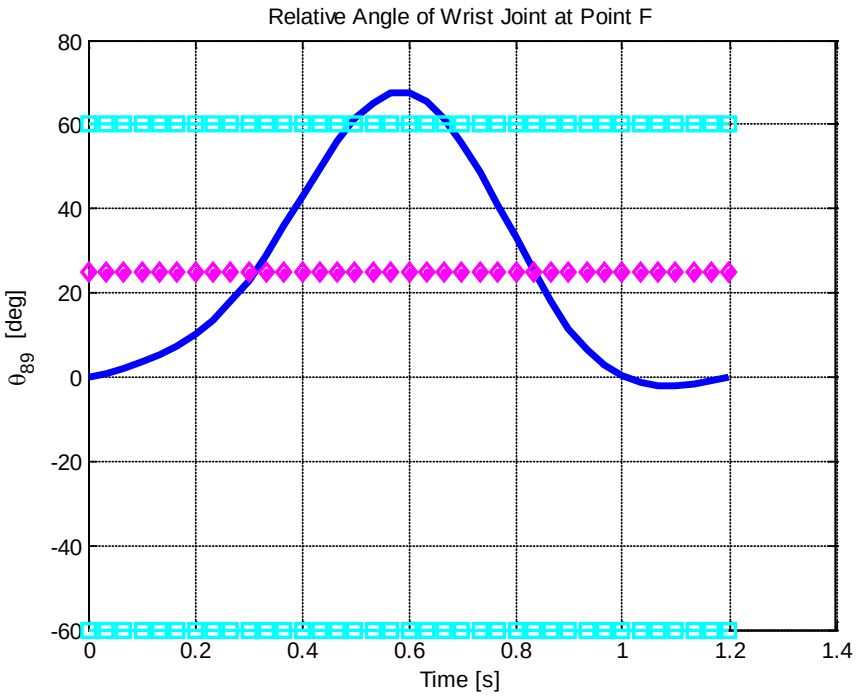

Figure 7.18 Relative Angle of Wrist Joint at Point F during sitting trot

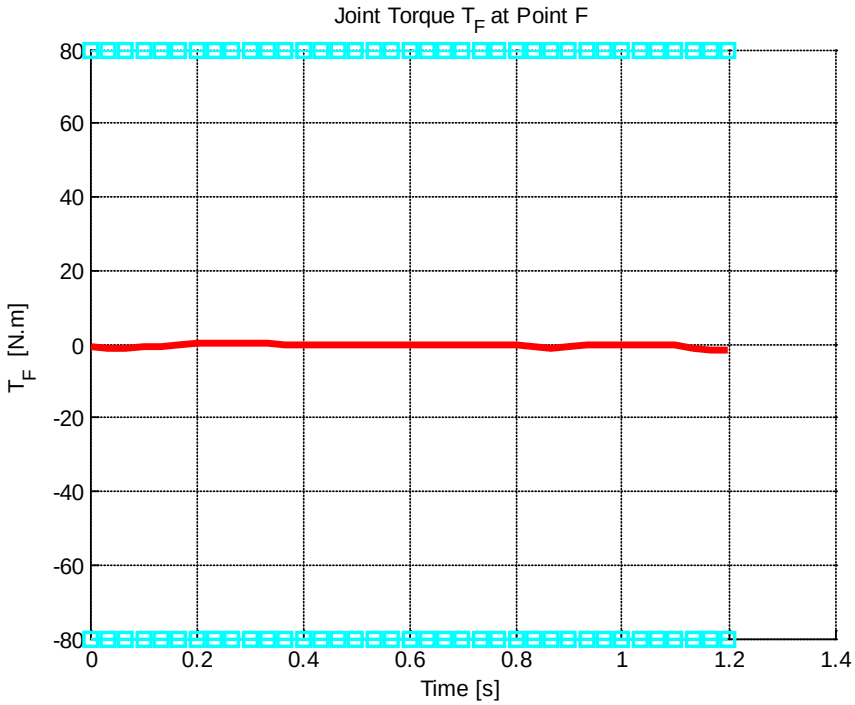

Figure 7.19 Joint Torque T_F at Point F during sitting trot

x) Link-10 Simulation Results

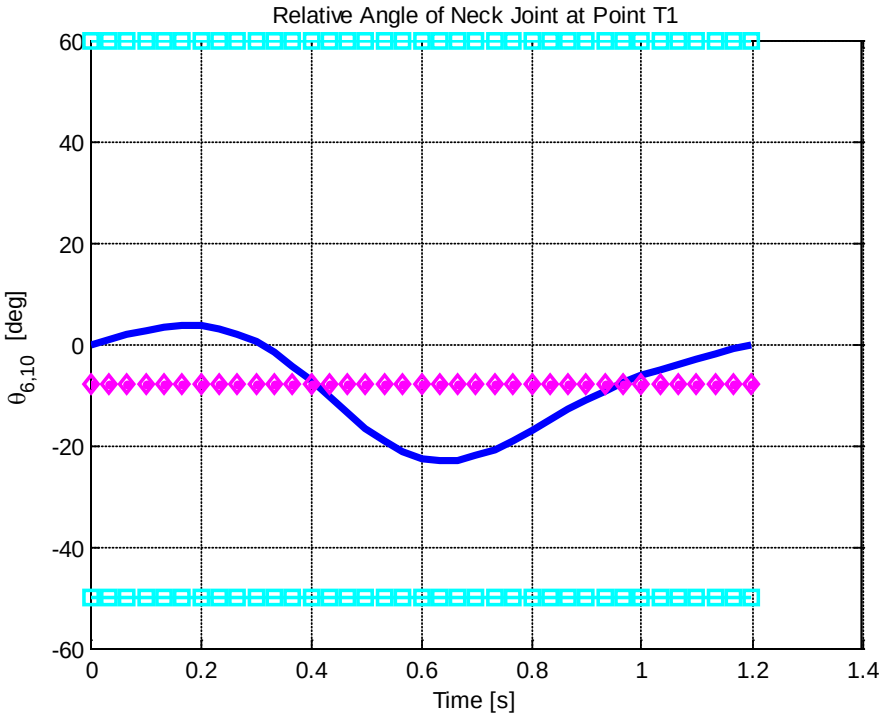

Figure 7.20 Relative Angle of Neck at Point T_1 during sitting trot

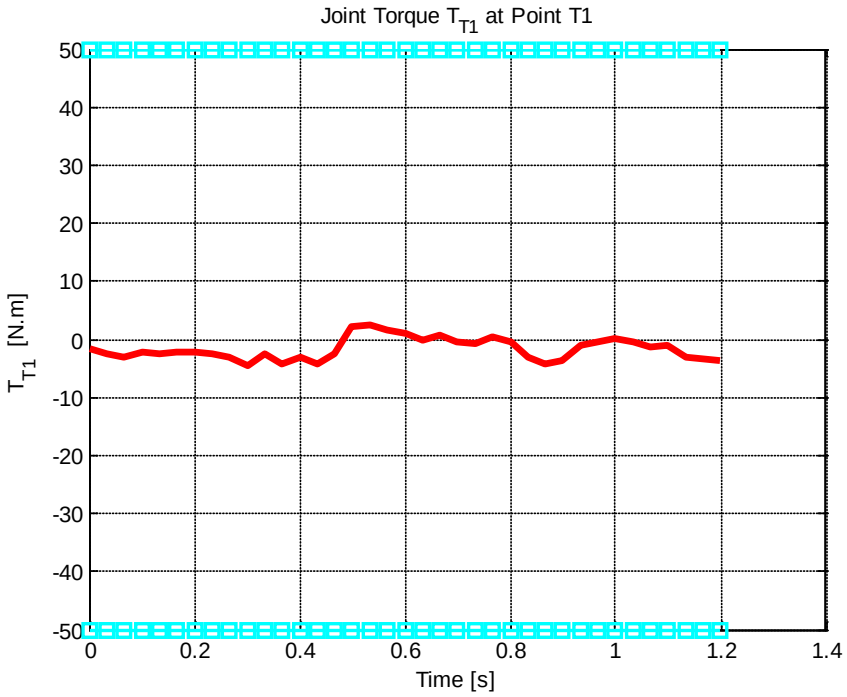

Figure 7.21 Joint Torque T_{T1} at Point T_1 during sitting trot

xi) Link-11 Simulation Results

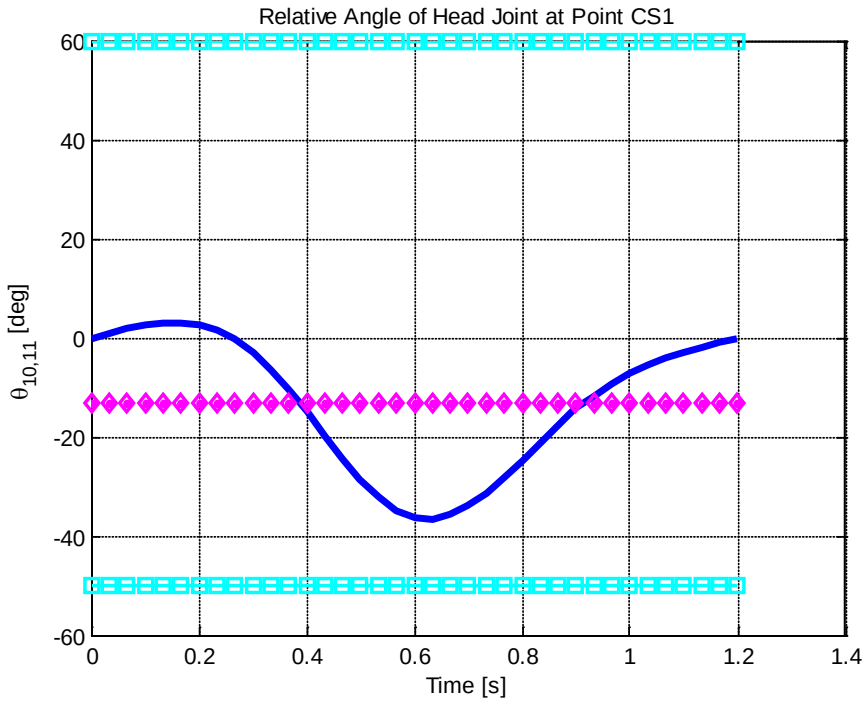

Figure 7.22 Relative Angle of Head Joint at Point CS_1 during sitting trot

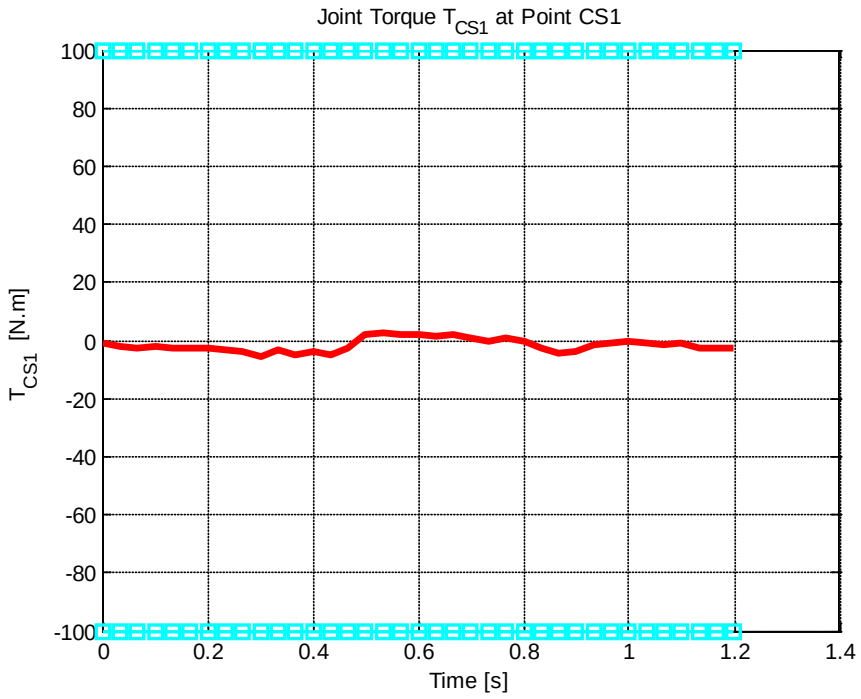

Figure 7.23 Joint Torque T_{CS1} at Point CS_1 during sitting trot

7.2 Minimization in Performance Measure during Sudden Stop

A sudden stop scenario is also created. In this scenario, the same performance measure is employed. During the sudden stop scenario, the nonlinear inequality constraints, $p_j{}^{nonlin}$, [which ensure that the joint torques are in range of minimum and maximum torque limits] are not considered for the optimization of $\overline{a}_m$. Hence the optimization process concerns only the linear inequality constraints, $p_j{}^{lin}$ (for limiting the joint angles in the minimum-maximum range) and the nonlinear equality constraints, $h_i{}^{nonlin}$ (ensuring that the rider center of gravity of the rider along x-direction will not change). After getting the optimum parameters which minimize the objective function, the joint torques are found. Then it is checked whether these torques are feasible or not.

Four piecewise continuous polynomials are created for the joint angles are created. These are 3rd degree polynomials with second degree of continuity at the knot points. The initial and final conditions of the joint angles as 0th, 1st and 2nd derivatives are defined and they are equal at t_0 and t_f. At the final time, t_f, the joint angles can take any value after sudden stop but since it can't be guessed the final posture, the rider is assumed to be the correct posture at final time also. (See Appendix Table A.21)

At the end, it is decided whether the rider can be prevented from falling down. In the following plots, the minimum and maximum limits of the joint angles and torques are represented by square-dotted (cyan color) lines and the mean values of the joint angles are shown as diamond-dotted (magenta color) lines. The optimization yields the optimal design variables and performance measure is given below.

$\overline{a}_m{}^*$ = [0.5919 0.1174 -0.6989 -0.7377 -1.2067 1.2939 0 -0.6759 -1.1745 -1.1408]

$J^*(\overline{a}_m) = 6.5420\text{e+}10\ (Nm)^2$

i) Link-1 Simulation Results

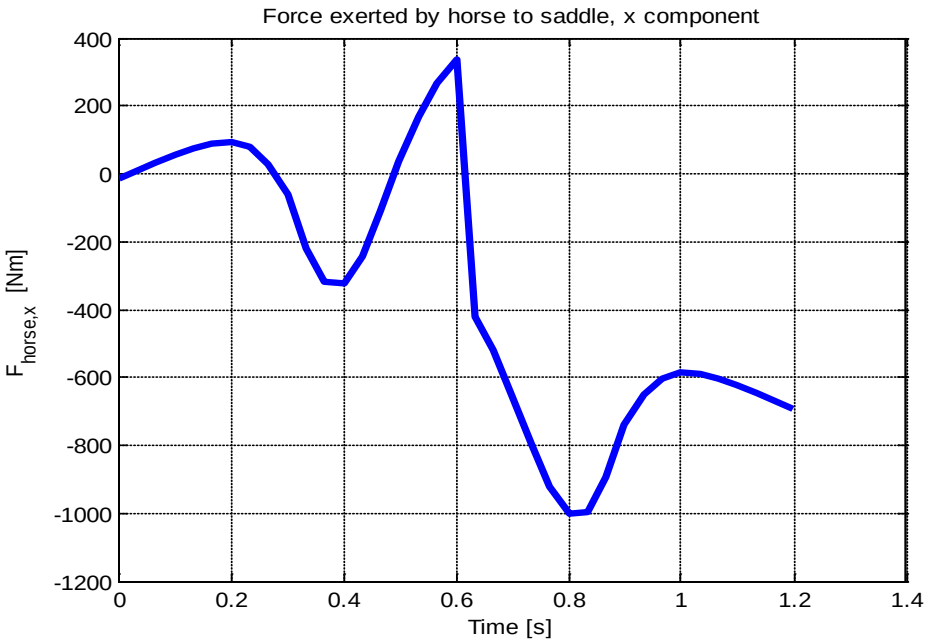

Figure 7.24 Force exerted by horse to saddle, x component during sudden stop

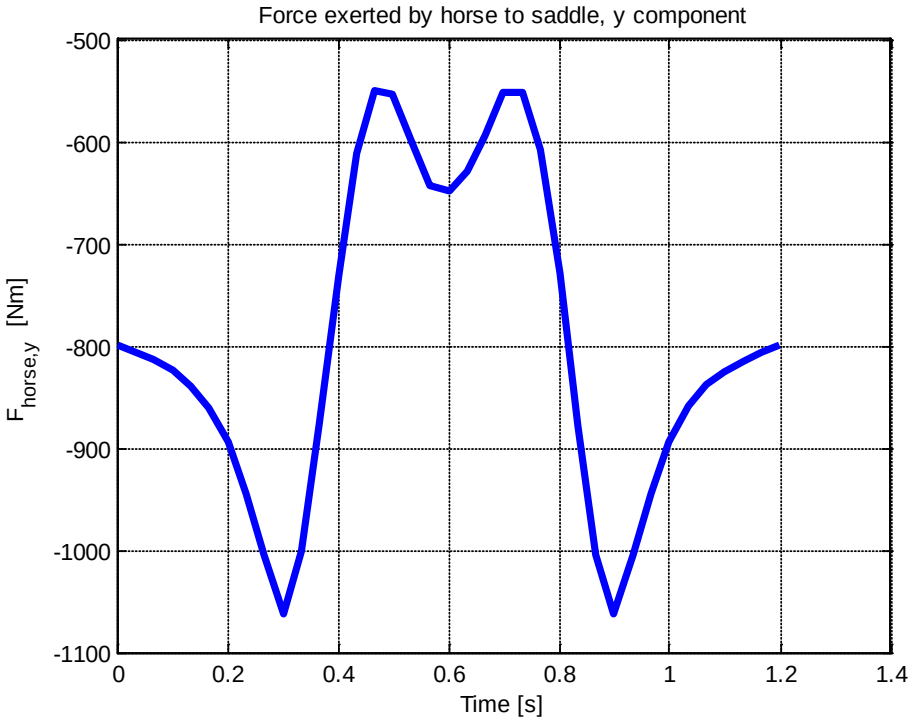

Figure 7.25 Force exerted by horse to saddle, y component during sudden stop

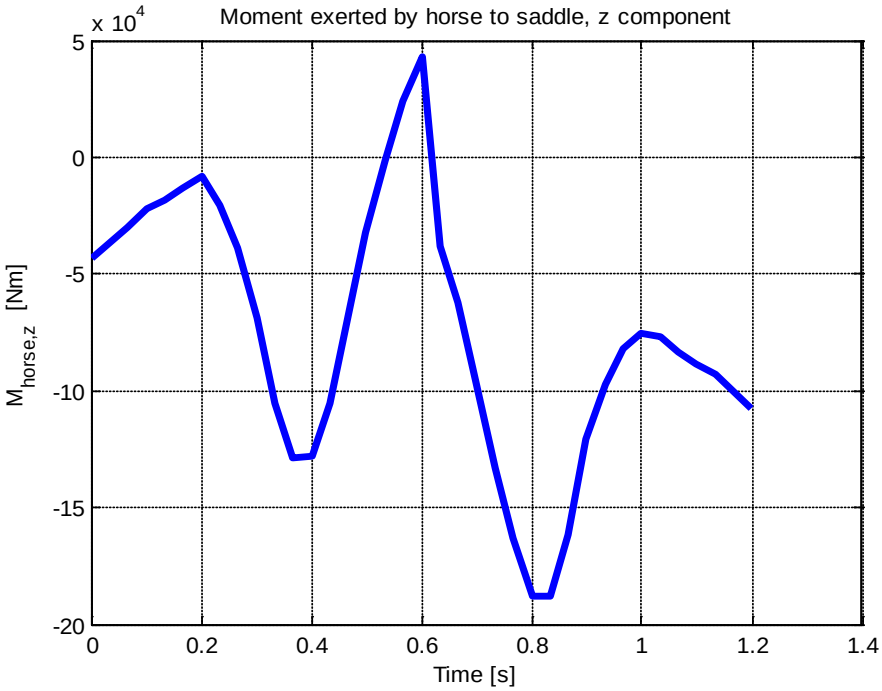

Figure 7.26 Moment exerted by horse to saddle, z component during sudden stop

ii) Link-2 Simulation Results

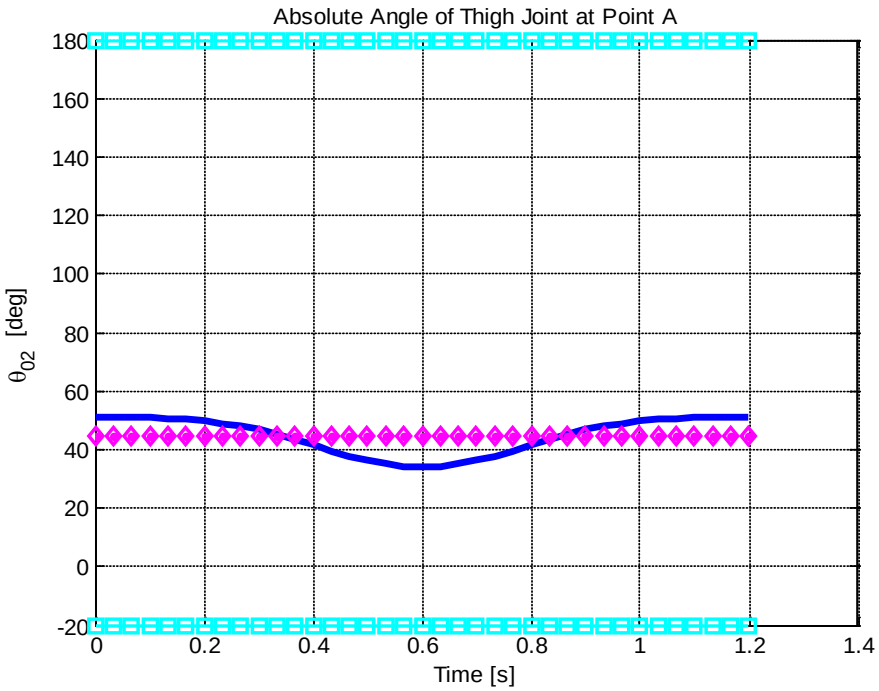

Figure 7.27 Relative Angle of Thigh Joint at Point A during sudden stop

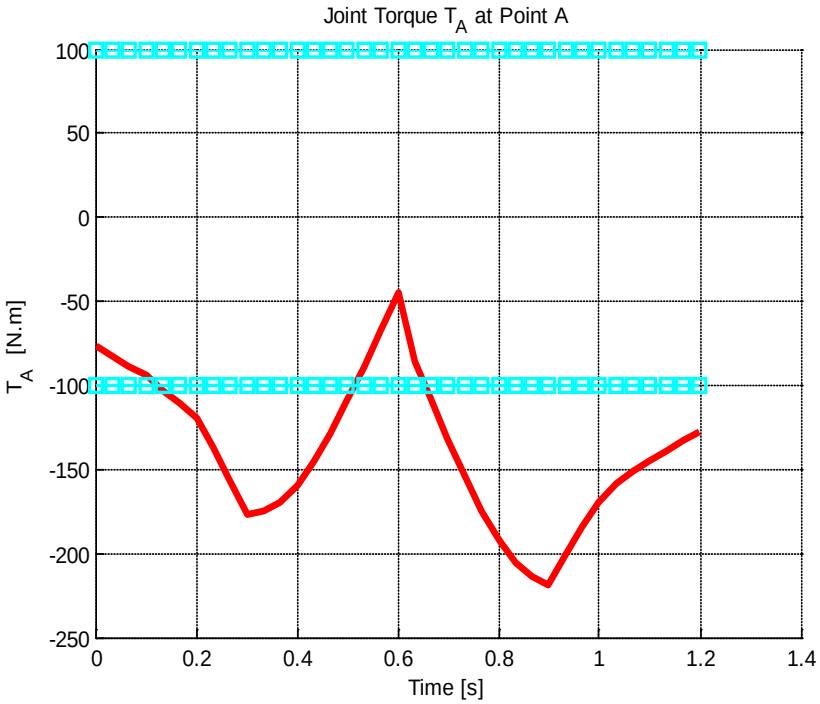

Figure 7.28 Joint Torque T_A at Point A during sudden stop

iii) Link-3 Simulation Results

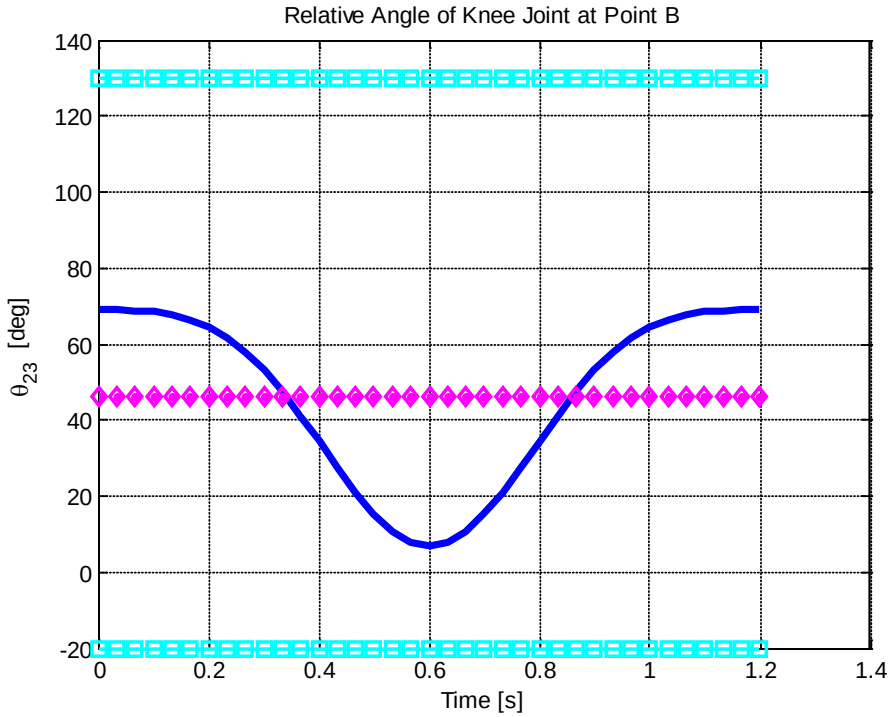

Figure 7.29 Relative Angle of Knee at Point A during sudden stop

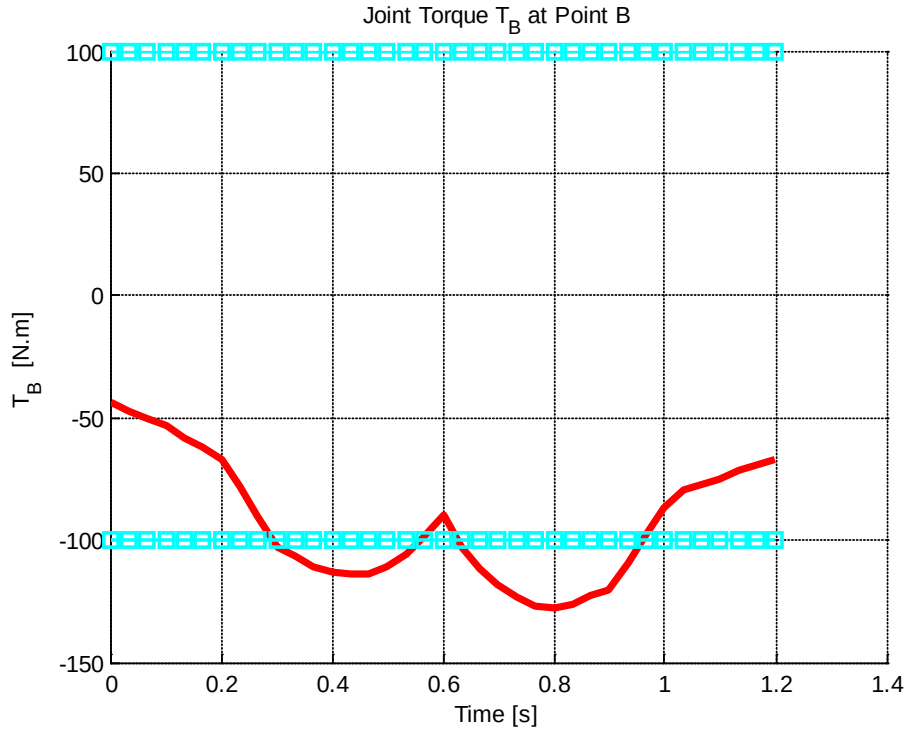

Figure 7.30 Joint Torque T_B at Point B during sudden stop

iv) Link-4 Simulation Results

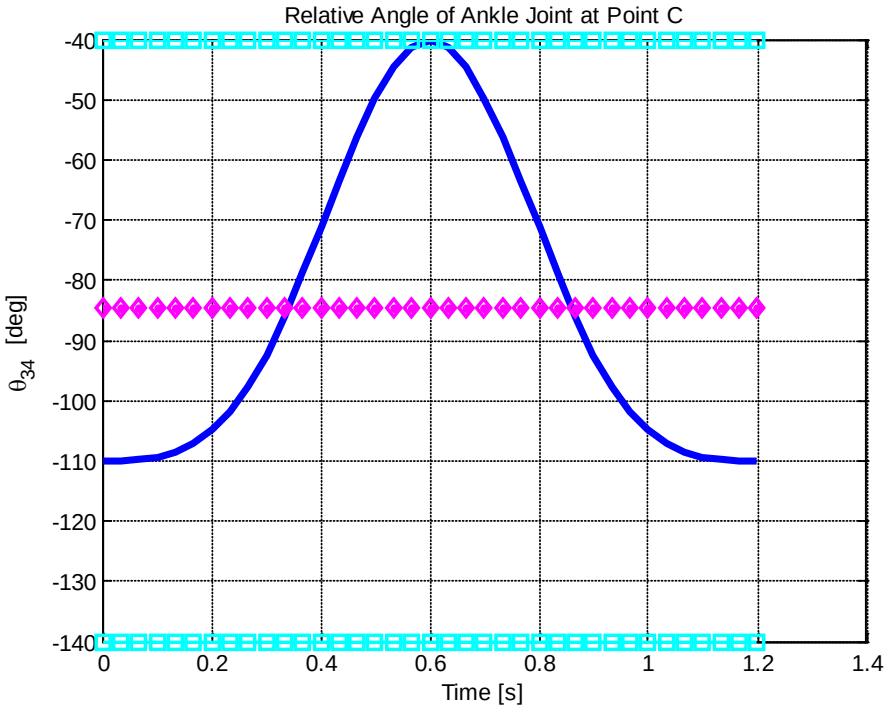

Figure 7.31 Relative Angle of Ankle Joint at Point C during sudden stop

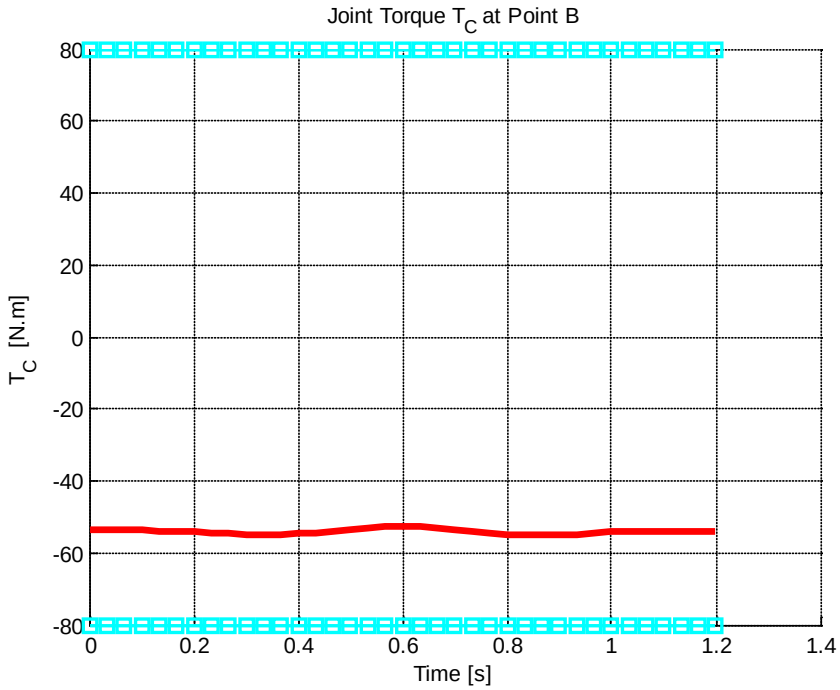

Figure 7.32 Joint Torque T_C at Point C during sudden stop

v) Link-5 Simulation Results

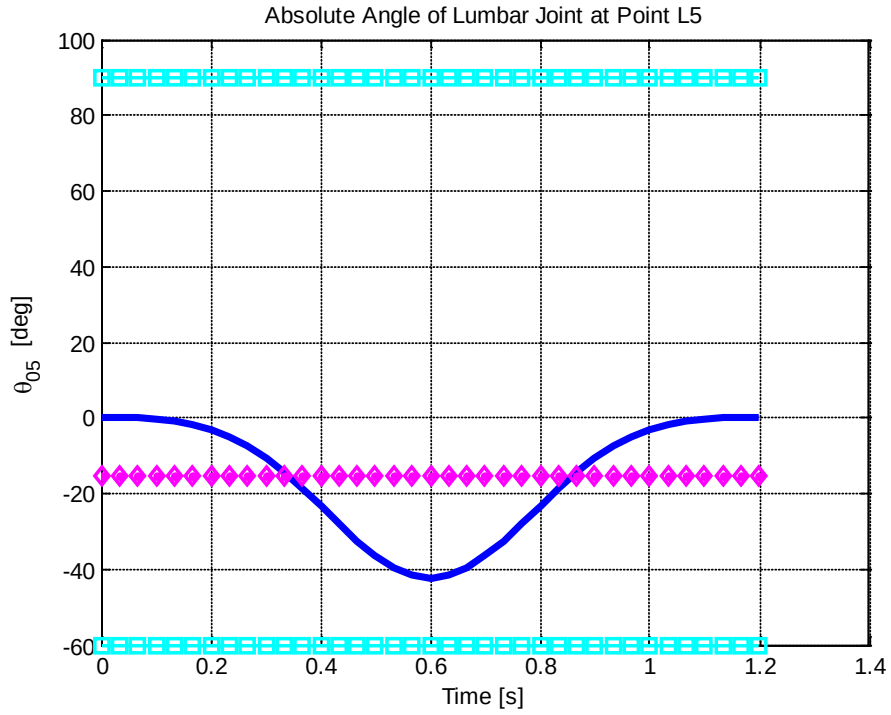

Figure 7.33 Relative Angle of Lumbar Joint at Point L_5 during sudden stop

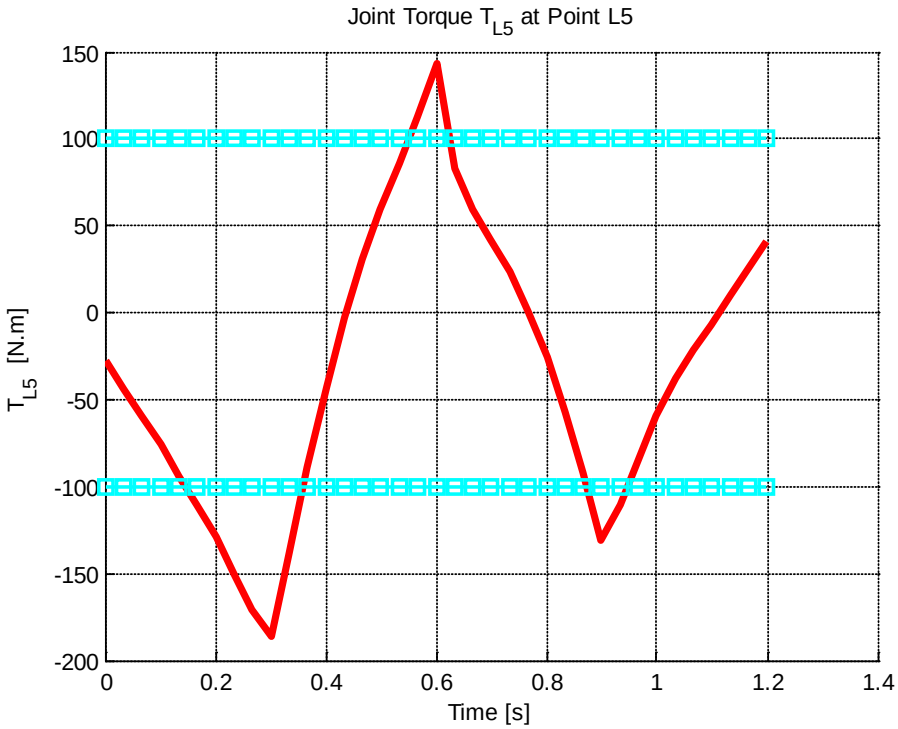

Figure 7.34 Joint Torque T_{L5} at Point L_5 during sudden stop

vi) Link-6 Simulation Results

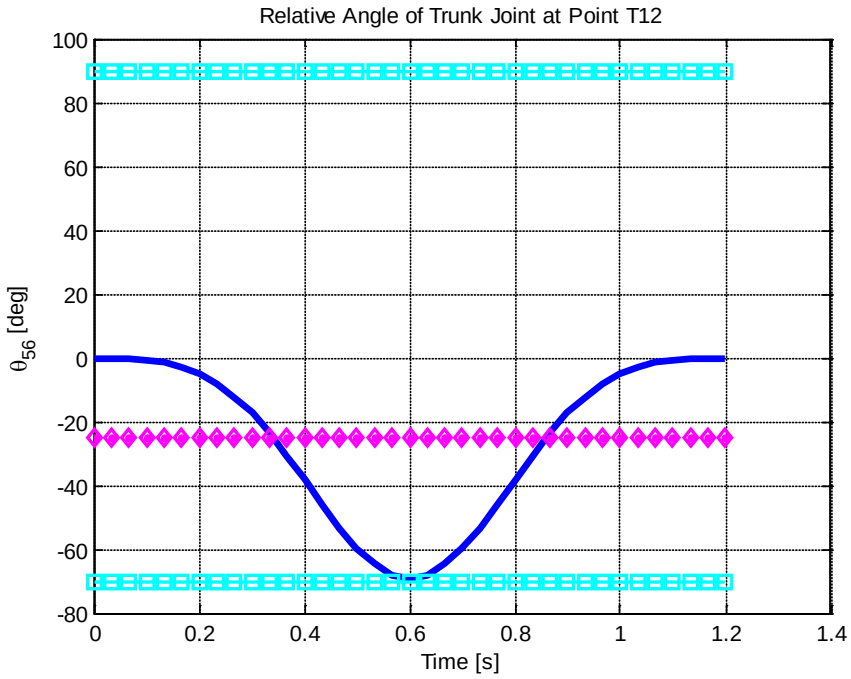

Figure 7.35 Relative Angle of Trunk at Point T_{12} during sudden stop

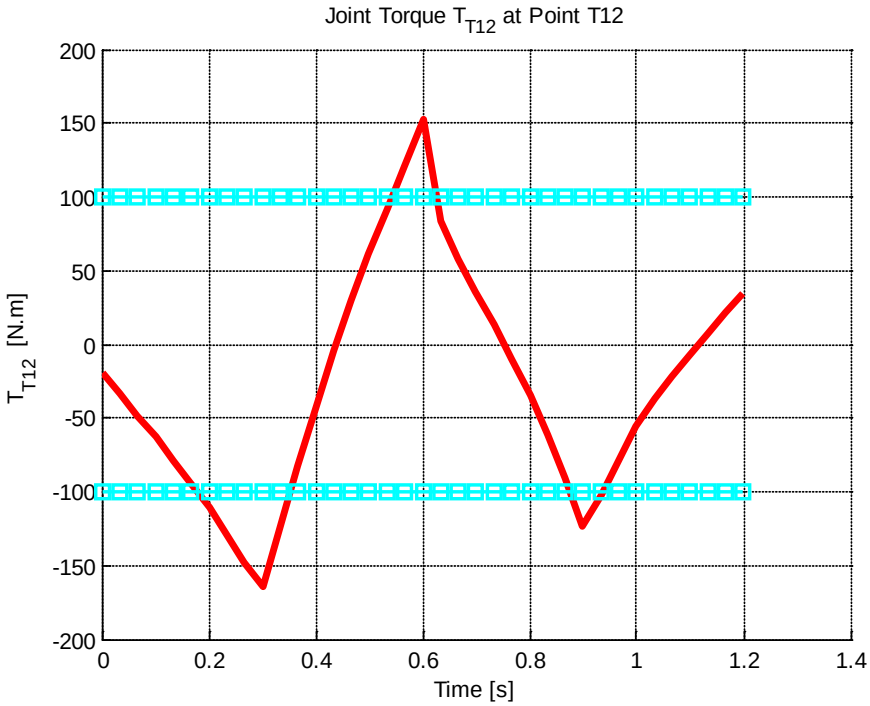

Figure 7.36 Joint Torque T_{T12} at Point T_{12} during sudden stop

vii) Link-7 Simulation Results

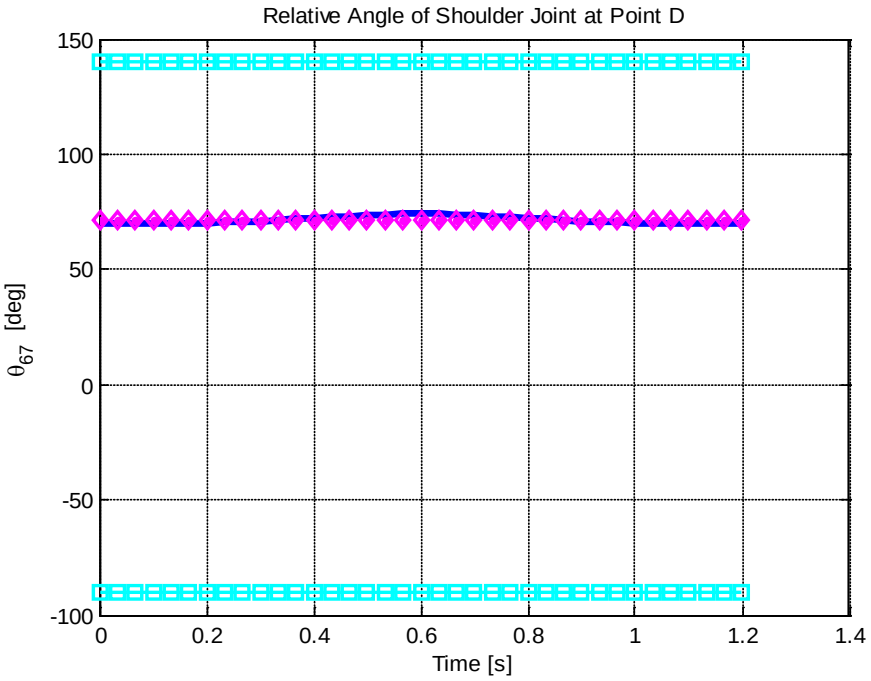

Figure 7.37 Relative Angle of Shoulder Joint at Point D during sudden stop

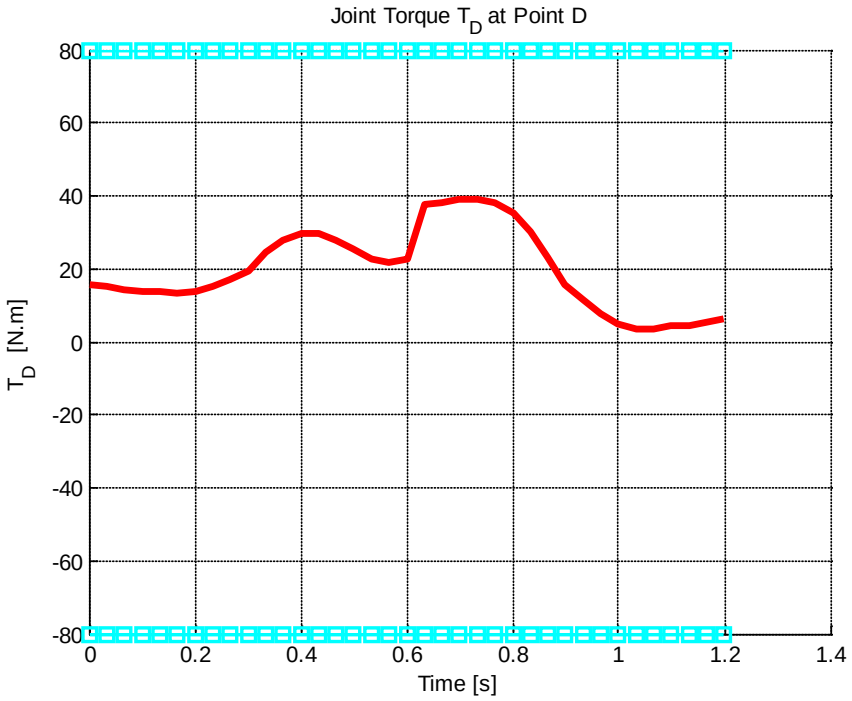

Figure 7.38 Joint Torque T_D at Point D during sudden stop

viii) Link-8 Simulation Results

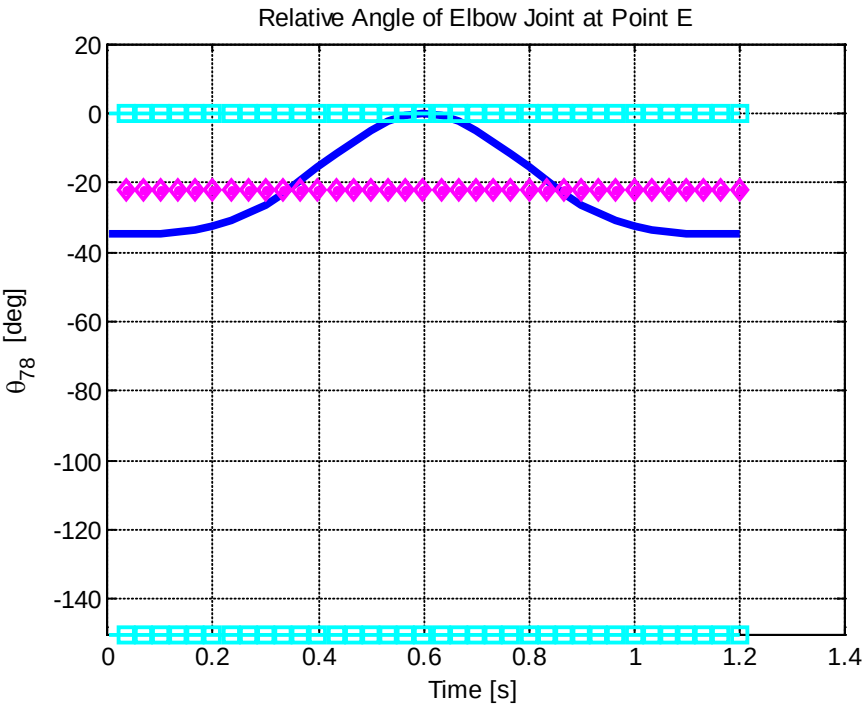

Figure 7.39 Relative Angle of Elbow Joint at Point E during sudden stop

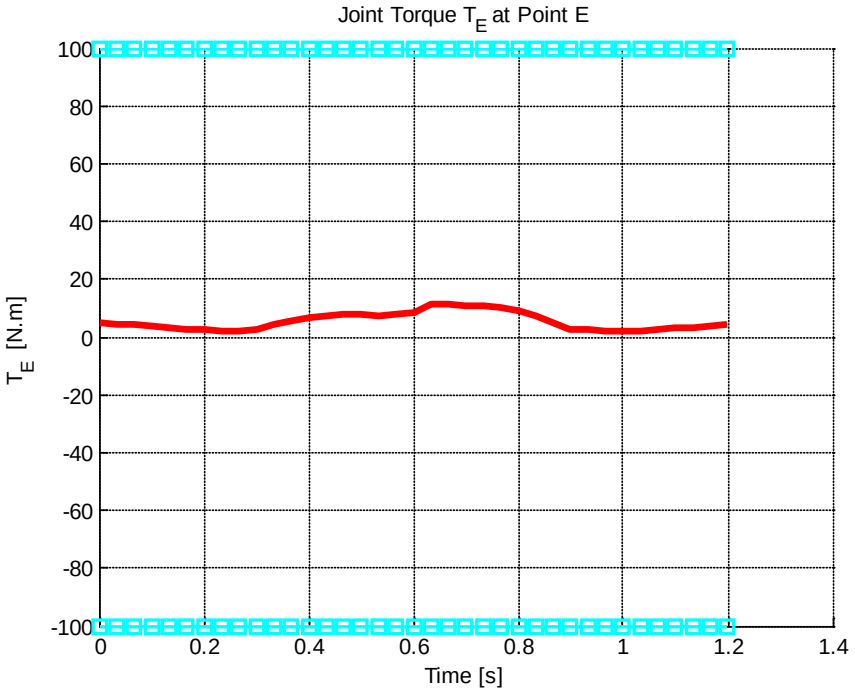

Figure 7.40 Joint Torque T_E at Point E during sudden stop

ix) Link-9 Simulation Results

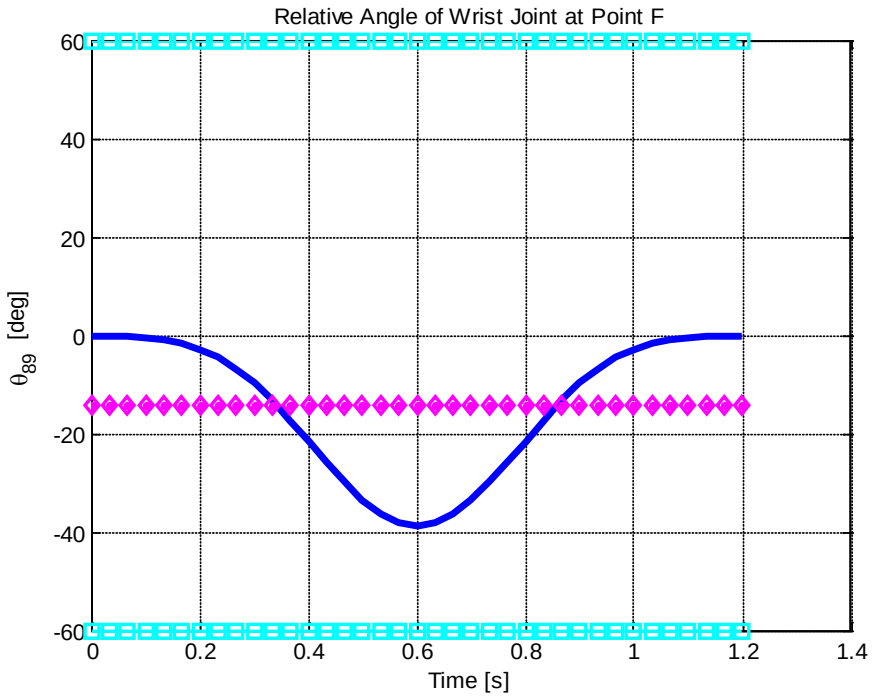

Figure 7.41 Relative Angle of Wrist Joint at Point F during sudden stop

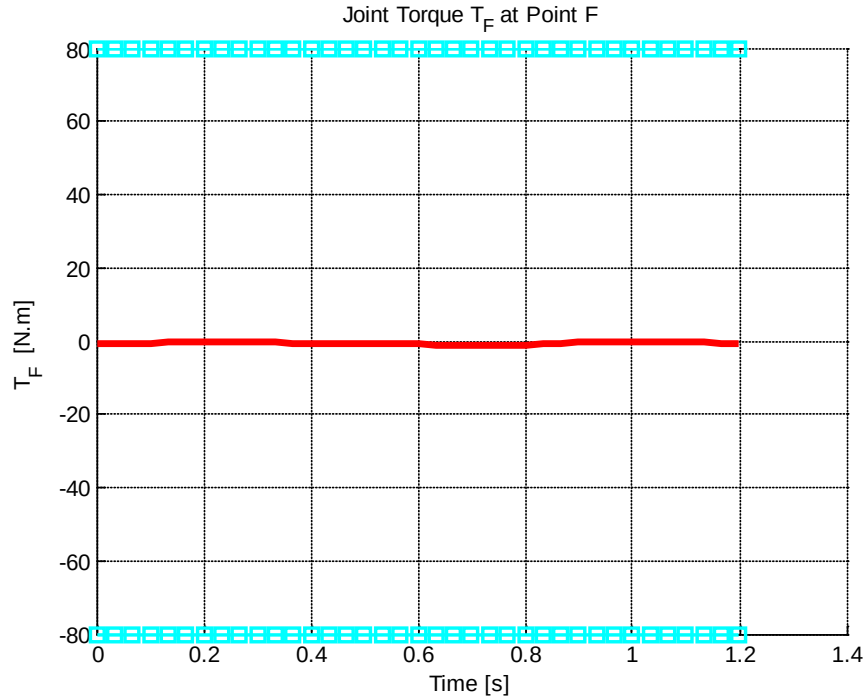

Figure 7.42 Joint Torque T_F at Point F during sudden stop

x) Link-10 Simulation Results

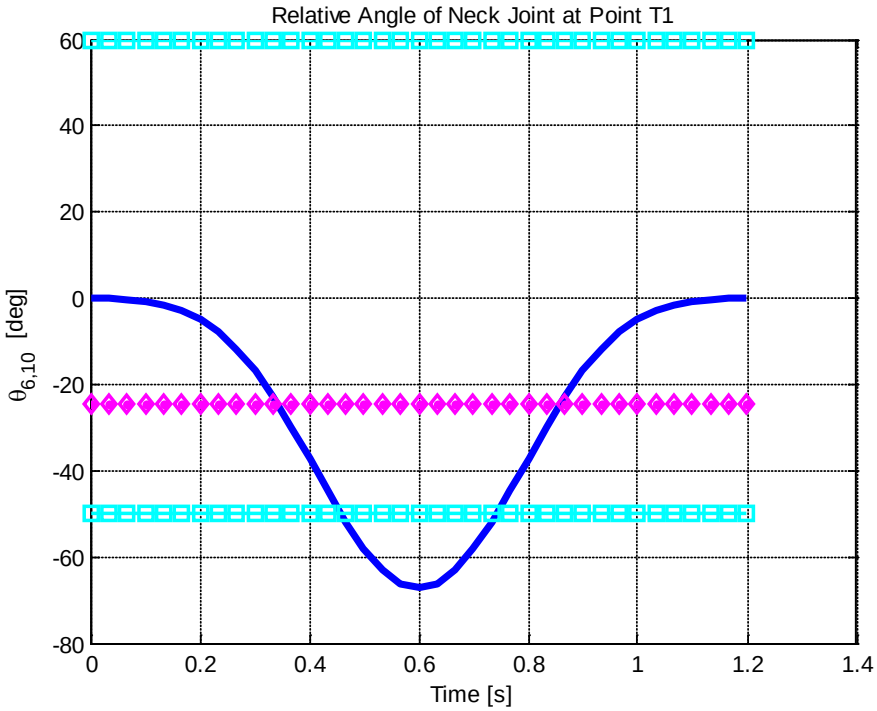

Figure 7.43 Relative Angle of Neck at Point T_1 during sudden stop

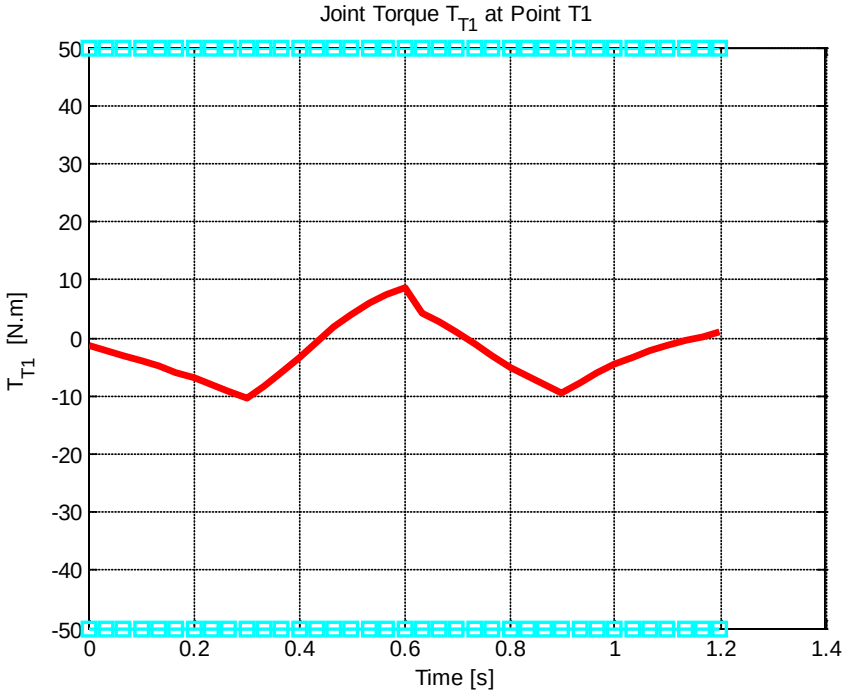

Figure 7.44 Joint Torque T_{T1} at Point T_1 during sudden stop

xi) Link-11 Simulation Results

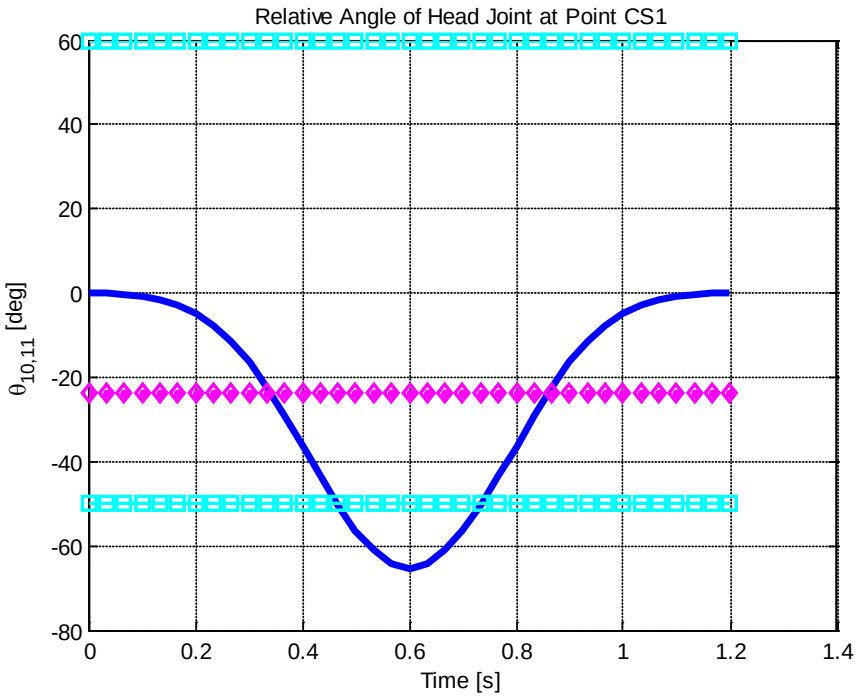

Figure 7.45 Relative Angle of Head Joint at Point CS_1 during sudden stop

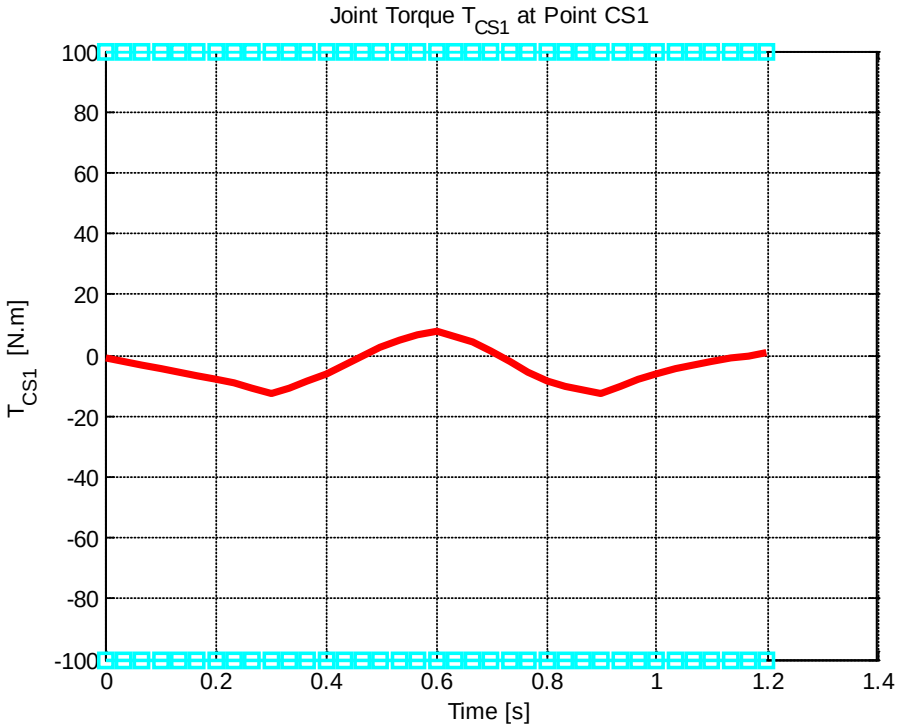

Figure 7.46 Joint Torque T_{CS1} at Point CS_1 during sudden stop

7.3 Discussion of Obtained Results

During the sitting trot, some of the joint angles exceed the limits at some time points (time increment=fps=1/30sec). However, the mean values of the joint angles are between the limits which are plotted in the figures also (magenta line with diamond shape). The joint torques during sitting trot lie in the feasible range In Figure 7.47, the posture change of the rider is plotted at certain points during one period of the horse motion 1.2 sec.

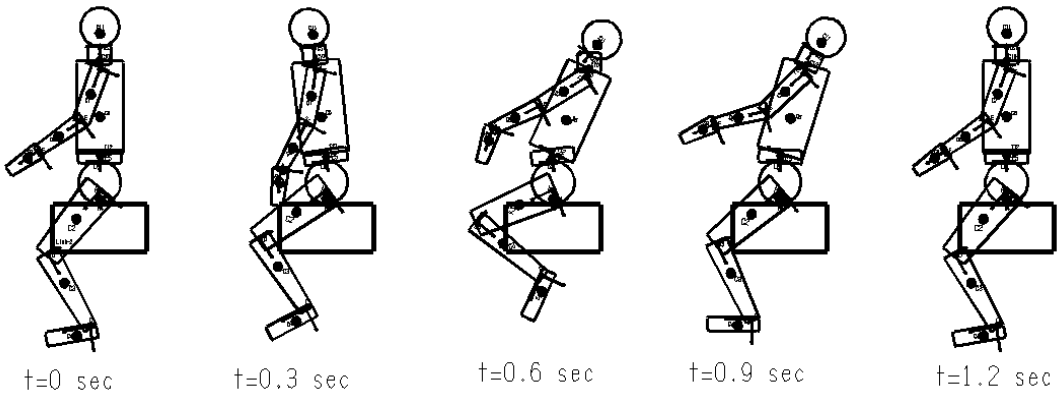

Figure 7.47 Posture change of the rider during sitting trot

In the sudden stop scenario, observing the figures of joint torques at each joint, it is noticed that the rider cannot provide some of the joint torques since these exceed the minimum and the maximum limits. The sudden stop occurs at t=0.6 sec, and the peak points of the joint angles and the joint actuation torques are seen at that time. In Figure 7.48, the rider's posture is plotted at certain time points during the period. The rider's body leans backward so much at the sudden stop time. Furthermore, the generated joint torques at L_5 (lumbar spine) and T_{12} are too high from the limits. Especially at Joint A, the joint torque T_A exceeds the limits by 100 Nm. Hence, although the joint angles are in the feasible range, the sudden stop of the rider is not possible since the joint torques are too high and the rider's position is extremely unrealistic and the joint torques are too high from the limits.

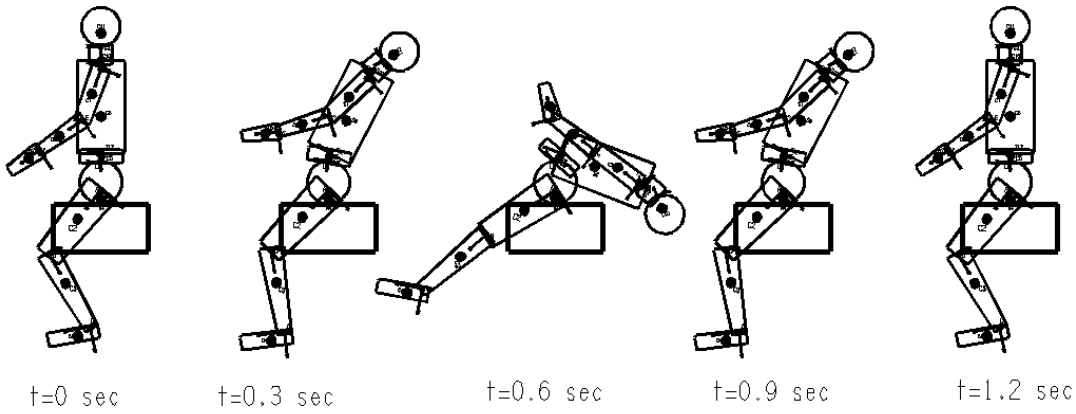

Figure 7.48 Posture change of the rider during sudden stop

At the sudden stop time, the rider's lower extremity goes forward and the upper extremity goes backward in order to satisfy the rider's center of mass constraint. So, since the relative distance between the rider's center of mass and 4^{th} marker is kept constant during riding, this posture happens at the sudden stop time.(see Figure 7.48) Indeed, the posture of the rider at this time values is not so realistic.

CHAPTER 8

CONCLUSION AND FUTURE WORK

In this thesis, a biomechanical dynamic model is developed for the motion of a rider on the horseback. The model is established based on a realistic segmentation of the human body. Each body segment is represented by a link and each link is connected by a 1-dof revolute joint. The mass, center of mass, inertia and geometric dimension data of each body segment used in this study, is taken from **[21]**.

In **[22]**, the kinematic data of Link-1 (saddle-hip) (i.e. position $\overline{r}$, velocity $\overline{v}$, acceleration $\overline{a}$, angular velocity $\overline{\omega}$ and angular acceleration $\overline{\alpha}$) have been obtained for the three gaits of the horse. These data are used in the position, velocity and acceleration analyses of the developed dynamic model.

The joint angles, angular velocities and the angular accelerations are modeled via creating parametric continuous piecewise polynomials with design parameters. These parametric continuous piecewise polynomials are used in the inverse dynamic analysis in order to find the joint reaction forces and joint actuation torques.

A performance measure is defined as the summation of the joint actuation torques squares, together with the horse-rider reaction forces and moments. The functional minimization problem is transformed into a nonlinear optimization problem which is solved by using MATLAB® *fmincon* function. The constraints are constructed so that the joint angles and the joint actuation torques do not violate the biological limits of the human body motion. Two additional constraints ensure that that the center of gravity of the rider in the x-direction does not change relative to the horse body, and, the stirrup length is always constant during riding. The minimization of the

performance measure is achieved considering all of these constraints. The optimization of the performance measure is done during two case studies, namely, the sitting trot and sudden stop scenario. Sitting trot kinematic data is known **[22],** on the other hand; the data related to the sudden stop scenario is generated in this study.

After solving the optimization problem, the optimal joint angles and joint actuation torques are plotted.

As a future work suggestion, the horse rider model can be extended to a 3D model; in this case all of the joint angle rotations about the three axes should be created as parametric piecewise continuous polynomials and implemented into the kinematic and dynamic analyses.

The horse rider model in this study is an application of human body modeling, which is based on a realistic segmentation. This model may be also used in other biomechanical modeling studies.

The performance measure created in this study may be also minimized with the same constraints during walk and canter gaits.

An animation code may be written in MATLAB® in order to visualize the motion of the rider.

REFERENCES

[1] C. Peham, A.B. Kotschwar, B. Borkenhagen, S. Kuhnke, J. Molsner, A.Baltacis, *A comparison of forces acting on the horse's back and the stability of the rider's seat in different positions at the trot*, The Veterinary Journal 184, 56-59, 2010.

[2] P. Cocq, M. Mooren, A. Dortmans, P.R. Weeren, M. Timmermans, M. Muller, J.L. Leeuwen, *Saddle and leg forces during lateral movements in dressage*, Equine Veterinary Journal 42 (Suppl. 38), 644-649, doi: 10.1111/j.2042-3306.2010.00201.x, 2010.

[3] L.E. Keener and M. Levy, *Quantification of Biomechanical Interactions between Dressage Horses and Riders,* http://www.asbweb.org/conferences/2005/315.pdf, last visited on June 21st, 2013.

[4] C. Peham, T. Licka, H. Schobesberger, E. Meschan, *Influence of the rider on the variability of the equine gait*, Human Movement Science 23, 663-671, 2004.

[5] Ok-Deuk Kang, Youn-Chul Ryu, Che-Cheong Ryew, Woon-Yong Oh, Chong-Eon Lee, Min-Soo Kang, *Comparative analyses of rider position according to skill levels during walk and trot in Jeju horse*, Human Movement Science 29, 956-963, 2010.

[6] J. Lagarde, C. Peham, T. Licka, J.A.S. Kelso, *Coordination Dynamics of the Horse-Rider System*, Journal of Motor Behavior 37, No. 6, 418–424 , 2005.

[7] K. Witte, H. Schobesberger, C. Peham, *Motion pattern analysis of gait in horseback riding by means of Principal Component Analysis*, Human Movement Science 28, 394–405, 2009.

[8] A. Byström, M. Rhodin, K. Von Peinen, M.A. Weishaupt, L. Roepstorff, *Kinematics of saddle and rider in high-level dressage horses performing collected walk on a treadmill*, Equine Veterinary Journal 42, 340-345, 2010.

[9] S.J. Schils, L.N. Greer, L.J. Stoner, C.N. Kobluk, *Kinematic analysis of the equestrian-Walk, posting trot and sitting trot*, Human Movement Science 12, 693-712, 1993.

[10] D. Symes, R. Ellis, *A preliminary study into rider asymmetry within equitation*, The Veterinary Journal 181, 34–37, 2009.

[11] L. Greve, S.Dyson, *The horse–saddle–rider interaction*, The Veterinary Journal, 195, 275-281, 2013.

[12] V. Keppler, *Analysis of the Biomechanical Interaction between Rider and Motorcycle by Means of an Active Rider Model*, Proceedings of Bicycle and Motorcycle Dynamics, Symposium on the Dynamics and Control of Single Track Vehicles, 2010.

[13] V. Keppler, *Biomechanical Rider for Motorcycle Simulations*, 2008, www.simpack.com/fileadmin/simpack/doc/newsletter/2008/SN_2_Nov2008_Biomechanical_Rider.pdf , last visited on June 21st, 2013.

[14] S.E. Harris, *Horse Gaits, Balance and Movement*, New York: Howell Book House, ISBN 0-87605-955-8, pp. 32–33, 1993.

[15] A.M. Swinker, 4H-Horse Project Manual, Colorado State University Cooperative Extension, Colorado Springs, Member's Manual, MA1500C.

[16] http://www.adsere.com/blog/2012/07/buying-secondhand-horse-riding-equipment/, last visited on July 21st, 2013.

[17] *How to improve your classical seat in horse riding*, http://www.videojug.com/film/how-to-improve-your-classical-seat-in-horse-riding, last visited on July 21st, 2013.

[18] Balance Rider, http://www.balancedrider.com/read.pdf, last visited on July 21st, 2013

[19]http://vichorse.com/forum/index.php?t=msg&goto=2722851&S=70a5bb544c863

14b1e 34155a9e859af0, last visited on July 21st, 2013

[20] Saddle Seat, http://www.imeha.org/imehaguidebook/SS/saddleseat.html, last visited on July 21st, 2013

[21] Naval Biodynamic Laboratory, *Anthropometry and Mass Distribution for Human Analogues*, Volume I: Military Male Aviators, U.S. Army, Airforce, and Navy, March 1988.

[22] Doğan, G., *"Development of a 3-camera vision system and the saddle motion analysis of horses via this system"*, MSc. Thesis, Dept. Mech. Eng, Middle East Technical University, Ankara, Turkey, 2009.

[23] M.K Özgören, *ME502 Advanced Dynamics Lecture Notes*, Middle East Technical University, Ankara, Turkey

[24] N.R. Jezar, *Advanced Dynamics: Rigid Body, Multi Body and Aerospace Applications*, John Wiley & Sons, Inc., 2011.

[25] F.E. van Beek et al., *Stirrup forces during horse riding: A comparison between sitting and rising trot*, The Veterinary Journal, doi:10.1016/j.tvjl.2011.10.007, 2011.

[26] A.K. Warren-Smith et al., Applied Animal Behaviour Science 108, 157–169, 2007.

[27] *Range of Joint Motion Evaluation Chart*, Department of Social Health Services, Washington State University, DSHS 13-585A (REV. 08/2002) (AC 01/2003).

[28] E.N. Horn, *"Optimization Based Dynamic Human Motion Prediction"*, MSc. Thesis, Dept. Mech. Eng, University of Iowa, USA, 2005.

[29] Mathworks Inc., http://www.mathworks.com/help/optim/ug/fmincon.html, last visited on October 14th, 2013.

[30] R.L. Burden, J.D. Faires, Numerical Analysis, 7th edition, Brooks/Cole, USA, 2001.

APPENDIX A

HUMAN BODY DIMENSIONS

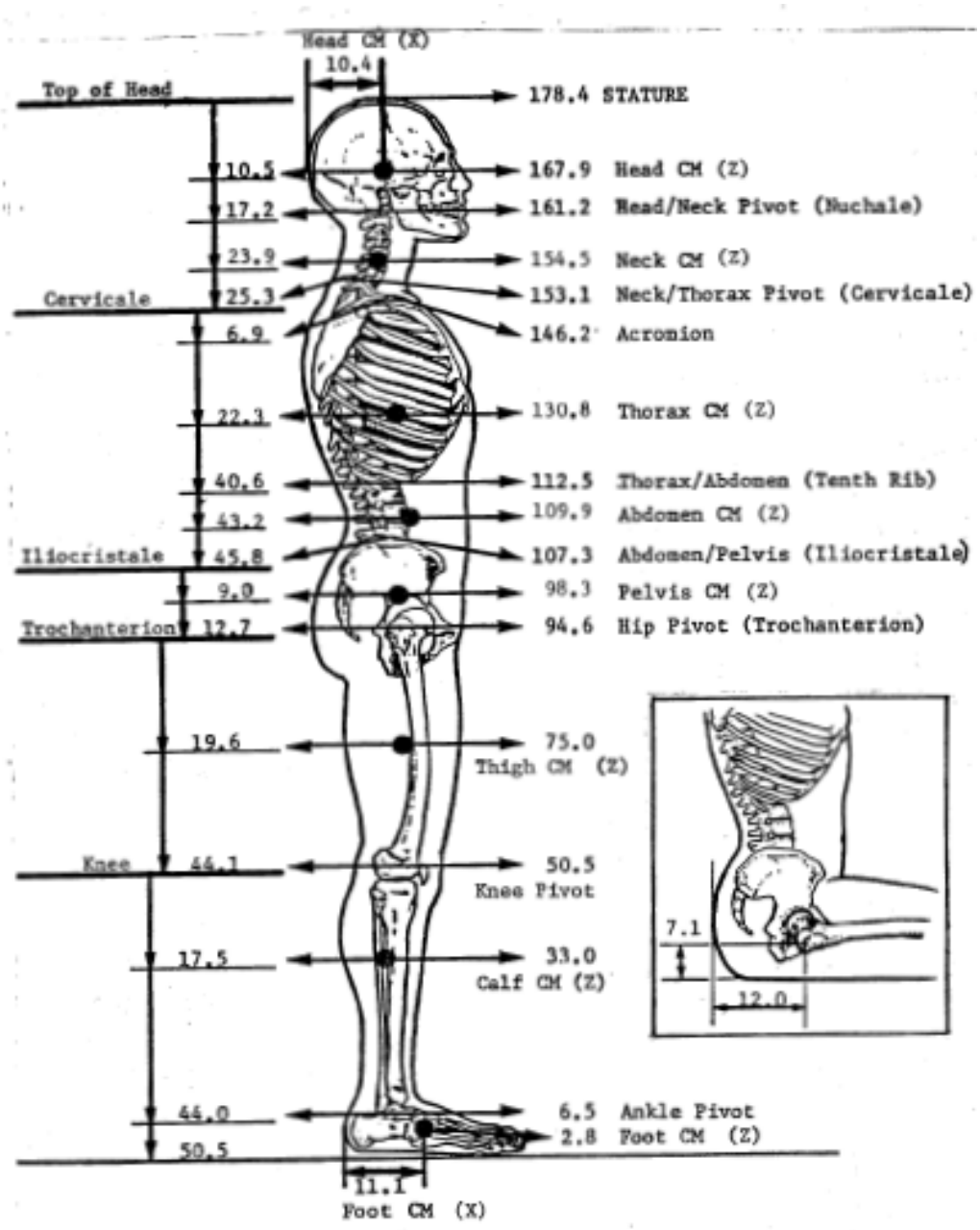

Figure A.1 Center of Mass Locations of Lower and Upper Extremity of Human Body **[21]**

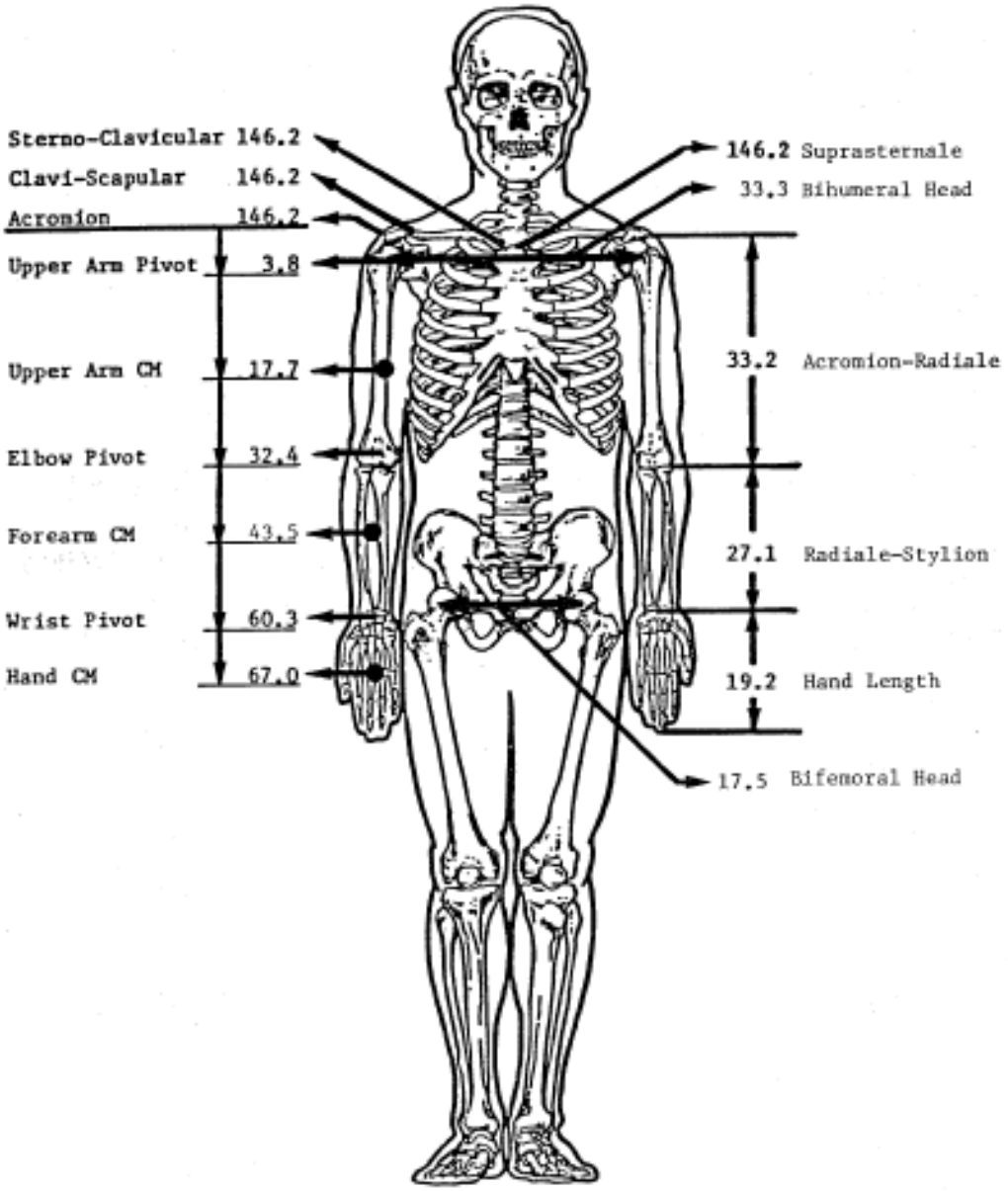

Figure A.2 Center of Mass Locations of Upper Arm, Fore Arm and Hand **[21]**

A.1 Mass Distrubution of the Body Segments

Head:

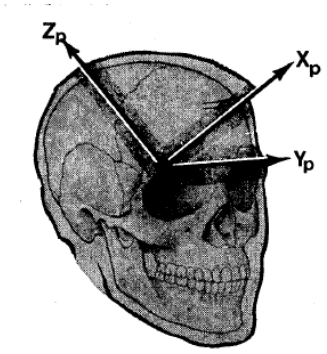

Table A. 1 Mass and Principal Moments of Inertias of Head **[21]**

	Moment of Inertias [kg.cm2]		
Segment Mass [kg]	**X**	**Y**	**Z**
4.2	**206**	**235**	**153**
The principal axes are rotated -36 deg about Y axis			

Neck:

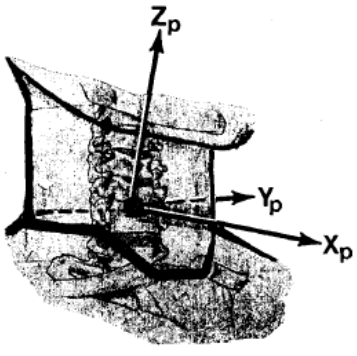

Table A.2 Mass and Principal Moments of Inertias of Neck **[21]**

	Moment of Inertias [kg.cm2]		
Segment Mass [kg]	**X**	**Y**	**Z**
1.1	**18**	**22**	**28**
The principal axes are rotated +22.2 deg about Y axis			

Trunk:

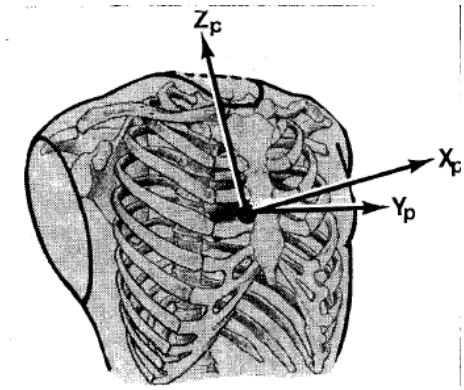

Table A. 3 Mass and Principal Moments of Inertias of Trunk **[21]**

	Moment of Inertias [kg.cm2]		
Segment Mass [kg]	**X**	**Y**	**Z**
24.9	**5224**	**3857**	**3284**
The principal axes are rotated -12 deg about Y axis			

Abdomen:

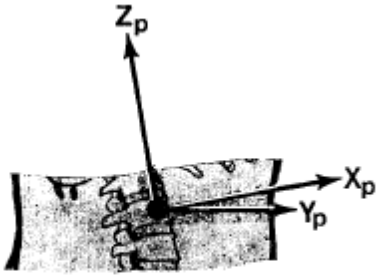

Table A. 4 Mass and Principal Moments of Inertias of Abdomen **[21]**

	Moment of Inertias [kg.cm2]		
Segment Mass [kg]	**X**	**Y**	**Z**
2.4	**175**	**99**	**266**
The principal axes are coincident with reference axes			

Pelvis:

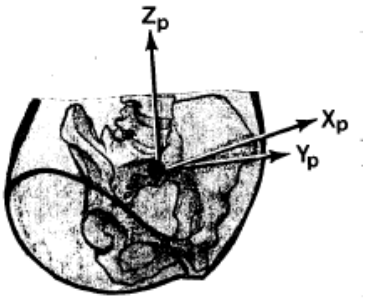

Table A. 5 Mass and Principal Moments of Inertias of Pelvis **[21]**

	Moment of Inertias [kg.cm2]		
Segment Mass [kg]	**X**	**Y**	**Z**
11.8	**1116**	**1028**	**1298**
The principal axes are rotated -24 deg about Y axis			

Upper Arm:

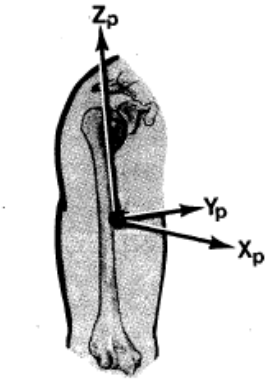

Table A.6 Mass and Principal Moments of Inertias of Upper Arm **[21]**

	Moment of Inertias [kg.cm2]		
Segment Mass [kg]	**X**	**Y**	**Z**
2.0	**141**	**141**	**29**
The principal axes are coincident with reference axes			

Fore Arm:

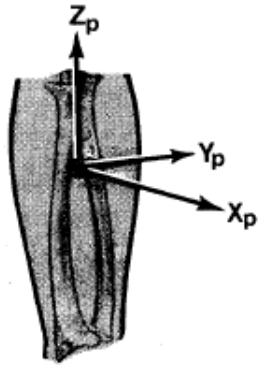

Table A. 7 Mass and Principal Moments of Inertias of Fore Arm **[21]**

	Moment of Inertias [kg.cm2]		
Segment Mass [kg]	**X**	**Y**	**Z**
1.4	**90**	**90**	**14**
The principal axes are coincident with reference axes			

Hand:

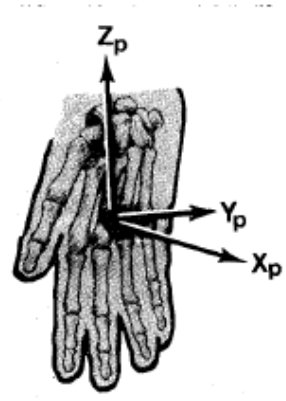

Table A. 8 Mass and Principal Moments of Inertias of Hand **[21]**

	Moment of Inertias [kg.cm2]		
Segment Mass [kg]	**X**	**Y**	**Z**
0.5	**13**	**11**	**4**
The principal axes are coincident with reference axes			

Thigh:

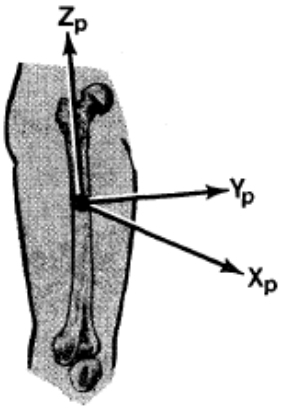

Table A. 9 Mass and Principal Moments of Inertias of Thigh **[21]**

	Moment of Inertias [kg.cm2]		
Segment Mass [kg]	**X**	**Y**	**Z**
9.8	**1652**	**1652**	**452**
The principal axes are coincident with reference axes			

Shank:

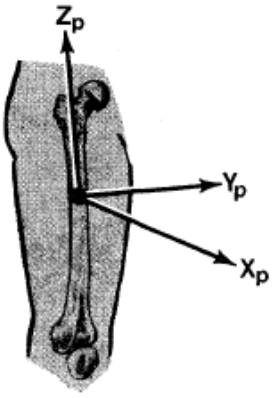

Table A. 10 Mass and Principal Moments of Inertias of Shank **[21]**

	Moment of Inertias [kg.cm2]		
Segment Mass [kg]	**X**	**Y**	**Z**
3.8	**606**	**606**	**71**
The principal axes are coincident with reference axes			

Foot:

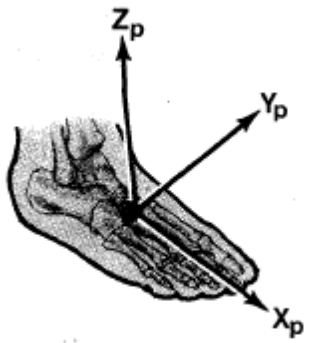

Table A. 11 Mass and Principal Moments of Inertias of Foot **[21]**

	Moment of Inertias [kg.cm2]		
Segment Mass [kg]	**X**	**Y**	**Z**
1.0	**8**	**44**	**46**
The principal axes are coincident with reference axes			

A.2 TORQUE LIMITS OF HUMAN BODY JOINTS

	Max. Value [N.m]	Min. Value [N.m]
T_A	100	-100
T_B	100	-100
T_C	80	-80
T_{L_5}	100	-100
$T_{T_{12}}$	100	-100
T_D	80	-80
T_E	100	-100
T_F	80	-80
T_{T_1}	50	-50
T_{CS_1}	100	-100

Table A.12 Torque Limits of Human Joints **[28]**

A.3 ANGLE LIMITS OF HUMAN BODY JOINTS

	Max. Value [deg]	Min. Value [deg]
θ_{12}	-20	180
θ_{23}	-20	130
θ_{34}	-140	-40
θ_{15}	-60	90
θ_{56}	-70	90
θ_{67}	-90	140
θ_{78}	-150	0
θ_{89}	-60	60
$\theta_{6,10}$	-50	60
$\theta_{10,11}$	-50	60

Table A.13 Angle Limits of Human Joints **[27]**

A.4 GEOMETRIC DIMENSIONS OF THE HUMAN BODY

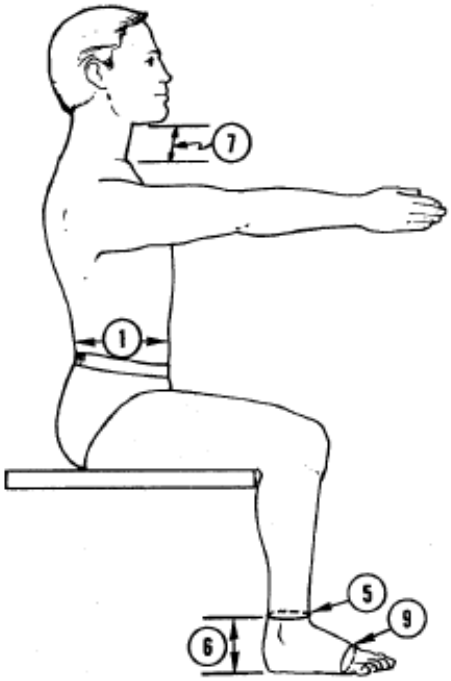

Figure A.3 Ankle, Foot and Waist Geometry **[21]**

Table A.14 Ankle, Foot and Waist Dimensions **[21]**

	Description	**Dimension**
1	**Abdominal Depth, Sitting :** "The maximum horizontal depth of the abdomen"	25.5 cm
5	**Ankle Circumference:** "The minimum horizontal circumference of the lower leg, calf."	22.7 cm
6	**Ankle Height:** "The vertical distance between the standing surface and the level of the ankle circumference."	13.8 cm
7	**Anterior Neck Length:** "The surface distance in the midsagittal plane between the points of the deepest depression of the top of the breastbone and the juncture of the neck and the jaw."	8.4 cm
9	**Ball of Foot Circumference:** "The circumference of the foot passing over the maximum protuberance of the first metatarsal bone and the fifth metatarsal bone."	25.0 cm

Figure A.4 Chest and Thigh Geometry **[21]**

Table A.15 Chest and Thigh Dimensions **[21]**

	Description	Dimension
29	**Buttock-Knee Length:** "The horizontal distance between the maximum protrusion of a buttock and the anterior point of the knee of a seated subject. The knee is flexed 90 degrees."	60.9 cm
30	**Buttock-Popliteal Length:** "The horizontal distance between the maximum protrusion of a buttock and the posterior surface of the knee of a seated subject. The knee is flexed 90 degrees."	50.8 cm
34	**Cervicale Height, Sitting:** "The vertical distance between the sitting surface and cervical."	68.4 cm
40	**Chest Height, Sitting:** "The vertical distance between the standing surface and the level of nipple."	130.1 cm

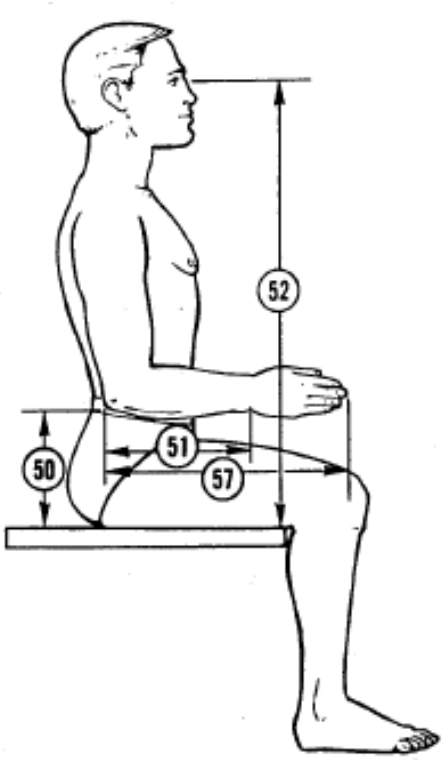

Figure A.5 Fore Arm, Elbow and Wrist Geometry **[21]**

Table A.16 Fore Arm, Elbow and Wrist Dimensions **[21]**

	Description	**Dimension**
50	**Elbow Rest Height:** "The vertical distance between the sitting surface and the bottom of the elbow with the arm hanging freely and the elbow is flexed 90 degrees."	25.4 cm
51	**Elbow-Wrist Length:** "The distance between the tip of the elbow and the distal length of the radius with the upper arm hanging freely and the elbow is flexed with 90 degrees."	30.2 cm
52	**Eye Height, Sitting:** "The vertical distance between the sitting surface and the outer corner of an eye."	81.4 cm
57	**Forearm-Hand Length, Sitting:** "The distance between the tip of the elbow and the tip of the middle finger when the upper arm is hanging freely and the elbow is flexed with 90 degrees."	49.3 cm

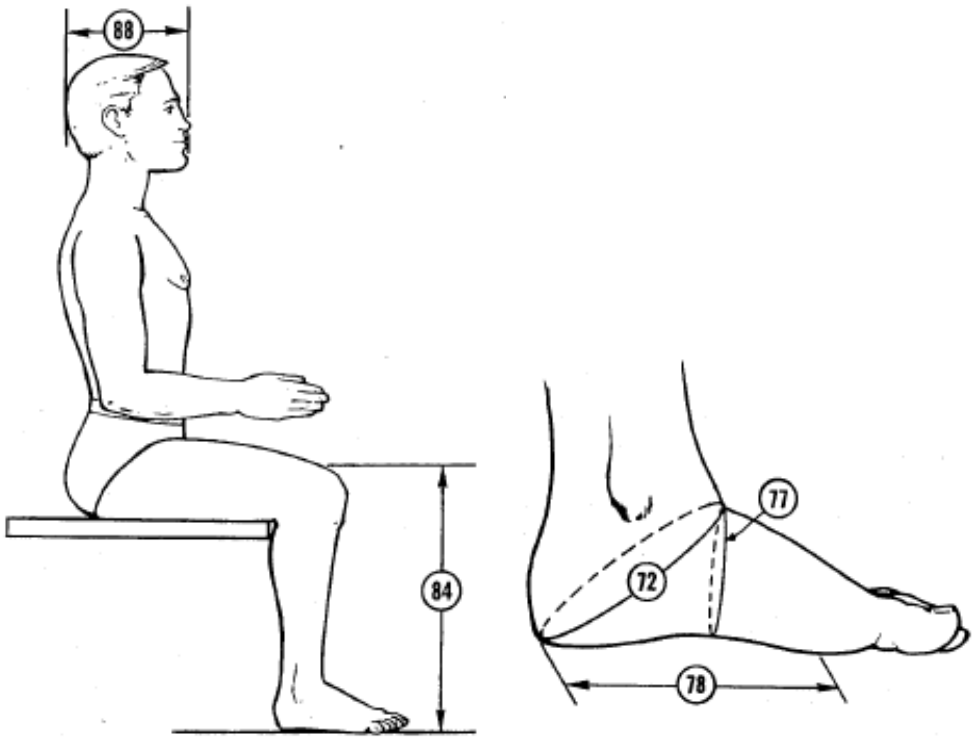

Figure A.6 Knee and Foot Geometry **[21]**

Table A.17 Knee and Foot Dimensions **[21]**

	Description	Dimension
72	**Heel-Ankle Circumference:** "The circumference of the foot and the ankle passing under the tip of the heel and over the anterior juncture of the foot with the ankle."	34.2 cm
77	**Instep Circumference:** "The vertical circumference of the arch of the foot"	25.9 cm
78	**Instep Length:** "The horizontal distance between the back of the heel and the level of maximum medial protrusion of the foot."	19.9 cm
84	**Knee Height, Sitting:** "The vertical distance between a footrest surface and the top of a knee of a seated subject. The knee is flexed 90 degrees."	56.2 cm

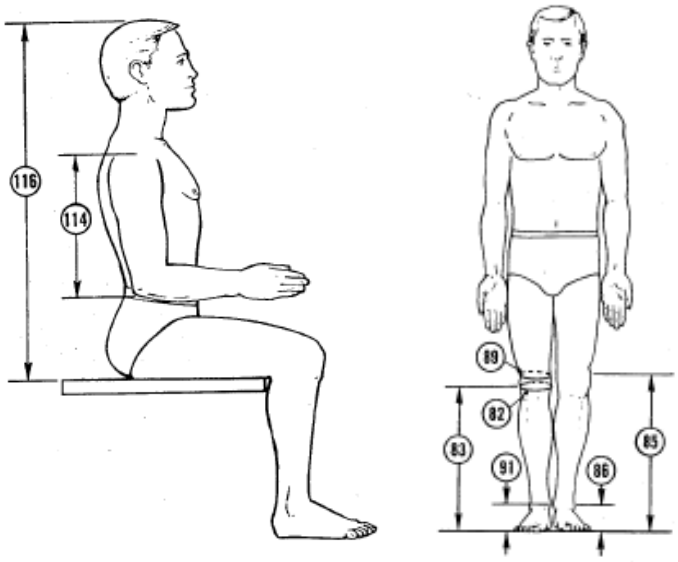

Figure A.7 Knee, Thigh and Shoulder Geometry **[21]**

Table A.18 Knee, Thigh and Shoulder Dimensions **[21]**

	Description	Dimension
82	**Knee Circumference:** "The horizontal circumference of the knee at the level of the middle of kneecap."	39.2 cm
83	**Knee Height:** "The vertical distance between the standing surface and the level of the middle of kneecap."	50.0 cm
85	**Lateral Femoral Epicondyle Height** : " The vertical distance between the standing surface and the level of the maximum protrusion of the lateral femoral epicondyle"	51.0 cm
86	**Lateral Malleous Height:** "The vertical distance between the standing surface and the lateral point of the ankle."	7.1 cm
89	**Lower Thigh Circumference:** "The circumference of the thigh just above the kneecap(patella)."	43.4 cm
91	**Medial Malleous Height:** " The vertical distance between the standing surface and the medial point of the ankle."	8.6 cm
114	**Shoulder-Elbow Length :** " The distance along the long axis of the upper arm, between the tip of the shoulder (acromion) and the bottom of the elbow (olecranon process) when the upperarm is hanging freely with the elbow flexed 90 degrees."	36.2 cm
116	**Sitting Height:** "The vertical distance between the sitting surface and the top of the head."	93.7 cm

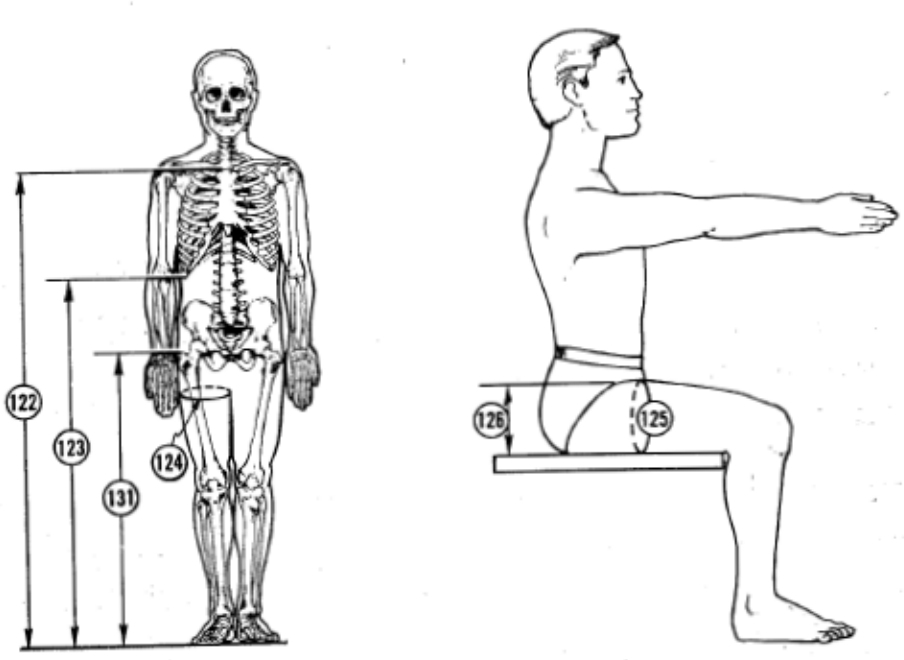

Figure A.8 Thigh and Rib Case Geometry **[21]**

Table A.19 Thigh and Rib Case Dimensions **[21]**

	Description	Dimension
122	**Suprasternale Height:** " The vertical distance between the standing surface and the point of deepest depression of the top of the breast-bone (supras ternale)"	146.2 cm
123	**Tenth Rib Height:** " The vertical distance between the standing surface and the level of the lowest point of the tenth rib."	112.5 cm
124	**Thigh Circumference:** " The circumference of the thigh perpendicular to its long axis at the lowest point of the juncture of a buttock with the thigh."	59.9 cm
125	**Thigh Circumference**, **Sitting: "** The vertical circumference of the thigh at its juncture with the groin of a seated subject"	58.9 cm
126	**Thigh Clearence:** "The vertical distance between t h e siting surface and the highest point on the thigh of a seated subject."	16.8 cm
131	**Trochanteric Height:** "The vertical distance between the standing surface and the top of the greater trochanter of the femur(trochanterion)".	94.6 cm

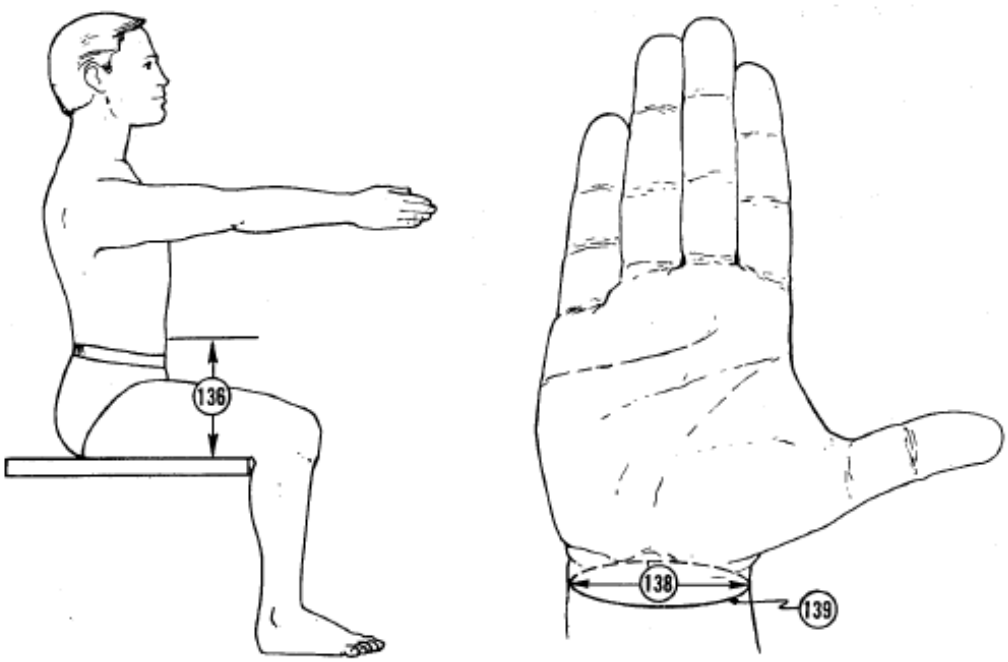

Figure A.9 Waist and Hand Geometry **[21]**

Table A.20 Waist and Hand Dimensions **[21]**

	Description	Dimension
136	**Waist Height, Sitting:** "The vertical distance between the seated surface and the navel."	22.4 cm
138	**Wrist Breadth (Bone):** "The maximum distance between the radial and ulnar styloid"	5.7 cm
139	**Wrist Circumference :** "The circumference of the wrist perpendicular to the long axis of the forearm at the level of the distal tip of the radius (stylion) ."	17.7 cm

A.5 SUDDEN STOP SCENERIO FUNCTIONS

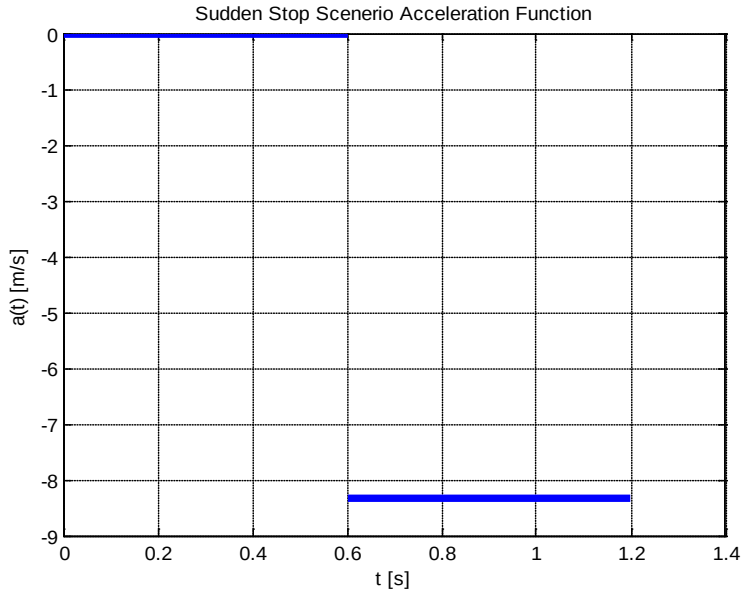

Figure A.10 Sudden Stop Scenario Acceleration Function

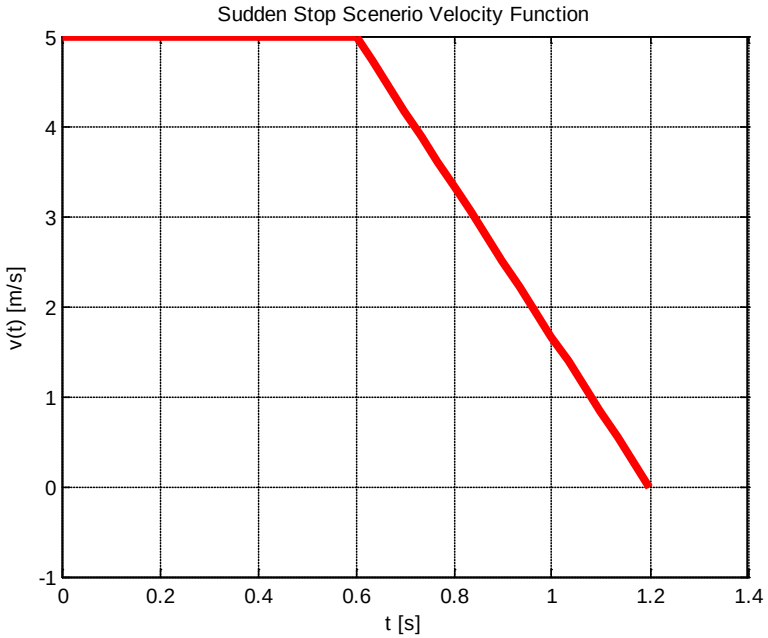

Figure A.11 Sudden Stop Scenario Velocity Function

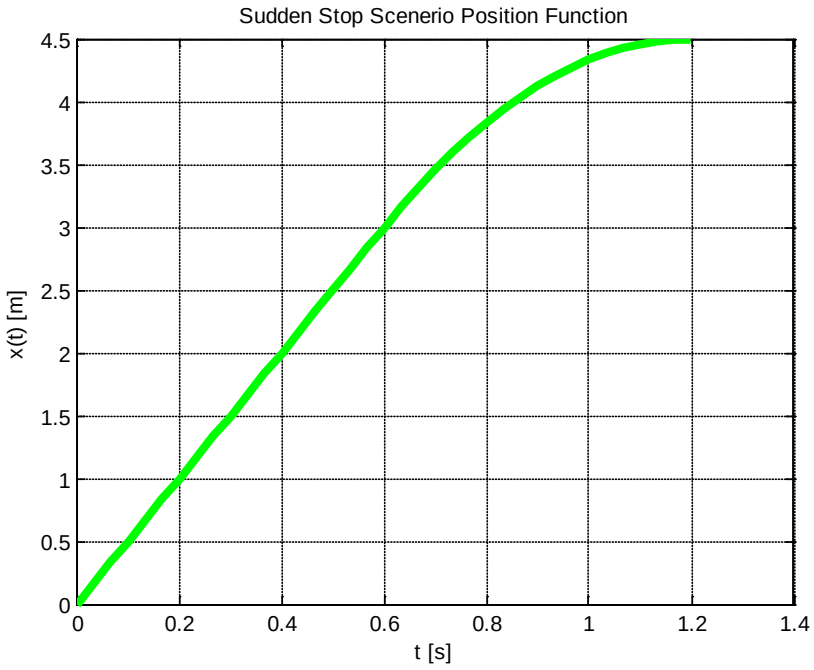

Figure A.12 Sudden Stop Scenario Displacement Function

A.6 CONTINIOUS PIECEWISE POLYNOMIALS (AN EXAMPLE)

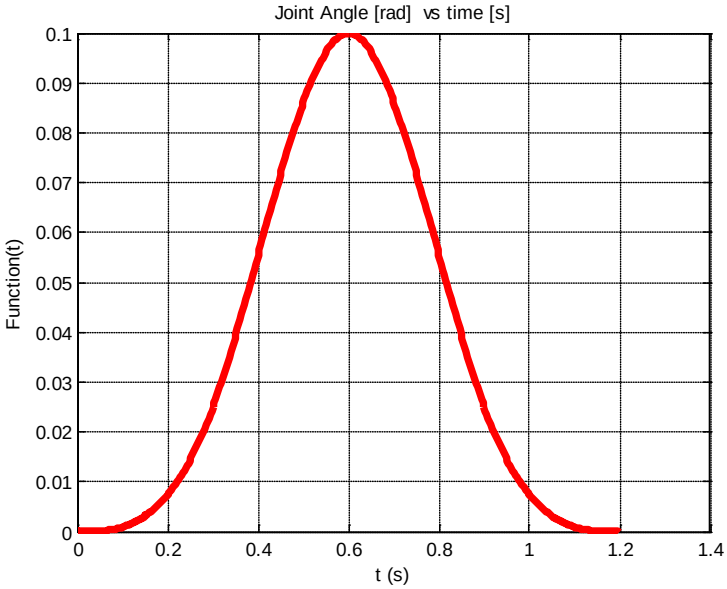

Figure A.13 A Created Example of Parametric Continuous Piecewise Polynomial

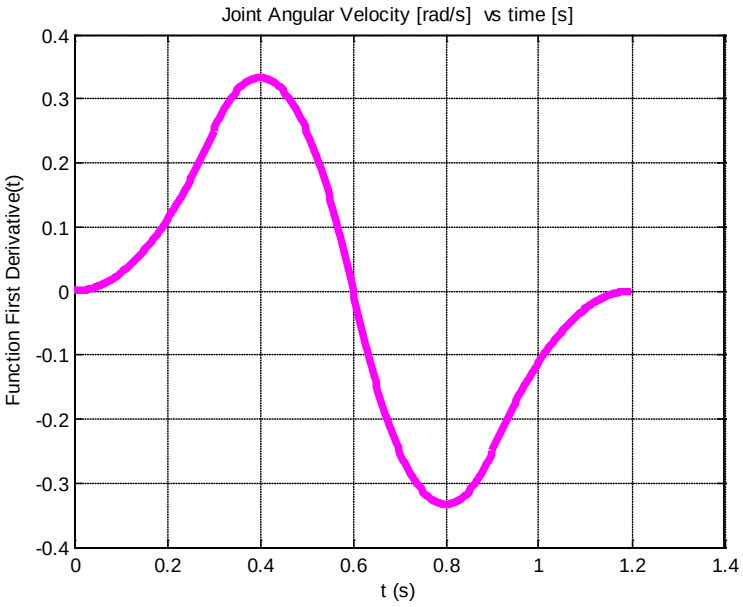

Figure A.14 A Created Example of Parametric Continuous Piecewise Polynomial's 1st derivative Function

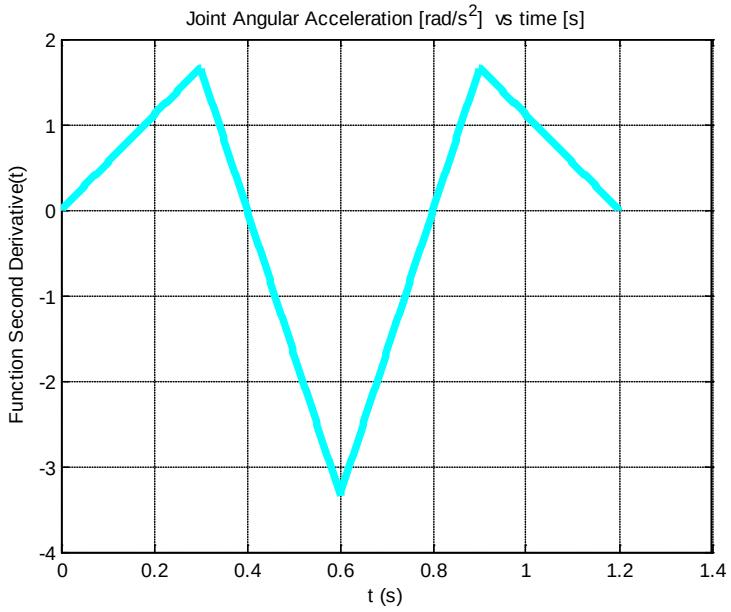

Figure A.15 A Created Example of Parametric Continuous Piecewise Polynomial's 2nd derivative Function

The inputs to the program are as follows:

t_0: 0

t_f: 1.2 (period of sitting trot)

n_p: 4

d_p: 3

d_c: 2

Table A.21 Initial and Final Conditions for the Continuous Piecewise Polynomials (created to be optimized during Sitting Trot and Sudden Stop)

Relative Angles	Initial and Final Conditions
θ_{12}	51 deg
θ_{23}	69 deg
θ_{34}	-110 deg
θ_{15}	0 deg
θ_{56}	0 deg
θ_{67}	70 deg
θ_{78}	-35 deg
θ_{89}	0 deg
$\theta_{6,10}$	0 deg
$\theta_{10,11}$	0 deg
$\dot{\theta}_0$	0.5 rad/s
$\ddot{\theta}_0$	0.5 rad/s^2

Periodicity Rule is;

$\theta_0\,(t_0) = \theta_f(t_f)$

$\dot{\theta}_0(t_0) = \dot{\theta}_f(t_f)$

$\ddot{\theta}_0(t_0) = \ddot{\theta}_f(t_f)$

A.7 KINEMATIC DATA OF 4th MARKER IN WORLD FIXED FRAME

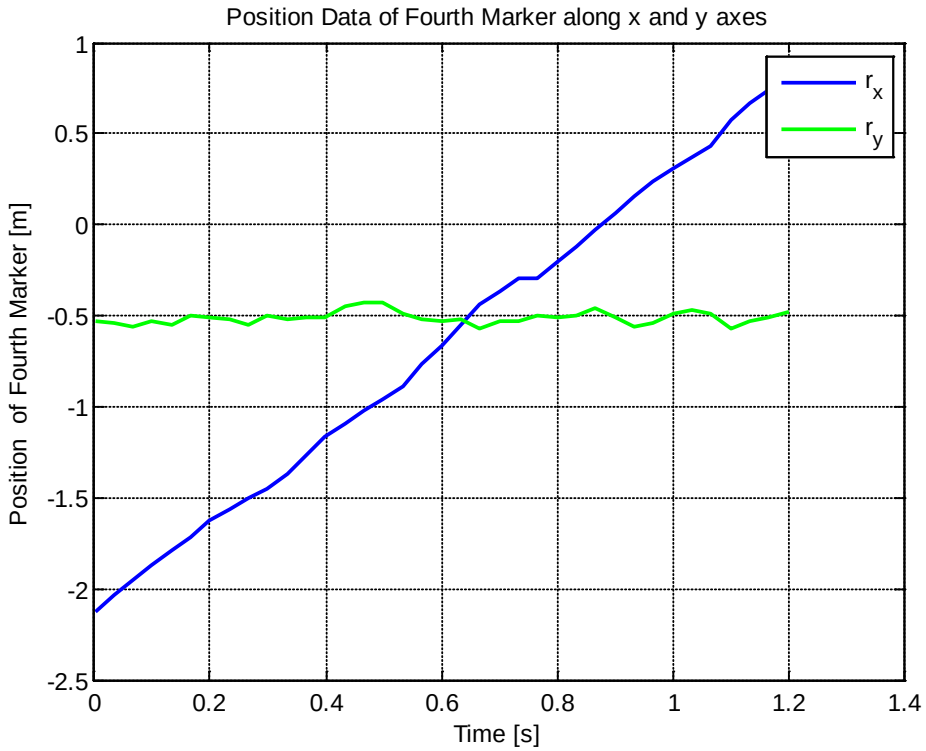

Figure A.16 Position Data of 4th Marker (x- and y- axes)

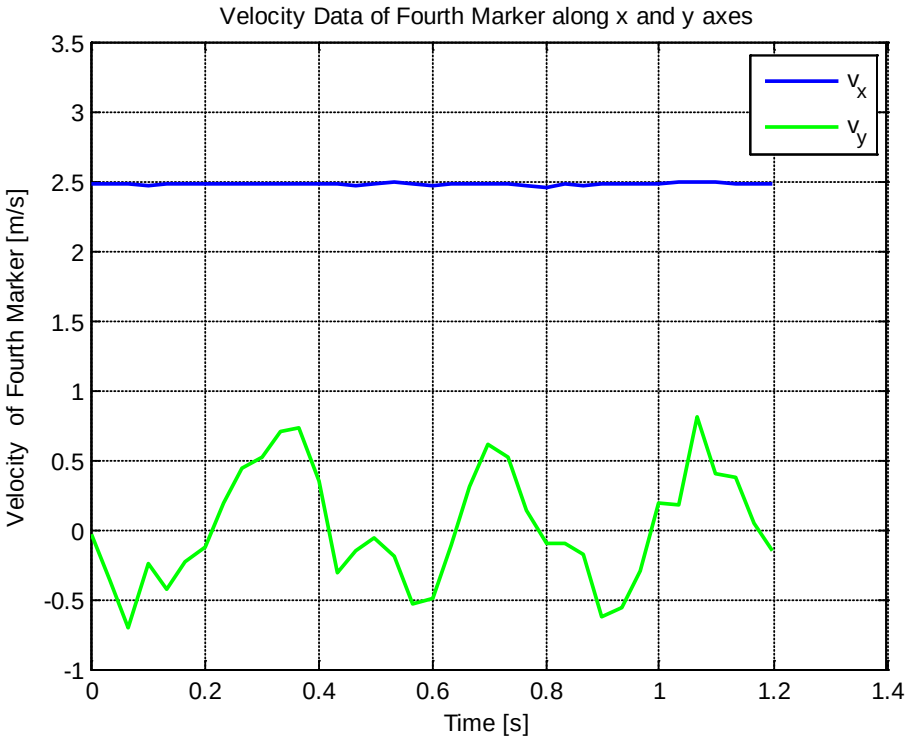

Figure A.17 Velocity Data of 4th Marker (x- and y- axes)

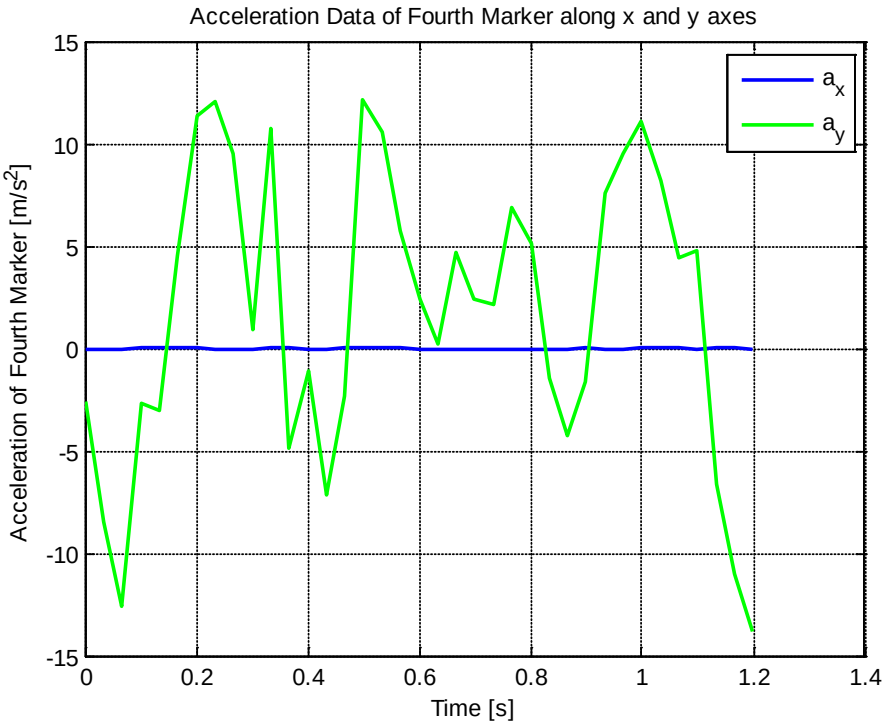

Figure A.18 Acceleration Data of 4th Marker (x- and y- axes)

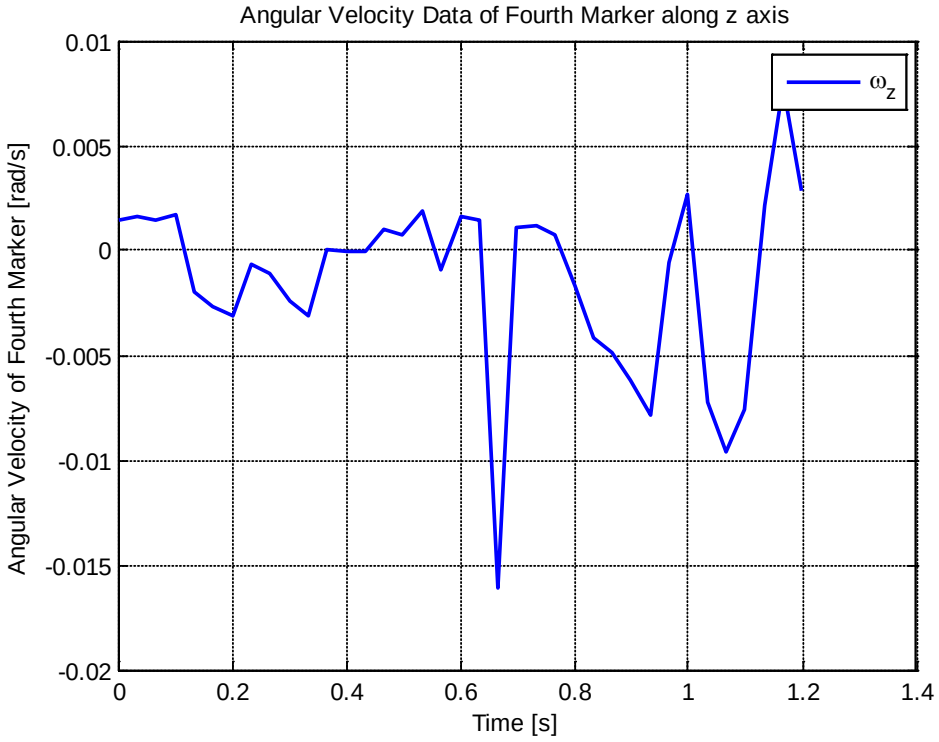

Figure A.19 Angular Velocity Data of 1st Link (z- axis)

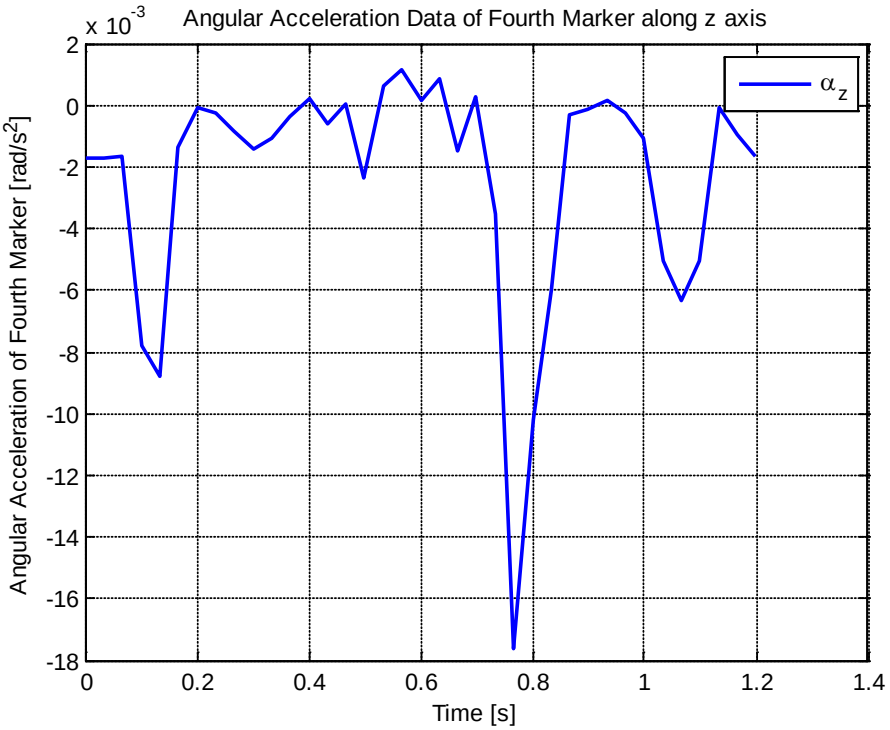

Figure A.20 Angular Acceleration Data of 1st Link (z- axis)